Handbook T-XIX
CIERMMI Women in Science
Biological Sciences

MARROQUÍN-DE JESÚS, Ángel
CASTILLO-MARTÍNEZ, Luz Carmen
SOTO-ÁLVAREZ, Sandra
CRUZ-CARPIO, Luis Eduardo

Coordinators

ECORFAN®

ECORFAN®

ISBN: 978-607-8695-86-7
ECORFAN Publishing Label: 607-8695
HSW Control Number: 2022-19
HSW Classification (2022): 121122-1901

Handbooks

Definition of Handbooks

Scientific Objectives

To support the International Scientific Community in its written production of Science, Technology and Innovation in the CONACYT and PRODEP research areas.

ECORFAN-Mexico, S.C. is a Scientific and Technological Company in contribution to the formation of Human Resources focused on the continuity in the critical analysis of International Research and is attached to the RENIECYT of CONACYT with number 1702902, its commitment is to disseminate research and contributions of the International Scientific Community, academic institutions, agencies and entities of the public and private sectors and contribute to the linkage of researchers who perform scientific activities, technological developments and training of specialized human resources with governments, businesses and social organizations.

To encourage the interlocution of the International Scientific Community with other study centres in Mexico and abroad and to promote a wide incorporation of academics, specialists and researchers to the serial publication in Science Niches of Autonomous Universities - State Public Universities - Federal IES - Polytechnic Universities - Technological Universities - Federal Technological Institutes - Teacher Training Colleges - Decentralised Technological Institutes - Intercultural Universities - S&T Councils - CONACYT Research Centres.

Scope, Coverage and Audience

Handbooks is a product edited by ECORFAN-Mexico S.C. in its Holding with repository in Mexico, it is a refereed and indexed scientific publication. It admits a wide range of contents that are evaluated by academic peers by the double-blind method, on topics related to the theory and practice of the CONACYT and PRODEP research areas respectively with diverse approaches and perspectives, which contribute to the dissemination of the development of Science, Technology and Innovation that allow arguments related to decision-making and influence the formulation of international policies in the field of Science. The editorial horizon of ECORFAN-Mexico® extends beyond academia and integrates other segments of research and analysis outside that field, as long as they meet the requirements of argumentative and scientific rigour, in addition to addressing issues of general and current interest of the International Scientific Society.

Editorial Board

Arbitration Committee

Assignment of Rights

By submitting a Scientific Work to ECORFAN Handbooks, the author undertakes not to submit it simultaneously to other scientific publications for consideration. To do so, the author must complete the Originality Form for his or her Scientific Work.

The authors sign the Authorisation Form for their Scientific Work to be disseminated by the means that ECORFAN-Mexico, S.C. in its Holding Mexico considers pertinent for the dissemination and diffusion of their Scientific Work, ceding their Scientific Work Rights.

Declaration of Authorship

Indicate the name of 1 Author and a maximum of 3 Co-authors in the participation of the Scientific Work and indicate in full the Institutional Affiliation indicating the Unit.

Identify the name of 1 author and a maximum of 3 co-authors with the CVU number - PNPC or SNI-CONACYT - indicating the level of researcher and their Google Scholar profile to verify their citation level and H index.

Identify the Name of 1 Author and 3 Co-authors maximum in the Science and Technology Profiles widely accepted by the International Scientific Community ORC ID - Researcher ID Thomson - arXiv Author ID - PubMed Author ID - Open ID respectively.

Indicate the contact for correspondence to the Author (Mail and Telephone) and indicate the Contributing Researcher as the first Author of the Scientific Work.

Plagiarism Detection

All Scientific Works will be tested by the PLAGSCAN plagiarism software. If a Positive plagiarism level is detected, the Scientific Work will not be sent to arbitration and the receipt of the Scientific Work will be rescinded, notifying the responsible Authors, claiming that academic plagiarism is typified as a crime in the Penal Code.

Refereeing Process

All Scientific Works will be evaluated by academic peers using the Double-Blind method. Approved refereeing is a requirement for the Editorial Board to make a final decision which will be final in all cases. MARVID® is a spin-off brand of ECORFAN® specialised in providing expert reviewers all of them with PhD degree and distinction of International Researchers in the respective Councils of Science and Technology and the counterpart of CONACYT for the chapters of America-Europe-Asia-Africa and Oceania. The identification of authorship should only appear on a first page, which can be removed, in order to ensure that the refereeing process is anonymous and covers the following stages: Identification of ECORFAN Handbooks with their author occupancy rate - Identification of Authors and Co-authors - PLAGSCAN Plagiarism Detection - Review of Authorisation and Originality Forms-Assignment to the Editorial Board - Assignment of the pair of Expert Referees - Notification of Opinion - Statement of Observations to the Author - Modified Scientific Work Package for Editing - Publication.

ECORFAN CIERMMI Women in Science

Volume XIX

The Handbook will offer volumes of selected contributions from researchers who contribute to the scientific dissemination activity of the Colegio de Ingenieros en Energías Renovables de Querétaro A.C. in their areas of research in Biological Sciences. In addition to having a total evaluation, in the hands of the directors of the Colegio de Ingenieros en Energías Renovables de Querétaro A.C., the quality and timeliness of its chapters, each individual contribution was refereed to international standards (RESEARCH GATE, MENDELEY, GOOGLE SCHOLAR and REDIB), the Handbook thus proposes to the academic community, recent reports on new developments in the most interesting and promising areas of research in the Biological Sciences.

For future volumes:
http://www.ecorfan.org/handbooks/

MARROQUÍN-DE JESÚS, Ángel. PhD
CASTILLO-MARTÍNEZ, Luz Carmen. MsC
SOTO-ÁLVAREZ, Sandra. MsC
CRUZ-CARPIO, Luis Eduardo. BsC

Coordinators

CIERMMI Women in Science T-XIX
Biological Sciences
Handbooks

Colegio de Ingenieros en Energías Renovables de Querétaro A.C. – Mexico. November, 2022

DOI: 10.35429/H.2022.6.1.1.123

Prologue

.

This book has been written by women involved in the world of science, where they work in what they believe in, whose mission lies in research, the authors call it their work, but in reality it is their life there, their time and perhaps it is also their family, their soul full of inspiration, this miraculous and indescribable symbiosis, called woman-science.

The works submitted to the CIERMMI Congress, cover the areas of knowledge indicated by the National Council of Science and Technology (CONACYT), which opens a range of possibilities to publish their work, which contributes to obtaining important recognition for their work, which also contributes to obtaining personal goals such as the desirable profile of the Program for the Professional Development of Teachers (PRODEP) and compete to obtain some distinction in the National System of Researchers (SNI).

As Jane Goodall said "The greatest danger that the future holds for us is apathy". In light of this truth, women researchers contribute with their work to the dissemination of their knowledge, in which they put their heart and their time, this book recognizes their valuable contributions in area I: Physics-Mathematics and Earth Sciences. As well as area II: Biology and Chemistry.

My recognition to these women, scientists, teachers, housewives, mothers, wives, daughters, etc., who put their wisdom and contribute in a real way to the development of science, which contributes to improve our common home: our planet and elucidate that perfect machine called living beings, to find and reconnect the homeostasis so sought and desired for humanity.

Castillo-Martínez, Luz Carmen. MsC
Full Time Professor
Attached to the Industrial Chemistry and Renewable Energies Educational Program.
Universidad Tecnológica de San Juan del Río
San Juan del Rio, Queretaro, November 2022

Introduction

The Colegio de Ingenieros en Energías Renovables de Querétaro A.C. (CIER-QUERÉTARO), and its chapters of Renewable Energy, Industrial Maintenance, Mechatronics and Informatics, technical sponsors of the International Interdisciplinary Congress on Renewable Energy, Maintenance, Mechatronics and Informatics, CIERMMI 2022 has as general objective to establish a space for discussion and reflection on issues related to the areas of: renewable energy, industrial maintenance, mechatronics and informatics with the participation of students, teachers, researchers and national and international speakers, promoting the formation and consolidation of research networks. Contributing to provide a space for dissemination and discussion of the presentations of students, graduates, academics and researchers, representatives of various higher education institutions, research centers in our country, as well as educational institutions beyond our borders. Promoting the formation of research networks between different institutions. Offering a space for undergraduate, master's, doctoral and postdoctoral students, in which they can present the progress of the research they carry out in their different educational centers. Providing a space in which study groups and members of academic bodies, linked to the curricular program of renewable energy, industrial maintenance, mechatronics and computer science careers, can present the research work developed within their institution and in collaboration with other national or international educational institutions. Establishing a training space for the attendees, through the development of specific lectures and conferences.

This volume, Women in Science T-XIX-2022 contains 9 refereed chapters dealing with these issues, chosen from among the contributions, we gathered some researchers and graduate students from the 32 states of our country. We thank the reviewers for their feedback that contributed greatly in improving the book chapters for publication in these proceedings by reviewing the manuscripts that were submitted.

ALTAMIRANO, VILLARREAL, HERNÁNDEZ and RESÉNDEZ open with Study of Hox protein-protein interactions in living cells using novel fluorescent techniques. *GUTIERREZ, CEDILLO and PERRUSQUÍA* submit molecular biology: tools for the study of re-emerging diseases. *TORRES, LOEZA, MORALES and MEDINA* investigate the used edible oils a latent threat in the contamination of water bodies. *URBANO, OJEDA and PRADO* develop the evaluation of activated carbon from cactus residues in the colour removal process in synthetic water. *ANTONIO, DEL ÁNGEL, PURATA and CÁCERES* research the removal of aluminium (Al) and lead (Pb) in contaminated water using carboxymethylcellulose (CMC) gel polymer. *FONSECA, MENDOZA, PEÑA and RAMÍREZ* develop the polyhydroxyalkanoates (PHA): natural polymers produced by bacteria, an option for the replacement of plastics. *GARCÍA, MACÍAS, LUGO and ALCÁZAR* assess the effects of selenium on yield, seed size, and phenolic compound content of common bean (*Phaseolus vulgaris* L.). *VÁZQUEZ & PEÑA* investigate the genetic improvement of polyester degrading enzymes. Finally, *RAMOS, ESCALANTE, ROSALES and REYES* submit Staphylococcus carnosus study as an alternative bio-collector for metal minerals.

MARROQUÍN-DE JESÚS, Ángel
CASTILLO-MARTÍNEZ, Luz Carmen
SOTO-ÁLVAREZ, Sandra
CRUZ-CARPIO, Luis Eduardo

Coordinators

Content

Chapter 1 Study of Hox protein-protein interactions in living cells using novel fluorescent techniques

Capítulo 1 Estudio de interacciones proteína-proteína Hox en células vivas utilizando técnicas novedosas de fluorescencia

ALTAMIRANO-TORRES, Claudia†, VILLARREAL-PUENTE, Alely, HERNÁNDEZ-BAUTISTA, Carolina and RESÉNDEZ-PÉREZ, Diana*

Universidad Autónoma de Nuevo León, Faculty of Biological Sciences, Department of Cell Biology and Genetics, Developmental Biology Unit, Mexico.

ID 1st Author: *Claudia, Altamirano-Torres* / **ORC ID:** 0000-0001-5919-0660, **CVU CONACYT ID:** 418086

ID 1st Co-author: *Alely, Villarreal-Puente* / **ORC ID:** 0000-0003-1770-0778, **CVU CONACYT ID:** 745887

ID 2nd Co-author: *Carolina, Hernández-Bautista* / **ORC ID:** 0000-0001-8576-4592, **CVU CONACYT ID:** 966599

ID 3rd Co-author: *Diana, Reséndez-Pérez* / **ORC ID:** 0000-0002-4709-7677, **CVU CONACYT ID:** 51004

DOI: 10.35429/H.2022.6.1.1.12

C. Altamirano, A. Villarreal, C. Hernández and D. Reséndez

* diana.resendezpr@uanl.edu.mx

A. Marroquín, L. Castillo, S. Soto, L. Cruz. (Coord.) CIERMMI Women in Science T-XIX Biological Sciences. Handbooks-

Abstract

Hox genes are master regulators of development that contain the homeobox, a highly conserved region of 180 base pairs. The homeobox codes for a 60-aminoacid domain called the homeodomain, which interacts with DNA to regulate gene expression with great specificity. How the homeodomain achieves this high level of specificity is one of the great questions in developmental biology. Besides interacting with DNA, the homeodomain also interacts with transcription factors, cofactors, and other proteins to regulate development. These protein-protein interactions are necessary to understand the functions and transcriptional regulation of homeoprotein target genes. In this review, we describe the different techniques used to study Hox protein-protein interactions. These novel fluorescent techniques can be used to verify these interactions in living cells and further analyze them in model organisms to elucidate functional implications of these interactions *in vivo*. As we discover more Hox interacting partners, these techniques will help us determine the essential role of protein-protein interactions within the interactome networks to control cellular functions and morphogenesis and organogenesis *in vivo*.

Protein-protein interactions, BiFC, FRET, Fluorescent techniques, Hox interactome, Cofactors, Transcription regulation, Homeodomain, Development

Resumen

Los genes Hox son reguladores maestros del desarrollo que contienen al “homeobox”, una región altamente conservada de 180 pares de bases. El “homeobox” codifica a una región de 60 aminoácidos llamada homeodominio, la cual interacciona con el ADN para regular la expresión genética con alta especificidad. El mecanismo de cómo el homeodominio logra este alto nivel de especificidad es una de las grandes preguntas en biología del desarrollo. Además de interaccionar con el ADN, el homeodominio también interacciona con factores de transcripción, cofactores, y otras proteínas que regulan el desarrollo. Estas interacciones proteína-proteína son necesarias para entender las funciones y regulación transcripcional de los genes blanco de las homeoproteínas. En esta revisión, describimos las diferentes técnicas utilizadas para estudiar las interacciones proteína-proteína de Hox. Estas novedosas técnicas fluorescentes pueden utilizarse para verificar las interacciones en células vivas y analizarlas en organismos modelo para elucidar las implicaciones funcionales de estas interacciones *in vivo*. Con el descubrimiento de más colaboradores que interaccionan con Hox, estas técnicas nos ayudarán a determinar el papel esencial de las interacciones proteína-proteína dentro de las redes del interactoma que controlan las funciones celulares, la morfogénesis y organogénesis *in vivo*.

Interacciones proteína-proteína, BiFC, FRET, Técnicas fluorescentes, interactoma Hox, Cofactores, Regulación de la transcripción, Homeodominio, Desarrollo

1.1 Introduction

Hox genes are a family of transcription factors (TFs) with a key role as master regulators of development, responsible for giving identity to the segments of the anteroposterior (A-P) axis of bilateral organisms (Lewis *et al*., 1978; Mann and Morata, 2000). All the homeotic genes share a highly conserved region of 180 base pairs (bp) called the homeotic box or "homeobox" (McGinnis *et al*., 1984, Scott & Weiner, 1984) that encodes a 60–amino acid DNA-binding domain known as the homeodomain (HD) (Gehring, 1987). The HD’s tridimensional structure consisting of three alpha-helixes allows it to bind to DNA, specifically through helix III—the recognition helix—that contains short regions rich in A-T present in the major groove of DNA (Svingen & Tonissen, 2006, Mann *et al*., 2009).

However, considering that the HD of all homeoproteins is highly similar and that the DNA regions to which they bind are also present multiple times throughout the entire genome. In addition, some Hox proteins bind cooperatively to chromatin (Arunachalam, *et al*., 2022; Latham & Zhang, 2022). It is therefore difficult to imagine how each of the homeoproteins is capable of specifically regulating target genes for the development of the segments along the A-P axis of the different organisms. This question is known as the “Hox paradox” (Prince *et al*., 2008; Hueber & Lohman, 2008).

Many transcriptional factors that interact with homeoproteins have been described in the complete map of protein interactions called the "Hox interactome" (Baëza *et al*., 2015). Protein-protein (PPI) interactions became relevant when it was determined that Extradenticle (Exd) can interact with homeoproteins through the YPWM motif, improving the specificity of DNA binding site compared to its monomeric form (Shanmugam *et al*.,1997; Joshi *et al*.,2007). Exd dimeric interaction with homeoproteins like Abdominal A (abdA), Ultrabithorax (Ubx), Sex combs reduced (Scr), and Antennapedia (Antp) (Passner *et al*.,1999; Joshi *et al*., 2007; Papadopoulos et al., 2011) increase the specificity of homeoproteins. Homothorax (Hth), another Hox cofactor that establishes interaction with homeoproteins, also interacts with Exd to allow active nuclear export (Rieckhof *et al*., 1997; Ryoo *et al*.,1999). Both cofactors interact with homeoproteins, forming trimeric Hox-Exd-Hth complexes that improve specificity, allowing the activation or repression of different genes. For example, Ubx-Exd-Hth and AbdA-Exd-Hth trimers can activate or repress transcription depending on the cis-regulatory module (CRM) to which it binds. (Merabet *et al*.,2007; Delker *et al*.,2019 Zandvakili *et al*., 2019). Although these trimeric complexes between homeoproteins with cofactors increase specificity, it is not enough to explain the transcriptional regulation given by homeoproteins.

To specify cellular identity, homeoproteins interact with cofactors such as Exd, but also with general transcription factors (GTF) that confer specificity. The first link of functional contact with a GTF found in *Drosophila* was between Antp and BIP2 (TAFII155, TAF3), a member of the TFIID complex (Prince *et al*., 2008). Other homeoprotein interactions include components of Pol II machinery, Med19 from the Mediator (MED) complex, and the transcription-pausing factor M1BP and TFIIEβ (Boube *et al*., 2014; Zouaz *et al*., 2019; Baëza *et al*., 2015). These interactions demonstrate Hox-driven transcription, but the molecular mechanisms behind transcriptional regulation remain elusive.

1.2 Analysis of protein-protein interactions

Protein-protein interactions (PPIs) are necessary to understand the functions and transcriptional regulation of homeoprotein target genes. Several techniques are used to study protein-protein interactions *in vitro*; of these, Co-IP, pull-down assays, affinity purification coupled to mass spectrometry (TAP-MS), and yeast two-hybrid have been used to study the Hox interactome and are described below.

In Co-IP, the target protein is recognized by a specific antibody that has been immobilized to a support, which is then used to co-precipitate the antibody-protein complex from the cell lysate. The complexes are detected and identified by western blot analysis or mass spectrometry (Free *et al*., 2009). Interactomes of the Hox proteins Abd-A, Antp, Scr and Ubx have been validated by Co-IP experiments (Baëza *et al*., 2015). Ubx partners have also been identified from nuclear extracts of embryos (Carnesecchi *et al*., 2020).

In pull-down assays, the detection system consists of a glutathione S-transferase (GST)-, polyHis- or streptavidin-tagged protein that is captured by agarose beads coated with the tag-specific ligand. The immobilized fusion-tagged protein captures its putative interacting partner from a cell lysate; the complexes are selectively eluted for in-gel or western blot analysis (Brymora *et al*., 2004). A great number of Hox PPIs have been identified by pull-down assays including cofactors, GTFs and other Hox proteins (Emili *et al*., 1994; Zhu and Kuziora 1996; Rieckhoff *et al*., 1997).

The TAP-MS assays require two tags instead of one in a sequential manner; typically, a combination of FLAG and HA peptides are used as affinity tags (Rigaut *et al*., 1999; Nakatani and Ogryzko 2003). In the first affinity step, the TAP-tagged protein is expressed in cells for association with its endogenous partners. In the second step, the complexes formed are purified by interaction with the corresponding tag ligand using immunoglobulins anchored on agarose beads. Once recovered, protein complexes can be processed for direct analysis by mass spectrometry (MS) or separated by SDS-PAGE for reducing sample complexity before MS analysis (Dunham *et al*., 2012; Adelmant *et al*., 2019). This approach has been used to capture lineage-specific Ubx partners at the subcellular level (Carnesecchi *et al*., 2020). Also, the interactome of the Hox cofactor Meis1a was analyzed using TAP-MS in absence or presence of its regulator Prep1 to gain insight into its oncogenic activity (Dardaei *et al*., 2014).

The yeast two-hybrid (Y2H) assay allows the identification of PPIs using the yeast Gal4 transcription factor. The DNA-binding domain and activation domain of Gal4 are fused to two proteins of interest. If both proteins interact, Gal4 transcription factor becomes functional, activating the expression of reporter genes under the control of the UAS (*GAL* promoter). This assay is used to confirm the interaction between two proteins of interest and discover novel PPIs (Fields and Song 1989). Y2H screenings identified Ubx interacting proteins like TFs and cell signaling regulators (Bondos et al., 2006). Another example is the identification of the homeodomain-interacting protein kinases as a novel family of Hox co-repressors that differentially interact with homeoproteins in living cells (Kim et al., 1998).

Overall, these *in vitro* techniques are very popular for PPI detection and could be used in large-screening approaches. However, there are some drawbacks that must be considered when choosing the most appropriate technique, because these methods rely on indirect detection of the PPI or require disruption of the cells. Some PPIs are transient or weak, or require a specific cellular environment, giving false positive or false negative results; in other words, only strong and stable PPIs can be detected. Also, since these methodologies require lysis of the cell, the compartment in which the PPI occurs cannot be determined.

Fluorescent labeling techniques can be used to detect protein-protein interactions in live conditions and visualize the location where they occur within the cell, allowing us to better understand protein function *in vivo*. For example, fluorescent fusion proteins have been used to visualize gene expression of the Hox locus at the subnuclear level in *Drosophila* imaginal discs (Delker *et al.*, 2022). Some techniques used to analyze PPIs are fluorescence anisotropy, fluorescence correlation spectroscopy (FCS), fluorescence lifetime image microscopy (FLIM) and photonic crystal (PC) biosensors. The most commonly used techniques to study PPIs are Bimolecular fluorescent complementation (BIFC), Förster resonance energy transfer (FRET), competitive BiFC, and the combined BiFC-FRET.

Bimolecular fluorescence complementation (BiFC) relies on a visible fluorescent signal. This assay is based on complementation between two fragments of a fluorescent protein that are each fused to a protein of interest. The interaction between these proteins brings the fragments together and reconstitutes the fluorescence, indicating protein-protein interaction (Figure 1). The first fluorescent protein used in complementation assays was the green fluorescent protein (GFP); now there are various GFP-derivatives such as the YFP, Venus or Cerulean (Hu *et al.*, 2002; Hu and Kerppola, 2003; Shyu *et al.*, 2006), red fluorescent variants like mRFP1 (Jach *et al.*, 2006) and lately the near infrared fluorescent protein iRFP (Chen *et al.*, 2015). Venus has been used to determine Antp-TFIIEβ interaction, showing a direct physical interaction of TFIIEβ with two aminoacidic positions on helix 2 of the Antp HD that is required for the ectopic function of Antp in thorax and antenna-to-tarsus transformations. Antp-TFIIEβ interaction showed the important relationship between Hox proteins and the general transcription machinery for transcriptional regulation (Altamirano-Torres *et al*., 2018).

Figure 1 Schematic representation of BIFC. Venus fragments (VN AND VC) are fused to A and B proteins of interest. The interaction of A and B proteins brings the Venus fragments together and enables Venus fluorescence, indicating an interaction between A and B

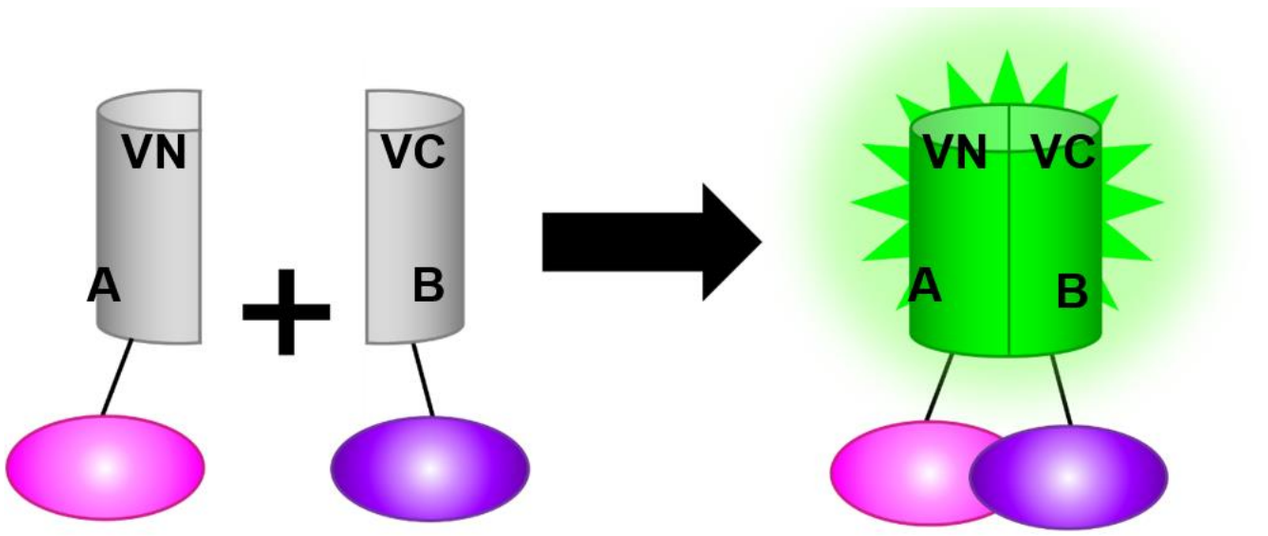

BiFC has been used successfully in yeast (Sung *et al*., 2013), plants (Lee *et al*., 2012), mammalian cells (Lee *et al*., 2011) and insects like *Drosophila melanogaster* (Plaza *et al*., 2008) allowing us to study PPIs in a tissue- and developmental stage–specific manner *in vivo*. Its main advantage is that the complementation between the two fragments causes covalent junctions, leading to the stabilization of the protein complex. Although it is not possible to monitor the temporal dynamics of PPIs, BiFC allows detection of transient and weak interactions that occur simultaneously, combining peptides of different fluorescent proteins (multicolor BiFC) (Bischof *et al*., 2018). This assay was applied to detect interactions in living embryos in *Drosophila* (Hudry *et al*., 2011) and to create a BiFC library consisting of a collection UAS-ORF fly lines that allows the simultaneous detection of PPIs in living embryos. This multicolor BiFC library is updated constantly and aims to cover all *Drosophila* TFs in the near future (Bischof *et al*., 2013).

Förster resonance energy transfer (FRET) is another method that enables the detection of interactions *in vivo.* FRET can measure the proximity between two fluorophores that are fused to interest proteins, upon excitation. The energy transfer between a donor and an acceptor molecule should occur within a small distance (less than 10 nm) to validate the close proximity between interest proteins and hence the interaction between them (Shyu, *et al.*, 2006, Truong & Ikura, 2001, Parsons *et al.*, 2004, Kenworthy, 2001). The efficiency of the energy transfer refers to donor excitation that results in energy transfer to the acceptor, thus the donor emission decreases whereas the acceptor emission increases, indicating PPI (Figure 2). A variation of FRET is BRET (bioluminescence resonance energy transfer), where a light-emitting enzyme (luciferase) is used as a donor, and a fluorescent protein is used as an acceptor (Harikumar *et al.*, 2017).

Figure 2 Schematic representation of FRET. Donor (CFP) is fused to protein A and acceptor (YFP), to protein B. When the donor is excited, energy is transferred to the acceptor, decreasing the donor's fluorescence, and indicating A and B interaction

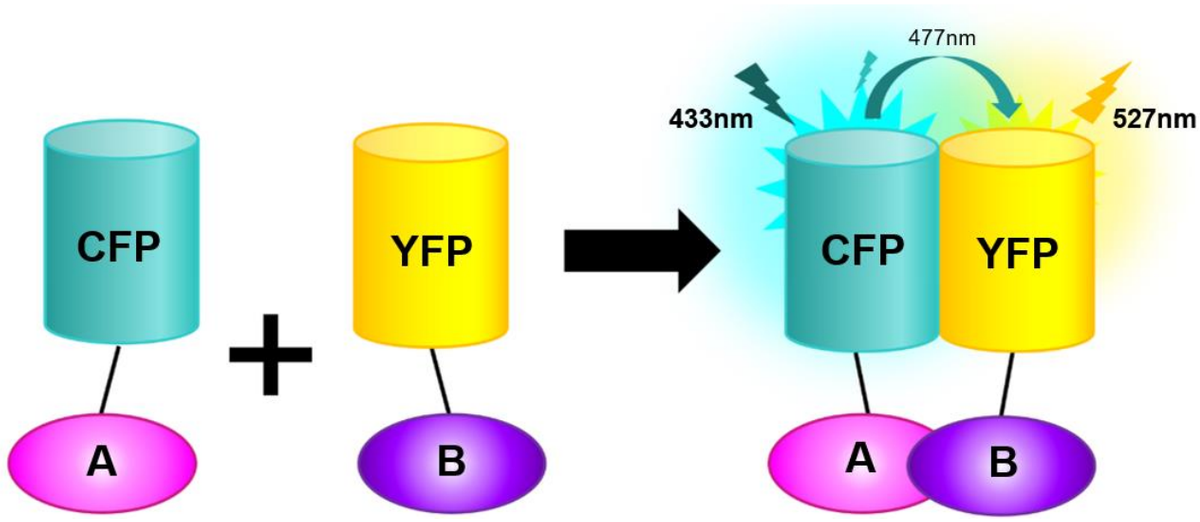

In FRET, the most commonly used fluorescent proteins are CFP and YFP, although the YFP mutant Venus and the CFP mutant Cerulean have been used successfully, showing better properties for live-cell imaging. These techniques require high levels of protein expression as well as specific interfaces to reliably interpret the few emitted signals and therefore cannot be used for large-scale applications.

BiFC and FRET assays allow the detection of dimeric interactions, and multicolor BiFC can detect several dimers simultaneously; detecting trimeric complexes, however, has proved to be a challenging task. In 2004, Galperin et al., developed a three chromophore–based FRET system that can measure the signals of three donor-acceptor pairs, such as CFP-YFP, CFP-mRFP and YFP-mRFP *in vitro* and *in vivo*, and can be used to visualize trimeric complexes in cells, but required sophisticated optical setup and data process.

One approach to indirectly detect possible candidates for trimeric interactions are competition experiments. Here, a “cold” competitive partner (not fused to a fluorescent protein fragment) is co-expressed with proteins fused to the amino and carboxyl ends of fluorophore, expecting a decrease in dimeric interaction (Baëza *et al*., 2015). An example is shown in Figure 3, where Antp and TFIIEβ interact in HEK293 cells, giving an interaction of 81%. When the “cold” proteins (TBP, BIP2 and EXD) were co-transfected with the Antp/TFIIEβ complex the interaction decreased, indicating the possible formation of trimeric interactions with these transcriptional factors.

Figure 3 Antp-TFIIEβ interaction is affected by TBP, BIP2 and Exd in competitive BiFC assays. The co-expression of Antp and TFIIEβ with TBP, BIP2 and Exd. A) Green fluorescence indicates the protein-protein interaction of Antp with TFIIEβ in 81% of the transfected cells. B) The addition of TFs to Antp-TFIIEβ decreased the interaction to 56% in TBP, 43% in BIP2 and 49% in Exd. pCAG-mCherry was used as an internal control for transfection

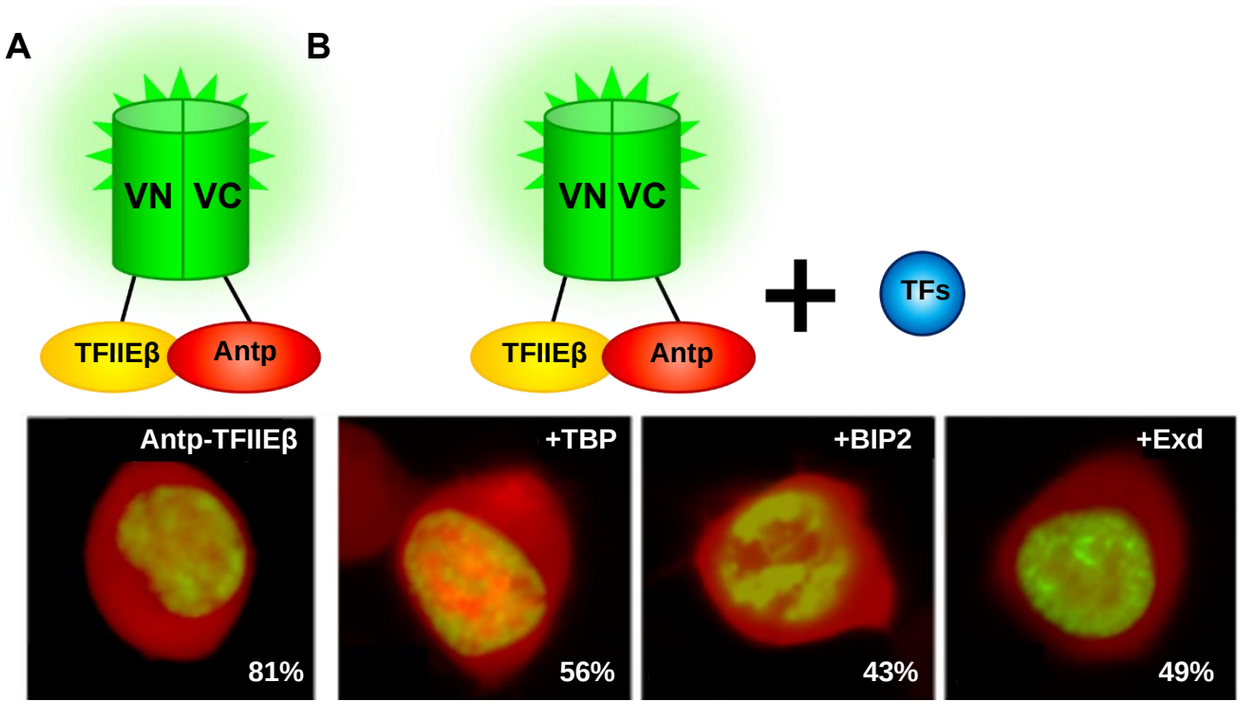

A better option to detect trimeric complexes directly is the combination of BiFC and FRET (BiFC-FRET) using Venus and Cerulean fluorescent proteins for visualization of trimeric complexes in living cells (Shyu *et al.,* 2008), avoiding the use of three chromophores. BiFC allows reconstitution of a fluorescent protein (with proteins of interest fused to the fragments) and can be used as a donor, plus Cerulean fused to another protein used as an acceptor. An example of BiFC-FRET being used to detect a trimeric interaction between p65-Jun-Fos is observed in Figure 4.

Figure 4 P65-Jun-Fos trimeric interaction by BiFC-FRET. (A) Schematic representation of p65 fused to Cerulean (Cerulean Channel), BiFC by Jun-Fos interaction (Venus channel) and energy transfer due to p65-Jun-Fos trimeric complex (FRET). Modified from Jiménez-Mejía *et al.*, 2018

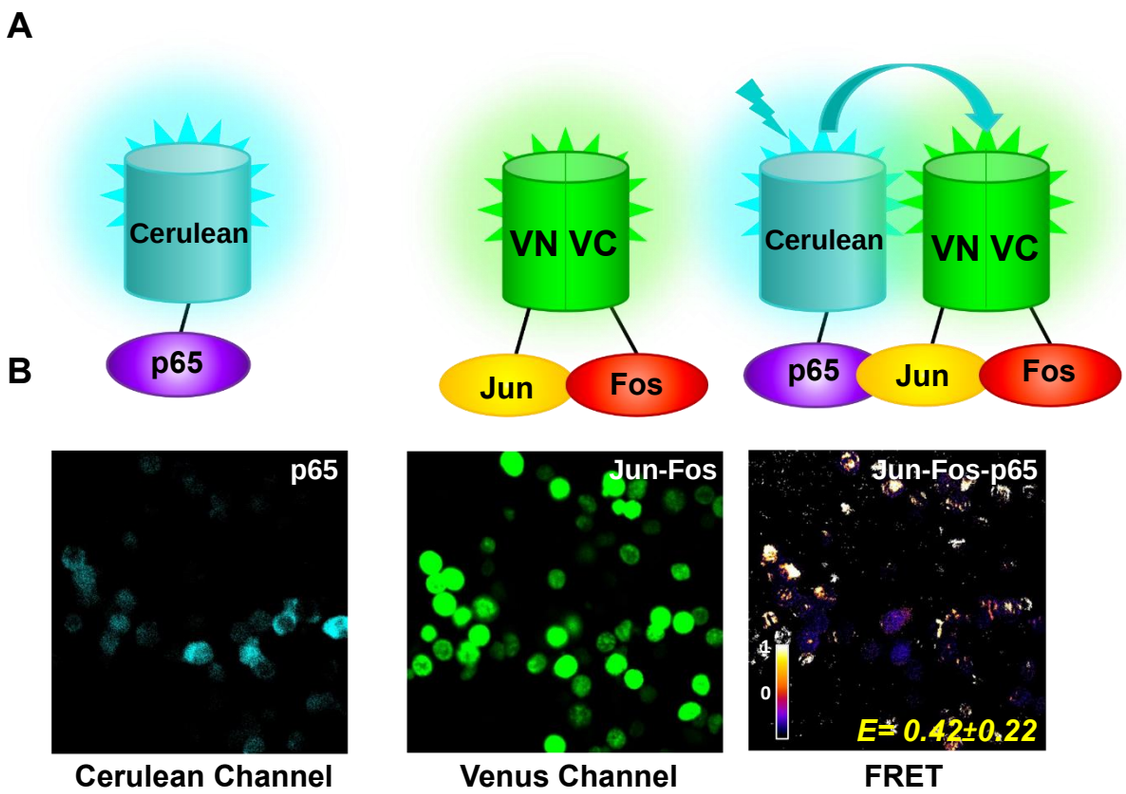

In summary, *in vivo* approaches enable detection of PPIs in their normal environment without disrupting the cell, and allowing their visualization and localization, all important aspects to determine their function during development. Moreover, these techniques can determine key interacting domains that could be useful, not only to elucidate function, but to find ways to disrupt interactions involved in pathologies such as cancer. These next-generation therapeutic approaches have been successfully used to disrupt the interaction between HOX proteins and their co-factors in neoplasms such as glioblastoma multiforme, leukemia and other neoplasms (Morgan *et al*., 2017; Arunachalam, *et al*., 2022).

1.3 Acknowledgements

We thank Consejo Nacional de Ciencia y Tecnologia (CONACyT) and Programa de Apoyo a la Investigación en Ciencia y Tecnología (PAICyT) for financial support.

1.4 Funding

The present work was financed by CONACYT, project number CF-2019-2280 and PAICyT project number CN1558-21. AVP received the scholarship number 717425 and CHB, scholarship number 790953.

1.5 Conclusion

Proteins control basically all biological systems; they rarely act alone and most of them interact with others to perform their biological activity in the cell. Protein-protein interactions are the physical contacts with molecular docking between proteins that allow them to achieve their biological functions both at cellular and organism level, integrating the so-called interactome. In this review we analyze how methods such as co-immunoprecipitation, pull-down assays, BiFC, FRET and BIFC can be used to analyze the PPIs of Hox proteins in order to understand the Hox interactome. These novel fluorescent techniques present the advantage to verify these interactions in living cells and further analyze them in whole in model organisms to elucidated functional implications of these interactions *in vivo.*

Although we have made significant progress in the study of Hox interacting partners to understand how multimeric complexes between homeoproteins and cofactors increase the specificity of transcriptional regulation to specify cellular identity, we still possess a limited understanding of how Hox PPIs control cellular functions and morphogenesis and organogenesis *in vivo*.

Moreover, data published in recent years with efficient large-scale technologies that measure proteome-wide physical connections produced a large collection of PPI databases that are available in public repositories. All these PPIs complexes should be analyzed in an adequate biological context to determine their essential role to build and analyze interactome networks.

1.6 References

Adelmant, G., Garg, B. K., Tavares, M., Card, J. D., & Marto, J. A. (2019). Tandem Affinity Purification and Mass Spectrometry (TAP-MS) for the Analysis of Protein Complexes. *Current protocols in protein science*, *96*(1), e84. DOI:10.1002/cpps.84
URL: currentprotocols.onlinelibrary.wiley.com/doi/10.1002/cpps.84

Altamirano-Torres, C., Salinas-Hernández, J. E., Cárdenas-Chávez, D. L., Rodríguez-Padilla, C., & Reséndez-Pérez, D. (2018). Transcription factor TFIIEβ interacts with two exposed positions in helix 2 of the Antennapedia homeodomain to control homeotic function in *Drosophila*. *Plos one*, *13*(10), e0205905. DOI:10.1371/journal.pone.0205905
URL: journals.plos.org/plosone/article?id=10.1371/journal.pone.0205905

Arunachalam, E., Rogers, W., Simpson, G. R., Möller-Levet, C., Bolton, G., Ismael, M., ... & Pandha, H. (2022). HOX and PBX gene dysregulation as a therapeutic target in glioblastoma multiforme. *BMC cancer*, *22*(1), 1-13. DOI: 10.1186/s12885-022-09466-8
URL: bmccancer.biomedcentral.com/articles/10.1186/s12885-022-09466-8
Baëza, M., Viala, S., Heim, M., Dard, A., Hudry, B., Duffraisse, M., ... & Merabet, S. (2015). Inhibitory activities of short linear motifs underlie Hox interactome specificity *in vivo*. Elife, 4, e06034. DOI: 10.7554/eLife.06034
URL: elifesciences.org/articles/06034

Bischof, J., Björklund, M., Furger, E., Schertel, C., Taipale, J., & Basler, K. (2013). A versatile platform for creating a comprehensive UAS-ORFeome library in Drosophila. *Development*, *140*(11), 2434-2442. DOI: 10.1242/dev.088757
URL: journals.biologists.com/dev/article/140/11/2434/45737/A-versatile-platform-for-creating-a-comprehensive

Bischof, J., Duffraisse, M., Furger, E., Ajuria, L., Giraud, G., Vanderperre, S., ... & Merabet, S. (2018). Generation of a versatile BiFC ORFeome library for analyzing protein–protein interactions in live Drosophila. *Elife*, *7*, e38853. DOI: 10.7554/eLife.38853
URL: journals.biologists.com/dev/article/140/11/2434/45737/A-versatile-platform-for creating-a-comprehensive

Brymora, A., Valova, V. A., & Robinson, P. J. (2004). Protein-protein interactions identified by pull-down experiments and mass spectrometry. Current protocols in cell biology, 22(1), 17-5. DOI: 10.1002/0471143030.cb1705s22
URL: currentprotocols.onlinelibrary.wiley.com/doi/10.1002/0471143030.cb1705s22

Bondos, S. E., Tan, X. X., & Matthews, K. S. (2006). Physical and genetic interactions link hox function with diverse transcription factors and cell signaling proteins. *Molecular & Cellular Proteomics*, *5*(5), 824-834. DOI: 10.1074/mcp.M500256-MCP200
URL: www.sciencedirect.com/science/article/pii/S1535947620303303?via%3Dihub

Boube, M., Hudry, B., Immarigeon, C., Carrier, Y., Bernat-Fabre, S., Merabet, S., ... & Cribbs, D. L. (2014). *Drosophila melanogaster* Hox transcription factors access the RNA polymerase II machinery through direct homeodomain binding to a conserved motif of mediator subunit Med19. PLoS genetics, 10(5), e1004303. DOI: 10.1371/journal.pgen.1004303
URL: journals.plos.org/plosgenetics/article?id=10.1371/journal.pgen.1004303

Carnesecchi, J., Sigismondo, G., Domsch, K. *et al.* Multi-level and lineage-specific interactomes of the Hox transcription factor Ubx contribute to its functional specificity. *Nat Commun* 11, 1388 (2020). DOI:10.1038/s41467-020-15223-x
URL: www.nature.com/articles/s41467-020-15223-x

Chen, M., Li, W., Zhang, Z., Liu, S., Zhang, X., Zhang, X. E., & Cui, Z. (2015). Novel near-infrared BiFC systems from a bacterial phytochrome for imaging protein interactions and drug evaluation under physiological conditions. *Biomaterials*, *48*, 97-107. DOI: 10.1016/j.biomaterials.2015.01.038
URL: www.sciencedirect.com/science/article/abs/pii/S0142961215000551?via%3Dihub

Dardaei, L., Longobardi, E., & Blasi, F. (2014). Prep1 and Meis1 competition for Pbx1 binding regulates protein stability and tumorigenesis. *Proceedings of the National Academy of Sciences*, *111*(10), E896-E905. DOI:10.1073/pnas.1321200111
URL: www.pnas.org/doi/full/10.1073/pnas.1321200111

Delker, R. K., Ranade, V., Loker, R., Voutev, R., & Mann, R. S. (2019). Low affinity binding sites in an activating CRM mediate negative autoregulation of the *Drosophila* Hox gene Ultrabithorax. PLoS genetics, 15(10), e1008444. DOI: 10.1371/journal.pgen.1008444
URL: journals.plos.org/plosgenetics/article?id=10.1371/journal.pgen.1008444

Delker, R. K., Munce, R. H., Hu, M., & Mann, R. S. (2022). Fluorescent labeling of genomic loci in *Drosophila* imaginal discs with heterologous DNA-binding proteins. Cell reports methods, 2(3), 100175. DOI: 10.1016/j.crmeth.2022.100175
URL: https://pubmed.ncbi.nlm.nih.gov/35475221/

Dunham, W. H., Mullin, M., & Gingras, A. C. (2012). Affinity-purification coupled to mass spectrometry: Basic principles and strategies. Proteomics, 12(10), 1576-1590.
DOI: 10.1039/C9EE00596J
URL: analyticalsciencejournals.onlinelibrary.wiley.com/doi/full/10.1002/pmic.201100523

Emili A, Greenblatt J, Ingles CJ. Species-specific interaction of the glutamine-rich activation domains of Sp1 with the TATA box-binding protein. Mol Cell Biol. 1994;14(3):1582–93
DOI: 10.1128/mcb.14.3.1582-1593.1994
URL: pubmed.ncbi.nlm.nih.gov/8114696/

Fields, S., & Song, O. K. (1989). A novel genetic system to detect protein–protein interactions. *Nature*, *340*(6230), 245-246. DOI: 10.1038/340245a0
URL: www.nature.com/articles/340245a0

Free, R. B., Hazelwood, L. A., & Sibley, D. R. (2009). Identifying novel protein-protein interactions using co-immunoprecipitation and mass spectroscopy. Current protocols in neuroscience, 46(1), 5-28. DOI: 10.1002/0471142301.ns0528s46
URL: currentprotocols.onlinelibrary.wiley.com/doi/abs/10.1002/0471142301.ns0528s46

Galperin, E., Verkhusha, V. V., & Sorkin, A. (2004). Three-chromophore FRET microscopy to analyze multiprotein interactions in living cells. *Nature methods*, *1*(3), 209-217. DOI: 10.1038/nmeth720
URL: www.nature.com/articles/nmeth720#citeas

Gehring, W. J. (1987). Homeo boxes in the study of development. Science, 236(4806), 1245-1252. DOI: 10.1126/science.2884726
URL: pubmed.ncbi.nlm.nih.gov/2884726/

Harikumar, K. G., Yan, Y., Xu, T. H., Melcher, K., Xu, H. E., & Miller, L. J. (2017). Bioluminescence resonance energy transfer (BRET) assay for determination of molecular interactions in living cells. *Bio-protocol*, *7*(22). DOI:10.21769/BioProtoc.2904
URL: bio-protocol.org/e2904

Hu, C. D., Chinenov, Y., & Kerppola, T. K. (2002). Visualization of interactions among bZIP and Rel family proteins in living cells using bimolecular fluorescence complementation. *Molecular cell*, *9*(4), 789-798. DOI: 10.1016/S1097-2765(02)00496-3
URL: https://pubmed.ncbi.nlm.nih.gov/11983170/

Hu, C. D., & Kerppola, T. K. (2003). Simultaneous visualization of multiple protein interactions in living cells using multicolor fluorescence complementation analysis. *Nature biotechnology*, *21*(5), 539-545. doi:10.1038/nbt816 URL: www.nature.com/articles/nbt816

Hudry, B., Viala, S., Graba, Y., & Merabet, S. (2011). Visualization of protein interactions in living *Drosophila* embryos by the bimolecular fluorescence complementation assay. *BMC biology*, *9*(1), 1-18. DOI:10.1186/1741-7007-9-5
URL: bmcbiol.biomedcentral.com/articles/10.1186/1741-7007-9-5

Hueber, S. D., & Lohmann, I. (2008). Shaping segments: Hox gene function in the genomic age. Bioessays, 30(10), 965-979. DOI: 10.1002/bies.20823
URL: onlinelibrary.wiley.com/doi/10.1002/bies.20823

Jach, G., Pesch, M., Richter, K., Frings, S., & Uhrig, J. F. (2006). An improved mRFP1 adds red to bimolecular fluorescence complementation. *Nature methods*, *3*(8), 597-600. DOI: 10.1038/nmeth901
URL: www.nature.com/articles/nmeth901

Jiménez Mejía, G. (2018). *Interacciones triméricas del complejo Antp-TBP con los factores TFIIEβ, BIP2 y la homeoproteína Exd* (Doctoral dissertation, Universidad Autónoma de Nuevo León).
URL: eprints.uanl.mx/17715/

Kenworthy, A. K. (2001). Imaging protein-protein interactions using fluorescence resonance energy transfer microscopy. *Methods*, *24*(3), 289-296. DOI: 10.1006/meth.2001.1189
URL: www.sciencedirect.com/science/article/abs/pii/S1046202301911892?via%3Dihub

Kim, Y. H., Choi, C. Y., Lee, S. J., Conti, M. A., & Kim, Y. (1998). Homeodomain-interacting protein kinases, a novel family of co-repressors for homeodomain transcription factors. *Journal of Biological Chemistry*, *273*(40), 25875-25879. DOI: 10.1074/jbc.273.40.25875
URL: www.sciencedirect.com/science/article/pii/S0021925819599008?via%3Dihub

Joshi, R., Passner, J. M., Rohs, R., Jain, R., Sosinsky, A., Crickmore, M. A., ... & Mann, R. S. (2007). Functional specificity of a Hox protein mediated by the recognition of minor groove structure. Cell, 131(3), 530-543. DOI: 10.1016/j.cell.2007.09.024
URL: www.sciencedirect.com/science/article/pii/S0092867407012123?via%3Dihub

Lee OH, Kim H, He Q, Baek HJ, Yang D, Chen LY, Liang J, Chae HK, Safari A, Liu D, Songyang Z. 2011. Genomewide YFP fluorescence complementation screen identifies new regulators for telomere signaling in human cells. Molecular & Cellular Proteomics 10:M110.001628. PMID: 21044950
DOI: 10.1074/mcp.M110.001628
URL: www.sciencedirect.com/science/article/pii/S1535947620328012?via%3Dihub

Lee LY, Wu FH, Hsu CT, Shen SC, Yeh HY, Liao DC, Fang MJ, Liu NT, Yen YC, Dokla´ dal L, Sykorova´ E, Gelvin SB, Lin CS. 2012. Screening a cDNA library for protein-protein interactions directly in planta. The Plant Cell 24: 1746–1759., PMID: 22623495 DOI: 10.1105/tpc.112.097998
URL: academic.oup.com/plcell/article/24/5/1746/6097375

Lewis, E. B. (1978). A gene complex controlling segmentation in *Drosophila*. In Genes, development and cancer (pp. 205-217). Springer, Boston, MA. DOI: 10.1007/978-1-4419-8981-9_13
URL: link.springer.com/chapter/10.1007/978-1-4419-8981-9_13

Mann, R. S., and Morata, G. (2000). The developmental and molecular biology of genes that subdivide the body of *Drosophila*. Annual review of cell and developmental biology, 16(1), 243-271.
DOI: 10.1146/annurev.cellbio.16.1.243
URL: www.annualreviews.org/doi/10.1146/annurev.cellbio.16.1.243

Mann, R. S., Lelli, K. M., & Joshi, R. (2009). Hox specificity: unique roles for cofactors and collaborators. Current topics in developmental biology, 88, 63-101.
DOI:10.1016/S0070-2153(09)88003-4
URL: www.sciencedirect.com/science/article/abs/pii/S0070215309880034?via%3Dihub

Merabet, S., Saadaoui, M., Sambrani, N., Hudry, B., Pradel, J., Affolter, M., & Graba, Y. (2007). A unique Extradenticle recruitment mode in the *Drosophila* Hox protein Ultrabithorax. Proceedings of the National Academy of Sciences, 104(43), 16946-16951. DOI: 10.1073/pnas.0705832104
URL: www.pnas.org/doi/full/10.1073/pnas.0705832104

McGinnis, W., Garber, R. L., Wirz, J., Kuroiwa, A., & Gehring, W. J. (1984). A homologous protein-coding sequence in *Drosophila* homeotic genes and its conservation in other metazoans. Cell, 37(2), 403-408. DOI: 10.1016/0092-8674(84)90370-2
URL: www.sciencedirect.com/science/article/abs/pii/0092867484903702?via%3Dihub

Morgan, R., El-Tanani, M., Hunter, K. D., Harrington, K. J., & Pandha, H. S. (2017). Targeting HOX/PBX dimers in cancer. *Oncotarget*, *8*(19), 32322. DOI: 10.18632/oncotarget.15971
URL: www.ncbi.nlm.nih.gov/pmc/articles/PMC5458287/

Nakatani Y, Ogryzko V. Immunoaffinity purification of mammalian protein complexes. Methods Enzymol. 2003; 370: 430-44. PMID: 14712665. DOI: 10.1016/S0076-6879(03)70037-8
URL: www.sciencedirect.com/science/article/abs/pii/S0076687903700378

Papadopoulos, D. K., Reséndez-Pérez, D., Cárdenas-Chávez, D. L., Villanueva-Segura, K., Canales-del-Castillo, R., Felix, D. A., ... & Gehring, W. J. (2011). Functional synthetic Antennapedia genes and the dual roles of YPWM motif and linker size in transcriptional activation and repression. Proceedings of the National Academy of Sciences, 108(29), 11959-11964. DOI:10.1073/pnas.1108686108
URL: www.pnas.org/doi/full/10.1073/pnas.1108686108

Parsons, M., Vojnovic, B., & Ameer-Beg, S. (2004). Imaging protein–protein interactions in cell motility using fluorescence resonance energy transfer (FRET). *Biochemical Society Transactions*, *32*(3), 431-433. DOI: 10.1042/bst0320431
URL: www.pnas.org/doi/full/10.1073/pnas.1108686108

Passner, J. M., Ryoo, H. D., Shen, L., Mann, R. S., & Aggarwal, A. K. (1999). Structure of a DNA-bound Ultrabithorax–Extradenticle homeodomain complex. Nature, 397(6721), 714-719. DOI: 10.1038/17833
URL: www.nature.com/articles/17833

Plaza, S., Prince, F., Adachi, Y., Punzo, C., Cribbs, D. L., & Gehring, W. J. (2008). Cross-regulatory protein–protein interactions between Hox and Pax transcription factors. *Proceedings of the National Academy of Sciences*, *105*(36), 13439-13444. DOI: 10.1073/pnas.0806106105
URL: www.pnas.org/doi/abs/10.1073/pnas.0806106105

Prince, F., Katsuyama, T., Oshima, Y., Plaza, S., Resendez-Perez, D., Berry, M., ... & Gehring, W. J. (2008). The YPWM motif links Antennapedia to the basal transcriptional machinery.
DOI: 10.1242/dev.018028
URL: journals.biologists.com/dev/article/135/9/1669/64942/The-YPWM-motif-links-Antennapedia-to-the-basal

Rieckhof, G. E., Casares, F., Ryoo, H. D., Abu-Shaar, M., & Mann, R. S. (1997). Nuclear translocation of extradenticle requires homothorax, which encodes an extradenticle-related homeodomain protein. Cell, 91(2), 171-183. DOI: 10.1016/S0092-8674(00)80400-6
URL: www.sciencedirect.com/science/article/pii/S0092867400804006?via%3Dihub

Rigaut G, Shevchenko A, Rutz B, Wilm M, Mann M, Séraphin B. A generic protein purification method for protein complex characterization and proteome exploration. Nat Biotechnol. 1999 Oct; 17 (10):1030-2. DOI: 10.1038/13732
URL: www.nature.com/articles/nbt1099_1030

Ryoo, H. D., Marty, T., Casares, F., Affolter, M., & Mann, R. S. (1999). Regulation of Hox target genes by a DNA bound Homothorax/Hox/Extradenticle complex. Development, 126(22), 5137-5148. DOI: 10.1242/dev.126.22.5137
URL: journals.biologists.com/dev/article/126/22/5137/40556/Regulation-of-Hox-target-genes-by-a-DNA-bound

Shanmugam, K., Featherstone, M. S., & Saragovi, H. U. (1997). Residues flanking the HOX YPWM motif contribute to cooperative interactions with PBX. Journal of Biological Chemistry, 272(30), 19081-19087. DOI: 10.1074/jbc.272.30.19081
URL: www.sciencedirect.com/science/article/pii/S0021925818390914?via%3Dihub

Shyu, Y. J., Liu, H., Deng, X., & Hu, C. D. (2006). Identification of new fluorescent protein fragments for bimolecular fluorescence complementation analysis under physiological conditions. Biotechniques, 40(1), 61-66. DOI: 10.2144/000112036
URL: www.future-science.com/doi/10.2144/000112036

Shyu, Y. J., Suarez, C. D., & Hu, C. D. (2008). Visualization of AP-1–NF-κB ternary complexes in living cells by using a BiFC-based FRET. *Proceedings of the National Academy of Sciences*, *105*(1), 151-156. DOI: 10.1073/pnas.0705181105
URL: www.pnas.org/doi/abs/10.1073/pnas.0705181105

Scott, M. P., & Weiner, A. J. (1984). Structural relationships among genes that control development: sequence homology between the Antennapedia, Ultrabithorax, and fushi tarazu loci of *Drosophila*. Proceedings of the National Academy of Sciences, 81(13), 4115-4119. DOI: 10.1073/pnas.81.13.4115
URL: www.pnas.org/doi/abs/10.1073/pnas.81.13.4115

Sung, M. K., Lim, G., Yi, D. G., Chang, Y. J., Yang, E. B., Lee, K., & Huh, W. K. (2013). Genome-wide bimolecular fluorescence complementation analysis of SUMO interactome in yeast. *Genome research*, *23*(4), 736-746. DOI:10.1101/gr.148346.112.
URL: genome.cshlp.org/content/23/4/736

Svingen, T., & Tonissen, K. F. (2006). Hox transcription factors and their elusive mammalian gene targets. Heredity, 97(2), 88-96. DOI: 10.1038/sj.hdy.6800847
URL: www.nature.com/articles/6800847

Truong, K., & Ikura, M. (2001). The use of FRET imaging microscopy to detect protein–protein interactions and protein conformational changes *in vivo*. *Current opinion in structural biology*, *11*(5), 573-578. DOI: 10.1016/S0959-440X(00)00249-9
URL: www.sciencedirect.com/science/article/abs/pii/S0959440X00002499?via%3Dihub

Zandvakili, A., Uhl, J. D., Campbell, I., Salomone, J., Song, Y. C., & Gebelein, B. (2019). The cis-regulatory logic underlying abdominal Hox-mediated repression versus activation of regulatory elements in *Drosophila*. Developmental biology, 445(2), 226-236. DOI: 10.1016/j.ydbio.2018.11.006
URL: www.sciencedirect.com/science/article/abs/pii/S0959440X00002499?via%3Dihub

Zhu A, Kuziora MA. Homeodomain interaction with the β subunit of the general transcription factor TFIIE. J Biol Chem. 1996;271(35):20993–6. DOI: 10.1074/jbc.271.35.20993
URL: www.sciencedirect.com/science/article/pii/S0021925819746031

Zouaz, A., Auradkar, A., Delfini, M. C., Macchi, M., Barthez, M., Ela Akoa, S., ... & Saurin, A. J. (2017). The Hox proteins Ubx and AbdA collaborate with the transcription pausing factor M1 BP to regulate gene transcription. The EMBO journal, 36(19), 2887-2906. DOI: 10.15252/embj.201695751
URL: www.embopress.org/doi/full/10.15252/embj.201695751

Chapter 2 Molecular biology: tools for the study of re-emerging diseases

Capítulo 2 Biología molecular: herramientas para el estudio de enfermedades reemergentes

GUTIÉRREZ-CEDILLO, Perla Mariana´†*, CEDILLO-BARRÓN, Leticia´´ and PERRUSQUÍA-LÓPEZ, Verónica´´

´Instituto Politécnico Nacional, Escuela Nacional de Ciencias Biológicas, México.
´´Instituto Politécnico Nacional, Departamento de Biomedicina Molecular-Centro de Investigación y Estudios Avanzados, México.

ID 1st Author: *Perla Mariana, Gutiérrez-Cedillo* / **ORC ID:** 0000-0003-3801-868X, **CVU CONACYT ID:** 1079086

ID 1st Co-author: *Leticia, Cedillo-Barrón* / **ORC ID:** 0000-0003-2642-3872, **CVU CONACYT ID:** 13822

ID 2nd Co-author: *Verónica, Perrusquía-López* / **ORC ID:** 0000-0001-6107-6277

DOI: 10.35429/H.2022.6.1.13.25

* perlamgc65@gmail.com

A. Marroquín, L. Castillo, S. Soto, L. Cruz. (Coord.) CIERMMI Women in Science TXIX Biological Sciences. Handbooks-©ECORFAN-México, Querétaro, 2022.

Abstract

Chikungunya fever is a disease caused by the chikungunya virus (CHIKV), which is transmitted by hematophagous female mosquitoes (Mohan, 2010). Chikungunya Fever is a re-emerging illness with a great global impact, causing severe public health problems (Mohan, 2010) (Gérardin, 2011) (Sebastian, 2009). CHIKV contains a single-stranded RNA genome (+) with two open reading frames (ORFs), one for nonstructural proteins and the other for structural proteins (Caglioti, 2013). Little is known about the specific role nonstructural proteins (NSPs) play during viral replication. Nevertheless, NSP1 is known to be involved in the induction of cytoskeleton and plasma membrane changes and cell prolongations such as filopodia (Laakkonen, 1998). Currently, there are no commercial antibodies to detect NSP1; hence, it is of utmost importance to design tools that would allow us to study the role of this protein during the viral cycle. In this study, primers for CHIKV NSP1 were designed and used to amplify cDNA, which was cloned into the pPROEX Htb expression vector. The optimal expression time for NSP1 was determined, and the expressed protein was purified. The recombinant NSP1 (rNSP1) protein obtained using this process was used to immunize rats to obtain polyclonal antibodies. These antibodies were tested in Vero cells infected with CHIKV and were observed using immunofluorescence assays, showing the recognition of viral proteins in their native form.

Chikungunya, NSP1, Antibody, Recombinant, Clonation, Purification

Resumen

La fiebre de Chikungunya es una enfermedad causada por el virus de Chikungunya (CHIKV), el cual es transmitido mediante la picadura de los moquitos hematófagos hembras (Mohan, 2010). La fiebre de Chikungunya es una enfermedad reemergente con un gran impacto global que ha causado severos problemas en salud pública (Mohan, 2010)(Gérardin, 2011) (Sebastian, 2009). CHIKV contiene una cadena monocatenaria de RNA y polaridad positiva. Este genoma tiene 2 marcos de lectura (ORFs) que codifican para dos poliproteínas: la no estructural y la estructural (Caglioti, 2013). Poco se conoce acerca de la actividad de las proteínas no estructurales (NSPs) durante la replicación del virus. Para NSP1, se ha observado que participa durante la formación de prolongaciones celulares (como los filopodios), así como en la remodelación del citoesqueleto y membranas plasmáticas (Laakkonen, 1998). Actualmente, en el mercado no hay anticuerpos específicos que detecten a NSP1, por lo que es de suma importancia el diseño de herramientas que nos permitan estudiar el papel de esta proteína durante el ciclo viral. En este estudio se diseñaron oligos para NSP1 y se emplearon para la amplificación del cDNA. Posteriormente este cDNA se clonó en el vector de expresión pPROEX Htb. La proteína recombinante NSP1 (rNSP1) fue purificada y utilizada para la inmunización de ratas. Los anticuerpos policlonales obtenidos fueron probados en células VERO infectadas con CHIKV y, mediante ensayos de inmunofluorescencia, se detectó a la proteína NSP1 en su forma nativa.

Chikungunya, NSP1, Anticuerpo, Recombinante, Clonación, Purificación

2.1 Introduction

CHIKV causes Chikungunya fever, which is considered a re-emerging illness and has a severe impact in public health. This is due to its debilitating and lasting sequelae, mainly of a rheumatological type, resulting in expensive treatments and therefore burdening the health sector of the countries in which they occur, such as Mexico, Argentina, Colombia and Bolivia, which have the most confirmed chikungunya cases (OMS, 2020).

Symptoms of CHIKV appear within 3-7 days of infection and most patients with acute infection show a fever higher than 38.9 °C, headache, rash, fatigue, nausea, vomiting, joint pain, and conjunctivitis. Almost all infected people develop severe polyarthralgia, more frequently in the wrists, elbows, fingers, knees and ankles, and it tends to weaken the patient. In some cases, joint pain, fatigue, and neuritis continue to be observed up to ten months after infection, with 43–75% of infected people reporting to have some late- or prolonged-onset symptoms (on average, two years after infection), such as recurrent joint pain or joint stiffness (Simon, 2007) (Gérardin, 2011) (Manimunda, 2010).

CHIKV belongs to the Togaviridae family and Alphavirus genus. Most alphaviruses are transmitted by mosquitoes to vertebrate hosts, such as humans, nonhuman primates, birds, amphibians, reptiles, rodents, and pigs (Chen, 2018). CHIKV has an icosahedral form with a diameter of 60-70 nm and is wrapped by a phospholipid layer. It contains a genome approximately 11.8 kb long, which is a single linear chain of positive RNA flanked by two UTRs (untranslated regions) at the 5′ end and a poly-A tail at the 3′ end (Caglioti, 2013). The CHIKV genome has two open reading frames (ORFs), the first of which encodes four nonstructural proteins (NSPs): NSP1, NSP2, NSP3, and NSP4. The second ORF encodes five structural proteins, including those that form the capsid (C) and the envelope glycoproteins E1, E2, E3, and 6k (Li, 2012).

Cell infection starts when CHIKV binds to the cell membrane, mainly through the interaction of the E2 protein. Next, the virus enters the cell via clathrin-dependent endocytosis. When an endosome is formed, the endosome pH begins to decrease, leading to a conformational rearrangement of the virus and E2-E1 heterodimer dissociation. E1 then participates as a fusogenic peptide, inducing the fusion of the endosome and the viral coat, allowing the RNA to be released into the cytosol. The nonstructural proteins are translated as polyproteins and a replicative complex (RC) is formed, wherein genomic RNA and other nonstructural proteins are cleaved to the plasma membrane where RNA synthesis occurs. The double-stranded RNA formed leads to the synthesis of genomic and subgenomic viral RNAs. Subgenomic RNA is translated to produce structural proteins that form the viral capsid, which interacts with genomic RNA, giving rise to new viruses, and leading to cell exit for the infection of new cells (Cunha, 2020).

Nonstructural protein 1 (NSP1) is highly involved in viral replication. This molecule is 535 amino acids long (~60 kDa) and has three domains: an N-terminal domain (NT) (with methyltransferase [MT] and guanylyltransferase functions), a membrane-binding domain (MB), and a C-terminal domain (CT). The NT domain is involved in the methylation and capping of viral RNA. The MB anchors the replication complex (CR) to the cell membrane. The function of C-terminal domain is not yet known (Kumar, 2018) (Cunha, 2020). Thus, NSP1 participates in binding the replication complex (RC) to the inner part of the plasma membrane and capping the genomic and subgenomic RNA (Ahola, 1995). Additionally, it is believed that NSP1 is involved in membrane reorganization during cell infection; however, many aspects of this phenomenon remain to be elucidated (Kumar,2018).

2.2 Methodology

2.2.1 Designing primers

Primers were designed to amplify the coding sequence for NSP1. The sequence of the complete CHIKV genome from the first clinical case in Mexico reported by InDRE (strain 51CHIK; GenBank: KP851709.1) was used as a template. Two primers were designed, which were approximately 20 to 25 base pairs in length and had an alignment temperature between 56 and 59 °C. The primers were then analyzed using NEBcutter V2.0 and Clustal Omega software to rule out other restriction sites of the enzymes to be used within the sequences and corroborate that their sequences were not complementary.

2.2.2 Viral RNA and cDNA preparation

A Vero cell culture was infected with Chikungunya virus at 5 MOI for 12 h. Subsequently, the cell monolayer was washed with Dulbecco's Modified Eagle Medium (DMEM) without Fetal Bovine Serum (FBS), and trizol reagent was added. The resulting solution was vigorously mixed at room temperature (20-25°C) for 5 min. Next, 200 µL of a cold solution of chloroform and isoamyl alcohol (49:1, v/v) was added, mixed via inversion, and centrifuged at 20,000 × g at 4°C for 15 min, and the aqueous phase was recovered. Next, 500 µL of cold isopropanol was added the aqueous phase, mixed via inversion, centrifuged at 20,000 × g for 10 min, and the supernatant was removed. The pellet was then washed with 75% ethanol. Finally, the isolated RNA was resuspended in DEPC water and quantified. A mixture containing dNTPs, DTT, 200 U/µL of the enzyme SuperScript III (reverse transcriptase), and the previously extracted RNA was added to specific primers previously designed to amplify the NSP1 sequence via RT-PCR.

The coding region for NSP1 was amplified using the designed primer pairs, and the synthesized cDNA was used as a template for further amplification. For this, 35 cycles were carried out as follows: initial denaturation at 95 °C for 5 min, primer annealing at 56.8 °C for 1 min, and cDNA extension at 72 °C for 7 min.

2.2.3 Construction design and obtaining recombinant *Escherichia coli* cells

The amplicon (NSP1) was ligated into a pJET transfer vector following the cloning protocol for blunt ends (CloneJET PCR Cloning kit, Thermo Scientific). Briefly, the PCR product was purified from the electrophoresis gel (QIA Quick Gel extraction kit) and digested to produce blunt ends. Nuclease-free water and the reaction buffer (Thermo Scientific, 1×) were mixed and incubated at 70 °C for 5 min. Subsequently, the vector and T4 DNA ligase (Thermo Scientific, 1×) were added and incubated at room temperature for 5 min. The above mixture was used to transform competent XL10 Gold E. coli cells, which were subject to heat shock at 42 °C for 45 s, placed on ice for 1 min, and 400 µL of LB medium was added. The transformed cells were then incubated at 37 °C for 1 h with constant agitation. Finally, the cells were spread onto plates with LB medium supplemented with 120 µg/mL ampicillin and incubated at 37 °C for 24 h to screen for positive transformants.

Next, the digestion of the expression vector pPROEX Htb was carried out using the restriction enzymes *BamHI* and *XhoI*. This was done for directed cloning during ligation, wherein the amplicon was inserted in the 5′-3′ direction, thus resulting in the appropriate reading frame.

The next step was the release of the NSP1 gene via digestion at 37 °C for 2 h with the enzymes *BamHI* and *XhoI* from the previous construct (NSP1-pJET) and transferring the gene into the expression vector pPROEX HTb. The transformation process was carried out using competent BL21 E. coli, as described previously for the XL10 Gold strain. General cloning strategy of NSP1 into the transfer pJET 1.2/ blunt and expression pPROEX HTb vectors is shown below (Figure 2.1).

Figure 2.1 Schematic representation of general cloning strategy for pJET1.2 and pPROEX Htb vectors and the final construction pPROEX HTb-NSP1 flanked by *BamHI* and *XhoI* restriction sites

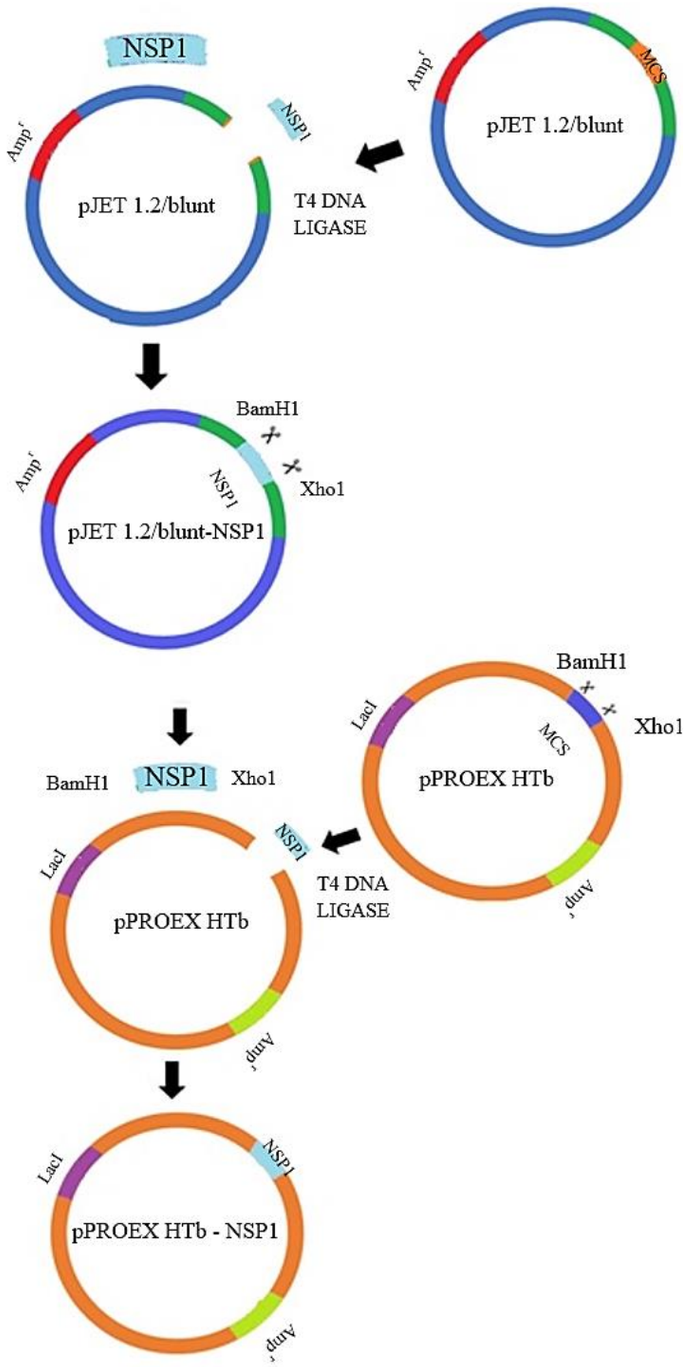

2.2.4 Evaluating the Expression and purification of NSP1

To elucidate the optimal expression time of NSP1, induction kinetics were evaluated in recombinant E. coli BL21 cells incubated at 37 °C with agitation, with or without induction agent (IPTG, 100 mM). Bacterial aliquots were taken at 0, 3, 6, 9, and 12 h post-induction. Recombinant bacterial cultures were lysed and analyzed via western blotting using an antibody against His-tag. The proteins were exposed using a Super Signal West Femto Maximum Sensitivity Substrate chemiluminescence kit (Thermo Fisher Scientific) and were analyzed with a ChemiDoc system (Bio-Rad).

To purify NSP1, it was produced in 1 L bacterial culture for 9 h post-induction, as previously standardized. Bacteria were centrifuged at 4,000 × g, resuspended in lysis buffer, stirred at room temperature for 60 min, centrifuged at 10,000 × g at room temperature for 30 min, and the supernatant was recovered.

Meanwhile, a NiNTA Resin 3x (QIAGEN) was washed with B lysis buffer (The QIAexpressionist™, QIAGEN; 100 mM NaH2PO4, 10 mM Tris-Cl, and 8 M urea; pH 8.0) and 100 µL of resin per 100 mL of culture was added. The lysates were mixed with the resin and incubated for 1 h at room temperature with gentle stirring. The mixture was passed through a column and the eluate was recovered. Subsequently, the mixture was washed twice with 4 mL of B lysis buffer (pH 8.0), followed by two washes with 4 mL of C buffer (pH 6.3). Afterward, 2 mL of D buffer (pH 5.9) was added, and eluates were recovered in 500-µL aliquots. Finally, 2 mL of E buffer (pH 4.5) (The QIAexpressionist ™: QIAGEN) was added, and 500-µL eluates were recovered.

2.2.5 Wistar rat immunization protocol and evaluation of hyperimmune serum by immunofluorescence

Two Wistar rats were immunized intraperitoneally with four doses of 150 µg purified NSP1. Each dose was administered at 15-day intervals (Figure 2.2). The first immunization included recombinant NSP1 protein mixed with complete Freund's adjuvant. The next dose was administered with incomplete Freund's adjuvant. After immunization, bleeding was performed to obtain the serum.

Figure 2.2 NSP1 immunization protocol

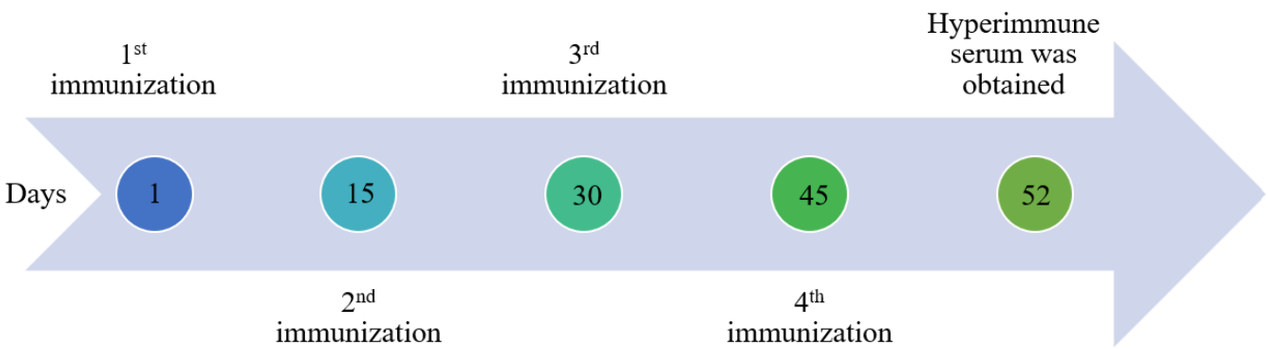

2.2.6 Immunofluorescence assay

Approximately 8×10^5 Vero cells were seeded in each well of a 24-well plate and grown until confluence. The monolayers were infected with CHIKV at 5 MOI for 5 and 24 h. After the infection, the cells were fixed with 300 µL of 4% paraformaldehyde for 20 min and washed twice with sterile 1× PBS. Subsequently, the cells were permeabilized by adding 300 µL of 0.1% Triton X-100 in PBS + 0.2% gelatin and incubated with agitation for 20 min in the dark. The cells were then blocked with 300 µL of 10% goat serum (PBSTCH) diluted in 0.1% PBS-Triton X-100 and incubated with agitation for 1 h. After incubation, the slides were placed with 20 µL of primary antibody from the immunized rats, diluted 1:100 in PBSTCH, and incubated for 1 h at room temperature. The corresponding secondary antibody (anti-rat IgG-FitC, diluted 1:50 in PBSTCH) was added, and the cells were incubated for another 1 h at room temperature in the dark. Finally, the slides were washed with 0.1% PBS-Triton. The slides were observed under an epifluorescence microscope (Leica) at 60× magnification or in a confocal microscope (Leica) at 40× magnification.

2.3 Results and Discussion

2.3.1 Design and cloning of recombinant plasmids

Two primers, 24 base pairs long each, were designed and flanked by the restriction sites of *XhoI* and *BamHI* in the forward and reverse directions, respectively, with an annealing temperature of 56.89 °C. After a series of amplification cycles, the gene encoding the NSP1 protein was obtained at an expected size of approximately 1,578 bp (Figure 2.3).

Figure 2.3 NSP1 RT-PCR electropherogram. The NSP1 sequence was amplified using the forward 5′-CGC-GGA-TCC-ATG-GAT-TCT-GTG-TAC-3′ and the reverse primer 5′-CTA-TCT-CGA-CCA-CGA-GAG-CTC-GAA-3′, which were flanked by the *BamHI* and *XhoI* restriction sites, respectively

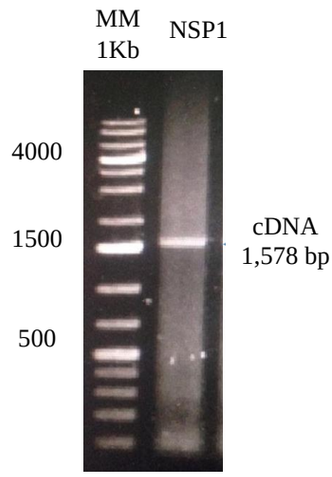

Besides, pJet blunt vector was selected since it can store large DNA sequences. Once the amplicon was ligated into the pJET transfer vector, its insertion was confirmed by digesting the construct with the *BglII* enzyme, which released the NSP1 gene, obtaining a fragment of the expected size (Figure 2.4).

Figure 2.4 pJET- NSP1 restriction electropherogram

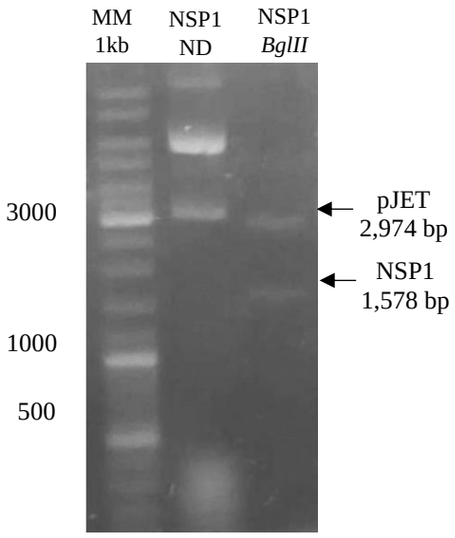

As mentioned previously, to perform targeted cloning, both the expression vector pPROEX Htb and the NSP1 insert were digested with the restriction enzymes XhoI and BamHI, resulting in the release of fragments of expected sizes (Figure 2.5).

Figure 2.5 Electropherogram of the pPROEX Htb plasmid and amplicons digested with the restriction enzymes *Bam*HI and *Xho*I

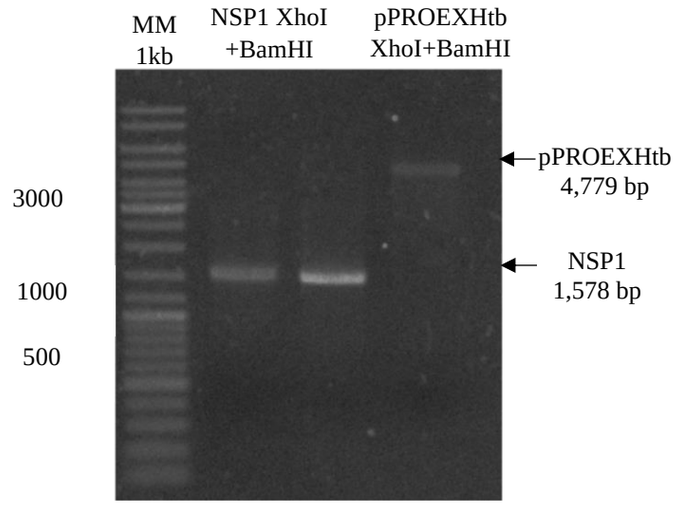

2.3.2 Expression and identification of recombinant protein NSP1

Additionally, to confirm the functionality of the pPROEX Htb-NSP1plasmid, *E. coli* cells were transformed, and the culture was incubated with IPTG to induce the expression of the NSP1 protein. To evaluate recombinant NSP1 expression, western blot analysis was performed using an anti-His antibody to detect the protein. It was observed that a higher protein production occurred at nine hours post-induction (hpi) (Figure 2.6). Additionally, several smaller bands were observed at 6, 9, and 12 hpi that did not correspond to the product of interest (NSP1). The appearance of these bands may be due to NSP1 degradation since the stationary phase begins after several hours. During this stage, DNA and RNA synthesis are decreased, while protein synthesis is increased (Ramírez-Santos, 2005); thus, these bands may correspond to different sizes of NSP1. On the other hand, at 9 and 12 h, the bacterial cultures without IPTG showed small amounts of NSP1 due to a phenomenon known as “leaking,” which consists of incomplete repression of the expression of the protein. This is because many promoters are not very well regulated, showing little expression before the addition of an induction agent; *lac* promoters are highly likely to present this phenomenon (Miroux, 1996).

Figure 2.6 NSP1 expression kinetics in *E. coli.* Western blot analysis shows that the best time of protein production was at 9 h post-induction

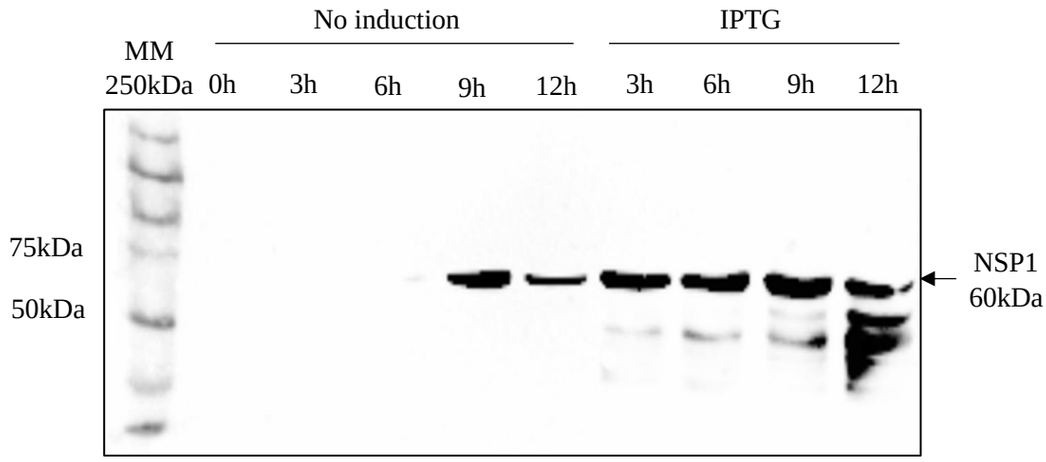

2.3.3 Purification of recombinant NSP1

Furthermore, recombinant NSP1 was purified under denaturing conditions using histidine columns and then analyzed via western blotting. Two bands were observed in lanes 2 and 3 (Figure 2.7); the first band showed a molecular weight of 60 kDa, which was in accordance with the size predicted for NSP1, confirming the successful purification of the protein. However, a second smaller band was also observed, which may indicate a truncated product due to the presence of a premature stop codon. Interestingly, this doublet has not been reported in the literature for NSP1 in Chikungunya. Although it has been reported for other alphaviruses such as SINV, truncated proteins are still expressed even when there is a mutation in the reading frame (Akhrymuk, 2012).

Figure 2.7 Purification of recombinant CHIK NSP1 using an Ni-NTA column. The eluted fractions were analyzed via western blot using a specific anti-His antibody

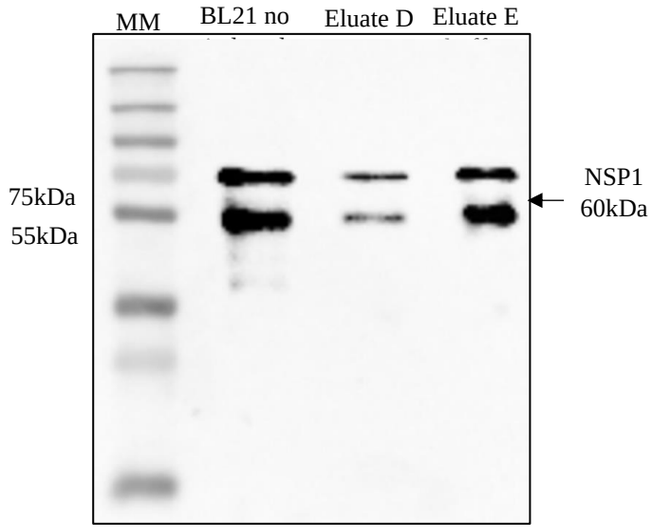

2.3.4 Evaluation of recombinant NSP1 to induce specific antibodies

Finally, recombinant NSP1 was used as an antigen to immunize rats, and the hyperimmune serum samples obtained were evaluated. We then addressed whether the antibodies raised in the immunized rats could recognize native CHIKV in infected Vero cells. Figure 2.8 shows Vero cells infected with CHIKV at an MOI of 5 and analyzed via IF at different times. The micrographs showed nuclei dyed with blue (DAPI) and green (FITC) staining was observed in the infected cells treated with the hyperimmune anti-NSP1 antibody. In contrast, the uninfected cells did not show the recognition of NSP1 by the antibody. However, during the first 5 h of infection, the positive signal was only faint, possibly because the production of NSP1 was not yet high. As previously reported, the transport of viral RNA is being carried out simultaneously with the synthesis of other nonstructural proteins (Kallio, 2015). However, at 24 h, the green signal is already stronger because late replication complexes, including genomic and subgenomic RNA, were already synthesized, and viral particles were released (Rana, 2014).

Figure 2.8 Specific recognition of NSP1 in Vero cells infected with CHIKV that were analyzed via immunofluorescence staining at 5 and 24 h post-infection. Serum samples from rats immunized with NSP1 were used as the primary antibody, and anti-mouse IgG-FITC was used as the secondary antibody. The Figure shows results from a representative experiment

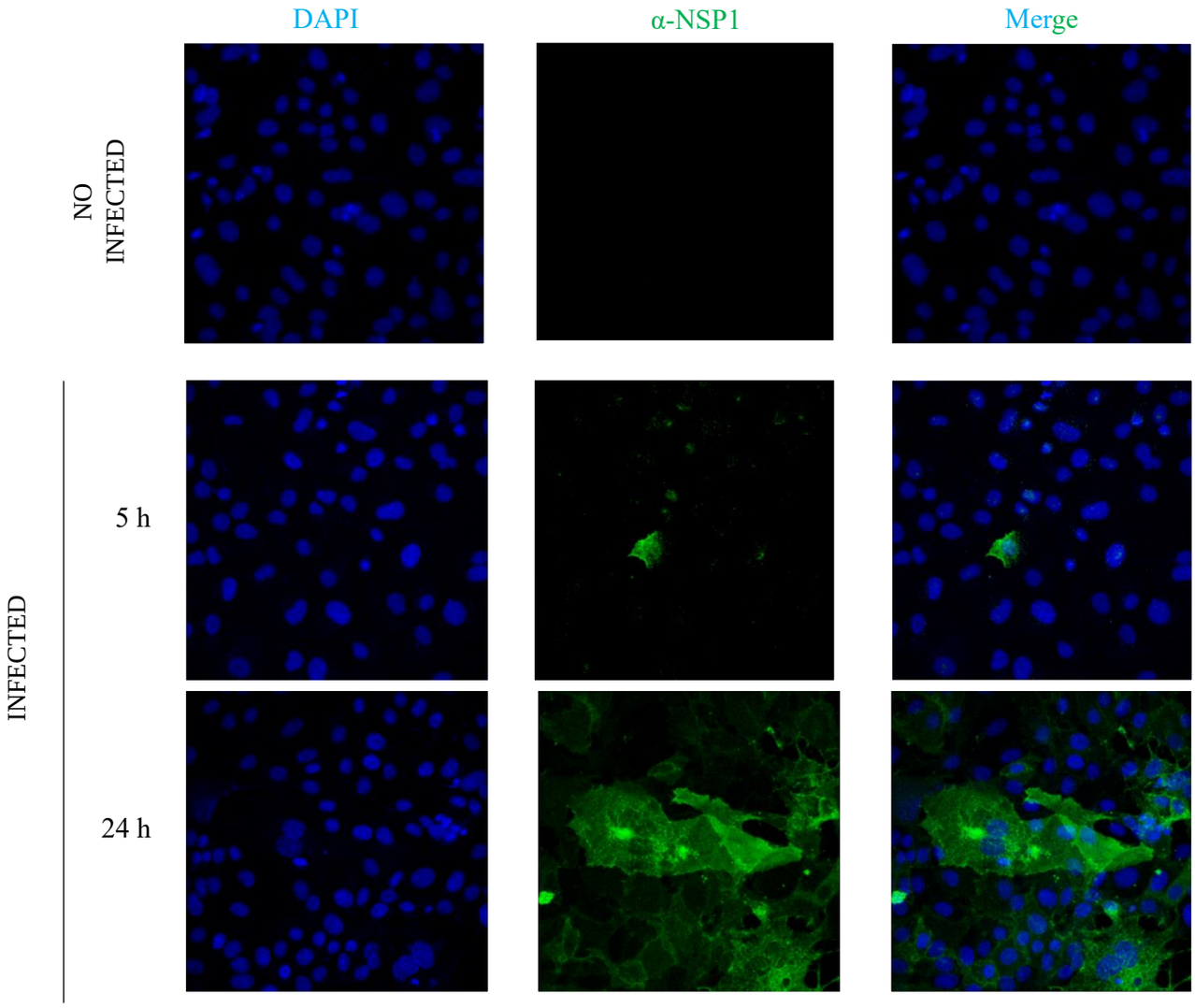

One of the most relevant domains of the NSP1 protein is the membrane-binding domain, which allows its association with cell membranes. The presence of α-helical loops and palmitoylation sites in this domain allows the protein and replication complex to anchor to the plasma membrane (Abu Bakar, 2018). Hence, the presence of NSP1 was more pronounced in the cell periphery, as evidenced by the strong fluorescence observed in this area. Previously, Kumar et al. (2018) have shown that NSP1 is mainly found in the plasma membrane of cells infected with CHIKV (at an MOI of 2) at 2 hpi. In contrast, at 4 and 6 hpi, NSP1 can already be observed in the cell cytoplasm.

Furthermore, it has been previously reported that cells infected with CHIKV induce filopodia formation (Laakkonen, 1998) and cytoskeleton rearrangement (Karo-Astover, 2010). However, much work remains to be done to elucidate the changes induced by CHIK infection in host cells. Using the hyperimmune serum generated in this study, we can highlight and follow the drastic changes in cell morphology, mainly in the cytoplasmic membrane from where projections come out, as reported by Laakkonen and Karo-Astover (1998 and 2010, respectively).

Finally, it has also been reported that anti-NSP antibodies might be useful for investigating the stages of viral replication, describing the expression patterns of different viral proteins, or determining the location of NSPs in different cell compartments at certain times during infection (Kumar, 2015). Therefore, obtaining antibodies against the native form of CHIKV NSP1 could provide a valuable tool to investigate and understand the host-pathogen relationship in Chikungunya fever.

2.4 Acknowledgments

We would like to thank García-Cordero, Julio. PhD for the support in the elaboration of experiments shown in this project.

2.5 Founding

This work has been funded by CONACYT [grant number 2462-QLCB].

2.6 Conclusions

Recombinant NSP1 is an immunogenic protein, which allowed us to obtain polyclonal antibodies against rNSP1 that recognize the native form of NSP1. The antiserum is a powerful tool to study aspects of the viral cycle of CHIKV.

2.7 References

Abu Bakar, F., & Ng, L. (2018). Nonstructural Proteins of Alphavirus-Potential Targets for Drug Development. Viruses, 10(2), 71. DOI: https://doi.org/10.3390/v10020071
URL: https://www.mdpi.com/1999-4915/10/2/71

Ahola, T., & Kääriäinen, L. (1995). Reaction in alphavirus mRNA capping: formation of a covalent complex of nonstructural protein nsP1 with 7-methyl-GMP. Proceedings of the National Academy of Sciences of the United States of America, 92(2), 507–511. DOI: https://doi.org/10.1073/pnas.92.2.507
URL: https://www.pnas.org/doi/abs/10.1073/pnas.92.2.507

Akhrymuk, I., Kulemzin, S. V., & Frolova, E. I. (2012). Evasion of the innate immune response: the Old World alphavirus nsP2 protein induces rapid degradation of Rpb1, a catalytic subunit of RNA polymerase II. Journal of virology, 86(13), 7180–7191. DOI: https://doi.org/10.1128/JVI.00541-12
URL: https://journals.asm.org/doi/10.1128/JVI.00541-12

Caglioti, C., Lalle, E., Castilletti, C., Carletti, F., Capobianchi, M. R., & Bordi, L. (2013). Chikungunya virus infection: an overview. The new microbiologica, 36(3), 211–227. PMID: 23912863.
URL: https://www.newmicrobiologica.org/PUB/allegati_pdf/2013/3/211.pdf

Chen, R., Mukhopadhyay, S., Merits, A., Bolling, B., Nasar, F., Coffey, L. L., Powers, A., Weaver, S. C., & Ictv Report Consortium (2018). ICTV Virus Taxonomy Profile: Togaviridae. The Journal of general virology, 99(6), 761–762. DOI: https://doi.org/10.1099/jgv.0.001072
URL: https://www.microbiologyresearch.org/content/journal/jgv/10.1099/jgv.0.001072

Cunha, M. S., Costa, P., Correa, I. A., de Souza, M., Calil, P. T., da Silva, G., Costa, S. M., Fonseca, V., & da Costa, L. J. (2020). Chikungunya Virus: An Emergent Arbovirus to the South American Continent and a Continuous Threat to the World. Frontiers in microbiology, 11, 1297.
DOI: https://doi.org/10.3389/fmicb.2020.01297
URL: https://www.frontiersin.org/articles/10.3389/fmicb.2020.01297/full

Gérardin, P., Fianu, A., Malvy, D., Mussard, C., Boussaïd, K., Rollot, O., Michault, A., Gaüzere, B. A., Bréart, G., & Favier, F. (2011). Perceived morbidity and community burden after a Chikungunya outbreak: the TELECHIK survey, a population-based cohort study. BMC medicine, 9, 5. DOI: https://doi.org/10.1186/1741-7015-9-5
URL: https://bmcmedicine.biomedcentral.com/articles/10.1186/1741-7015-9-5

Kallio, K., Hellström, K., Jokitalo, E., & Ahola, T. (2015). RNA Replication and Membrane Modification Require the Same Functions of Alphavirus Nonstructural Proteins. Journal of virology, 90(3), 1687–1692. DOI: https://doi.org/10.1128/JVI.02484-15
URL: https://journals.asm.org/doi/10.1128/JVI.02484-15

Karo-Astover, L., Sarova, O., Merits, A., & Zusinaite, E. (2010). The infection of mammalian and insect cells with SFV bearing nsP1 palmitoylation mutations. Virus research, 153(2), 277–287. DOI: https://doi.org/10.1016/j.virusres.2010.08.019
URL: https://www.sciencedirect.com/science/article/abs/pii/S0168170210002960?via%3Dihub

Kumar, S., Kumar, A., Mamidi, P., Tiwari, A., Kumar, S., Mayavannan, A., Mudulli, S., Singh, A. K., Subudhi, B. B., & Chattopadhyay, S. (2018). Chikungunya virus nsP1 interacts directly with nsP2 and modulates its ATPase activity. Scientific reports, 8(1), 1045. DOI: https://doi.org/10.1038/s41598-018-19295-0
URL: https://www.nature.com/articles/s41598-018-19295-0

Kumar, S., Mamidi, P., Kumar, A., Basantray, I., Bramha, U., Dixit, A., Maiti, P. K., Singh, S., Suryawanshi, A. R., Chattopadhyay, S., & Chattopadhyay, S. (2015). Development of novel antibodies against non-structural proteins nsP1, nsP3 and nsP4 of chikungunya virus: potential use in basic research. Archives of virology, 160(11), 2749–2761. DOI: https://doi.org/10.1007/s00705-015-2564-2
URL: https://link.springer.com/article/10.1007/s00705-015-2564-2

Laakkonen, P., Auvinen, P., Kujala, P., & Kääriäinen, L. (1998). Alphavirus replicase protein NSP1 induces filopodia and rearrangement of actin filaments. Journal of virology, 72(12), 10265–10269. DOI: https://doi.org/10.1128/JVI.72.12.10265-10269.1998
URL: https://journals.asm.org/doi/10.1128/JVI.72.12.10265-10269.1998

Li, X. F., Jiang, T., Deng, Y. Q., Zhao, H., Yu, X. D., Ye, Q., Wang, H. J., Zhu, S. Y., Zhang, F. C., Qin, E. D., & Qin, C. F. (2012). Complete genome sequence of a chikungunya virus isolated in Guangdong, China. Journal of virology, 86(16), 8904–8905. DOI: https://doi.org/10.1128/JVI.01289-12
URL: https://journals.asm.org/doi/10.1128/JVI.01289-12

Manimunda, S. P., Vijayachari, P., Uppoor, R., Sugunan, A. P., Singh, S. S., Rai, S. K., Sudeep, A. B., Muruganandam, N., Chaitanya, I. K., & Guruprasad, D. R. (2010). Clinical progression of chikungunya fever during acute and chronic arthritic stages and the changes in joint morphology as revealed by imaging. Transactions of the Royal Society of Tropical Medicine and Hygiene, 104(6), 392–399. DOI: https://doi.org/10.1016/j.trstmh.2010.01.011
URL: https://academic.oup.com/trstmh/article-abstract/104/6/392/1941200?redirectedFrom=fulltext

Miroux, B., & Walker, J. E. (1996). Over-production of proteins in Escherichia coli: mutant hosts that allow synthesis of some membrane proteins and globular proteins at high levels. Journal of molecular biology, 260(3), 289–298. DOI: https://doi.org/10.1006/jmbi.1996.0399
URL: https://www.sciencedirect.com/science/article/pii/S002228369690399X?via%3Dihub

Mohan, A., Kiran, D. H., Manohar, I. C., & Kumar, D. P. (2010). Epidemiology, clinical manifestations, and diagnosis of Chikungunya fever: lessons learned from the re-emerging epidemic. Indian journal of dermatology, 55, 54–63. DOI: https://doi.org/10.4103/0019-5154.60355
URL: https://www.e-ijd.org/article.asp?issn=0019-5154;year=2010;volume=55;issue=1;spage=54;epage=63;aulast=Mohan

OMS: Chikungunya [(retrieved on March 20, 2022)]; Available online: https://www.who.int/es/news-room/fact-sheets/detail/chikungunya

Ramírez Santos, J., Contreras Ferrat, G., & Gómez Eichelmann, M. C. (2005). La fase estacionaria en la bacteria Escherichia coli [Stationary phase in Escherichia coli]. Revista latinoamericana de microbiologia, 47(3-4), 92–101. PMID: 17061534
URL: https://www.medigraphic.com/pdfs/lamicro/mi-2005/mi05-3_4f.pdf

Rana, J., Rajasekharan, S., Gulati, S., Dudha, N., Gupta, A., Chaudhary, V. K., & Gupta, S. (2014). Network mapping among the functional domains of Chikungunya virus nonstructural proteins. Proteins, 82(10), 2403–2411. DOI: https://doi.org/10.1002/prot.24602
URL: https://onlinelibrary.wiley.com/doi/10.1002/prot.24602

Sebastian, M. R., Lodha, R., & Kabra, S. K. (2009). Chikungunya infection in children. Indian journal of pediatrics, 76(2), 185–189. DOI: https://doi.org/10.1007/s12098-009-0049-6
URL: https://link.springer.com/article/10.1007/s12098-009-0049-6

Simon, F., Parola, P., Grandadam, M., Fourcade, S., Oliver, M., Brouqui, P., Hance, P., Kraemer, P., Mohamed, A. A., de Lamballerie, X., Charrel, R., & Tolou, H. (2007). Chikungunya infection: an emerging rheumatism among travelers returned from Indian Ocean islands. Report of 47 cases. Medicine, 86(3), 123–137. DOI: https://doi.org/10.1097/MD/0b013e31806010a5
URL: https://journals.lww.com/md-journal/Fulltext/2007/05000/Chikungunya_Infection__An_Emerging_Rheumatism.1.aspx

Chapter 3 Used edible oils a latent threat in the contamination of water bodies

Capítulo 3 Aceites comestibles usados una amenaza latente en la contaminación de los cuerpos de agua

TORRES-RIVERO, Ligia†*, LOEZA-CRUZ, María Samantha, MORALES-ORTIZ, Verónica and MEDINA-DÍAZ, Emery

Tecnológico Nacional de México - Instituto Tecnológico de Cancún, México.

ID 1st Author: *Ligia, Torres-Rivero* / **ORC ID:** 0000-0002-3303-3437, **CVU CONACYT ID:** 316421

D 1st Co-author: *María Samantha, Loeza-Cruz*

ID 2nd Co-author: *Verónica, Morales-Ortiz* / **ORC ID:** 0000-0002-9640-4848

ID 3rd Co-author: *Emery, Medina-Díaz* / **ORC ID:** 0000-0002-8921-8924

DOI: 10.35429/H.2022.6.1.26.39

* ligia.tr@cancun.tecnm.mx

A. Marroquín, L. Castillo, S. Soto, L. Cruz. (Coord.) CIERMMI Women in Science TXIX Biological Sciences. Handbooks-©ECORFAN-México, Querétaro, 2022.

Abstract

This article refers to the poor disposal of used vegetable oil management, in cheap kitchens and in homes in regions 226, 249, 238, 235, 233, New Jerusalem New Millennium, a body of water is located, an irregular settlement. It is essential to create awareness for the management and disposal of used vegetable oils, national and international legislation that departs from the importance of the impact caused by the dumping of used edible oils, but it is necessary at the local level for proper management. of used vegetable oil, a total of 100 surveys were applied on the management and disposal of used edible oils, in the regions and irregular settlement of the Municipality of Benito Juárez Quintana ROO with a snowball statistical treatment, non-probabilistic sampling. The application of the surveys shows us that 70% of the population pours residual oils into the drain, 45% have a body of water nearby, to the drain or put it in a plastic bag in the garbage, 6% take it to the center collection, used cooking oils, after receiving adequate treatment, become raw material to produce biodiesel

Disposal, Used edible oils, Spills, Water bodies

Resumen

Este artículo alude la mala disposición del manejo del aceite vegetal usado, en cocinas económicas y en los hogares de las regiones 226, 249, 238, 235,233, Nueva Jerusalén Nuevo Milenio, se sitúa un cuerpo de agua, asentamiento irregular. Es primordial crear conciencia para el manejo y disposición de los aceites vegetales usados, las legislaciones a nivel nacional e internacional que departen de la importancia del impacto que ocasiona el vertido de los aceites comestibles usados, pero hace falta en el ámbito local para el adecuado manejo del aceite vegetal usado, se aplicaron un total de 100 encuestas sobre el manejo y disposición de los aceites comestibles usados, en las regiones y asentamiento irregular del Municipio de Benito Juárez Quintana ROO con un tratamiento estadístico bola de nieve, muestreo no probabilístico. La aplicación de las encuestas nos arroja que el 70% de la población vierte los aceites residuales al drenaje, el 45% tiene cuerpo de agua cerca, al drenaje o lo ponen en bolsa de plástico en la basura, el 6% lo lleva al centro de acopio, los aceites usados de cocina, después de recibir un adecuado tratamiento se convierte en materia prima para la elaboración de biodiesel.

Disposición, Aceites comestibles usados, Contaminación, Cuerpos de agua

3.1 Introduction

Used edible oils are a latent environmental problem in this globalized world, because it is easier to dispose of them in sinks, sinks, than to take them to a collection center for treatment, without thinking about the damage that such discharges may cause to the water table, they are materials of oily type obtained as a residue of fried foods that, when they are discarded, are mostly mixtures of vegetable oils of different composition, sometimes contaminated with tallow fats, lard, during cooking, some with residues of processed foods with high moisture content, and protein, of animal origin, presents an inadequate management of used vegetable cooking oils. The application of the survey consisted of knowing if the housewives, economic kitchens where they dispose of the waste of the edible oils used in the frying process.

3.1.1 Types of fats

Fats or tallows: Solid at room temperature, formed mainly by saturated fatty acids (palmitic acid, stearic acid, etc.). The most harmful fats for man and are the main components in beef and mutton tallow.
Oils: Liquid at room temperature, formed mainly by unsaturated fatty acids (oleic acid, palmitoleic acid, linolenic acid, etc.

3.1.2 Classification of fats

Fats by their origin are divided into:

Vegetable fats: “They come from the fruits and seeds of oilseeds, not being entirely edible, especially olive oil stands out.

Animal fats: This group includes butter, lard, tallow, and oils from marine animals.

3.1.3 Fat quality

The quality of the fat depends on the content of free fatty acids, moisture, color, odor and hardness. Common fatty acids found in plant lipids range from C12 - C18. The melting point determines whether the triglyceride is liquid or solid at room temperature. The melting point depends primarily on the degree of unsaturation and to a lesser extent on the chain length of the fatty acids. Plant triglycerides typically contain 70-80% unsaturated fatty acids and tend to remain in a liquid state (oils) at room temperature. On the other hand, animal fats contain 40-50% saturated fatty acids and tend to stay in a solid state (fat or tallow).

Generic term for a class of lipids produced by biosynthetic processes in animals and plants. They are formed by the union of three fatty acids with glycerin through an esterification reaction. For this reason, they are also called triglycerides or triacyl glycerides

All fats are insoluble in water, and soluble in organic solvents such as ethyl ether, n-hexane, chloroform, etc., with a density significantly less than unity (they float on water).

3.1.4 Environmental problem caused by the dumping of used edible oils

In the global environmental problem, used vegetable oil is one of the residues that is not handled correctly, due to ignorance of the environmental effects towards its surroundings, and the consequences of dumping the oils in the sinks. that goes directly to the drainage or septic tanks without receiving prior treatment, which has harmful consequences for the environment and the bodies of water that are close to their homes. This residue is generated by subjecting edible oils to high cooking temperatures, after which this oil is no longer suitable for further frying.

Used cooking oil is currently one of the main causes of contamination of urban wastewater, since once used and reused, it is discharged into the sewage network, polluting the environment, producing obstructions and bad odors in the pipes and a large number of environmental problems, as shown in Figure 3.1, when residual oils are mixed with other residues that are poured into the sinks, soaps, food scraps, water, they form solids that when mixed form large obstructions, the figure shows the solidified fat extracted from the drainage system of a neighbor's house, it generated obstruction, and its gray water was not discharged to the municipal drainage system.

Figure 3.1 Solidified grease extracted from the drainage, causing obstruction and bad odors, this was due to the direct discharge of used vegetable cooking oil from a dwelling house into the sink

Source: Own elaboration

Used edible oil and other types of fats also cause problems in the drainage pipes in our houses, clogging them and generating bad odors, and creating an ideal food for the proliferation of rodents and cockroaches, as shown in Figure 3.2 completely. clogged by large oil residue and other debris causing blockage, and damage to the drainage system.

Figure 3.2 This occurs when the oil is poured directly onto the kitchen sink, it is a clear example of what this malpractice causes within the home, economic kitchens, etc.

Source: Own elaboration

And as for the drainage network, and particularly in the rainy season, the reduction in flow due to the accumulation of vegetable oil mixed with soaps and detergents (converted into a solid that adheres to the upper part of the pipes or channels), generates severe waterlogging, see Figure 3.3. The lack of adequate management of used edible oils discharged into the drainage, in the areas of invasions, irregular settlements lacking drainage, go directly to the garbage during the rainy season, leachates, runoffs go to the bodies of water, which are located in those areas, given the hydrology of the state of Quintana ROO, characteristic of the karstity of the limestone that makes it up, representing from tiny cavities to large depressions in where decalcification clays accumulate, in some of which the water table appears (locally called cenotes), it also has floodable areas, the largest of which are located in the northern portion of the state. INEGI. In our own homes, the amounts are smaller, being able to generate an approximate average of two liters per month, which happens with cheap meals, they must produce approximately 5 liters or more per month, if in the cafeteria of the weekly ITCancún a total of approximately 4 liters, this being one of the sources that provide the plant in the production of biodiesel.

What leads us to the lack of specific legislation for the management of oils from edible uses means that the traditional way of disposing of these used oils is to leave them together with other household waste, organic remains, plastics, glass, cardboard, paper, etc. to be removed by the garbage collection service, the destination of this waste being the municipal dumps.

Figure 3.3 Solidified used edible oils generating clogging of wastewater pipes, generated in homes causing economic losses, due to poor disposal of used edible oil residues

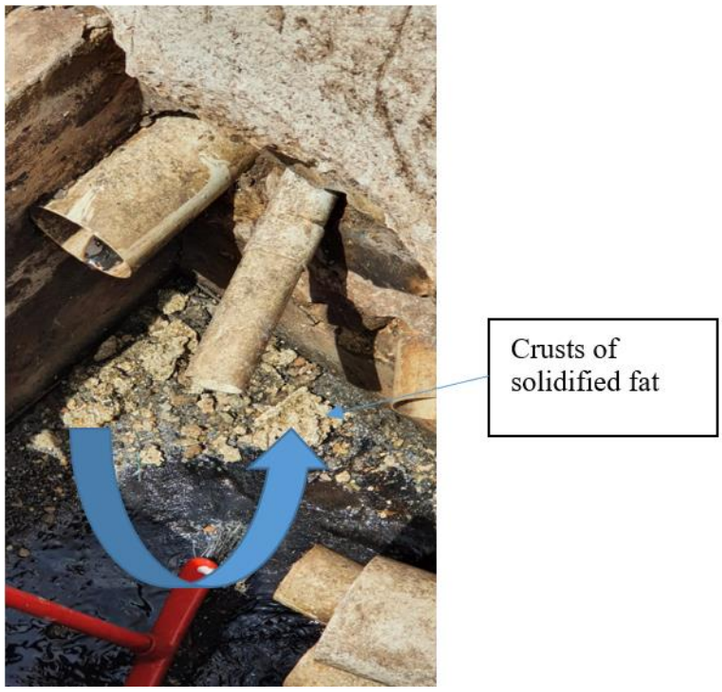

Source: Own elaboration

3.1.5 Problems in water treatment systems due to used cooking oils

In bodies of water, these spills form hard or oily films on the surface that prevent the passage of sunlight, which limits photosynthesis and thus the lack of oxygen causing eutrophication, excess organic matter, bad odors, causing alterations in ecosystems, even the disappearance of these. (NADF-012-AMBT-2015). When improperly, used cooking oils are poured down the sink or into the garbage, or due to spills on the ground, it is absorbed and reaches the groundwater, due to runoff generated by leachates, they are a source of contamination of bodies of water. that are inserted in areas of high population, where some are irregular settlements, that do not have drinking water, electricity and therefore drainage, causing problems in the sanitation networks in the Wastewater Treatment plants in the pretreatment they receive the water the fats, sometimes it is necessary to clean with a degreaser since the fat can clog the holes that are very small, preventing this phase from being adequate and costly to remove the adhesions due to the direct pouring of used cooking oils directly to the sewage system.

The removal of fats and oils can be carried out in primary settlers; dissolved air flotation systems are also used for this purpose, (National Water Commission) they are a source of latent contamination which has not been given enough attention, that this discharge causes that for each liter of used oil can to contaminate 40,000 liters of water, in addition, once cold it hardens and can clog pipes or tubes, as shown in figure No. 2, it is essential that the inhabitants of the Benito Juárez municipality (Cancún), separate the fats and Used edible oils, whether of animal or vegetable origin, fats, rancid or expired oils, and those from grease traps in large restaurant chains, hotel kitchens, also harm the soil, making it less fertile and eroding it, which is why it is It is extremely important to deposit them directly in properly closed containers with lids, in the collection centers destined to be subjected to treatment and disposal (data.se dema.cdmx.gob.mx), González-Canal, Iñigo et all (2015) mention that a liter of used oil has the following average composition of used edible oil:

- 85% oil.
- 10% is water with traces of oil and organic matter.
- 5% are sludge whose composition is 60% oil, 30% organic matter and 10% Water.
- Relative density: 0.91.

Uses of used edible oils.

Used edible oils are used in the production of soap, liquid soap as a recycling method and why not generate a circular economy for them.

Development of biodiesel as a clean alternative energy at the international level, this is since it reduces the environmental impact as an alternative to contribute to reducing the carbon footprint in the reduction of fossil fuel consumption day by day new research is carried out to improve production and improve the methods of obtaining.

Glycerin is a by-product of the production of biodiesel, which can also be used in the soap industry, giving it a purification treatment to eliminate traces of soda and alcohol. Waxes, candles, organic fertilizer among others.

Regulations governing the disposal of used edible oils

The Secretariat of the Environment (SEDEMA) of the Government of Mexico City published on June 12, 2018, in the Official Gazette of the capital, the Environmental Standard for the Federal District NADF-012-AMBT-015, which establishes the conditions and technical specifications for the comprehensive management of waste fats and oils of animal and/or vegetable origin in the territory of Mexico City.

Official Mexican STANDARD NOM-068-ECOL-1994, which establishes the maximum permissible limits of contaminants in wastewater discharges to receiving bodies from the edible oil and fat industry of animal and vegetable origin.

The problem of used oil waste, as well as that of urban solid waste in general, should address the recommendations of the Waste chapter of the so-called Agenda 21, Rio 92 Earth Summit, regarding the "Ecologically Sound Management of Solid Waste and Sewage Related Issues (Earth Summit 2002)

3.2 Methodology

The application of the surveys was carried out using the snowball statistical treatment, non-probabilistic sampling. And convenience sampling, non-probabilistic sampling, for low-incidence populations and on this occasion for individuals that are difficult to access because they are areas of irregular settlements New Millennium, New Jerusalem, and the selected individuals allow the sample size to grow as that the selected individuals invite their acquaintances to participate, regions 226, 249, 238, 235,233, see the location map, this was the treatment carried out on the samples from these regions, given the epidemiological conditions that emerged in the years 2020-2021, they are practically newly created regions, with a lack of environmental policies, the lack of regulation directly affects nature, causing environmental damage in its surroundings. A total of 100 surveys were applied, supported by the students who lived in those areas, using the statistical treatment.

Which consisted of a total of 10 questions, in situ, to the people in charge of the household, economic kitchen business, which allowed to collect information in a clear way in both sampled points in order to know the disposal and elimination of waste of edible oils. with a type of qualitative and quantitative approach forging an analysis of the field work carried out. With the participation and collaboration of students who live on the outskirts of the regions, superblock settlements, in an organized fifteen-day process given the health contingency conditions due to COVID-19.

The objective of this work was to know the management of edible oil residues in households and economic food. The information derived from this survey made us aware of the management of this waste that generates high pollution due to spills in kitchen drains and thrown in the garbage. Generating environmental problems due to the poor disposal of the edible oils used in the frying process.

Figure 3.4 Map of the regions that served as a sample for the application of the surveys

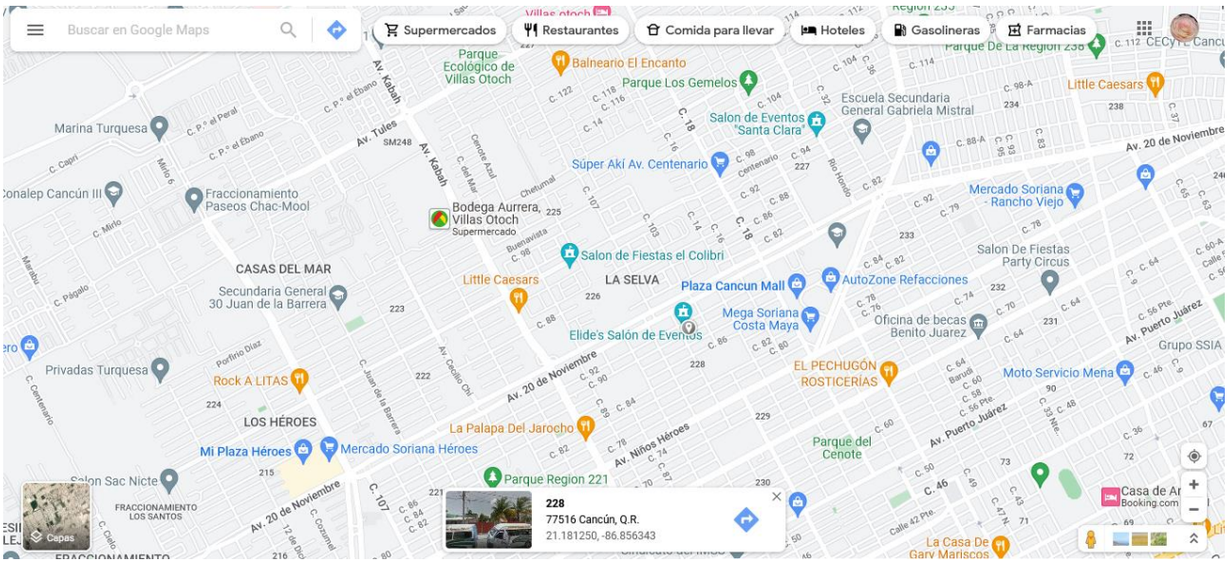

Source: Own elaboration

3.2.1 Survey design

The collection and analysis of data was carried out a survey with 10 questions, addressed to housewives, people in charge of economic kitchens, and the disposal, storage of used edible oils, if there is a body of water close to their home which, due to runoff, may be contaminated by the poor disposal of oils and/or discharges, as well as knowing the area or region where there is a poor disposal of used edible oils and therefore the location of said cenotes if they were close to their homes.

3.2.2 Analysis of the applied instrument

Once the interviews were carried out, the respective diagnosis of the problem was carried out, the processing and interpretation of the information obtained was carried out, to determine if the stated objective, as well as the proposed hypothesis, is accepted or rejected, and in this way give an answer. to the question about the final disposal of used edible oils.

3.3 Results

With respect to the data collected from the regions, superblock, and irregular settlements, the results obtained from the application of the survey are presented, which consists of 6 questions, which are quick response, we are interested in the response of housewives who generate waste. of the edible oils used in the cooking or frying process and of some economic kitchens located near the home of the students who supported us with the application of said survey, see table No. 1, due to the health contingency we only refer to some regions, and 2 irregular settlements, we leave the superblocks for another job, and for protocol and protection of the students. See table 3.1.

Table 3.1 Surveys applied by IT Cancún students, according to the area where their home is located, the questions of interest for the stated objectives are shown

Questions	Answer
What do you do for a living?	a) Housewife b) sale of food (cheap kitchens)
The cooking oil once it has been used in the frying process where it is disposed of or disposed of	a) I take it to a collection center b) I throw it in the drain c) throw it in the trash
What type of container do you use to keep (store) the oil once it has been reused	a) Glass jars b) Plastic bottles c) I reuse detergent bottles e) I reuse large mayonnaise jars d) I don't store it
How long do you store cooking oil before discarding	a) One week b) One month until the container is full c) 15 days d) I don't store it
How many liters of oil do you use per week approximately	a) 1 to 2 liters per week b) 4 to 5 liters per week
Near your house there is a cenote, wetland	a) Yes b) No

Source: Own elaboration

The disposal of used edible oils, and if there are bodies of water close to their homes, obtaining 45% of the total population that, if there is any body of water, and by runoff and the type of hydrogeology of the Yucatan Peninsula there are leachates that are filtering directly towards said bodies as can be seen in figure no.5, due to the disposition they make of them, it is shown in Table 3.2 and the corresponding graph of question no. two.

Cooking oil once it has been used in the frying process where it is disposed of or disposed of, obtaining that 70% of the total population surveyed disposes of it in the kitchen sink. Table 3.2 shows us the results obtained by the selected regions and the two irregular settlements, which have 0% of taking the used edible oil to the collection centers due to the distance where they are located every 2 months, which is in the recycling case.

Table 3.2 Disposal of used edible oils generated by region and irregular settlement

Irregular settlement region	Ítems	226	249	238	235	233	Nuevo Milenio	Nueva Jerusalén
Housewives	They throw in the sink	32	20	29	23	18	30	34
	They throw it away	16	12	14	26	12	20	21
	Collection center	4	2	1	1	2	0	0
Economic kitchens	They throw in the sink	8	8	4	3	6	6	8
	They throw it away	12	15	10	3	4	6	5
	Collection center	4	3	8	4	5	0	0

Source: Own elaboration

According to the response obtained from the people surveyed, they answered that approximately 70% or more of them throw the oil in the sink once it has been used in the process of frying food, in the region 235 housewives throw the oil to the trash in bags, or they pour it directly on their organic trash, or they leave it outside their house until the trash pick-up. In the irregular settlements they do not have the basic services to cover the minimum needs, so it is the same for them to throw the oil in the sink as it is to throw it in the garbage, see Graphic 3.1.

Graphic 3.1 Disposal of used edible oils by housewives and economic kitchens

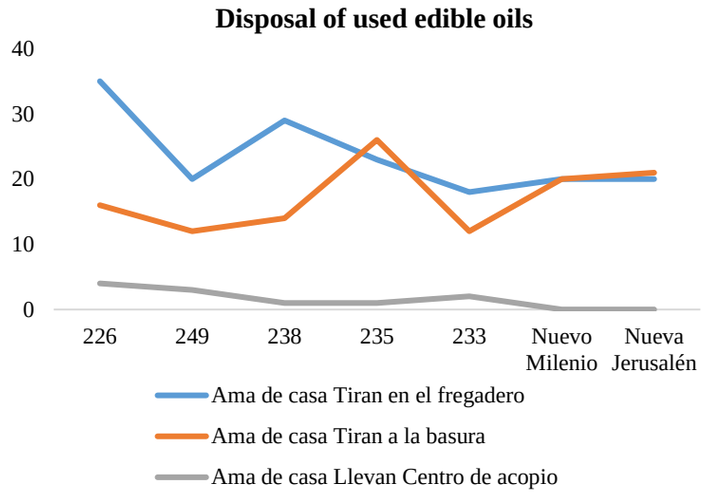

Source: Own elaboration

In Graphic 3.2 it indicates the disposal of used edible oils generated by economic kitchens, the number of economic kitchens surveyed was between 3 to 4 since due to the 2020-2021 health contingency the economy was affected by closing small businesses established, giving rise to the sale of food in residential homes, generating twice the amount of used edible oil that is poured into sinks and thrown away, and a null disposal in the collection centers.

Graphic 3.2 Disposal of the edible oils used by the economic kitchens in the regions, irregular settlements, it is observed that said residues are thrown in the garbage, in bottles, in plastic bags, or dumped directly into the garbage

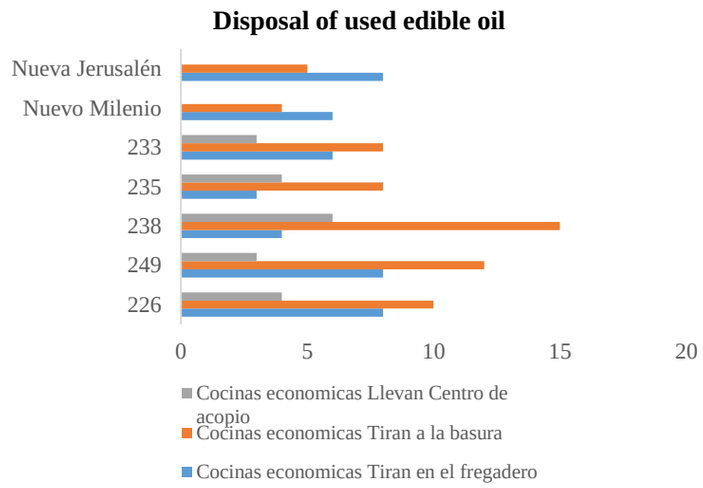

Source: Own elaboration

The answers to the question near where you live is there a body of water, was that 60% were affirmative. in region 235 there is a cenote that is located in the urban area as shown in Figure 3.5, which are areas that have adequate drainage for which the dumping of used edible oils in the sinks, or they throw it into garbage, reach the bodies of water by leachates, filtrations by the cavernous type of Geology.

Figure 3.5 Cenote located in region 235 which is within the populated area and lacks environmental policy, there is no drainage system so the disposal of used edible oils should not be adequate

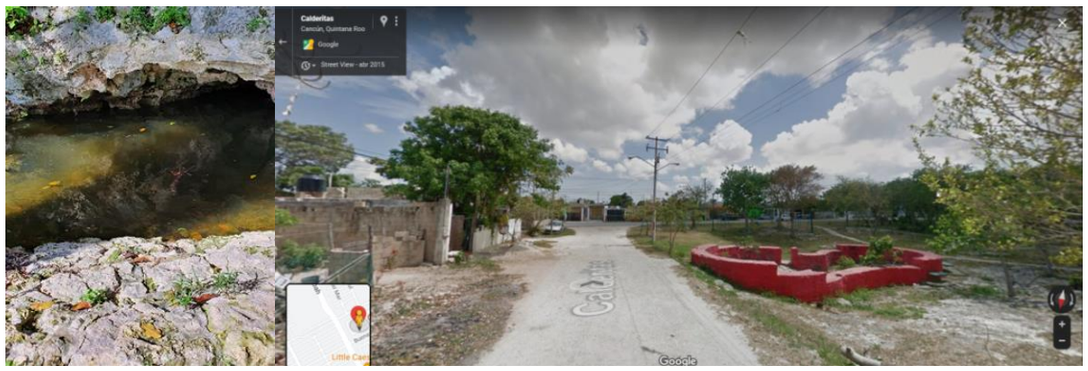

Source: Own elaboration with Google maps

The question about whether they find a body of water near their homes. in region 233 there is a cenote that is located in the urban area as shown in Figure 3.6, which are areas that have adequate drainage through which the dumping of used edible oils in the sinks, or what throw them away, electrical appliances in irregular settlements do not have basic services such as the lack of drainage, they reach bodies of water by leachate, leaks into the cenotes that are cavernous type that can be closed or open.

Figure 3.6 Cenote located at 233 which is within the populated area and lacks environmental policy, there is no drainage system so the region for disposal of used edible oils should not be adequate

Source: Own elaboration

Graphics 3.3 and 3.4 there are bodies of water in the different regions and irregular settlements that, on many occasions, are used as garbage dumps. Causing damage to the ecosystem of water bodies.

Graphic 3.3 Bodies of water (Cenotes, Wetlands) located in the regions, irregular settlements

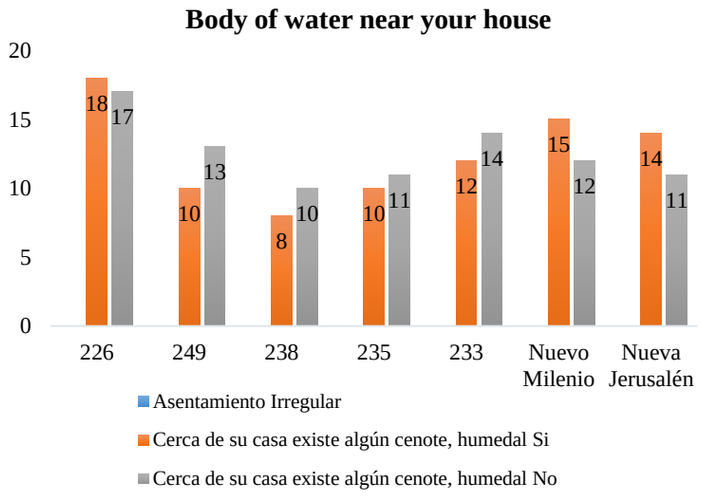

Source: Own elaboration

Graphic 3.4 Bodies of water near your home

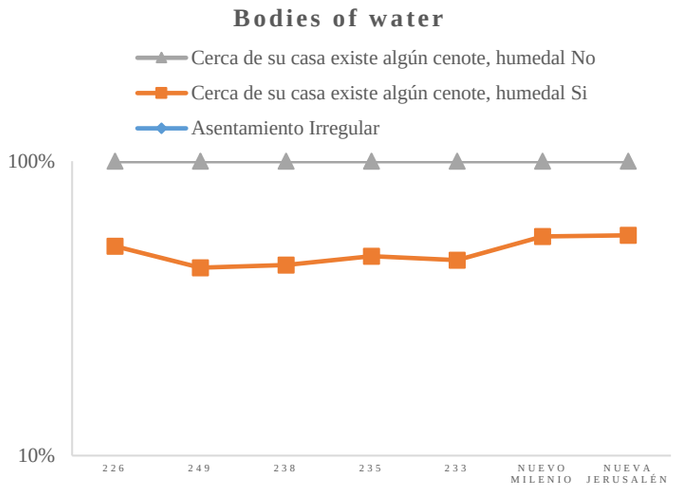

Source: Own elaboration

Figure 3.7 Body of water located within the urban area, region 226

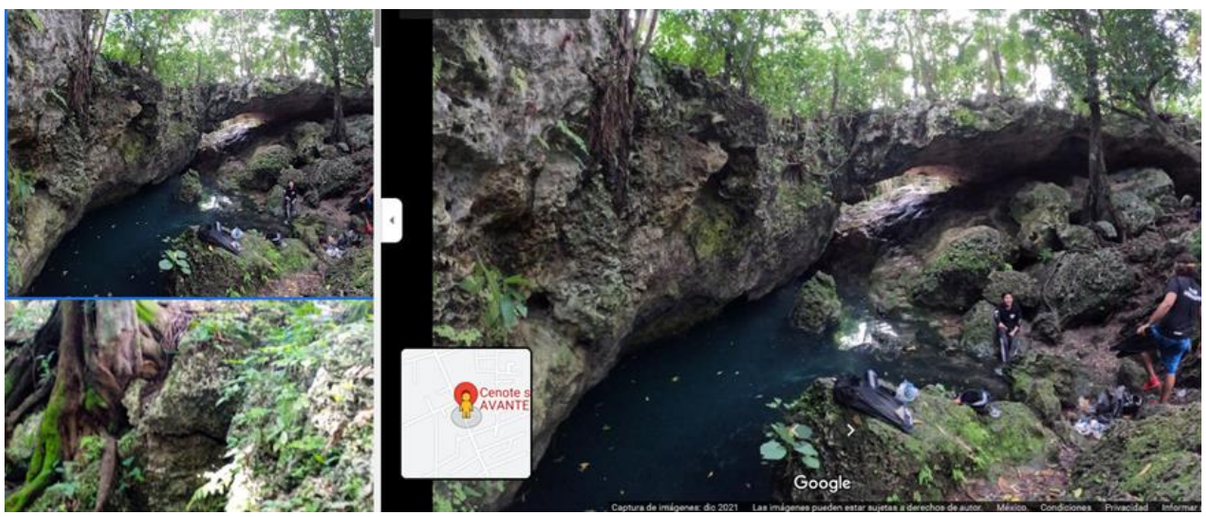

Source: Own elaboration

The number of liters of edible oil during the COVID-19 pandemic increased due to quarantine confinement, the family was at home 24 hours a day. the consumption of food was increasing, as well as fried foods, being one of the responses given by those surveyed, both housewives and those in charge of economic kitchens.

All the people surveyed indicated that they knew the effects of dumping the oil in the drain. The people of the irregular settlements 19 respondents indicated knowing such consequences and 21 said they did not know. Finally, in the regions 223 233 235,226 if they knew and 30 revealed that they did not know them.

The main effects, according to those surveyed, are damage to the pipeline, undervaluing the effects in the waters or the environment in general (Figure 3.1, 3.2 and 3.3). This indicates the need to generate information for housewives as well as those in charge of cheap kitchens, which proliferated as a means of livelihood during the Pandemic, not only about how to manage waste, but also about the reasons why a good disposition of this must be made.

41.81% of those surveyed indicated that space should be allocated for the disposal of used edible oil. 36.88% answered that only a radio campaign be carried out on the disposal of used vegetable oil and not pour it into the drain, kitchen sinks, thus avoiding contaminating the bodies of water that are within the urban sprawl of their regions and irregular settlements, and 16.48% that they be given a workshop on how to take advantage of that oil that they no longer use 65% of those surveyed indicated that they do not store it to later leave it in the collection centers, the disposal of used edible oil is made by pouring it directly into garbage bags or placing it in containers to throw it in the garbage and/or throw it in kitchen clothes. 36.88% answered that they only do not know if throwing away the used edible oil contaminates the cenote that is close to their home.

Graphic 3.5 Liters of oils used in a week by economic kitchens and home

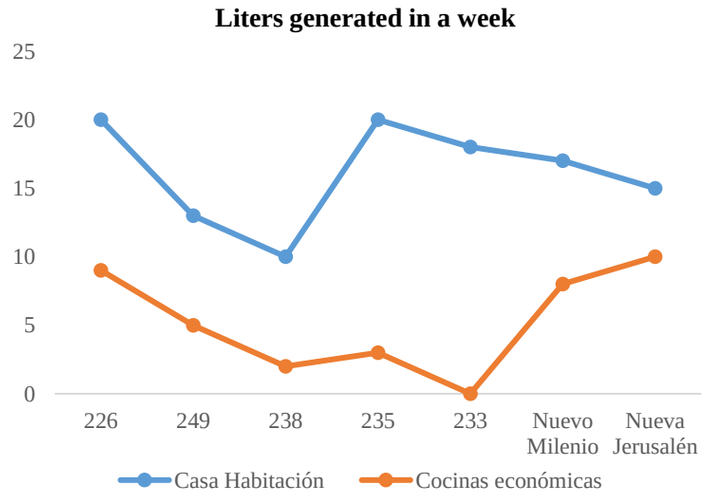

Source: Own elaboration

3.4 Gratitude

To the TECNM/Instituto Tecnológico de Cancún, for the support received to carry out the project, Characterization of edible oils used in the production of biodiesel.

3.5 Conclusions

The degree of affectation caused by the poor disposal of used vegetable oils is very high, this is increased during the COVID 19 health contingency, since the families were locked up, the existence of bodies of water near their home is almost 50%. of those surveyed that if there is a body of water, the other 40% there are no bodies of water near their home, 10% do not know if there is any body of water, cenotes or wetlands, sometimes they are used as garbage dumps, and therefore residues of the oils used in the frying of food that are poured directly into the sinks, few are the people who take the residues of oils to a collection center, another 40% throw it away in plastic bags, or they just throw it straight into the dumpster. The lack of knowledge of the proper management of frying oils, the absence of legislation and the lack of supervision by those charged with environmental sanitation, we are experiencing a problem of lack of water, we must take care of it, and protect the bodies of water since in the medium term they will be sources of water supply. We do not throw garbage, nor use them as a system to eliminate sewage where there are no sanitary drainage services.

3.6 References

Andrade, N., & Moncada, J. (Julio - diciembre de 2020). Manejo de los residuos de aceite comestible en los expendios de comida. Ibarra, Ecuador. Sathiri: sembrador, 15(2), 185-198. https://doi.org/10.32645/13906925.987

Espitia Romero, J. D., & Ortiz Mahecha, J. L. (2022). Formulación del plan de manejo ambiental para la finca Tao ubicada en el municipio de Natagaima-Tolima.

Henao González, A. M. (2022). Impacto ambiental en la microcuenca Cascabel ocasionado por la actividad minera del municipio de Marmato, Caldas.
https://repository.eia.edu.co/handle/11190/5330

González-Canal, Iñigo y González-Ubierna, José Antonio. Aceites usados de cocina. Problemática Ambiental, incidencias en redes de saneamiento y coste del tratamiento en depuradoras. Consorcio de Aguas de Bilbao Bizkaia. Available in: residusrecursos.cat/uploads/activitats/docs/20170427092548.pdf

NADF-012-AMBT-2015. Available in: data.sedema.cdmx.gob.mx

NORMA Oficial Mexicana NOM-068-ECOL-1994, Que establece los límites máximos permisibles de contaminantes en las descargas de aguas residuales a cuerpos receptores provenientes de la industria de aceites y grasas comestibles de origen animal y vegetal. Available in: https://dof.gob.mx/

Gioia Germán. Gestión Integral de Aceites Vegetales Usados (AVU's). Available in: www.placc.org/ramcc/buenas-practicas/item/830-plan-de-bioenergia.html

Mujica Bueno Sayda Estela. Sustentos para que los aceites comestibles residuales (ACR) sean considerados dentro del régimen especial de gestión del residuo de bienes priorizados del Perú. Espacio y Desarrollo N° 32, 2018, pp. 125-136 (ISSN 1016-9148). Available in: https://doi.org/10.18800/espacioydesarrollo.201802.006

La Cumbre de la Tierra. ECO 92U 58-v Universidad para la Paz et al. Visiones Diferentes: Eco'92 / Universidad para la Paz, Consejo de la Tierra, GTZ, IICA y OmCed. - 2 ed. San José, C.R.: University for Peace, 2002. 454 p.:20 cm. ISBN: 9977-925-14-3. Available in:
https://www.bivica.org/files/cumbre-tierra.pdf

Manual de Agua Potable, Alcantarillado y Saneamiento, Operación y mantenimiento de plantas de tratamiento de aguas residuales municipales: Pretratamiento y tratamiento primario. ISBN: 978-607-626-016-6. Comisión Nacional del Agua, Available in: www.conagua.gob.mx

Moya-Salazar Marcia M. Moya-Salazar Jael (2021) Biodegradación de residuos de aceite usado de cocina por hongos lipolíticos: un estudio in vitro.

Revista internacional de contaminación ambiental versión impresa ISSN 0188-4999. Rev. Int. Contam. Ambient vol.36 no.2 Ciudad de México may. 2020 Epub 04-Mayo-2021. Available in: https://doi.org/10.20937/rica.53054

Posada Hernández, J. A. (2022). La apropiación del territorio por parte de la comunidad de la vereda El Cardal frente al ecoturismo y los recursos naturales que presenta el entorno y la Reserva Natural de la Sociedad Civil" Lusitania" del municipio de La Unión Antioquia. Available in: PosadaJenifer_2022_ComunidadApropiaciónEcoturismo.pdf

Rincón Vija, L. A. (2018). Reutilización de aceites de cocina usados en la producción de aceites epoxidados. [En línea] (Trabajo de titulación) *Ingeniería Química*. Available in: https://repositorio.unal.edu.co/handle/unal/68873

Rodríguez Palma, D. (2022). Análisis de riesgos por residuos sólidos en la laguna el limón en la colonia el Carmen de Reforma, Chiapas. Available in: https://hdl.handle.net/20.500.12753/4392

Rodriguez Bustamante, Josué Iván; Meza Gago, Dennys José y Gutiérrez Rodriguez, Iliana Del Carmen. Biodiesel production performance by transesterification from used soybean oil. *Fides Et Ratio* [online]. 2022, vol.23, n.23, pp.149-176. ISSN 2071-081X.

Rojas-Vargas, J. A. & Benavides-Araya, N. (2019). Diagnóstico de la gestión de los aceites usados de cocina en las sodas de las Universidad Nacional de Costa Rica. En Y. Morales-López (Ed.), Memorias del I Congreso Internacional de Ciencias Exactas y Naturales de la Universidad Nacional, Costa Rica, 2019 (e111, pp.1-9). Heredia: Universidad Nacional. Doi http://dx.doi.org/10.15359/cicen.1.19 ISBN: 978-9968-9661-6-0

Urda y Mg Harold Chirinos, Bocardo Delgado Edwin: Characterization off Recycled Edible Oils in their Physicochemical Properties as a Source of Bioglycerin and Biodiesel, in the city of Arequipa Digital Object Identifier (DOI): http://dx.doi.org/10.18687/LACCEI2020.1.1.204
ISBN: 978-958-52071-4-1 ISSN: 2414-6390

Chapter 4 Evaluation of activated carbon from cactus residues in the colour removal process in synthetic water

Capítulo 4 Evaluación de carbón activado de residuos de nopal en el proceso de remoción de color en agua sintética

URBANO-HERNÁNDEZ, Marta†, OJEDA-CASTILLO, Valeria, PRADO-SALAZAR, María del Rosario*

Universidad Tecnológica de Jalisco, División de Química Aplicada, México.

ID 1st Author: *Marta, Urbano-Hernández* / **ORC ID:** 0000-0002-2897-6158

ID 1st Co-author: *Valeria, Ojeda-Castillo* / **ORC ID:** 0000-0002-1397-0589, **CVU CONACYT ID:** 417629

ID 2nd Co-author: *María del Rosario, Prado-Salazar* / **ORC ID:** 0000-0002-6366-1944, **CVU CONACYT ID:** 100541

DOI: 10.35429/H.2022.6.1.40.46

M. Urbano, V. Ojeda and M. Prado

* mprado@utj.edu.mx

A. Marroquín, L. Castillo, S. Soto, L. Cruz. (Coord.) CIERMMI Women in Science TXIX Biological Sciences. Handbooks-©ECORFAN-México, Querétaro, 2022.

Abstract

The removal efficiency of activated carbons prepared from *Opuntia* spp. cladodes in the adsorption of Crystal Violet from the synthetic wastewater was investigated in a 3^2 factorial design (two factors and three levels). *Opuntia* spp. powder was processed into activated carbon by carbonizing at 650 ºC and activated with acetic acid (60% v/v) for 1 h. Then, synthetic solutions of crystal violet were prepared and the adsorption process was carried out by varying initial crystal violet concentration and carbon activated dose, at room temperature. The results showed that 77.8% of adsorption of crystal violet from the syntethic water and an adsorption of 622.3 mg/g at room temperature and 10 min of contact.

Dyes, Remotion, Wastewater, Cristal-violet

Resumen

Se investigó la eficacia de eliminación de carbones activados preparados a partir de cladodios de *Opuntia* spp. en la adsorción de Violeta de Cristal de las aguas residuales sintéticas en un diseño factorial de 3^2 (dos factores y tres niveles). El polvo de *Opuntia* spp. se transformó en carbón activado mediante carbonización a 650 ºC y se activó con ácido acético (60% v/v) durante 1 h. A continuación, se prepararon soluciones sintéticas de violeta de cristal y se llevó a cabo el proceso de adsorción variando la concentración inicial de violeta de cristal y la dosis de carbón activado, a temperatura ambiente. Los resultados mostraron un 77,8% de adsorción de violeta de cristal del agua sintética y una adsorción de 622.3 mg/g a temperatura ambiente y 10 min de contacto.

Colorantes, Remoción, Aguas residuales, Cristal-violeta

4.1 Introduction

A significant impact of dyes is observed in the environment due to their important production of several goods, notably papers, textiles, plastics, leather, rubber, cosmetics, and food. For example, the textile industry can produce 7x metric tons of dye annually. The widespread of these dyes and immense utilization increasingly contribute to the wastewater, causing a detrimental effect on the environment. Along with it, the color effluents present in the dyes negatively impact the penetration capacity of the sunlight, which is harmful to the aquatic environment (Al-Shahrani, 2020).

Dyes can be described as colored substances chemically bonded to an applied substrate, conveying the desired color to that material. The dye's chemical bond (fastness) with the substrate can be improved using a mordant. Pigments are also dyeing agents. However, pigments do not chemically bond; rather, they adhere by physical adsorption, covalent bond formation, or mechanical retention. The organic dye molecules comprise delocalized electronic systems with conjugated double bonds that possess exclusive chemistry. It usually consists of a chromophore component, capable of absorbing a visible range of the light spectrum imparting toward color development for the dye molecules, and an auxochrome constituent that generally increases its affinity toward the substrate (Roy and Sahaa, 2021).

Dyes used in industry are classified into three categories of cationic dyes (all base dyes), anionic (direct, acidic, and reactive dyes), and non-ionic (disperse dyes). Cationic dyes, being more dangerous than other types, are widely used. It is reported that 12% of the annual production (about 700,000 tons) of cationic dyes is wasted through industrial water streams polluting the environment. Crystal violet (CV) dye is a cationic triphenylmethane dye with high intensity. It is used in various industries such as pharmaceuticals, paper, textiles, and printing inks (Foroutan *et al*., 2021). CV dye is more toxic than negative dye and, if present in water, can reduce the penetration of sunlight and disrupt the process of photosynthesis. In addition, CV dye in certain concentrations can cause various diseases and illnesses such as respiratory failure, eye irritation, increased heart rate, skin irritation, blindness, cyanosis, cancer, and mutagenesis (Essandoh *et al*., 2021, Mittal *et al*., 2021). Therefore, removing the CV dye from industrial wastewater streams is necessary before entering the environment.

In Mexico, arid and semi-arid lands constitute 49.20% of the national territory. Therefore, Mexico is also considered one of the main diversity centers of cacti. There are 586 species of cacti and the highest number of native species in Mexico (Ortega-Baes *et al*., 2010). The cacti of greatest economic importance globally are the *Opuntia spp*., commonly named "nopales". There is a big interest in valorizing nopales; for example, it has been used as reagent material in wastewater treatment (Vishali and Karthikeyan, 2015; Barbera and Gurnari, 2018). The production of nopales for consumption generates waste at agricultural and industrial levels. For example, in Mexico City, each year dethroning process of nopal generates around 40,000 tons of waste (Marin-Bustamante *et al*., 2017). This can become a focus of contamination (insects and microorganisms) (Colín-Chávez *et al*., 2021)

On the other hand, to improve the quality of water bodies, the recent modifications in Mexican regulations have included the removal of color in wastewater, which is why industries need to implement efficient, cheap, and sustainable treatments. That is why the objective of the present study was to evaluate the efficiency of crystal violet removal from aqueous solutions using high surface area activated carbon prepared from *Opuntia* spp. cladodes by chemical activation of acetic acid as a cheap and readily available adsorbent.

4.2 Metodology

4.2.1 Sample preparation

First, spines were removed from the *Opuntia* spp. cladodes (referred to now as nopal), then the cladodes were washed and cut into 1-2 cm squares and dried in an oven at 100° C for 24 h. Grinding was carried out in an industrial blender until a homogeneous powder was obtained. The powder was sieved to retain the particle sizes <1 mm.

4.2.2 Activated carbon

Cactus powder with particle sizes less than 1 mm was taken. The impregnation was carried out with a 1:1.5 ratio of powder: acetic acid (60% v/v), and subsequently, the temperature was brought to 650 ºC and maintained for one h.

4.2.3 Crystal violet dye

Synthetic water was prepared with Crystal Violet Dye ($C_{25}H_{30}CIN_3$ CAS#548-62-9) and distilled water. A calibration curve was arranged for the Crystal Violet dye. Nine points were used: 0, 400, 800, 1200, 2000, 4000, 4800, 5600, and 6400 ng/ml; the absorbance was measured at a wavelength of 590 nm using a visible spectrophotometer (Thermo Fisher Scientific type Genesys 20 4001/4). The equation of the curve $y = 163.91x - 0.0716$ was obtained with a linear fit of $R^2 = 0.9907$.

Figure 4.1 Crystal violet

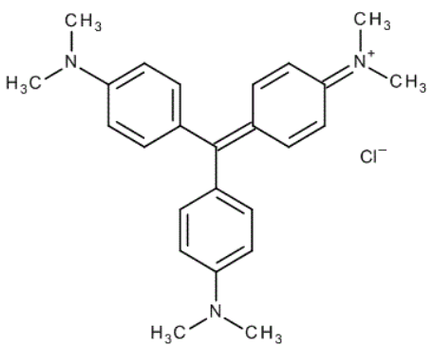

4.2.4 Experimental Design

A 3^2 factorial design (two factors and three levels) was used to optimize the removal of crystal violet dye (CV) in synthetic water. The initial dye concentration and the nopal activated carbon dose were selected as the main independent variables (factors), which varied at two levels (low and high) with central points.

Different combinations of conical tubes with 10 ml of synthetic water with CV and activated carbon of nopal were prepared according to the 3^2 factorial design proposals at room temperature. All the combinations used in the experiment are presented in Table 4.1. After termination of the adsorption experiments, the remaining concentration of CV in each sample dye was investigated as a dependent variable (response). It was measured by UV spectroscopy after 10 min of contact. Subsequently, it was centrifuged to separate the carbon solids from the liquid phase at 3000 rpm for 1 min. Statgraphics Centurion XVI software generated and evaluated the statistical experimental design. The percentage removal (%) was calculated using the following equation:

$$\%\, removal = \frac{(C_0 - C_e)}{(C_0)} \times 100 \quad (1)$$

The amount of adsorption at equilibrium q_e (mg/g) was calculated as follows:

$$q_e = \frac{(C_0 - C_e)}{(V/M)} \quad (2)$$

Where C_0 is the liquid-phase concentration of dye at initial (mg/L), and C_e is the liquid-phase concentration of dye at final (mg/L), V is the volume of the solution (L), and M is the mass of activated carbon used (g).

Table 4.2 Experimental design

Run	Independent variables			
	Coded values		Uncoded values	
	X_1	X_2	X_1	X_2
1	0	-1	8000	300
2	1	-1	16000	300
3	0	1	8000	500
4	-1	0	4000	400
5	1	0	16000	400
6	0	0	8000	400
7	-1	-1	4000	300
8	1	1	16000	500
9	-1	1	4000	500
X_1: CV concentration (ng/ml), X_2: activated carbon dose (mg).				

Source: Own elaboration, 2022

4.3 Results and Discussions

4.3.1 Color remotion

According to the 3^2 factorial design, the color removal tests were prepared using the combinations indicated in Table 4.1. The general description of the experimental test and the observed responses are presented in Table 4.2. The results of the ANOVA showed that the initial concentration of crystal violet color ($p<0.05$) and the interaction of the initial concentration of crystal violet with the dose of activated carbon has a significant effect ($p<0.05$) on the final residual concentration of dye.

Table 4.2 Observed responses to experimental design

Run	Independent variables		Dependent variables		
	X_1	X_2	Y_1	Y_2	Y_3
1	0	-1	3841.1	52.0	124.8
2	1	-1	6525.5	59.2	284.2
3	0	1	4329.2	45.9	183.5
4	-1	0	2340.3	41.5	66.4
5	1	0	5470.1	65.8	421.2
6	0	0	3066.3	61.7	197.3
7	-1	-1	2047.5	48.8	58.6
8	1	1	3554.4	77.8	622.3
9	-1	1	2987.0	25.3	50.7

X_1: CV concentration (ng/ml), X_2: Activated Carbon dose (mg), Y_1: residual concentration of Crystal Violet dye (ng/ml), Y_2: color remotion (%), Y_3: amount of adsorption at equilibrium q_e (mg/g)

Source: Own elaboration, 2022

Statgraphics Centurion XVI software provided an equation involving individual principal factors and interaction factors after fitting these data. The model equation relating the residual color concentration as a response became:

$$Y_1 = 3575.4 + 1362.54 \cdot X_1 - 257.255 \cdot X_2 + 75.2445 \cdot X_1\text{^}2 - 977.671 \cdot X_1 \cdot X_2 + 255.221 \cdot X_2\text{^}2 \quad (3)$$

Graphic 4.1 Main effects plot for CV residual concentration

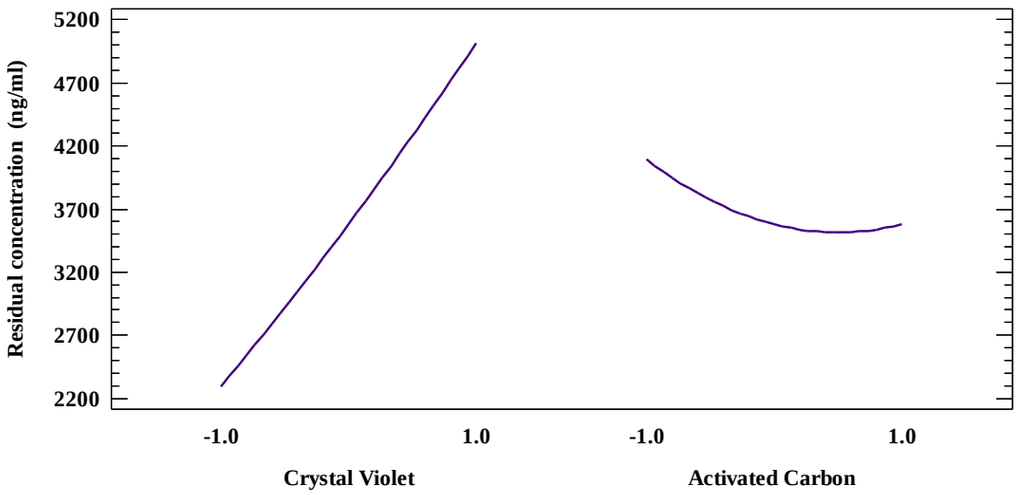

Source: Own elaboration, 2022

Graphic 4.1 shows the main effects of the residual concentration of CV. It is observed that a lower final concentration is obtained with a lower initial concentration of CV; this can be explained by the adsorption capacity of the material and the saturation of its pores. For Prías *et al*., (2015), activated carbon is a compound that contains carbon chains with structures and properties like graphite; its morphological formation is crystalline, carbon is determined by its high porosity, and because it can form extensive surface areas approximately between 500-1500 m^2 per gram of carbon, this is directly proportional to the chemical activation process that is carried out. Foroutan *et al*., (2021) mention that the initial concentration of the CV can have a significant effect on the efficiency and adsorption capacity of the process because it provides the necessary driving force for the mass transfer between the aqueous phase (aqueous solution containing dye) and the solid phase (adsorbent) (Sulyman, Namieśnik,& Gierak *et al*., 2016). On the other hand, a maximum q_e of 622.3 mg/g was obtained at high levels (1) of initial CV and carbon dose, while the minimum of 58.6 mg/g was found at low levels (-1). For various materials and dyes, for example, a q_{max} of 203.34 mg/g is reported for activated carbon from Waste tea activated carbon with Acid Blue 25 dye (Auta & Hameed, 2011) and one of 340.0 mg/g for activated carbon from date stones with Methylene Blue (Jassem *et al*., 2011). This represents a potential material for higher initial concentrations and controlling constant agitation.

Graphic 4.2 Main effects plot of CV residual concentration

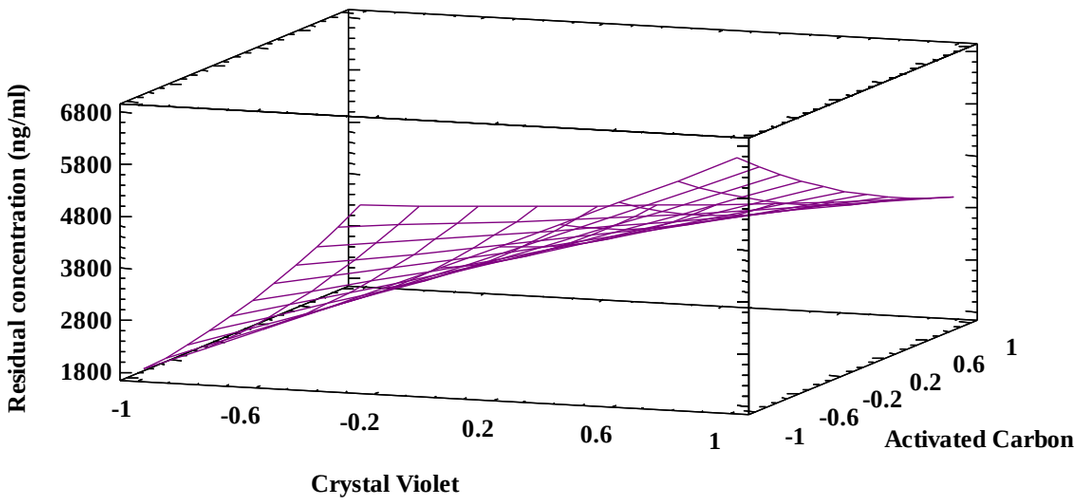

Source: Own elaboration, 2022

Table 4.3 Optimization values obtained by the mathematical model

Factor	Low	High	Optimium
CV concentration (ng/ml)	-1.0	1.0	-1.0
Activated Carbon dose (mg)	-1.0	1.0	-1.0

Source: Own elaboration, 2022

4.4 Conclusions

It was confirmed that the activated carbon obtained from nopal bagasse and activated with acetic acid removes the crystal violet dye at 16,000 ng/ml and below it in synthetic waters. The analysis of the results obtained allows us to establish that the activated carbon reached an efficiency of 77.8% in the conditions handled during the tests. Therefore, it was identified that other levels of activated carbon dose should be experimented with to determine the maximum capacity of adsorption of the active sites and to evaluate the influence of agitation on the adsorbent-adsorbate contact. On the other hand, the material shows a good adsorption potential at room temperature compared to other materials.

4.5 Funding

The authors declare that no funds were received for this work development.

4.6 References

Al-Shahrani, S. (2020). Phenomena of removal of crystal violet from wastewater using Khulays natural bentonite. Journal of Chemistry, 2020. https://doi.org/10.1155/2020/4607657

Auta, M., & Hameed, B. H. (2011). Preparation of waste tea activated carbon using potassium acetate as an activating agent for adsorption of Acid Blue 25 dye. Chemical engineering journal, 171(2), 502-509. https://doi.org/10.1016/j.cej.2011.04.017

Barbera, M., & Gurnari, G. (2018). Quality standards for recycled water: Opuntia ficus-indica as sorbent material. In Wastewater Treatment and Reuse in the Food Industry (pp. 29-47). Springer, Cham. https://doi.org/10.1007/978-3-319-68442-0_4

Colín-Chávez, C., Soto-Valdez, H., Turrado-Saucedo, J., Rodríguez-Félix, A., Peralta, E., Saucedo-Corona, A. R., & Guzmán-Corona, M. (2021). Papermaking as Potential Use of Fibers from Mexican Opuntia ficus-indica Waste. Biotecnia, 23(1), 141-150. https://doi.org/10.18633/biotecnia.v23i1.1315

Essandoh, M., Garcia, R. A., Palochik, V. L., Gayle, M. R., & Liang, C. (2021). Simultaneous adsorption of acidic and basic dyes onto magnetized polypeptidylated-Hb composites. Separation and Purification Technology, 255, 117701. https://doi.org/10.1016/j.seppur.2020.117701

Foroutan, R., Peighambardoust, S. J., Peighambardoust, S. H., Pateiro, M., & Lorenzo, J. M. (2021). Adsorption of crystal violet dye using activated carbon of lemon wood and activated carbon/Fe3O4 magnetic nanocomposite from aqueous solutions: a kinetic, equilibrium and thermodynamic study. Molecules, 26(8), 2241. https://doi.org/10.3390/molecules26082241

Jassem M.S., Abdulkarim M.S., Firyal M.A., Batch adsorption study of methylene blue dye onto date stone activated carbon, Al-Mustansiriyah J. Sci. 2011, 22, 6.

Marin-Bustamante, M. Q., Chanona-Pérez, J. J., Güemes-Vera, N., Cásarez-Santiago, R., PereaFlores, M. J., Arzate-Vázquez, I., & Calderón-Domínguez, G. (2017). Production and characterization of cellulose nanoparticles from nopal waste by means of high impact milling. Procedia engineering, 200, 428-433. https://doi.org/10.1016/j.proeng.2017.07.060

Mittal, H., Al Alili, A., Morajkar, P. P., & Alhassan, S. M. (2021). Graphene oxide crosslinked hydrogel nanocomposites of xanthan gum for the adsorption of crystal violet dye. Journal of Molecular Liquids, 323, 115034. https://doi.org.10.1016/j.molliq.2020.115034

Ortega-Baes, P., Sühring, S., Sajama, J., Sotola, E., Alonso-Pedano, M., Bravo, S., & Godínez-Alvarez, H. (2010). Diversity and conservation in the cactus family. In Desert plants (pp. 157-173). Springer, Berlin, Heidelberg. https://doi.org.10.1007/978-3-642-02550-1_8

Roy, M., & Saha, R. (2021). Dyes and their removal technologies from wastewater: A critical review. Intelligent Environmental Data Monitoring for Pollution Management, 127-160. https://doi.org/10.1016/b978-0-12-819671-7.00006-3

Sulyman, M., Namieśnik, J., & Gierak, A. (2016). Adsorptive removal of aqueous phase crystal violet dye by low-cost activated carbon obtained from Date palm (L.) dead leaflets. Inżynieria i Ochrona Środowiska, 19. https://doi.org.10.17512/ios.2016.4.14

Vishali, S., & Karthikeyan, R. (2015). Cactus opuntia (ficus-indica): an eco-friendly alternative coagulant in the treatment of paint effluent. Desalination and Water Treatment, 56(6), 1489-1497. https://doi.org/10.1080/19443994.2014.945487.

Chapter 5 Removal of aluminium (Al) and lead (Pb) in contaminated water using carboxymethylcellulose (CMC) gel polymer

Capítulo 5 Eliminación de aluminio (Al) y plomo (Pb) en agua contaminada utilizando un polímero de gel de carboximetilcelulosa (CMC)

ANTONIO-CRUZ, Rocío†*, DEL ÁNGEL-MAYA, Flor Elena, PURATA-PÉREZ, Nora Alicia and CÁCERES-JAVIER, José Luis

Tecnológico Nacional de México Campus Villahermosa, Departamento de Ingeniería Química, Bioquímica y Ambiental. Carretera Villahermosa-Frontera km 3.5 Ciudad Industrial, Villahermosa, Tabasco, México.

ID 1st Author: *Rocío, Antonio-Cruz* / **ORC ID:** 0000-0003-3638-5152, **CVU CONACYT ID:** 25705

ID 1st Co-author: *Flor Elena, del Ángel-Maya* / **ORC ID:** 0000-0001-8209-9574, **CVU CONACYT ID:** 942200

ID 2nd Co-author: *Nora Alicia, Purata-Pérez* / (**ORC ID:** 0000-0002-6823-6912, **CVU CONACYT ID:** 328771

ID 3rd Co-author: *José Luis, Cáceres-Javier* / **ORC ID:** 0000-0002-5455-5891, **CVU CONACYT ID:** 813537

DOI: 10.35429/H.2022.6.1.47.63

* rocio.ac@villahermosa.tecnm.mx

A. Marroquín, L. Castillo, S. Soto, L. Cruz. (Coord.) CIERMMI Women in Science TXIX Biological Sciences. Handbooks-

Abstract

Water is a renewable resource, very important for living beings and essential for various activities. However, when it is contaminated, it becomes a non-renewable resource and it is necessary to investigate and know how to preserve it. Nowadays, water is a highly polluted resource, mainly due to human and industrial activities, due to this, a treatment is sought to solve one of the problems, such as the presence of heavy metals such as: lead, cadmium, arsenic and mercury, which are very toxic and accumulate by the organisms that absorb them, which in turn are a source of contamination of food chains that, when ingested by man, cause blindness, amnesia, rickets, myasthenia or even death (Covarrubias and Peña, 2017). On the other hand, aluminum has a wide application in the food, pharmaceutical, paper and construction industries and in the treatment of drinking water and wastewater. However, the possible damage to health caused by the consumption of this element has not been emphasized. One of the diseases that has been associated with the intake of this element is Alzheimer's and there is a risk of developing other conditions (Trejo *et al*., 2004). Currently, the use of clean technologies is being promoted, which are products, tools or processes that seek to reduce environmental pollution. An example are gels, these are cross-linked hydrophilic polymers capable of expanding their volumes due to their high expansion in water and are widely used in wastewater purification. There are different types of absorbent materials such as activated carbon, minerals, zeolites, ion exchange resins, biosorbents (biomasses) and cross-linked polymers. In this research work, a polymer (carboxymethylcellulose gel) was synthesized, using glutaraldehyde (GA) as a binding agent. crosslinking and hydrochloric acid (HCl) as reaction catalyst. The carboxymethylcellulose (CMC) gel was in contact with the contaminated water containing Al and Pb ions, these were retained by the absorption process within the cross-linked network of the CMC gel, and by atomic absorption (AA) analysis. the amount of Al and Pb ions removed from the contaminated water was determined.

Aluminum, Lead, Gels, Carboxymethylcellulose

Resumen

El agua es un recurso renovable, muy importante para los seres vivos y fundamental para diversas actividades. Sin embargo, cuando se encuentra contaminada se convierten en un recurso no renovable y, es necesario investigar y conocer la manera de preservarla. Hoy en día el agua es un recurso muy contaminado principalmente por las actividades humanas e industriales, debido a eso, se busca un tratamiento para resolver uno de los problemas como son, la presencia de metales pesado como: plomo, cadmio, arsénico y mercurio, los cuales son muy tóxicos y acumulables por los organismos que lo absorben, los cuales a su vez son fuente de contaminación de las cadenas alimenticias que al ser ingeridos por el hombre provocan, ceguera, amnesia, raquitismo, miastenia o hasta la muerte (Covarrubias y Peña, 2017). Por otro lado, el aluminio tiene una amplia aplicación en la industria alimenticia, farmacéutica, del papel, de la construcción y en el tratamiento de agua para beber y agua residual. Sin embargo, no se ha dado énfasis a los posibles daños a la salud originados por el consumo de este elemento. Una de las enfermedades que ha sido asociada a la ingesta de este elemento es el Alzheimer y se corre el riesgo de desarrollar otros padecimientos (Trejo *et al*., 2004). En la actualidad se está fomentando el uso de tecnologías limpias que son productos, herramientas o procesos que buscan reducir la contaminación del medio ambiental. Un ejemplo, son los geles, estos son polímeros hidrófilos reticulados capaces de ampliar sus volúmenes debido a su alta expansión en el agua y son ampliamente utilizados en la purificación de aguas residuales. Existen diferentes tipos de materiales absorbentes como carbón activado, minerales, zeolitas, resinas de intercambio iónico, biosorbentes (biomasas) y polímeros entrecruzados, en este trabajo de investigación se sintetizó un polímero (gel de carboximetilcelulosa), utilizando glutaraldehído (GA) como agente de entrecruzamiento y ácido clorhídrico (HCl) como catalizador de la reacción. El gel de carboximetilcelulosa (CMC) estuvo en contacto con el agua contaminada que contiene iones de Al y Pb, estos fueron retenidos mediante el proceso de absorción dentro de la red entrecruzada del gel de CMC, y mediante el análisis de absorción atómica (AA) se determinó la cantidad de iones de Al y Pb eliminados del agua contaminada.

Aluminio, Plomo, Geles, Carboximetilcelulosa

5.1 Introduction

For many years, surface waters such as rivers, streams, lakes and estuaries were used as a vehicle to dispose of all kinds of waste and there was not enough knowledge about the impact that these pollutants could have on ecosystems and human health.

The Santiago River in the state of Jalisco, Mexico, is an example of the above and has generated a socio-environmental conflict because on the health and well-being of the surrounding population. Contamination is identified through the spectacular foamy fall and nauseating waterfall of the Santiago River, by the Juanacatlán Fall. In 2012, Greenpeace Mexico used that image as part of a campaign to denounce toxic rivers, when brave volunteers wearing protective gear entered the river below the waterfall in inflatable canoes and were almost overwhelmed by white foam.

The Santiago River receives municipal wastewater without treatment (or with low levels of treatment), especially discharges in the Guadalajara Metropolitan Area, in addition to industrial discharges, leachate from landfills located nearby, and agricultural runoff.

In addition to this, the problem of contamination in the agricultural area of the Barranca de Metztitlán Hidalgo Biosphere Reserve, Mexico, is caused by the contribution of residual water that is made through the aquifers that irrigate the area, has generated that this site is exposed to a great risk of contamination by heavy metals, hydrocarbons and other contaminants, which remain bioavailable to plants and indirectly there is a high possibility of entering the food chain of animals and finally to humans, with the risks that this would generate for the inhabitants and final consumers of the agricultural products that are generated there.

The most frequent contaminants in water are organic matter, microorganisms, hydrocarbons, industrial waste, heavy metals, pesticides, household chemicals and radioactive waste. These, heavy metals are considered among the most serious pollutants in aquatic ecosystems, since they are generally not removed by natural processes like organic pollutants and they can enter food chains through bioaccumulation, bioconcentration and biomagnification processes. Toxic elements such as Hg, Cd, Cr, Cu and As are accumulated in the sediment where it can be suspended in bioavailable chemical forms producing acute or chronic poisoning. (Tejeda *et al*., 2011).

Heavy metals in high concentrations are harmful to humans, aquatic and terrestrial flora and fauna. The harmful capacity of metals is mainly since most of them are non-biodegradable. For this reason, it is necessary to prevent the entry of toxic metals into aquatic environments and, above all, for industries to reduce their concentration to levels that do not generate toxicity problems. Consequently, controlling the discharge of heavy metals and their removal from the water has become a challenge for this new century.

Recently and in response to this problem, procedures have been developed to try to counteract pollution in water bodies. Conventional methods for the treatment of effluents with heavy metals include precipitation, oxidation, reduction, ion exchange, filtration, electrochemical treatment and membrane technologies, or chemical processes that have the drawbacks of high costs, low efficiency for dilute solutions and in some cases the production of sludge that is difficult to manage or dispose of (Tenorio-Rivas, 2006). One of the new developments for metal removal in recent years is the use of bio-absorption.

Bio-adsorption is a surface property by which certain solids (of biological origin) preferentially capture certain metals from a solution, concentrating them on their surface. For which many materials of biological origin have been studied as adsorbents to remove metal ions from water in industrial effluents (Bayramoglu *et al*., 2002).

Chitosan is a biomaterial that has been used for the adsorption of heavy metals such as Cu (II), Cd (II), Zn (II), Pb (II), Fe (II), Mn (II), Ag (II), this fact is due to the ability of this polymer to undergo chelation reactions (Rhaza *et al*., 2002). One of the disadvantages of using this material is that in solutions with a low pH, chitosan suffers some dissolution. One way to avoid dissolution in an acid medium is by modifying it structurally and functionally through chemical crosslinking reactions.

Carboxymethylcellulose (CMC) is a water-soluble biopolymer derived from cellulose with anionic behavior. This colloid is a physiologically inert, rapidly soluble protector that can form films, as well as being able to thicken, suspend, stabilize and disperse. These properties give it a wide industrial application and a special interest in its application as bio-absorbent and/or coagulant-flocculant for water treatment.

This book chapter aims to synthesize a polymeric material from a cellulose derivative such as carboxymethylcellulose (CMC), which is a CMC gel that has the purpose of absorbing the metals aluminum (Al) and lead (Pb) of the water contaminated with these metals and thus recover the contaminated water and be able to reuse it in other processes.

The techniques that were used for the development of this research work were: (1) Swelling tests, where the optimal absorption time was determined, (2) Infrared spectroscopy (IR) showed the functional groups of the CMC gel before and after being in contact with water contaminated with Al and Pb, (3) Scanning Electron Microscopy (SEM) presented the morphological surface of the CMC gel before and after being exposed to water contaminated with Al and Pb and (4) Absorption Atomic (AA) allowed to quantify the amount of metal eliminated in the water contaminated by the metals under study.

5.2 Background

The increase in recent years of industrial production activities in our country has brought with it environmental problems such as contamination of national waters by heavy and non-heavy metals from extractive and manufacturing companies.

A clear example of the above is the case of the Upper Course of the Lerma River (CARL), which is part of the Lerma-Chapala-Santiago hydrological system, which is a very active industrial area with very important agricultural production and accelerated urban growth. and industrial, which has caused an overexploitation of its aquifers, as well as the contamination of its residual water bodies and agricultural runoff. Much of the wastewater generated is treated in several treatment plants and is later discharged directly into the Lerma River, thus this body has become a collector of industrial and domestic waste that channels, and streams drag. Due to this contamination, the quality of the river's water and sediments have seriously deteriorated, causing in turn an alteration of the trophic chains and the disappearance of fish and other aquatic organisms, surviving in some areas, only those organisms that are highly resistant such as the water lily (Eichhornia crassipies), some species of nematodes and plankton, among others (Government of the State of Mexico, 2005).

Recent research works on the evaluation of the water quality of the Lerma river during a hydrological cycle (Tejeda et al., 2006) show the presence and distribution of heavy metals such as Cr, Mn, Fe, Cu, Zn and Pb in the matter. suspended, with Fe being the element found in the highest concentration (average 4244 mg/kg), Cr and Cu with a measurement of 34 mg/kg, and Zn with an average value of 158 mg/kg; Mn and Pb present an average of 172 mg/kg respectively.

The World Health Organization in 2010, published that Lead is a toxic chemical element with the characteristic of accumulating and affecting numerous parts of the body, such as the neurological, hematological, gastrointestinal, cardiovascular and renal systems. Children are vulnerable to the neurotoxic effects of lead, which even at low levels of exposure to said metal can cause serious neurological damage and in some cases irreversible, there is no level of exposure to lead that is safe for health.

They also published that Cadmium has toxic effects on the kidney and on the bone and respiratory systems and is also classified as carcinogenic to humans. Arsenic in its inorganic form is soluble and highly toxic, the alterations it causes can take years to appear, this is in relation to the level of exposure; The toxic effects of arsenic are the generation of skin lesions, peripheral neuropathy, gastrointestinal symptoms, diabetes, kidney problems, cardiovascular diseases and cancer.

Finally, Mercury is a metal that is toxic to human health and a threat to the proper development of the fetus in the womb. This substance can be presented in various forms: elemental (or metallic); inorganic (for example mercuric chloride) and organic (for example methyl and ethylmercury), each form in which mercury occurs generates different toxic effects, in general mercury affects the nervous, digestive and immune systems, as well as the lungs, kidneys, skin, and eyes.

Heavy metal contamination of water resources is of great interest due to the toxic effects to humans and other animals and plants in the environment. The sources of heavy and non-heavy metals as pollutants are usually industries such as mining, electrolytic finishing, manufacturing of electrical products, among others. For example, Salas et al., in 2019 published that lead is a metal that has had a great impact on environmental contamination. It is found naturally in the soil, air, water, and fresh and processed foods of plant origin. The presence of this metal has caused numerous health problems and death in individuals.

They also reported that irrigation water contaminated by industrial waste or fertilizer remains is one of the main factors of lead contamination, while in industry contamination can occur in different areas such as: glass, plastic, combustion anti-knocks, batteries. (accumulators), etc. In addition, lead is a metal present in the environment and highly harmful to human health, its contamination has spread to fresh, processed foods and even kitchen utensils, causing serious health problems and affecting the quality of life of individuals.

On the other hand, the high concentrations of fluorides in the drinking water of states such as Aguascalientes, San Luis Potosí, Durango, Zacatecas, Jalisco, Hidalgo, Chihuahua, Guanajuato and others, and the fact that aluminum compounds are present in the purification processes of the water with unknown concentrations, there is a risk not yet evaluated, due to exposure of the population to alumina fluoride compounds whose effects occur in the long term, and most of the human intake of aluminum comes from food, through different sources and In the pharmaceutical industry, aluminum is used as the main compound of medicines used to counteract heartburn, diarrhea and other gastrointestinal problems. (Trejo and Hernandez, 2004).

Therefore, it is important to detect measures to prevent contamination, which can help reduce the risk of contamination by these metals (Al and Pb). Currently, research work is in search of clean technologies and every day it grows very rapidly. Given this scenario, research centers, organizations or institutions seek alternatives to develop new or better products or procedures that allow the elimination or reduction of metals present in contaminated water.

5.3 Theoretical framework

Removal of metals in wastewater

Environmental contamination with heavy metals represents one of the biggest problems in the world. Cleanup methodologies are based on energy-intensive engineering processes, which are complicated and expensive. Within these technologies are chemical precipitation, electrodeposition, ion exchange, membranes and adsorption. Of these methods, chemical precipitation, for example with OH^- or S^{-2}, has the lowest operating cost, but is inefficient for dilute solutions. Furthermore, the biggest drawback is the formation of sludge which must be subject to restrictions.

Ion exchange and reverse osmosis are generally effective but have high operation and maintenance costs and are subject to scaling. Adsorption is a promising alternative for this purpose, especially using low-cost adsorbents such as clays, agricultural residues, and shellfish processing residues (Bailey *et al*., 2008).

On the other hand, biopolymers are a potential tool that provides ample opportunity for chemical reactions with metals, soil particles, and other biopolymers. In addition, they may have the ability to create interpenetrating cross-linking networks that manage to encapsulate contaminants (Etemadi *et al*., 2008).

One of these polymeric materials of great interest in recent research for the removal of heavy metal ions present in wastewater has been chitosan [poly (β-1-4)-2-amino-2-deoxy-D-glucopyranose] a derivative of the N-deacetylation of chitin, a natural biopolymer from crustaceans or the biomass of fungi capable of removing ions such as mercury, lead, cadmium, etc. by physical or chemical adsorption. This material has the advantage of adsorption at very low concentrations of the ion, in addition to being widely available and friendly to the environment (Li and Bai, 2009).

Adsorption of metals in aqueous solution

Adsorption is the adherence or retention of a thin layer of molecules of a gas or liquid mixture in contact with a solid surface, because of force fields on that surface. Due to the fact that the surface can present different affinities to the various components of the fluid, causing the composition of the adsorbed layer to be different from the composition of the fluid, this phenomenon is an excellent means of removing contaminants, since the unwanted components of a fluid mixture, in addition to the fact that the amounts removed can be very high compared to other methods (Ruthven, 2003).

In general, there are three stages involved in the sorption of contaminants within the solid sorbent: (1) transport of the contaminant from solution to the sorbent surface (2) adsorption on the particle surface; (3) transport within the sorbent particle (Crini, 2010).

Due to the complexity of the materials used and the specific characteristics (such as the presence of complex chemical groups, small surface area, poor porosity), the sorption mechanism in polysaccharide-based materials is different from other conventional adsorbents. These mechanisms are, in general, complicated because they imply the presence of different interactions. Furthermore, a wide range of chemical structures, pH, salt concentrations, and the presence of bonds often complicate the process (Kumar *et al*., 2009).

Some of the interactions reported for the contaminant adsorption process with polysaccharide-based materials are: ion exchange, complex formation, coordination/chelation, electrostatic, acid-base, hydrophobic, hydrogen bond, physical adsorption and precipitation interactions (Crini, 2010).

On the other hand, for the selection of the best adsorbent, the surface area, the type of solute and the solvent that act in the process must be considered, as well as the possible associations that are established between the adsorbent and the adsorbate. Recognizing the type of association, the process can be classified as chemical or physical adsorption, also called chemisorption or physisorption, respectively (Maron and Pruton, 1978).

If the Van der Waals forces justify the association of the adsorbate on the surface, this process is of the physical adsorption type. In this case, the process releases an amount of heat known as heat of adsorption. It is known that the amount of adsorbed matter, in the case of physical adsorption, increases with decreasing temperature. The process is interpreted as the accumulation of multiple layers of adsorbate on the adsorbent (Tryebal, 2005).

Chemical adsorption is justified by the sharing of electrons between the adsorbate and the adsorbent. With this, the formation of a bond justified by the release of energy known as heat of reaction is proposed. This process is known to restrict adsorption to monolayer formations. The amount of adsorbate fixed in this type of process is greater with increasing temperature (Mc Cabe *et al*., 1998).

Bioadsorption

Bioadsorption is a physicochemical process that includes the phenomena of adsorption and absorption of molecules and ions. This unconventional method mainly seeks the removal of heavy metals in wastewater from the industrial sector, using different materials of biological origin (alive or dead) as sorbent, such as: algae, fungi, bacteria, fruit peels, agricultural products and some types of biopolymers. These materials are inexpensive and are found in great abundance in nature, and their transformation to biosorbent is not an expensive process.

The bioadsorption process involves a solid phase (biomass) and a liquid phase (water) containing dissolved substances of interest to be adsorbed (in this case, metal ions). For the bioadsorption process to be carried out successfully, there must be a great affinity between the functional groups of the biomass and the contaminant, since the latter must be attracted to the solid and bound by different mechanisms.

The phenomenon of bioadsorption of metal ions, using biological materials as adsorbents, can be carried out through various physicochemical and metabolic mechanisms in which the process of capturing heavy metals can differ, and there are two methods:

1. Bioaccumulation: It is the adsorption of metallic species by means of accumulation mechanisms inside living biomass cells.

2. Bioadsorption: It is the adsorption of ions on the cell surface. This occurs by ion exchange, precipitation, complexation, or electrostatic attraction.

The bioaccumulation process involves a first stage that is bioadsorption, however, it is followed by other stages that allow the transport of contaminants through an active transport system that provides energy consumption inside the cell.

Due to the above, it is established that bioadsorption can be considered as the best alternative for the elimination of metallic ions present in wastewater, since it does not use living organisms as biosorbent materials; since these can be affected by the high concentrations of said contaminants, interrupting the adsorption process due to their death. Therefore, by using dead biomass, the rapid deterioration of the biosorbent material can be avoided, and certain variables can even be adjusted to increase the efficiency of the process.

Carboxymethylcellulose

Carboxymethylcellulose (CMC) is a derivative of cellulose with carboxymethyl groups (-CH_2-COOH) well known for its superabsorbent properties. It is a water-soluble anionic polymer that is produced by reacting cellulosic alkali with an esterifying agent known as sodium monochloroacetate. Its production is simpler than that of cellulose ethers because all the reagents are solid or liquid and allow working at atmospheric pressure. It is soluble in water and is very useful for its super absorbent characteristic.

All grades of CMC are white, odorless and non-toxic. Its dispersion and aqueous dissolution are not complicated, however, since it is a polymer it tends to agglomerate and form lumps when it is moistened, for which it is necessary to disperse and dissolve it in water, adding it very slowly and with vigorous stirring.

Among the most important physical properties are its hydrophilic character, high viscosity in diluted solutions, ability to form films, innocuousness, ability to act as a water-retaining agent, null toxicity, biocompatibility and excellent behavior as a colloid, protector and adhesive, make that CMC can be widely used in the pharmaceutical industry for tablet coatings (because it is insoluble in the acidic environment of the stomach but soluble in the basic medium of the intestine), as a drug-carrying gel former, tablet disintegrator and stabilizer for suspensions, emulsions, aerosols and bioadhesives in tablets that adhere internally to the mucus of some part of the body, in agriculture in pesticides and water-based sprays, CMC acts as a suspending agent. Also, it works as a glue after application to bind the insecticide to plant leaves. On some occasions, CMC is used as an aid in the degradation of some highly polluting fertilizers, among others.

Gels

A gel is a three-dimensional network made up of flexible polymer chains that absorb considerable amounts of water. These polymers have well-known characteristics, such as being hydrophilic, soft, elastic and insoluble in water, in addition to swelling in its presence, increasing their volume appreciably while maintaining their shape until reaching physical-chemical equilibrium. Additionally, they can have great mechanical resistance depending on the method with which they are obtained. Its three-dimensional conformation occurs in concentrated aqueous solutions when the initial polymer is capable of gelling with the consequent formation of non-covalent spatial networks. The hydrophilic character is due to the presence of hydrophilic functional groups such as: OH, COOH, CONH, among others. (Arredondo *et al*., 2009).

Since gels are very brittle, it is necessary to improve their mechanical properties in the swollen state. Due to the above, research has been carried out on hydrogels of semi-interpenetrated polymeric networks based on cross-linked polyacrylamide (PAAm) and having poly N-isopropylacrylamine (PNIPAAm) inside, presenting qualitatively good mechanical properties, even in a swollen state (Muñoz y Zuluaga, 2009).

Polymeric materials can undergo temporary deformations when a stress is applied to them. This behavior is called elasticity and is related to the molecular flexibility of polymers when the material is cross-linked (either through chemical or physical bonds) forming a mesh and can withstand much greater stresses without losing its original shape, since intermolecular bonds prevent the displacement of some chains with respect to others.

Some derivatives of natural polymers such as xanthan gum or cellulose (methylcellulose, ethylhydroxyethylcellulose, hydroxypropylmethylcellulose) and certain synthetic copolymers, gelation occurs because of a change in temperature. Cellulose derivatives can chemically cross-link forming a three-dimensional hydrophilic network through intermolecular covalent bonds between polymer molecules. Methylcellulose (MC) has been chemically crosslinked with a di-aldehyde (GA) in the presence of a strong acid (HCl) to generate a hydrogel (Park *et al*., 2001).

Due to their wide field of applications, gels have great technological and economic importance. The presence of water is beneficial for the biocompatibility of hydrogels, but it causes a decrease in the mechanical properties, which is why it is necessary to develop them with a high absorption capacity, while maintaining good mechanical properties.

In general, polymeric gels are capable of being polymerized in long linear chains that chemically or physically intersect to form a three-dimensional network. In the case of chemical gels, using bifunctional monomers in small amounts, crosslinking of the chains is achieved, while in physical gels this crosslinking is due to non-covalent secondary interactions (Muñoz y Zuluaga, 2009).

The two possible states of a gel are: the collapsed state and the swollen state, in the dry state it is called xerogel, but when a solvent is added it swells until it reaches the swelling equilibrium, so that the solvent is retained inside. (Sáez *et al*., 2003).

Aluminum

Aluminum is the third most abundant element in the earth's crust. Even when its toxicity has been demonstrated, geochemical control maintains its bioavailability within harmless parameters. However, natural modifications and anthropogenic interventions contribute to its release, increasing the incidence of diseases in the population and generating harmful accumulations in the environment. The most important sources of non-occupational exposure to aluminum are food, water, certain medications and cosmetics, as well as the containers and utensils used for food preparation (Torrellas, 2013).

Aluminum is found in the natural environment in the form of the ionic species Al^{+3}. In soils it is combined in minerals and rocks of aluminosilicates (feldspars, imogolite, kaolinite), phosphates (variscite), sulfates (jurbanite) and hydroxides (gibbsite) (Soon, 1993).

From a chemical point of view, this ion with a small ionic radius (0.50 Å) and a strong charge produces an intense electric field that attracts electrons. Aqueous solutions of aluminum salts are acidic due to hydrolysis of the Al^{+3} species (Cotton, 1989).

The concentration of the Al^{+3} ion in water is much higher than that of other biologically important cations such as Mg^{+2}, Fe^{+3} or Zn^{+2}. Aluminum is not an essential element for living organisms in ecosystems and has been found to be a toxic agent (Bondy, 2010; Lewis, 1989). The main reason why this toxic ionic species does not affect organisms in their natural environment is because aluminum readily reacts with silicon, the most abundant element on the planet, thereby forming aluminosilicates and bauxite with oxygen. Thus, geochemical control maintains the bioavailability of aluminum within harmless parameters. However, interventions in the environment are increasing its bioavailability and, consequently, causing impacts (Gustafsson, 2001).

Lead

Lead is a heavy metal whose density is 11.34 $g \cdot cm^{-3}$ at 20°C and its atomic mass is 207.19 $g \cdot mol^{-1}$. This metal can be found naturally in the environment, more specifically in the earth's crust. Its proportion in the earth's crust is approximately 15 $mg \cdot kg^{-1}$, whose total amount is estimated at $3.8 \cdot 10^{14}$ tons. Also, it can be found anthropogenicly due to human activities such as the burning of fossil fuels and mining. (Jacobs y Belaire, 2017).

Lead exposure can occur through ingestion of contaminated food and drinking water, and through inadvertent ingestion such as lead paint or dust particles from soil. Furthermore, 95% of inorganic lead is absorbed by inhalation.

This chemical element is toxic, dense and cumulative, which affects both living organisms and humans, and can enter food chains. Currently, the intake of this metal is reduced due to the controls established by regulations at the industrial level, leading to a lower risk of exposure (Londoño *et al*., 2016).

Lead is used as a metal in 40%, and of that percentage, 25% is used for applications in alloys and 35% is used as chemical compounds of both organic and inorganic origin. Some of the main applications are lead oxide in the production of paints and car battery components (Ubillus, 2003).

5.4 Methodology

Synthesis of carboxymethylcellulose gel

In a batch-type glass reactor with a capacity of 500 ml, 10 g of CMC and distilled water were added until a 5% solution by weight was obtained and mixed for 1 hour, maintaining constant stirring and a controlled temperature of 80°C. Subsequently, 4 ml of glutaraldehyde were added as a crosslinking agent and 4 ml of hydrochloric acid as a catalyst for the synthesis reaction, and it was kept under constant stirring at 80°C for a reaction time of 2 hours. After this time, the mixture was poured into polycarbonate molds and placed in an oven at 60°C for 48 hours until a completely dry film of constant weight of the CMC gel was obtained. Finally, the films were removed from the molds and used in the recovery treatment of water contaminated by Al and Pb.

Swelling tests

This technique consisted of evaluating the absorption capacity of the CMC gel, maintaining constant temperature and pH. In this test approx. 200 mg of the gel with dimensions of 1 cm^2 and dried in an oven at 45 °C for 24 hours until constant weight was obtained. Subsequently, they were placed in vials with a capacity of 20 ml and 0.1 ml of distilled water was added every hour for 24 hours until the gel reached its maximum swelling.

These swelling tests were carried out at a temperature of 40 °C and agitation at 120 rpm in a bath with agitation and controlled temperature. The amount of water absorbed by the gels was determined using equation 1, expressed as a percentage (Rivas et al., 2010).

$$H = \frac{(W - W_o)}{W_o} x\ 100\% \quad (1)$$

Where:

H = Swelling, %

W = Weight of swollen gel, g (at different contact times)

W_o = Initial dry gel weight, g

Infrared Spectroscopy (IR)

Infrared spectroscopy has the potential to determine a myriad of substances by virtue of almost any species absorbing in this region, it allows identifying and establishing the structure of organic, inorganic and biochemical species.

The infrared (IR) region of the electromagnetic spectrum covers the upper visible range (7.8×10^{-7} m), but only medium absorption (from 4000 cm^{-1} - 400 cm^{-1}) is used for organic chemical compounds. IR radiation energy levels range from 48 kJ/mol to 4.88 kJ/mol (11.5 to 1.15 kcal/mol). This tool is mainly used in organic chemistry to detect functional groups, identify compounds, and analyze mixtures (McMurry, 2009).

The IR characterization technique was carried out to identify the different characteristic groups of the CMC, which make up the gels, and it was also corroborated whether Al or Pb was found in the polymeric network of the gel. For this analysis, the Varian 640-IR model Fourier transform spectrophotometer was used, using the ATR technique with 12 scans and a frequency range of 4000 - 400 cm^{-1}. In this interval, the main functional groups of the CMC gel were observed, and it was verified if secondary reactions were present.

Preparation of Al and Pb solutions at laboratory level

The calculations were made to prepare the Al and Pb solutions that will have contact with the CMC gel called "substrate" and its function is to remove the two metals to be studied. The preparation consisted of the following: 11.8 mg of $AlK(SO_4)_2$ were weighed out and added to 1 l volumetric flask and deionized water was added. Subsequently, 11.8 mg of $Pb(NO_3)_2$ was weighed and added to another 1 l volumetric flask and deionized water was also added.

15 ml of the Al solution was added to a 20 ml capacity vial, which contains the substrate (CMC gel), this was done in triplicate. The same procedure was performed for the Pb solution. Subsequently, the 6 vials were placed in a bath with controlled temperature and agitation, and the optimal contact time for removing the two metals was found. In addition, the amount of metal absorbed by the substrate was determined using the atomic absorption technique.

Atomic Absorption

In analytical chemistry, atomic absorption spectrometry is a technique for determining the concentration of a given metallic element in a sample and is used to analyze the concentration of more than 62 different metals in a solution. The technique makes use of absorption spectrometry to assess the concentration of an analyte in a sample. It is largely based on the Beer-Lambert law. In short, the electrons of the atoms in the atomizer can be promoted to higher orbitals for an instant by absorbing an amount of energy (i.e. light of a certain wavelength). This amount of energy (or wavelength) specifically refers to one electron transition in an element, and in general, each wavelength corresponds to a single element.

Since the amount of energy that is put into the flame is known, and the amount remaining on the other side (the detector) can be measured, it is possible, from the Beer-Lambert law, to calculate how many of these transitions take place, and thus obtain a signal that is proportional to the concentration of the element being measured.

In this analysis, the amount of aluminum (Al) and lead (Pb) ions present in the water solutions, before and after being in contact with the CMC gel, was determined using the atomic absorption equipment, model AA 240Z, and PSD 120, VARIAN brand, using an acetylene/air gas ratio and a lamp for detection of aluminum and lead. Once the initial (stock solution) and final concentration were determined, the amount of Al and Pb absorbed per dry gram base of the CMC gel, q (mg/g), was calculated using equation 2.

$$q(mg/g) = \frac{V(C_o - C_f)}{m} \quad (2)$$

Where:

q = Amount of metal absorbed per gram of substrate, mg/g

V = volume of metal solution, l

C_o = Initial concentration, mg/l

C_f = Final concentration, mg/l

m = mass of substrate (CMC gel) on a dry basis, g

5.5 Results

Figure 5.1 shows the film obtained from the synthesis of the carboxymethylcellulose gel, with a transparent appearance and flexible to the touch, presenting an adequate homogeneity to be used in the tests of absorption and elimination of metals (Al and Pb).

Figure 5.1 Carboxymethylcellulose gel film

Source: Own elaboration

200 mg of film cut into vials approximately 1 cm^2 was added and placed in an oven at 45°C until a constant weight was obtained, proceeding with the swelling tests and determining the maximum degree of absorption. Table 5.1 shows the results of the weights obtained in the swelling tests, to determine the absorption capacity of the CMC gel with a degree of substitution (DS) of 0.7 at 25°C for 24 h.

Table 5.1 Increase in swelling with respect to time

Time (min)	Swelling (%)
1	43.8212
2	77.7491
3	113.8293
4	163.7598
5	204.9231
6	242.2268
7	277.4690
8	322.0128
9	350.8397
10	391.3876
11	444.0103
12	475.2322
13	473.0119
14	527.1385
15	564.5464
16	610.1092
17	639.4191
18	639.4191
19	709.4710
20	749.9724
21	783.37298
22	816.9908
23	852.2581
24	889.5588

Source: Own elaboration

The data obtained were plotted in figure 5.2 using Excel to observe the behavior of the CMC gel with respect to time, maintaining the temperature and controlled agitation of 40°C and 120 rpm, respectively, showing that the gel absorbs around 889. 5% in a period of 24 hours.

Figure 5.2 Percentage of swelling of carboxymethylcellulose gel

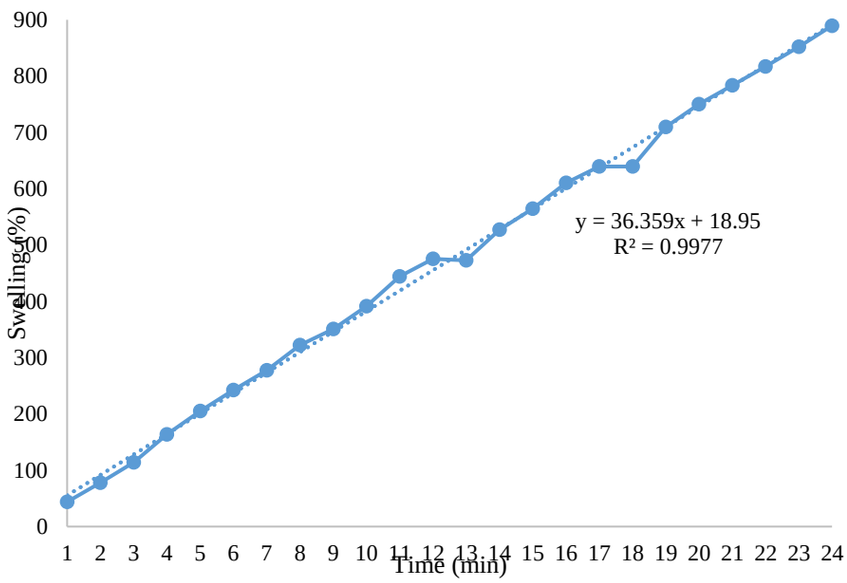

Source: Own elaboration

Figure 5.3 shows the infrared spectrum of CMC gel before being incorporated into water contaminated with Al and Pb, showing the characteristic functional groups, at a wavelength of 3271 cm^{-1} the characteristic –OH group of CMC is observed. the structure of carboxymethylcellulose, while at 2904 cm^{-1} the CH_2 group was found, at 1591 cm^{-1} and at 1417 cm^{-1} there is a stretch band due to the carbonyl and carboxyl groups, respectively. On the other hand, the bending by the -CH_2- groups at 1323 cm^{-1} are shown and finally in the region of 1038 cm^{-1} we find the C-C bonds, characteristic of cellulose.

Figure 5.3 IR spectrum of carboxymethylcellulose gel

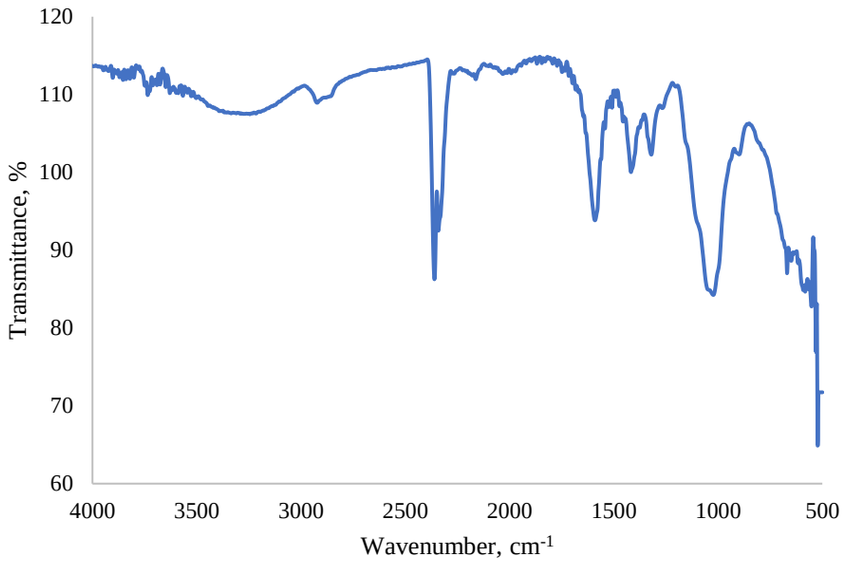

Source: Own elaboration

Figure 5.4 shows the IR spectrum of the carboxymethylcellulose gel after being in contact for 12 h in an Al solution and using 200 mg of substrate (CMC gel), showing a broad band at 3253 cm^{-1} of the group - OH characteristic of the CMC structure, at 2904 cm^{-1} a weak signal of the CH2 group is present, at 1597 cm-1 and 1417 cm^{-1} a stretching of the carbonyl and carboxyl group is shown, respectively. On the other hand, at 1319 cm^{-1} a bending of the -CH^2- group is observed and in the region of 1026 cm^{-1} the C-C bond, characteristic of cellulose, was present.

Figure 5.4 IR spectrum of carboxymethylcellulose gel after exposure to water contaminated with Al metal

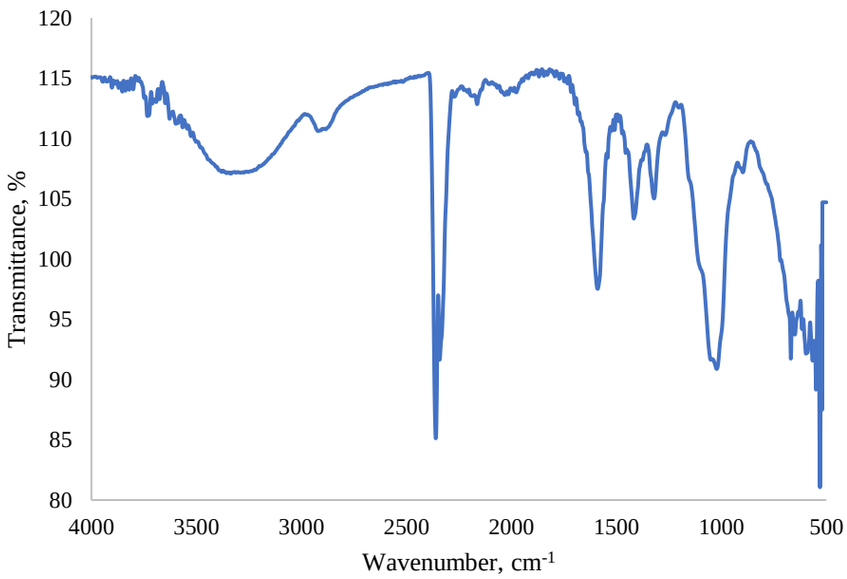

Source: Own elaboration

Figure 5.5 shows the IR spectrum of the carboxymethylcellulose gel after being in contact for 12 h in a Pb solution and using 200 mg of substrate (CMC gel), showing a broad band at 3298 cm^{-1} of the group -OH characteristic of the CMC structure, at 2910 cm^{-1} a weak signal of the CH_2 group is present, at 1587 cm^{-1} and 1419 cm^{-1} a stretching of the carbonyl and carboxyl group is shown, respectively. On the other hand, at 1325 cm^{-1} a bending of the -CH_2- group is observed and in the region of 1049 cm^{-1} the C-C bond, characteristic of cellulose, was present. In addition, at 895 cm-1 a peak appears due to out-of-plane twisting of the carboxyl group dimer.

Figure 3.5 IR spectrum of carboxymethylcellulose gel after exposure to water contaminated with the Pb metal

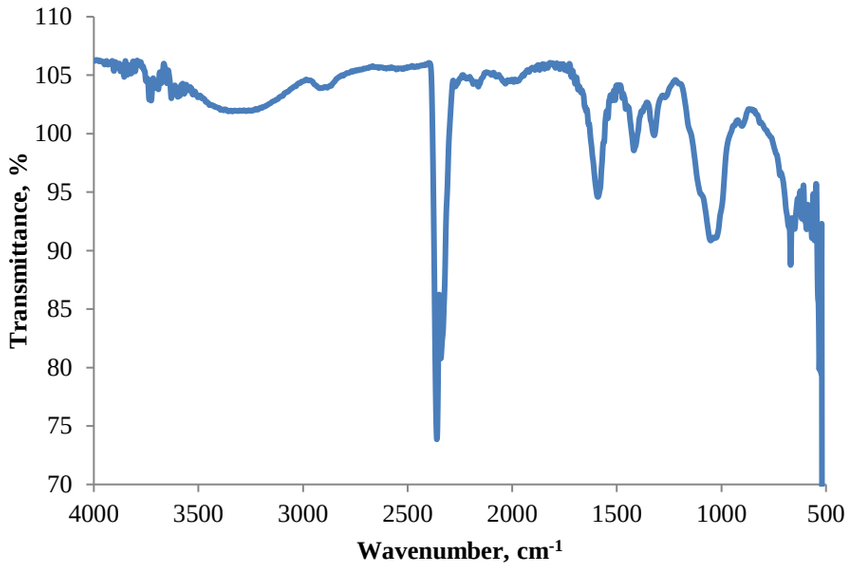

Source: Own elaboration

The effect of the substrate (CMC gel) was studied in each of the prepared solutions of Al and Pb, and it was carried out in triplicate for each solution, keeping the temperature constant at 25°C, agitation at 120 rpm and contact time at 12 h, after that time, the amount of Al and Pb that was removed from the contaminated water was determined, using the Atomic Absorption technique.

Figure 6.6 shows the data obtained by atomic absorption analysis (AA), where the results for metal removal (Al and Pb) are observed, obtaining a reduction of 92.4% and 90.33% for Al and Pb, respectively.

Figure 6.6 Concentration of Al and Pb after being exposed with the carboxymethylcellulose gel

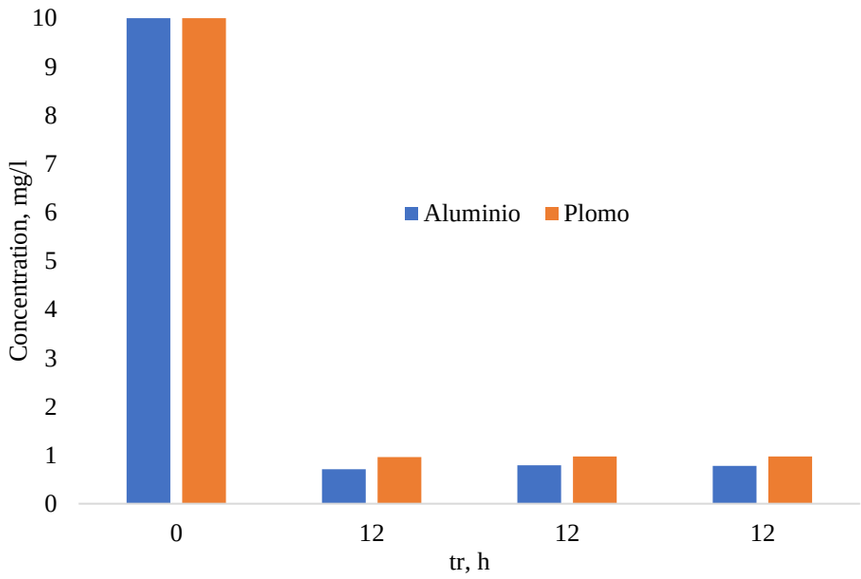

Source: Own elaboration

The initial concentration (Co) of the Al and Pb solutions that were prepared was 10 mg/l; and 15 ml of solution was added to 0.2 g of CMC gel contained in 20 ml vials and kept in contact for 12 h, and then the AA analysis was performed, reaching the final concentrations of Al and Pb of 0.76 mg/ l and 0.97 mg/ml, respectively. Subsequently, equation 2 was used to determine the amount of metal absorbed per gram of substrate, obtaining 9.24 mg/g for Al and 9.03 mg/g for Pb.

5.6 Acknowledgement

The authors wish to thank the Tecnológico Nacional de México (TECNM), for the support granted to carry out this work through the financing granted with code 13437.21-P.

5.7 Conclusions

The CMC gel was obtained according to the conditions described in the methodology, presenting favorable characteristics for the swelling tests, these were performed in triplicate and the values were averaged, obtaining a maximum absorption value of 889.5% in 24 h, after that time. the gel collapses and its structure are no longer cross-linked, that is, the material cannot capture or retain more liquid.

By means of FTIR, the hydroxyl, carboxyl and carbonyl functional groups that are part of the structure of carboxymethylcellulose were observed and the Atomic Absorption analysis showed a retention of Al and Pb of 92% and 90%, respectively. In addition, it was shown that when using 1 g of substrate (CMC gel) around 9 mg of metal is retained per gram of substrate, which is advantageous for treating water contaminated by these metals.

5.8 References

Arredondo Peñaranda Alejandro, Londoño Lopéz Martha Elena. (2009). Hidrogeles, Potenciales biomateriales para la liberación controlada de medicamentos. Revista Ingeniería Química, 3 (5), 83-94. http://www.scielo.org.co/pdf/rinbi/v3n5/v3n5a13.pdf

Bailey, S. E., Olin, T. J., Bricka, R, M y Adrian, D.D. (2008). A review of potentiallylow-cost sorbents for heavy metals. Water Research, 33 (11), 2469-279. https://doi.org/10.1016/S0043-1354(98)00475-8

Baker R. (1980). Controlled Release of Bioactie Materials. *Academic Press Inc*., New York. Web: https://books.google.com.mx/books?hl=es&lr=&id=tNrk9IXSjAsC&oi=fnd&pg=PP1&dq=Controlled+Release+of+Bioactive+Materials&ots=AmfOIXQdZH&sig=f49j54PmzJGfoa9jFe3ahCCDgwM#v=onepage&q=Controlled%20Release%20of%20Bioactive%20Materials&f=false

Bayramoglu, G., Denizli, A., Sektas, S., Arica, M.Y. (2002). Entrapment of lentinus sajor-caju into Ca-alginate gel beads for removal Cd (II) ions from aqueos solution: Preparation and kinetics analysis. Microchem Journal, 72 (1), 63-76. https://doi.org/10.1016/S0026-265X(01)00151-5

Cotton, F. A. & Wilkinson, G. (1989). Advanced Inorganic Chemistry. New York, NY: Oxford University Press.
https://chemistlibrary.files.wordpress.com/2015/05/cotton-wilkinson-advanced-inorganic-chemistry.pdf

Covarrubias Sergio Abraham y Peña Cabriales Juan Jose. (2017). Contaminación ambiental por metales pesados en México: Problemática y estrategias de fitorremediación. *Rev. Int. Contam. Ambie.* 33 (Especial Biotecnología e ingeniería ambiental), 7-21. https://doi.org/10.20937/RICA.2017.33.esp01.01

Crini, Gregorio. (2010). Recent developments in polysaccharide-based materials used as adsorbents in wastewater treatment. Progress in Polymer Sciencie, 30 (1), 38-70. https://doi.org/10.1016/j.progpolymsci.2004.11.002

Etemadi, Omid, I.G. Petrisor, D. Kim, M. Wan, and T.F. Yen. (2008). Stabilizacion of metals in subsurface by biopolymers: Laboratory Drainage Flow Studies. Soil and Sediment Contamination, 12, 647-661. https://doi.org/10.1080/714037712

Gustafsoon, J. P. (2001). Aluminium Solubility Mechanisms in Moderately Acid Bs Horizons of Podzolized Soils. European Journal of Soil Science, 52, 655-665. https://doi.org/10.1046/j.1365-2389.2001.00400.x

Jacobs-Fantassi, B., y Belaire-Cervantes, A.C. (2017). Tratamiento de aguas contaminadas por plomo (II) mediante una técnica en continuo de bioadsorción en columna de corcho. *Trabajo de fin de grado: Universidad Autónoma de Barcelona.*
https://ddd.uab.cat/pub/tfg/2017/190174/TFG_BelaireJacobs_article.pdf

Kumar M., Tripathi B.P., Shani, V. K. (2009). Surface states of PVA/ chitosan blended hydrogels. Polymer, 41 (12), 4461-4465. https://doi.org/10.1016/S0032-3861(99)00675-8

Lewis, T. E. (1989). Environmental Chemistry and Toxicology of Aluminium. Michigan: Lewis Publishers Inc.
https://books.google.com.mx/books?hl=es&lr=&id=VOtklUR71ywC&oi=fnd&pg=PA1&dq=Lewis,+T.+E.+(1989).+Environmental+Chemistry+and+Toxicology+of+Aluminium.+Michigan:+Lewis+Publishers.&ots=7oW8-Fad9Y&sig=1v_RNXjfj0L1vSWiITc2dEZltGU#v=onepage&q&f=false

Li, N., Bai, R. (2009). Copper adsorpotion on chitosan-cellulose hydrogel beads: behaviors and mechanisms. Separation and Purification Technology, 42, 237-247. https://doi.org/10.1016/j.seppur.2004.08.002

Londoño, L. F., Londoño, P. t., & Muñoz, F. G. (2016). Risk of heavy metals in human and animal health. Rev.Bio.Agro. 14 (2), 145-153. https://doi.org/10.18684/BSAA(14)145-153

Maron, S. H., Prutton, C.F (1978). Fisicoquimica Fundamental. Editorial Limusa. México. Capítulo 19. https://conalepfelixtovar.files.wordpress.com/2015/08/fundamentos-fisicoquimica-maron-y-prutton.pdf

McCabe W., Smith C.J y Harriot P. (1998). Operaciones unitarias en ingeniería química 4ª. Edicion. McGraww Hill. España. http://librodigital.sangregorio.edu.ec/librosusgp/14698.pdf

McMurry, John (2009). Organic Chemistry, 5ª. E. Cornell University. Brooks/Cole. USA.
https://gtu.ge/Agro-Lib/McMurry%20J.E.%20-%20Fundamentals%20of%20Organic%20Chemistry,%207th%20ed.%20-%202010.pdf

Muñoz, G.A., and Zuluaga F. (2009). Síntesis de hidrogeles a partir de acrilamida y ácido alilmalónico y su utilización en la liberación controlada de fármacos. Rev. Acad. Colomb. Cienc. 33 (129), 539-548.
https://www.researchgate.net/profile/Gustavo-Munoz-4/publication/275833408_SINTESIS_DE_HIDROGELES_A_PARTIR_DE_ACRILAMIDA_Y_ACIDO_ALILMALONICO_Y_SU_UTILIZACION_EN_LA_LIBERACION_CONTROLADA_DE_FARMACOS_Por/links/55481b220cf2e2031b3863ea/SINTESIS-DE-HIDROGELES-A-PARTIR-DE-ACRILAMIDA-Y-ACIDO-ALILMALONICO-Y-SU-UTILIZACION-EN-LA-LIBERACION-CONTROLADA-DE-FARMACOS-Por.pdf

Park J.S., Park J.W., Ruckenstein E. (2001). Thermal and dynamic mechanical anlysis of PVA/MC blend hydrogels. Adv, Drug Deliv. Revs., 11, 1-35. https://doi.org/10.1016/S0032-3861(00)00768-0

Peppas N.A., Hilt J. Z, Khademhosseini, Langer R. (2009). Hydrogels in biology and medicine: from molecular principles to bionanotecnology. Advanced Materials, 18. 1345-1360.
https://tissueeng.net/lab/papers/Peppas%20et%20al..%20Hydrogels%20in%20Biology%20and%20Medicine%20From%20Molecular%20Principles%20to%20Bionanotechnology.%20Advanced%20Materials.%202006.pdf

Rhaza, M., Desbrieres, J. Tolaimate, A., Rinaudo, M., Vottero, P. Alagui. (2002). Contribution to the study of Cooper by chitosan and oligomers. Polymer, 43(4), 1267-1276. https://doi.org/10.1016/S0032-3861(01)00685-1

Rivas-Orta, V., Antonio-Cruz, R., Rivera-Armenta, J. L., Mendoza-Martínez, A. M., Ramírez-Mesa, R. (2010). Synthesis and characterization of organogel from poly (acrylic acid) with cellulose acetate. *e-Polymers*. 144. https://www.degruyter.com/document/doi/10.1515/epoly.2010.10.1.1613/html

Ruthven, D. M. (2003). Adsorption (Chemical engineering). Encyclopedia of Physical Science and Technoogy. https://doi.org/10.1016/B0-12-227410-5/00013-2

Saéz V., Hernández E., Sanz A.L. (2003). Liberación controlada de fármacos. Revista Iberoamericana de Polímeros, 4 (1) 46-47.
https://reviberpol.files.wordpress.com/2019/08/2003-virginia.pdf

Salas-Marcial, Cindy, Garduño-Ayala, María A., Mendiola-Ortíz, Paulina, Vences-García, Jesús H., ZetinaRomán, Vanessa C., Martínez-Ramírez O.C., Ramos-García, Margarita D.L. (2019). Fuentes de contaminación por plomo en alimentos, efectos en la salud y estrategias de prevención. Revista Iberoamericana de Tecnología Postcosecha, 20 (1). https://www.redalyc.org/journal/813/81359562002/

Shibayama M., Tanaka T. (1993). Volumen pase transition and related phenomena of polymer gels. Advanced polymer Sciencie, 109, 1-62. https://doi.org/10.1007/3-540-56791-7_1

Soon, Y. K. (1993). Fractionation of Extractable Aluminum in Acid Soils: A Review and a Proposed Procedure. https://doi.org/10.1080/00103629309368908

Tejeda S; Zarazúa-Ortega, G; Ávila-Pérez-Mejía, Mejía, A; Carapia-Morales, L. y Díaz-Delgado, C. (2011). Major and trace elements in sedimets of the upper course of Lerma river. Journal of Radioanalytica and Nuclear Chmistry, 270, 9-14. https://doi.org/10.1007/s10967-006-0342-z

Tenorio-Rivas G. (2006). Caracterización de la biosorción de cromo con hueso de aceituna. Tesis Doctoral. Editorial de la Universidad de Granada. España. https://digibug.ugr.es/bitstream/handle/10481/1350/16476736.pdf?sequence=1&isAllowed=y

Torrellas Hidalgo, Rosabel. (2013). La exposición al aluminio y su relación con el ambiente y la salud. Revista Tecnogestión, 9 (1), 3-11.
https://revistas.udistrital.edu.co/index.php/tecges/article/view/5646/7164

Trejo Vázquez, Rodolfo; Hernández Montoya, Virginia. (2004). Riesgos a la salud por presencia del aluminio en el agua potable. Conciencia Tecnológica, (25). https://www.redalyc.org/articulo.oa?id=94402508

Treybal R. E (2005). Operaciones de transferencia de masa. 2ª. Edicion. Mc Graw Hill. México. https://fenomenosdetransporte.files.wordpress.com/2008/05/operaciones-de-transferencia-de-masa-robert-e-treybal.pdf Treyb

Ubillus Limo, J. (2003). Estudio sobre la presencia de plomo en el medio ambiente de talara en el año 2003. *Tesis de Ingeniero Químico*. Universidad Nacional Mayor de San Marcos. https://sisbib.unmsm.edu.pe/bibvirtualdata/Tesis/Ingenie/ubillus_lj/ubillus_lj.PDF

Chapter 6 Polyhydroxyalkanoates (PHA): natural polymers produced by bacteria, an option for the replacement of plastics

Capítulo 6 Polihidroxialcanoatos (PHA): polímeros naturales producidos por bacterias, una opción para el remplazo de los plásticos

FONSECA-BARRERA, Itzel del Carmen†*, MENDOZA-GARCÍA, Patricia Guillermina, PEÑA-MONTES, Carolina and RAMÍREZ-HIGUERA, Abril

Tecnológico Nacional de México - I. T. Veracruz, Unidad de Investigación y Desarrollo de Alimentos, Av. Miguel Ángel de Quevedo No. 2779, Col. Formando hogar, 91987 Veracruz, Ver, México.

ID 1st Author: *Itzel del Carmen, Fonseca-Barrera* / **ORC ID:** 0000-0003-3562-9899, **CVU CONACYT ID:** 950657

ID 1st Co-author: *Patricia Guillermina, Mendoza-García* / **ORC ID:** 0000-00001-6838-0861, **CVU CONACYT ID:** 270773, **SNI CONACYT ID:** 77817

ID 2nd Co-author: *Carolina, Peña-Montes* / **ORC ID:** 0000-0002-4767-1210, **CVU CONACYT ID:** 277236

ID 3rd Co-author: *Abril, Ramírez-Higuera* / **ORC ID:** 0000-0002-1430-2689, **CVU CONACYT ID:** 242658

DOI: 10.35429/H.2022.6.1.64.81

I. Fonseca, P. Mendoza, C. Peña and A. Ramírez

* patricia.mg@veracruz.tecnm.mx

A. Marroquín, L. Castillo, S. Soto, L. Cruz. (Coord.) CIERMMI Women in Science TXIX Biological Sciences. Handbooks-©ECORFAN-México, Querétaro, 2022.

Abstract

Synthetic plastics have facilitated the transport of food and various products; however, their time to degrade has caused severe environmental problems due to their accumulation in seas and rivers. Polyhydroxyalkanoates (PHA) have been proposed as an alternative to synthetic plastics due to their biodegradable characteristics and similar properties to polypropylene and polystyrene. PHA are polymers produced by bacteria such as *Bacillus* spp., *Streptomyces* spp., *Staphylococcus* spp., *Cupriavidus necator*, *R. eutropha* and *Alcaligenes latus* that accumulate the polymer in intracellular lipid granules that serve as their energy source. This review aims to provide an overview of research in recent years on identifying PHA-producing strains, methods for their extraction, factors affecting their production, the study of their structure and film-forming characteristics, and their applications and future developments related to PHA.

Polyhydroxyalkanoates, Intracellular, Bioplastics, Environmental

Resumen

Los plásticos sintéticos han facilitado el transporte de alimentos y de diversos productos, sin embargo, el tiempo que requieren para degradarse ha ocasionado graves problemas ambientales debido a su acumulación en mares y ríos. Los polihidroxialcanoatos (PHA) han sido propuestos como una alternativa para la reducción al uso de sintéticos plásticos debido a sus características biodegradables y propiedades similares al polipropileno y al poliestireno. Los PHA son polímeros producidos por bacterias, por ejemplo, *Bacillus* spp., *Streptomyces* spp., *Staphylococcus* spp., *Cupriavidus necator*, *Rastonia eutropha* y *Alcaligenes latus* que acumulan al polímero en gránulos lipídicos intracelulares que sirven como su fuente de energía. El objetivo de esta recopilación es proporcionar un panorama sobre las investigaciones que se han realizado en los últimos años acerca de la identificación de cepas productoras de PHA, los métodos para su extracción, factores que afecten su producción, el estudio de su estructura y características para la formación de películas; así como las aplicaciones y los futuros avances relacionados con los PHA.

Polihidroxialcanoatos, Intracelular, Bioplásticos, Ambiental

6.1 Introduction

The increase in the production of plastics by industry has caused their accumulation in the seas and soils, causing dramatic changes in the biosphere and affecting the survival of several species (Luengo *et al.*, 2003). The production of plastics has increased significantly, reaching 350 million tons annually. One of the main reasons for this is the advantages of these materials, such as durability, flexibility, and low production cost. However, it is estimated that more than 250 000 tons of plastic float in the sea, negatively affecting marine wildlife (Heidbreder *et al.*, 2019). In most cases, plastic waste reaches the ocean after being mismanaged on land. Plastic pollution has gained political attention, causing challenges for its reduction. Globally, it has been estimated that plastic pollution causes about $13 billion in financial damages annually (Nielsen *et al.*, 2019). It has been reported that the five countries originating the most significant amounts of plastic pollution are China, Indonesia, the Philippines, Vietnam, and Sri Lanka, which are responsible for more than half of the plastic leakage from land to sea. However, the leading cause of these leaks is the export of waste from other countries, so measures have been taken, such as the return of waste to the exporting countries (UNEP, 2014; Gregson and Crang, 2018; Nielsen *et al.*, 2019).

New alternatives have been sought to reduce the production and use of plastics worldwide. Polyhydroxyalkanoates (PHA) are polyesters stored intracellularly by different bacteria as a carbon source. They are made up of fatty acid chains with ester bonds between their hydroxyl group and the carbonyl group of the following monomer (Muhammadi *et al.*, 2015). Due to their characteristics, like conventional plastics, have been taken as an alternative to replace synthetic polymers. According to the ScienceDirect database, the number of publications on PHA production increased from 238 articles in 2011 to 1139 by 2021 (Graphic 6.1). Studies have focused on increasing the yield in the production of PHAs, their biomedical applications, the use of low-cost carbon sources, physicochemical modifications of the polymer to improve its characteristics and the search for new PHA-producing strains.

At the industrial level, countries such as the United States, China, Italy, Canada, and Germany produce polyhydroxyalkanoates such as polyhydroxybutyrate (PHB) and PHB-co-hydroxyvalerate (PHV) copolymers from bacteria such as *Rastonia eutropha*, *Cupriavidus necator*, *Aeromonas hydrophila* and *Pseudomonas putida*. TianAn, a Chinese PHA producing company, has reported PHA production of 10 thousand to 50 thousand tons per year. Nodax, a U.S. company, annually produces 91 thousand tons of different types of PHA. The thermoplastic nature of PHA makes it a candidate for a wide range of standard manufacturing techniques, including injection molding, extrusion, film-forming and blow molding. This compilation aims to provide an overview of the research carried out in recent years on identifying PHA-producing strains, methods for their extraction, factors affecting their production, the study of their structure and film-forming characteristics, as well as applications and future developments related to PHA.

Graphic 6.1 Articles published in Sciencedirect on Polyhydroxyalkanoates

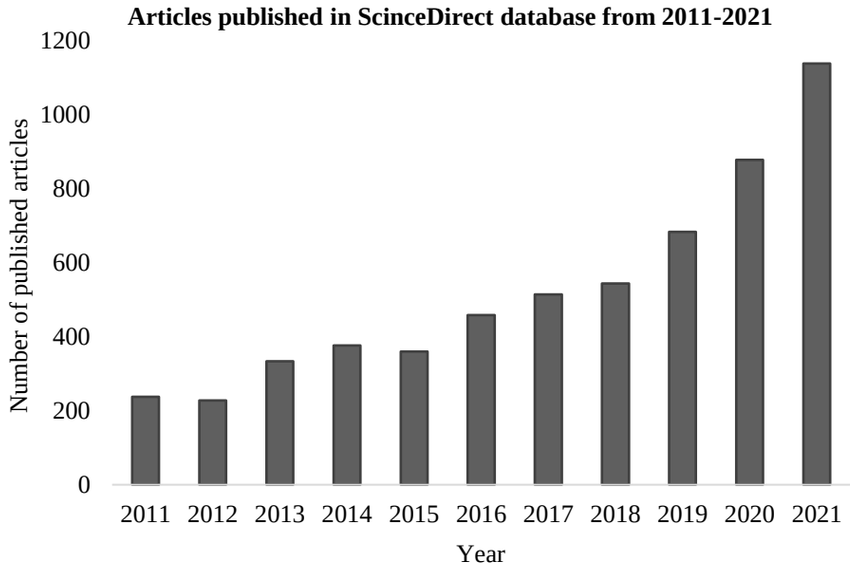

6.2 Chemical structure of PHA

PHAs are polyesters of 3,4,5 and 6 hydroxyalkanoic acids with a general structure shown in Figure 6.1. The radical group is regularly substituted by an unsaturated or saturated alkyl group ranging from C_1 to C_{13}. PHAs are linear polymers that form ester bonds between the carboxyl group of one monomer and the hydroxyl group of the next. More than 150 types of hydroxycarboxylic acids have been identified as PHA monomers. In all PHAs that have been characterized, the hydroxyl-substituted carbon atom has the R configuration due to the stereo-specificity of PHA biosynthetic enzymes. Because of this chirality at the center of the structure, the chemical synthesis of PHAs is complex. The monomer composition, macromolecular structure, and physicochemical properties of PHA vary depending on the microorganism and carbon source used for their growth (Berezina and Martelli, 2014; Muhammadi *et al.*, 2015; Prados and Maicas, 2016).

Figure 6.1 The general structure of PHAs

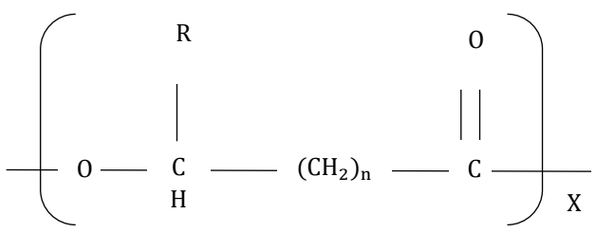

R group	No. of carbons	PHA polymer
Metyl	C_4	Poly (3-Hydroxybutyrate)
Etyl	C_5	Poly (3- hidroxivalerate)
Propyl	C_6	Poly (3-hydroxyhexanoate)
Butyl	C_7	Poly (3-hydroxyheptanoate)
Pentyl	C_8	Poly (3-hydroxyoctanoate)
Hexyl	C_9	Poly (3-hydroxynonanoate)
Heptyl	C_{10}	Poly (3-hydroxydecanoate)
Octyl	C_{11}	Poly (3-hydroxyundecanoate)
Nonyl	C_{12}	Poly (3-hydroxydodecanoate)

*Source: Muhammadi et al.,*2015

According to their chain size, PHA can be classified into short-chain (3-5 carbon atoms), medium-chain (6-14 carbon atoms) and long-chain (more than 14 carbon atoms) hydroxyalkanoic acids. It has been reported that strains such as *Alcaligenes eutrophus* can only synthesize short-chain PHA. On the other hand, *Pseudomonas oleovorans* are associated with the production of medium-chain PHA (Muhammadi *et al.,* 2015). The synthesis of both short-chain and medium-chain PHA has also been reported. For example, in the presence of propionic and valeric acid, *Alcaligenes eutrophus* produces copolymers of 3-hydroxybutyrate acid and 3-hydroxyvalerate acid (Anderson *et al.*, 1990). *Aeromonas caviae* is another bacterial strain that produces a copolymer of hydroxybutyrate and 3-hydroxyhexanoate. Boyadin *et al.* (2008) reported that *Photobacterium leiognathi* and *Vibrio harveyi* produced 2 to 3 PHA heteropolymers (hydroxybutyric, hydroxyvaleric and hydroxyhexanoic acid). As observed in these studies, the type of PHA depends on the producing bacteria; therefore, in the following section, different sources of isolation of PHA-producing strains and some of their yields will be mentioned.

6.3 PHA-producing microorganisms, isolation sources and nutritional factors that affect its production

Some bacteria accumulate substances, such as PHA, when external energy exceeds the cell need for growth. PHA is utilized when external energy input is insufficient to maintain cell growth, division, or viability. About 300 different bacteria, including Gram-positive and Gram-negative bacteria, have been reported to accumulate PHA. These bacteria accumulate PHA intracellularly in lipid granules in the presence of excess carbon sources and limited nitrogen source conditions. Once the microorganism depletes this carbon source, PHA is depolymerized and metabolized to act as a carbon and energy source (Muhammadi *et al.*, 2015; Prados and Maicas, 2016).

Several genera capable of synthesizing PHA have been identified, among which the *Bacillus* and *Pseudomonas* genera stand out. The source of isolation can be soil samples, marine sediments, dairy products, used oils or waste from different industries, for example. Ching *et al.* (2007) isolated bacteria from marine sediments, four of the twenty phenotypically different colonies were positive in the Nile red staining test. The bacteria were PHA producers. They identified by 16S rDNA sequencing that the four isolates belonged to the genus *Vibrio* with 98% identification. In the same year, Jamil *et al.* isolated a PHA-producing strain from sediment samples from the Karachi coast. The 16S rRNA gene analysis identified it as *Pseudomonas* sp. with 94 % homology. Sangkharak and Prasertsan (2012) isolated PHA-producing bacteria from different sources (pickle waste, nitrogen-rich soils, cow and chicken manure, and municipal garbage). In total, fifty strains were isolated and tested positive with Nile blue. Six different genera were identified, including *Bacillus* spp., *Proteus* spp., *Pseudomonas* spp., *Aeromonas* spp., *Alcaligenes sp*. and *Chromobacterium* spp. Nevertheless, the bacterium identified as *Bacillus licheniformis* JN 162418 was determined to have the highest PHA production (6.58 g /L).

In 2019, Alshehrei collected soil samples from Saudi Arabia to determine the presence of PHA-producing bacteria. Twenty strains tested positive for PHA production using Sudan black. It was determined that strain F15 belonged to the *Bacillus* genus and had the highest PHA production (4.3 g/L). Mohammed *et al.* in 2019, isolated two different PHA-producing *Bacillus* species from plastic waste landfills. Both bacteria tested positive using Sudan black B and Nile blue A. They reported that the highest PHA production for *Bacillus* BPPI-14 (49.46 ±2.79%) was obtained using glucose as a carbon source, a temperature of 37 °C and a pH of 7. It has also been possible to isolate PHA-producing strains from oil-contaminated soils. Al-Ardawy and Taj-Aldeen (2020) identified the presence of PHA granules in *Lactiplantibacillus plantarum* isolated from dairy products and *Pseudomonas* isolated from oil. They determined that *Lactiplantilactobacillus plantarum* had the highest PHA production (1.5 g /L) compared to *Pseudomonas* spp. 1 (0.95 g/L).

Isolation sources of PHA-producing bacteria can be varied, and their production conditions can also be a significant effect when considering their yield. Yüksekdag *et al.*, (2007) analyzed different carbon and nitrogen sources in PHB production from *Streptococcus thermophilus* Ba21S; their results showed that the percentage of PHB increased when using sucrose (35.56%) compared to the control (glucose) (12.47%) opposite case when changing the nitrogen source where it decreased from 21.15% (Protease peptone) to 3.69 % when using L-cysteine. Sharma *et al.*, (2012) studied PHA production in a *Pseudomonas putida* LS46 at high and low concentrations of ammonium sulfate (4 g/L and 1 g/L). They determined that the highest production occurred when using nitrogen at low concentrations in a 48h incubation period. Other examples of PHA-producing genus and their isolation source, as well as their PHA production and carbon source used for PHA synthesis, are shown in Table 6.1. Each bacterium synthesizes PHA differently depending on the carbon source and the enzymes involved in the process. In section 6.3, some of the most common routes for PHA synthesis will be described.

Table 6.1 PHA-producing bacteria isolated from different sources and their polymer production yield using different carbon sources

Bacteria	Insulation source	Carbon source	PHA (g/L)	Author
Vibrio MK4	Soil samples from Katch Island.	Sesame oil	4.22	Arun *et al.*, 2009
Lactiplantilactobacillus plantarum CW10 *L. casei* WWD3	Fermented milk Whey	Starch	3.5 3.3	Monilola and Makinde, 2020
Bacillus subtilis MSBN17	Sea sponge Callyspongia diffusa	waste pulp, tamarind powder and palm sugar	2.46	Sathiyanarayanan *et al.*, 2013
Bacillus spp.	Liquid wastewater samples from the "salwa" industry	Fructose	2.2	Ataei *et al.*, 2008
L. casei *L. plantarum* A *L. brevis* C3 *P. halophilus* B1 *S. thermophilus* E1	Different dairy products	Glucose	1.9 0.66 0.86 0.11 0.19	Aslim *et al.*, 1998
Pseudomonas chlororaphis PA23	Soybeans	Nonanoic acid	0.9601	Sharma *et al.*, 2017
Halomonas AT1214	Shrimp shell	Yeast extract	0.270	Simon-Colin *et al.*, 2008
Pseudomonas aeruginosa AU1292	Sediments from the Karachi coast	Yeast extract	0.376	Jamil *et al.*, 2007
Vibrio M20	Marine sediment	Glucose	0.176	Chien *et al.*, 2007

6.4 Metabolic pathways for the synthesis of PHA

A total of 14 pathways have been reported for PHA synthesis (Figure 6.2). Regularly, short-chain PHA is synthesized by pathway I, where two molecules of acetoacetyl-CoA are condensed to one molecule of acetoacetyl-CoA by the enzyme β-ketothiolase (PhaA). Acetoacetyl-CoA is converted to 3-hydroxybutyrate-CoA by the enzyme NADPH-acetoacetyl-CoA reductase (PhaB). Subsequently, the ester bond is catalyzed by PHA synthase (PhaC) action to form poly (3-hydroxybutyrate). In pathway II, the substrates originated from the β-oxidation of fatty acids. In this pathway, different hydroxyalkanoate monomers are generated by the action of (R)-enoyl-CoA hydratase (PhaJ), acyl-CoA oxidase and 3-ketoacyl-CoA reductase (Sharma *et al.*, 2021). The V-XIV pathways are engineered pathways leading to the production of unconventional PHA, for example, the use of a recombinant *E. coli* to produce poly-4-hydroxybutyrate using glucose as a carbon source. This strain contained genes encoding succinate degradation from *Clostridium kluyvery* and PHA synthase from *Ralstonia eutropha*. The native succinate semialdehyde dehydrogenase genes (*sad* and *gabD*) in *E. coli* were inactivated to enhance carbon flux to poly-4-hydroxybutyrate biosynthesis via pathway 5 (Zhou *et al.*, 2012).

Figure 6.2 Pathways for PHA synthesis

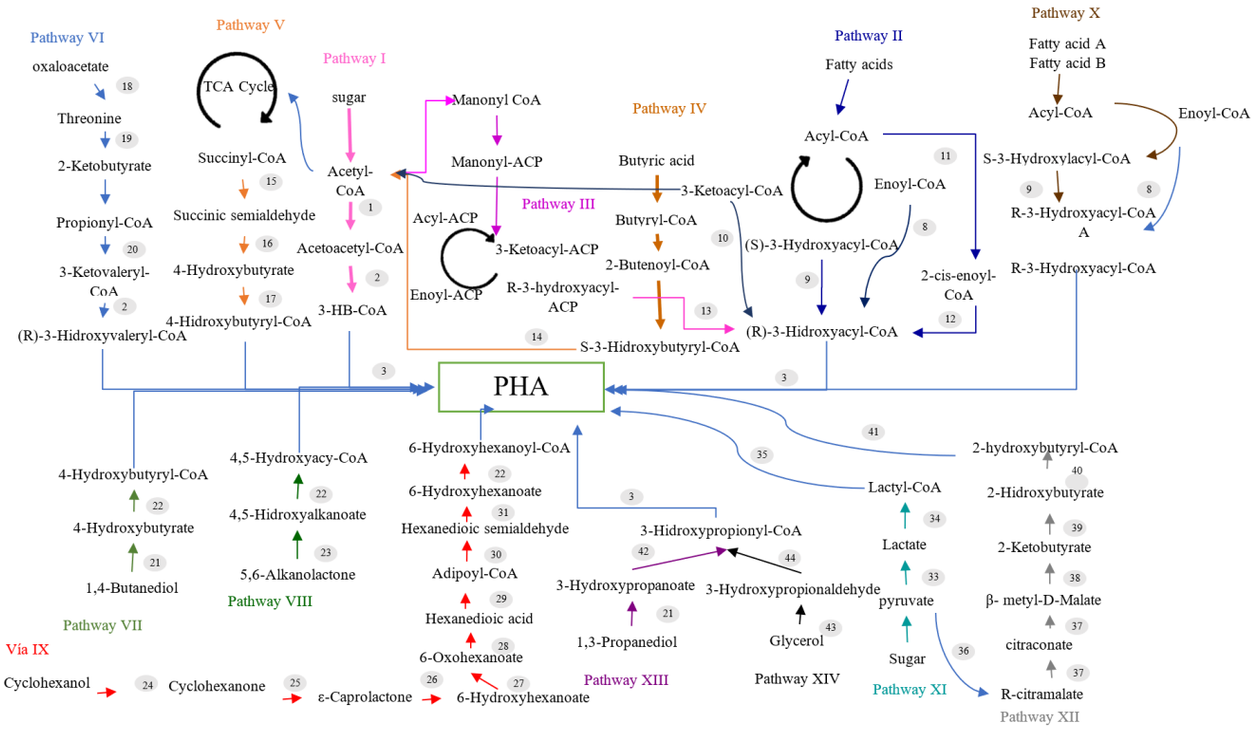

Enzymes for PHA synthesis: 1(β-Ketothiolase);2 (NADPH dependent acetoacetyl-CoA); 3(PHA synthase); 8 (R-Enoyl-CoA hydratase); 9 (Epimerase); 10(3-ketoacyl-CoA reductase);11(Acyl-CoA oxidase, putative); 12 (Enoyl-CoA hydratase, putative); 13 (3-Hydroxyacyl-ACP-CoA transferase); 14 (NADH-dependent acetoacetyl-CoA reductase);15 (Succinic semoaldehyde dehydrogenase); 16 (4-Hydroxybutyrate dehydrogenase); 17(4-Hydroxybutyrate-CoA transferase); 18 (Aspartokinase I, Homoserine kinase, Threonine synthase); 19 (Threonine deaminase); 20 (BktB(PhaA)); 21 (Alcohol dehydrogenase, Aldehyde dehydrogenase); 22 (Hydroxyacyl-CoA synthase, putative); 23 (Lactonase, putative); 24 (Cyclohexanol dehydrogenase); 25(Cyclohexanone monooxygenase); 26 (Caprolactone hydrolase); 27 (6-Hydroxyhexanoate dehydrogenase); 28 (6-Oxohexanoate dehydrogenase); 29 (Semialdehyde dehydrogenase, putative); 30 (6-Hydroxyhexanoate dehydrogenase, putative); 31 (Hydroxyacyl-CoA synthase, putative); 32 (3-Ketoacyl-CoA thiolase, 3-hydroxyacyl-CoA dehydrogenase); 33 (Lactate dehydrogenase); 34(Propionate CoA-transferase); 35 (Type II PHA syhthase); 36(α-Isopropylmalate synthase); 37(3-Isopropylmalate dehydratase); 38 (3-Isopropylmalate dehydrogenase); 39 (2-Hydroxybutyrate dehydrogenase); 40 (Propionate CoA-transferase);41(Type II PHA syhthase); 42 (Propionyl-CoA synthase); 43 (Glycerol dehydratases); 44 (Propionaldehyde dehydrogenase)

Source: Modified from Meng et al., 2014

Each pathway involves several enzymes that play an essential role in PHA synthesis. However, PHA synthase is one of the enzymes in charge of defining the chain length size of PHA. The different PHA synthases are classified into four categories based on their structure, composition and chain length. Class I comprises a subunit that polymerizes short-chain PHA, and class II comprises a subunit that polymerizes medium-chain PHA. Class III and IV are heterodimer enzymes formed by two subunits, class III is constituted by a subunit of PhaC and another subunit of PhaE, and class IV comprises two subunits, one of PhaC and PhaR (Tripathi *et al.*, 2021). PhaC from *Rastonia eutropha* has been known to polymerize PHA monomers consisting of 3 to 5 carbons such as poly(3-hydroxypropionate), poly(3-hydroxybutyrate), poly(4-hydroxybutyrate), poly(3-hydroxyvalerate) and copolymers of hydroxypropionate and 4-hydroxybutyrate).

Once PHA is formed, it is stored in lipid granules inside the cell, where their number and size depend on the producing bacterium. About 8-13 granules ranging from 0.2 to 0.5 µm have been reported for *Alcaligenes eutrophus*. However, in *Pseudomonas oleovorans*, it is estimated to accumulate around one to two large granules (Muhammadi *et al.*, 2015). On the other hand, PhaC identified in the *Pseudomonas* genus can polymerize 6 to 14 carbon monomers (Meng *et al.*, 2014). Once PHA is formed, it is stored in lipid granules inside the cell, where their number and size depend on the producing bacterium. About 8 to13 granules ranging from 0.2 to 0.5 µm have been reported for *A. eutrophus*. However, in *P. oleovorans,* it is estimated to accumulate around one to two large granules (Muhammadi *et al.*, 2015).

The variety of PHA, synthesized by the different pathways, has led to this polymer having physicochemical properties that differ from one other giving them applications in different areas. Some examples of different PHA synthesized and their physicochemical properties will be mentioned in section 6.5.

6.5 Physicochemical properties of PHAs

PHAs are biodegradable thermoplastics that are insoluble in water but soluble in chlorinated hydrocarbons such as chloroform. They have poor resistance to acids and bases. The properties of PHAs differ depending on their chemical composition. In some cases, their properties can be similar to common polymers. The PHB has some characteristics similar to polypropylene (Table 6.2). PHBs found in pure form are brittle because it presents an elongation percentage lower than 15 %. However, they have Young's modulus above 1 GPa, indicating that it is a rigid material (Bugnicourt *et al.*, 2014). The use of a polyhydroxybutyrate/polyhydroxyvalerate (PHB-HV) blend reduces the percentage crystallinity and Young's modulus from 60 % (PHB) to 53 % and from 1700 MPa to 1200 MPa, respectively (El-Hadi *et al.*, 2002). Another author who studied the blend of these polymers was Arcos-Hernandez *et al.* (2013), who studied the properties of a 38%mol PHB -62%mol HV copolymer. Their data determined that this presented Young's modulus of 867 MPA and an elongation percentage of 5%. A glass transition temperature of -12.4 °C and a degradation temperature of 268.1 °C.

Corre *et al.* (2012) studied the properties of different commercial PHA (Enmat Y1000P, Mirel F1006, Mirel F3002 and P226). Their results showed that the commercial PHA Enmat Y1000P presented values of Young's modulus (2624 MPa) and maximum tensile stress (32.2 MPa) higher than P226 and Mirel F3002, in addition to Young's modulus increased from 2624 MPa at day 0 to 4329 MPa at day 74. This process could be due to a secondary crystallization presented by this type of material.

Wecker *et al.* (2015) analyzed PHA synthesized by an *Enterobacter* sp. FAK 1384 determined that the PHA was a medium-chain of different polymers (3-hydroxydecanoate, 3-hydroxyoctanoate, 3-hydroxydodecenoate, 3-hydroxydodecanoate and 3-hydroxyhexanoate and 3-hydroxytetradecanoate). They determined that it had a crystallinity index of 0.26, a melting point temperature of 47 °C and a glass transition temperature of -47 °C. In 2016, Ray *et al.* analyzed PHA by the strain *Pannonibacter phragmitetus* ERC8. They determined by the nuclear magnetic resonance that the synthesized PHA was a copolymer of 3HB and 3HA (medium-chain PHA). The polymer's melting temperature was 163.29 °C with a percentage crystallinity of 48.55 %. The thermogravimetric analysis determined that requiring 500 °C for its complete degradation.

Perez-Arauz *et al.* (2019) reported the production of a heteropolymer composed of 98.2% mol HB, 0.75% mol HV and 1% mol HA from the *Cupriavidus necator* strain. They determined that the melting temperature for this polymer was 159.4°C with a crystallinity percentage of 22.2 %. Regarding its mechanical properties, the maximum stress of 2.7 MPa and an elongation of 25.7 % were obtained. The films elaborated from this polymer also showed a water vapor permeability (2.59×10^{-13} kg m s^{-1} $Pa^{-1}m^{-2}$) lower than that reported for those elaborated from PHB (6.9^{-7} kg m s^{-1} $Pa^{-1}m^{-2}$)

Table 6.2 Maximum tensile stress, % elongation and degradation temperature of different PHB copolymers and traditional synthetic polymers

Samples	Tm	σ (MPa)	ε (%)
PHB	177	43	5
P(3HB-co-20%mol3HV)	145	20	50
P(3HB-co-16%mol4HB)	150	26	444
P(3HB-co-15%mol 3HHx)	115	23	760
P(HB-co-10%mol HV)	150	25	20
P(HB-co-20%mol HV)	135	20	100
P(HB-co-10%mol HHx)	127	21	400
P(HB-co-17%mol HHx)	120	20	850
Polypropylene	170	34	400
Polystrene	110	50	-
Polyethylene	130	-	500
HDPE	135	29	620
LDPE	130	10	7300
PET	262	56	-

Tm: melting temperature.
σ: Tensile strength.
ε: Elongation at break.
HDPE: high-density polyethylene.
LDPE:low-density polyethylene.
PET: poly(ethylene terephthalate).

Source: Modified of Muhammady et al., 2015

6.5 Methods for the identification of PHA-producing bacteria

A method traditionally used for the detention of PHA granules is the use of Sudan black dye B, which consists of growing colonies in agar culture media where the dye previously dissolved in 96% ethanol is added. Once the dye is added for 20 minutes, the dye is decanted, and 96% ethanol is added for 1 minute. The colonies that present a bluish-black will be taken as positive for the production of the polymer. It is a convenient method for arresting a large number of PHA-producing bacteria (Schlegel *et al.*, 1970; Godbole, 2016). Phanse *et al.*, 2011, used this method to screen bacteria isolated from different sources (including domestic and industrial wastewater, dairy waste and soil samples). Twenty-three isolates tested positive for PHA production, showing a blue-black staining of their colonies, of which twelve belonged to the genus *Bacillu*s, five to the genus *Pseudomonas*, and four to the genus *Azotobacter* and two isolates to *Staphylococcus*.

Another dye employed for the detection of PHA is the use of Nile blue, a basic water-soluble oxazine. Heat-fixed smears are stained with 1% Nile blue A at 55 °C for 10 minutes and then washed with water and 8% acetic acid for one minute to remove excess dye. The stained smears are examined at 460 nm because PHA granules show orange fluorescence (Ostle and Holt, 1982). In 2017, Mascarenhas and Aruna identified PHA-producing bacteria isolated from different sources (raw honey samples, sugar industry waste, used machine oil and petroleum-contaminated soil) using Sudan black B and Nile blue. Their results showed that 81 strains isolated from these sources were positive when screened with Sudan black B. However, only 34 positive strains fluoresced in ultraviolet light when secondary screening was performed with Nile blue. Evangeline and Sridharan (2019) identified one PHA-producing bacterium out of the five isolated soil samples collected from the Ranipet area using Sudan black B and Nile blue as the screen. The bacterium was identified as *Bacillus cereus* VIT-SSR1.

Nile red, a derivative of Nile blue, is a sensitive screening method that allows observation of PHA accumulation in viable bacteria and is proposed by Spikerman *et al.* (1999). This method uses a stock solution of 0.25 mg of Nile red dissolved in 1 mL of dimethyl sulfoxide. This solution is poured into the sterile culture medium with a final concentration of 0.5 μg of Nile red per milliliter. The agar plates are exposed to ultraviolet light at 312 nm; as with blue, samples positive for PHA accumulation will fluoresce.

6.6 Methods used for PHA extraction

Cell disruption and removal of the protein sheet surrounding the PHA granules are necessary to extract PHA granules. Several protocols have been described for obtaining PHA. Among the methods mentioned in the literature are solvent extraction, chemical digestion, and enzymatic and physical methods (Visakh, 2014; Muhammadi *et al.*, 2015).

Most of the extraction methods use solvents such as chloroform and methanol. Modification in permeability of cell walls and dissolution of PHA in the solvent are the mechanisms of PHA extraction. Separation of PHA from the solvent can be performed by evaporation or precipitation of the polymer with a non-solvent material (Visakh, 2014). Due to the degradation of endotoxins present in Gram-negative bacteria, extraction by this method has been used for medical applications (Mohammadi and Ghaffari-Moghaddam, 2014). Regularly, the solvent ratio used is 20 parts for one part of the polymer, making it a costly method for the industry. (Perez-Rivero *et al.*, 2019). Currently, strategies have been sought for the use of chloroform, such as dimethyl carbonate. Samori *et al.* (2015) used this solvent to extract PHA from mixed cultures (*Amaricoccus sp.*, *Azoarcus sp*. and *Thauera*). They obtained a purity of 98 % and a polymer molecular weight of 1.2 MDa.

Another method studied is digestion, where sodium hypochlorite dissolves cellular substances such as proteins, carbohydrates, lipids and nucleic acids. PHA can be separated from the solution by centrifugation. Despite being a less expensive method, it has been reported that it can reduce up to 50% of the molecular weight of PHA because it is a potent oxidant, so the extraction conditions must be adequately designed to control the decrease in molecular weight (Tripathi *et al.*, 2021). Ramsay *et al.* (1990) extracted PHB from *Alcaligenes eutrophus* using sodium hypochlorite and surfactants (SDS and Triton X-100). They obtained purity of 97 to 98 % with a molecular weight between 730000 Da and 790000 Da when using surfactants, higher than that obtained by using only sodium hypochlorite (87% purity and molecular weight of 680000 Da). Heinrich *et al.* (2012) extracted PHB from *Ralstonia eutropha* H16 strain using sodium hypochlorite 13 % (v/v). They determined that they obtained a purity of 95.66% with an extraction percentage of 91.32%. Using gas chromatography, they determined that the weight of the extracted polymer was in the range of 460000 and 830000 Da lower than that reported for PHA extracted by chloroform (1700000kDa). The reduction in the molecular weight of PHA has led to the use of sodium hypochlorite and chloroform for polymer extraction. Hahn *et al.* (1994) obtained PHB from *A. eutrophus* using 30% concentrated hypochlorite and chloroform in a 1:1 ratio. Their results showed that polymer recovery was higher using this combination (97%) than sodium hypochlorite alone (91%). They also reported that the molecular weight of PHA did not significantly reduce its molecular weight (1020000 Da) with the control (chloroform: 1272000 Da). In 2013, Hamieh *et al.* used a sodium hypochlorite solution to lyse the *Lactobacillus acidophilus* cell wall for 24 hours. Chloroform was added to dissolve the PHA, and the polymer was precipitated with an acetone-ethanol solution 1:1 (v/v) to remove the membrane lipids. Chloroform was evaporated at 70 °C to obtain polymer crystals (Jacquel *et al.*, 2008).

Homes and Lim (1989) developed the enzymatic digestion method as an alternative to solvent extraction. The procedure starts with heat treatment of the cell mass, followed by enzymatic hydrolysis, treatment with surfactants and final decolorization with hydrogen peroxide. Although enzymes lead to high recovery levels, their high cost is a disadvantage. Some enzymes have high activity in protein dissolution but little effect on PHA degradation. Yasotha *et al*., (2006) extracted a medium-chain PHA synthesized by *Pseudomonas putida* using the commercial protease enzyme Alcalase. Their results showed a purity of 92.6% with an extraction of 90%. Another author who used this enzyme to obtain PHA was Kathiraser *et al.* (2007), who obtained a medium-chain PHA synthesized by *Pseudomonas putida*. Their analysis determined a purity of 92.63 % lower than that reported using chloroform (96.6%). In 2012, Neves and Müller studied the use of the proteases Corolase® L10, Alcalase® 2.4L, Corolase® 7089 and Protemax® FC and glycosidases Celumax® BC, Rohament® CL and Rohalase® for the extraction of P(3HB) and P(3HB-co-3HV) synthesized by *Cupriavidus necator*. The Celumax® BC enzyme obtained the cell membrane's best lysis, obtaining a recovery of 93.2 % of P(3HB-co-3HV) with a purity of 94%. Like the previous ones, the enzymatic digestion method has been combined with other methods.

Extraction using high pressure has also been used for the industrial extraction of PHA. The instruments used in this method destroy the cell wall. For its use, the pressure, temperature, biomass concentration, size, shape and strength of the cell wall must be considered. Cultures in the logarithmic phase have a lower resistance to cell wall rupture, while in the stationary phase, the resistance increases due to the increase in wall thickness (Tripathi *et al.,* 2021). Ghatnekar *et al.* (2002) extracted PHA produced by *Methylobacterium* sp. V49 using a ceramic cell disruption valve (APV Gaulin). Using a pressure of 400 kg cm^{-2} and two homogenization cycles resulted in 95 % recovery and 80 % purity of PHA. Hwang *et al.* (2006) obtained PHA and synthesized *Haloferax mediterranei* using ultrasonication with an amplitude of 20 kHz and a power of 525 W.

6.7 Methods for structural characterization of PHA

One of the most common methods used for the structural characterization of PHA is Fourier transform infrared spectroscopy (FTIR). It is a technique used to obtain an absorption spectrum of a sample. This method has been used for the detection of PHA in intact bacteria. This method can identify the carbonyl group in the fatty acid chain depending on the absorption peak. According to Hong *et al.* (1999), using this technique has identified PHA of short chains (such as hydroxybutyrate), medium chains (such as hydroxyoctanoate and hydroxydecanoate) or the combination of both, showing characteristic absorbance bands at wavelengths of 1728 cm^{-1}, 1740 cm^{-1} and 1732 cm^{-1}. Table 6.3 shows the characteristic bands of short- and medium-chain PHAs synthesized by *Azotobacter vinelandii* UWD, *Pseudomonas mendocina* AS 1.2329 and *Pseudomonas pseudoalcaligenes* AS 1.2328.

Table 6.3 Comparison of results from Fourier-transform infrared (FTIR) spectra and gas chromatography (G.C.) for component analysis of polyhydroxyalkanoates (PHA)

FTIR analysis		GC analysis:
Wave-number (cm^{-1})	**Possible PHA components**	**PHA monomer composition (%)**
1728 1262	PHB	100HB
1739 1261 2925	HB and mclHA	92HB, 8HD
1739 1260 2924	HB and mclHA	98HB, 2HO
1744 1165 2926	mclHA	0.3HB, 58HO, 41HD
1744 1162 2926	mclHA	22HO,78 HD
1744 1665 2928	mclHA	0.6HB,19HO, 80HD
1744 1165 2928	mclHA	0.4HB,20HO, 80HD
1739 1257 2926	HB and mclHA	23HB, 39HO, 38HD
1739 1258 2926	HB and mclHA	14HB, 50HO, 36HD
1739 1257 2926	HB and mclHA	22HB, 40HO, 38HD
1744 1168 2929	mclPHA	0.3HB, 59HO, 41HD
HA: polyhydroxyalkanoate. HB: polyhydroxybutyrate. HO: polyhydroxyoctanoate. HD: polyhydroxydecanoate. mcl: medium chains		

Source Hong et al.,1999

In 2013, Sathiyanarayanan *et al.* identified PHA synthesized from *Bacillus subtilis* isolated from a marine sponge (*Callypongia diffusa*) by FTIR analysis, reporting absorption bands at 1728 cm^{-1} and 1283 cm^{-1} corresponding to the C=O and C-O, respectively. The bands at 1230 cm^{-1}, 1382 cm^{-1} and 1184 cm^{-1} represented the $-CH_2$, $-CH_3$ and C-O-C. Finally, they reported an absorption band at 3450 cm^{-1} corresponding to the hydroxyl group. Another study with similar results was by Evangeline and Sridharan (2019), who extracted PHA synthesized by *Bacillus cereus* VIT-SSR1 and identified it by FTIR using KBr and a wavelength of 4000 cm^{-1} at 400 cm^{-1}. Their results showed an absorption band at 1724.34 cm^{-1} corresponding to the carbonyl group, characteristic of short chains of PHB monomers. The absorption bands at 3419.79 cm^{-1} correspond to the hydroxyl group.

This method can be combined with gas chromatography coupled to mass (GCMS) which helps to quantify and determine the proportion in which each PHA is present in the structure. To perform this analysis, a methanolysis of PHA is necessary. In addition to the use, the temperatures to use the equipment and the temperature increase must be contemplated. Sathinarayanan *et al.* (2013) analyzed by GCMS the PHA synthesized by *Bacillus subtilis* MSBN17 and determined the presence of a retention peak at 2,548 min corresponding to a PHB. This value was close to that reported by Evangeline and Sridharan (2019) using an elite-5MS capillary column. They analyzed PHA produced by *Bacillus cereus* VIT-SSR1 peaks at times 3.69 (3-HB), 11.81, 17.26 and 21.40. However, this is non-pure, so it presented other retention peaks. Wecker *et al.* (2015) analyzed PHA synthesized by an *Enterobacter* sp. FAK 1384 was isolated from a marine source by GCMS. Their results determined a PHA consisting of 62% mol-3-hydroxydecanoate, 18% mol 3-hydroxyoctanoate, 12% mol of 3-hydroxydodecenoate, 7.6% mol of 3-hydroxydodecanoate and a small fraction of 0.3% mol 3-hydroxyhexanoate and 1.3% mol of 3-hydroxytetradecanoate. The composition of the medium-chain PHA induced a higher elasticity and elongation of the extracted polymer, having a crystallinity index of 0.26, indicating an amorphous polymer.

Another method used to identify PHA is nuclear magnetic resonance (NMR). The composition of the hydroxyalkanoate units can be identified by analyzing the nuclear magnetic field of the NMR spectra. This method allows for a differentiation between blends and hetero polymers of PHA and provides details about the topology and functional groups in the polymers. Another advantage is that the hydrolysis step of the polymer can be avoided (Godbole, 2016). Kathiraser *et al*., (2007) used this technique to compare the structural variation of PHA synthesized *by Pseudomonas putida* extracted by two different methods (solvent and enzymatic). Their results showed that there was no variation in the structure of PHA. The spectra showed a peak at 2.58, corresponding to CH_2. The peak at 5.1 ppm belonged to the CH group. The peaks at 5.30 ppm and 5.52 ppm determine the presence of a side chain where protons bind to two ethylene carbon sequences (-CH=CH-) associated with the unsaturated monomer. The signal at 1.5 ppm represents the first side chain of the monomers and at 1.3 is attributed to the methyl (CH_2) of the monomers. The bit at 0.89 ppm indicates the terminal methyl group (CH_3). In 2017, Sharma *et al.* used this technique to analyze PHA synthesized by *P. chlororaphis* PA23-63. The spectrum identified five peaks corresponding to protons on the methylene group, a hydroxyl group, a methyl group attached to a carbonyl group, a saturated methyl side-chain group, a methyl group and a terminal methyl group. FTIR identified the presence of different functional groups such as aliphatic C-H bonds, = C-H bonds, =CH bonds and =C-O bonds, and stretching of the =O bond and deformation of the =C-H bond. It was observed that the C-H methylene peaks were more prominent in the medium-chain PHA.

6.8 Biodegradability of PHAs

PHAs are biodegradable in different environments, making them an attractive option for replacing plastics. The general degradation process consists of the breakdown of the polymer into shorter chains by hydrolytic depolymerase, followed by the PHA trimers or dimers being processed by lipases and hydrolases. PHA depolymerizes are carboxylesterases that have a catalytic triad (serine-Histidine-aspartic acid) as their active site (Knoll *et al.,* 2009). Extracellular PHA depolymerase is the most studied protein that consists of three main domains: (III) a binding domain responsible for surface adsorption and breakdown of the polymer structure; (II) a linker domain that joins the binding domain to the catalytic domain; and (I) a catalytic domain that cleaves the PHA and any available dimer/trimer in two parts (Figure 6.3). Hydrolytic enzymes have excellent adhesion to amorphous surfaces due to their less ordered structure, making them more accessible to enzyme action (Meereboer *et al.*, 2020).

Figure 6.3 Single PHB crystal enzymatic degradation by PHB depolymerase

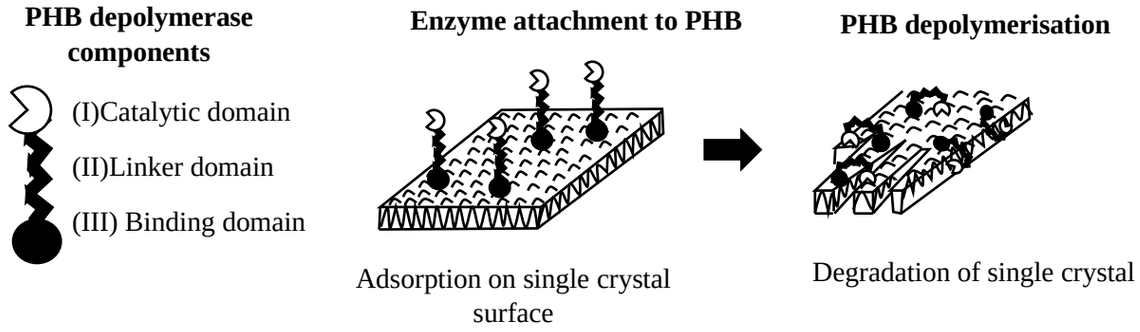

Source: Meereboer et al., 2020

The short and medium-chain PHA can be degraded by many bacterial genera such as *Bacillus*, *Clostridium*, *Comamonas*, *Enterobacter*, *Klebsiella*, *Pseudomonas*, *Staphylococcus*, *Streptomyces*, among others. Different fungi have also been used for PHA degradation, such as *Acremonium*, *Aspergillus, Candida*, *Paecilomyces* and *Emericelopsia* (Kim *et al.*, 2013; Bugnicourt *et al.*, 2014; Meereboer *et al.*, 2020).

In 2016, Ong and Sudesh analyzed three different PHA (poly 3-hydroxybutyrate and combinations of PHB and Polyhydroxyhexanoate) and their effect on the soil microbial community. Films made from these PHAs were buried in the soil for eight weeks. The results concluded that poly 3-hydroxybutyrate-co-21%mol 3-hydroxyhexanoate showed the presence of holes three weeks after initiation of the test. Metagenomic analysis revealed that some of the significant Phyla found at the site included *Actinobacteria, Firmicutes*, and *Proteobacteria* that can degrade PHA. In the following year, Volova *et al.* (2017) studied the microbial degradation of polyhydroxyalkanoates with different chemical compositions. They determined that the surface community of bacteria differed between polymers. The polyhydroxybutyrate was degraded by bacteria of the genus *Mitsuaria, Chitinophaga* and *Acidovorax*, which could not degrade the other three types of pHA. *Roseateles depolymerans*, *Streptomyces gardneri* and *Cupriavidus*, were poly(3HB/4HB)-degrading species. *Roseomonas massiliae* and *Delftia acidovorans* degraded poly(3HB/3-hydroxyvalerate), and poly(3HB/3-hydroxyhexanoate) was degraded by species of *Pseudoxanthomonas* sp., *Pseudomonas fluorescens*, *Ensifer adhaerens*, and *Bacillus pumilus*. The microbial community formed on the polymer surface and the soil microbial community differed depending on the polymer composition.

6.9 Applications of the PHA

The properties of this compound and the mixture of different PHA have broadened the possible applications for its use. Due to their biocompatibility, biodegradability and low cytotoxicity to cells, PHA has been used for packaging, medical equipment (gloves) and fishing nets. It has been proposed to manufacture resorbable saturates, pharmaceuticals, and transplants for tissue engineering and pharmacology (Chee *et al.*, 2010).

Shishatskaya *et al.* (2004) used PHA synthesized by the bacterium *Ralstonia eutropha* to realize monofilament sutures. The preparation uses PHB (340000 Da) and a copolymer of PHB and polyhydroxyvalerate (PHV). Their results showed that the suture adequately held the muscle-fascial incision in animals and that the animals did not show any adverse reaction to the PHA fibers. Hufenus *et al.* (2011) elaborated on polylactic acid fibers and a mixture of PHB and 8mol% of 3-hydroxyvalerate (Tianan). They studied their biocompatibility in human dermal fibroblasts. Their results showed that there was no toxicity. The fibroblasts that grew were adhering to the fibers covering after a culture period of 1 week. Degradation tests showed a reduction of maximum stress up to 33% after four weeks of incubation. Another biomedical application given to PHA is in bone tissue engineering, Meischel *et al.* (2016) evaluated the response of bone to PHA composite implants in rat femurs. PHB constituted these implants with zirconia dioxide, Herafill® and Mgalloy WZ21. Their results showed that implants with 30% Herafill, PHB and zirconium dioxide possessed the highest bone accretion values and that the mechanical properties were similar to that of bone. In agriculture, this polymer has been used to reduce ghost fishing caused by nets made of synthetic polymers that, when discarded, cause a negative economic and ecological impact as they continue to catch and retain fish (Amelia *et al.*,2019).

Another application of PHA in agriculture is the controlled release of pesticides and insecticides, producing films for crop protection or seed encapsulation (Sharma *et al.*, 2021). PHA has also been used to make shopping bags, containers, and utensils such as rakes, feminine hygiene products, and cosmetic containers, among others (Chen, 2009).

6.10 Financing

This work has been funded by CONACYT [scholarship number: 815355, 2022]; Tecnológico Nacional de México [Project TecNM code: 14073.22-P].

6.11 Conclusions

The accumulation of plastics in the soil and the oceans is becoming more evident and alarming. It is enough to walk along the streets or beaches of some countries to observe this accumulation. Garbage on the streets has become so common that people walk through this waste without caring. This problem is caused due to poor waste management by governments. This does not exempt us as citizens from blame since the industry's increased plastic production is due to the growing consumer demand. Recyclable materials have been proposed to reduce the accumulation of plastics. However, people's lack of awareness causes the recycling process to be inefficient. It is easier to throw garbage on the streets where we walk than find a recycling point.

Using biodegradable polymers has been another option studied for years to replace plastic. While many are easy to degrade, their mechanical properties are inadequate to match or resemble the properties of currently used synthetic plastics. PHAs, as mentioned in this chapter, have the advantage of the show a wide variety of structures that can be used individually or in combination to improve their characteristics. PHB is the most reported biodegradable polymer for plastics in the literature because it is produced by a wide variety of bacteria and has properties similar to polypropylene. Another advantage of PHA is that it can be degraded by enzymes of the PHA-producing bacteria or bacteria living naturally in soils and seas. They can be degraded in less than two months, depending on environmental conditions. Since they are fatty acid monomers, their applications have been widely studied in medicine. However, applications have also been proposed in agriculture. The varied applications of PHA have led to their industrial production in different countries such as China, the United States and Canada. Despite more sources of isolation of producing bacteria, genetic modifications to increase polymer production and chemical modifications of the polymer to give them other applications are still being studied. PHAs have proven to be a viable candidate to replace the use of plastics, but industry and individuals have yet to determine if their value is less than that of plastics.

6.12 References

Al-Ardawy, Y. J. H., & Taj-Aldeen, W. R. (2020). Study of gentamicin combined with polyhydroxyalkanoates extracted from *lactobacillus plantarum*. EurAsian Journal of BioSciences, 14(2), 2903-2910. https://www.proquest.com/openview/9a893b783035eeb545602424b12d2b05/1?pq-origsite=gscholar&cbl=2042720

Alshehrei, F. (2019). Production of polyhydroxybutyrate (PHB) by bacteria isolated from soil of Saudi Arabia. J. Pure Appl. Microbiol, 13, 897-904. doi: 10.22207/JPAM.13.2.26

Amelia, T. S. M., Govindasamy, S., Tamothran, A. M., Vigneswari, S., & Bhubalan, K. (2019). Applications of PHA in Agriculture. Biotechnological Applications of Polyhydroxyalkanoates, 347–361. doi:10.1007/978-981-13-3759-8_13

Anderson, A. J., Haywood, G. W., & Dawes, E. A. (1990). Biosynthesis and composition of bacterial poly(hydroxyalkanoates). International Journal of Biological Macromolecules, 12(2), 102–105. doi:10.1016/0141-8130(90)90060-n

Arcos-Hernández, M. V., Laycock, B., Donose, B. C., Pratt, S., Halley, P., Al-Luaibi, S., … Lant, P. A. (2013). Physicochemical and mechanical properties of mixed culture polyhydroxyalkanoate (PHBV). European Polymer Journal, 49(4), 904–913. doi:10.1016/j.eurpolymj.2012.10.025

Arun, A., Arthi, R., Shanmugabalaji, V., & Eyini, M. (2009). Microbial production of poly-β-hydroxybutyrate by marine microbes isolated from various marine environments. Bioresource Technology, 100(7), 2320–2323. doi:10.1016/j.biortech.2008.08.037

Aslım, B., Çalışkan, F., Beyatlı, Y., & Gündüz, U. (1998). Poly-β-hydroxybutyrate production by lactic acid bacteria. FEMS microbiology letters, 159(2), 293-297. doi:10.1111/j.1574-6968.1998.tb12874.x

Ataei, S. A., Vasheghani-Farahani, E., Shojaosadati, S. A., & Tehrani, H. A. (2008). Isolation of PHA-Producing Bacteria from Date Syrup Waste. Macromolecular Symposia, 269(1), 11–16. doi:10.1002/masy.200850903

Berezina, N., & Martelli, S. M. (2014). Polyhydroxyalkanoates: Structure, Properties and Sources. In Polyhydroxyalkanoate (PHA) based Blends, Composites and Nanocomposites (pp. 18-46). doi: 10.1039/9781782622314-00018

Boyandin, A. N., Kalacheva, G. S., Rodicheva, E. K., & Volova, T. G. (2008). Synthesis of reserve polyhydroxyalkanoates by luminescent bacteria. Microbiology, 77(3), 318–323. doi:10.1134/s0026261708030119

Bugnicourt, E., Cinelli, P., Lazzeri, A., & Alvarez, V. (2014). Polyhydroxyalkanoate (PHA): Review of synthesis, characteristics, processing and potential applications in packaging. Express Polymer Letters, 8(11), 791–808. doi: 10.3144/expresspolymlett.2014.82

Chee, J. Y., Yoga, S. S., Lau, N. S., Ling, S. C., Abed, R. M., & Sudesh, K. (2010). Bacterially produced polyhydroxyalkanoate (PHA): converting renewable resources into bioplastics. Current research, technology and education topics in Applied Microbiology and Microbial Biotechnology, 2, 1395-1404. https://www.researchgate.net/profile/JiunYeeChee/publication/216173367_Bacterially_produced_polyhydroxyalkanoate_PHA_Converting_renewable_resources_into_bioplastic/links/02eee579cc0226978c593e10/Bacterially-produced-polyhydroxyalkanoate-PHA-Converting-renewable-resources-into bioplastic.pdf

Chen, G.-Q. (2009). A microbial polyhydroxyalkanoates (PHA) based bio- and materials industry. Chemical Society Reviews, 38(8), 2434. doi:10.1039/b812677c

Chien, C., Chen, C., Choi, M., Kung, S., & Wei, Y. (2007). Production of poly-β-hydroxybutyrate (PHB) by *Vibrio spp*. isolated from marine environment. Journal of Biotechnology, 132(3), 259–263. doi:10.1016/j.jbiotec.2007.03.002

Corre, Y.M., Bruzaud, S., Audic, J. L., & Grohens, Y. (2012). Morphology and functional properties of commercial polyhydroxyalkanoates: A comprehensive and comparative study. Polymer Testing, 31(2), 226–235. doi: 10.1016/j.polymertesting.2011.11.002

El-Hadi, A., Schnabel, R., Straube, E., Müller, G., & Henning, S. (2002). Correlation between degree of crystallinity, morphology, glass temperature, mechanical properties and biodegradation of poly (3-hydroxyalkanoate) PHAs and their blends. Polymer Testing, 21(6), 665–674. doi:10.1016/s0142-9418(01)00142-8

Evangeline, S., & Sridharan, T. B. (2019). Biosynthesis and statistical optimization of polyhydroxyalkanoate (PHA) produced by *Bacillus cereus* VIT-SSR1 and fabrication of biopolymer films for sustained drug release. International Journal of Biological Macromolecules. doi: 10.1016/j.ijbiomac.2019.05.163

Ghatnekar, M., Pai, J., & Ganesh, M. (2002). Production and recovery of poly-3-hydroxybutyrate from *Methylobacterium* sp V49. Journal of Chemical Technology & Biotechnology, 77(4), 444–448. doi:10.1002/jctb.570

Godbole, S. (2016). Methods for identification, quantification and characterization of polyhydroxyalkanoates-a review. International Journal of Bioassays, 5(4), 2016.

Gregson, N., & Crang, M. (2018). Made in China and the new world of secondary resource recovery. Environment and Planning A: Economy and Space, 0308518X1879117. doi:10.1177/0308518x18791175

Hahn, S. K., Chang, Y. K., Kim, B. S., & Chang, H. N. (1994). Optimization of microbial poly(3-hydroxybutyrate) recover using dispersions of sodium hypochlorite solution and chloroform. Biotechnology and Bioengineering, 44(2), 256–261. doi:10.1002/bit.260440215

Hamieh, A., Olama, Z., & Holail, H. (2013). Microbial production of polyhydroxybutyrate, a biodegradable plastic using agro-industrial waste products. Glo Adv Res J Microbiol, 2(3), 54-64.

Heidbreder, L. M., Bablok, I., Drews, S., & Menzel, C. (2019). Tackling the plastic problem: A review on perceptions, behaviors, and interventions. Science of The Total Environment. doi: 10.1016/j.scitotenv.2019.02.437

Heinrich, D., Madkour, M. H., Al-Ghamdi, M. A., Shabbaj, I. I., & Steinbüchel, A. (2012). Large scale extraction of poly (3-hydroxybutyrate) from *Ralstonia eutropha* H16 using sodium hypochlorite. AMB express, 2(1), 1-6. doi: 10.1186/2191-0855-2-59

Homes, P.A. & Lim, G.B. (1989). Separation process, U.S. No. 4,910,145.

Hong, K., Sun, S., Tian, W., Chen, G. Q., & Huang, W. (1999). A rapid method for detecting bacterial polyhydroxyalkanoates in intact cells by Fourier transform infrared spectroscopy. Applied Microbiology and Biotechnology, 51(4), 523–526. doi:10.1007/s002530051427

Hufenus, R., Reifler, F. A., Maniura-Weber, K., Spierings, A., & Zinn, M. (2012). Biodegradable bicomponent fibers from renewable sources: melt-spinning of poly (lactic acid) and poly [(3-hydroxybutyrate)-co-(3-hydroxyvalerate)]. Macromolecular Materials and Engineering, 297(1), 75-84. doi: 10.1002/mame.201100063

Hwang, K. J., You, S. F., & Don, T. M. (2006). Disruption kinetics of bacterial cells during purification of poly-beta-hydroxyalkanoate using ultrasonication. J. Chin. Inst. Chem. Engrs, 37(3), 1-8. https://www.researchgate.net/profile/Trong-Ming-Don/publication/288358845_Disruption_kinetics_of_bacterial_cells_during_purification_of_poly-b-hydroxyalkanoate_using_ultrasonication/links/59adef42aca272f8a1618d80/Disruption-kinetics-of-bacterial-cells-during-purification-of-poly-b-hydroxyalkanoate-using-ultrasonication.pdf

Jacquel, N., Lo, C. W., Wei, Y. H., Wu, H. S., & Wang, S. S. (2008). Isolation and purification of bacterial poly (3-hydroxyalkanoates). Biochemical engineering journal, 39(1), 15-27. doi: 10.1016/j.bej.2007.11.029

Jamil, N., Ahmed, N., & Edwards, D. H. (2007). Characterization of biopolymer produced by *Pseudomonas sp*. CMG607w of marine origin. The Journal of General and Applied Microbiology, 53(2), 105-109. doi: 10.2323/jgam.53.105

Kathiraser, Y., Aroua, M. K., Ramachandran, K. B., & Tan, I. K. P. (2007). Chemical characterization of medium-chain-length polyhydroxyalkanoates (PHAs) recovered by enzymatic treatment and ultrafiltration. Journal of Chemical Technology & Biotechnology, 82(9), 847–855. doi:10.1002/jctb.1751

Kim, J. K., Won, Y. J., Nikoh, N., Nakayama, H., Han, S. H., Kikuchi, Y., ... & Lee, B. L. (2013). Polyester synthesis genes associated with stress resistance are involved in an insect–bacterium symbiosis. Proceedings of the National Academy of Sciences, 110(26), E2381-E2389. doi: 10.1073/pnas.1303228110

Knoll, M., Hamm, T. M., Wagner, F., Martinez, V., & Pleiss, J. (2009). The PHA Depolymerase Engineering Database: A systematic analysis tool for the diverse family of polyhydroxyalkanoate (PHA) depolymerases. BMC Bioinformatics, 10(1), 89. doi:10.1186/1471-2105-10-89

Luengo, J. M., García, B., Sandoval, A., Naharro, G., & Olivera, E. R. (2003). Bioplastics from microorganisms. Current Opinion in Microbiology, 6(3), 251–260. doi:10.1016/s1369-5274(03)00040-7

Mascarenhas, J., & Aruna, K. (2017). Screening of polyhydroxyalkonates (PHA) accumulating bacteria from diverse habitats. J global biosci, 6(3), 4835-4848. https://www.mutagens.co.in/jgb/vol.06/3/060304.pdf

Meereboer, K. W., Misra, M., & Mohanty, A. K. (2020). Review of recent advances in the biodegradability of polyhydroxyalkanoate (PHA) bioplastics and their composites. Green Chemistry. doi:10.1039/d0gc01647k

Meischel, M., Eichler, J., Martinelli, E., Karr, U., Weigel, J., Schmöller, G., … Stanzl-Tschegg, S. E. (2016). Adhesive strength of bone-implant interfaces and in-vivo degradation of PHB composites for load-bearing applications. Journal of the Mechanical Behavior of Biomedical Materials, 53, 104–118. doi:10.1016/j.jmbbm.2015.08.004

Meng, D.-C., Shen, R., Yao, H., Chen, J.-C., Wu, Q., & Chen, G.-Q. (2014). Engineering the diversity of polyesters. Current Opinion in Biotechnology, 29, 24–33. doi:10.1016/j.copbio.2014.02.013

Mohammadi, M., & Ghaffari-Moghaddam, M. (2014). Recovery and Extraction of Polyhydroxyalkanoates (PHAs). Polyhydroxyalkanoate (PHA) based Blends, Composites and Nanocomposites, 47-65. Doi: 10.1039/9781782622314-00047

Mohammed, S., Panda, A. N., & Ray, L. (2019). An investigation for recovery of polyhydroxyalkanoates (PHA) from *Bacillus sp*. BPPI-14 and *Bacillus sp*. BPPI-19 isolated from plastic waste landfill. International Journal of Biological Macromolecules. doi: 10.1016/j.ijbiomac.2019.05.155

Monilola, W. S., & Makinde, O. E. (2020). Production and Characterization of Polyhydroxyalkanoates from Lactic Acid Bacteria Isolated from Dairy Wastewater, Fermented Cow Milk and'Ogi'. Jamb, 31-46. doi: 10.9734/JAMB/2020/v20i930279

Muhammadi, Shabina, Afzal, M., & Hameed, S. (2015). Bacterial polyhydroxyalkanoates-eco-friendly next generation plastic: Production, biocompatibility, biodegradation, physical properties and applications. Green Chemistry Letters and Reviews, 8(3-4), 56–77. doi:10.1080/17518253.2015.1109715

Neves, A., & Müller, J. (2012). Use of enzymes in extraction of polyhydroxyalkanoates produced by *Cupriavidus necator*. Biotechnology Progress, 28(6), 1575–1580. doi:10.1002/btpr.1624

Nielsen, T. D., Hasselbalch, J., Holmberg, K., & Stripple, J. (2019). Politics and the plastic crisis: A review throughout the plastic life cycle. Wiley Interdisciplinary Reviews: Energy and Environment. doi:10.1002/wene.360

Ong, S. Y., & Sudesh, K. (2016). Effects of polyhydroxyalkanoate degradation on soil microbial community. Polymer Degradation and Stability, 131, 9–19. doi: 10.1016/j.polymdegradstab.2016.06.024
Ostle, A. G., & Holt, J. G. (1982). Nile blue A as a fluorescent stain for poly-beta-hydroxybutyrate. Applied and environmental microbiology, 44(1), 238-241. doi: 10.1128/aem.44.1.238-241.1982

Pérez-Arauz, A. O., Aguilar-Rabiela, A. E., Vargas-Torres, A., Rodríguez-Hernández, A. I., Chavarría-Hernández, N., Vergara-Porras, B., & López-Cuellar, M. R. (2019). Production and characterization of biodegradable films of a novel polyhydroxyalkanoate (PHA) synthesized from peanut oil. Food Packaging and Shelf Life, 20, 100297. doi: 10.1016/j.fpsl.2019.01.001

Pérez-Rivero, C., López-Gómez, J. P., & Roy, I. (2019). A sustainable approach for the downstream processing of bacterial polyhydroxyalkanoates: State-of-the-art and latest developments. Biochemical Engineering Journal, 150, 107283. doi:10.1016/j.bej.2019.107283

Phanse, N., Chincholikar, A., Patel, B., Rathore, P., Vyas, P., & Patel, M. (2011). Screening of PHA (poly hydroxyalkanoate) producing bacteria from diverse sources. Int J Biosci, 1(6), 27-32. https://www.researchgate.net/profile/Dr-Pragya-Rathore/publication/257230200_Screening_of_PHA_producing_bacteria_from_diverse_sources/links/549b89ad0cf2d6581ab2e414/Screening-of-PHA-producing-bacteria-from-diverse-sources.pdf

Prados, E., & Maicas, S. (2016). Bacterial production of hydroxyalkanoates (PHA). Universal Journal of Microbiology Research, 4(1), 23-30. doi: 10.13189/ujmr.2016.040104

Ramsay, B. A., Lomaliza, K., Chavarie, C., Dube, B., Bataille, P., & Ramsay, J. (1990). Production of poly-(beta-hydroxybutyric-co-beta-hydroxyvaleric) acids. Applied and environmental Microbiology, 56(7), 2093-2098. doi: 10.1128/aem.56.7.2093-2098.1990

Ray, S., Prajapati, V., Patel, K., & Trivedi, U. (2016). Optimization and characterization of PHA from isolate *Pannonibacter phragmitetus* ERC8 using glycerol waste. International Journal of Biological Macromolecules, 86, 741–749. doi:10.1016/j.ijbiomac.2016.02.002

Samorì, C., Abbondanzi, F., Galletti, P., Giorgini, L., Mazzocchetti, L., Torri, C., & Tagliavini, E. (2015). Extraction of polyhydroxyalkanoates from mixed microbial cultures: Impact on polymer quality and recovery. Bioresource Technology, 189, 195–202. doi: 10.1016/j.biortech.2015.03.062

Sangkharak, K., & Prasertsan, P. (2012). Screening and identification of polyhydroxyalkanoates producing bacteria and biochemical characterization of their possible application. The Journal of general and applied microbiology, 58(3), 173-182. doi: 10.2323/jgam.58.173

Sathiyanarayanan, G., Saibaba, G., Seghal Kiran, G., & Selvin, J. (2013). A statistical approach for optimization of polyhydroxybutyrate production by marine *Bacillus subtilis* MSBN17. International Journal of Biological Macromolecules, 59, 170–177. doi:10.1016/j.ijbiomac.2013.04.04

Schlegel, H. G., Lafferty, R., & Krauss, I. (1970). The isolation of mutants not accumulating poly-β-hydroxybutyric acid. Archiv für mikrobiologie, 71(3), 283-294. doi:10.1007/BF00410161

Sharma, P. K., Fu, J., Cicek, N., Sparling, R., & Levin, D. B. (2012). Kinetics of medium-chain-length polyhydroxyalkanoate production by a novel isolate of *Pseudomonas putida* LS46. Canadian Journal of Microbiology, 58(8), 982–989. doi:10.1139/w2012-074

Sharma, P. K., Munir, R. I., de Kievit, T., & Levin, D. B. (2017). Synthesis of polyhydroxyalkanoates (PHAs) from vegetable oils and free fatty acids by wild-type and mutant strains of *Pseudomonas chlororaphis.* Canadian journal of microbiology, 63(12), 1009-1024. doi: 10.1139/cjm-2017-0412

Sharma, V., Sehgal, R., & Gupta, R. (2021). Polyhydroxyalkanoate (PHA): properties and modifications. Polymer, 212, 123161. doi: 10.1016/j.polymer.2020.123161

Shishatskaya, E. I., Volova, T. G., Puzyr, A. P., Mogilnaya, O. A., & Efremov, S. N. (2004). Tissue response to the implantation of biodegradable polyhydroxyalkanoate sutures. Journal of Materials Science: Materials in Medicine, 15(6), 719–728. doi: 10.1023/B:JMSM.0000030215.49991.0d

Simon-Colin, C., Raguénès, G., Cozien, J., & Guezennec, J. G. (2008). *Halomonas profundus* sp. nov., a new PHA-producing bacterium isolated from a deep-sea hydrothermal vent shrimp. Journal of applied microbiology, 104(5), 1425-1432. doi: 10.1111/j.1365-2672.2007.03667.x

Spiekermann, P., Rehm, B. H. A., Kalscheuer, R., Baumeister, D., & Steinbüchel, A. (1999). A sensitive, viable-colony staining method using Nile red for direct screening of bacteria that accumulate polyhydroxyalkanoic acids and other lipid storage compounds. Archives of Microbiology, 171(2), 73–80. doi:10.1007/s002030050681

Tripathi, A. D., Paul, V., Agarwal, A., Sharma, R., Hashempour-Baltork, F., Rashidi, L., & Darani, K. K. (2021). Production of polyhydroxyalkanoates using dairy processing waste–a review. Bioresource Technology, 326, 124735. doi: 10.1016/j.biortech.2021.124735

UNEP. (2014). Valuing plastics: The business case for measuring, managing and disclosing plastic use in the consumer goods industry. Nairobi, Kenya: United Nations Environment Programme. Recovered from: https://wedocs.unep.org/20.500.11822/9238

Visakh, P. M. (2014). Polyhydroxyalkanoates (PHAs), their blends, composites and nanocomposites: State of the art, new challenges and opportunities. doi: 10.1039/9781782622314-00001

Volova, T. G., Prudnikova, S. V., Vinogradova, O. N., Syrvacheva, D. A., & Shishatskaya, E. I. (2016). Microbial Degradation of Polyhydroxyalkanoates with Different Chemical Compositions and Their Biodegradability. Microbial Ecology, 73(2), 353–367. doi:10.1007/s00248-016-0852-3

Wecker, P., Moppert, X., Simon-Colin, C., Costa, B., & Berteaux-Lecellier, V. (2015). Discovery of a mcl-PHA with unexpected biotechnical properties: the marine environment of French Polynesia as a source for PHA-producing bacteria. AMB Express, 5(1). doi:10.1186/s13568-015-0163-y

Yasotha, K., Aroua, M. K., Ramachandran, K. B., & Tan, I. K. P. (2006). Recovery of medium-chain-length polyhydroxyalkanoates (PHAs) through enzymatic digestion treatments and ultrafiltration. Biochemical Engineering Journal, 30(3), 260–268. doi:10.1016/j.bej.2006.05.008

Yüksekdag, Z. N., & Beyatli, Y. (2007). Production of poly-beta-hydroxybutyrate (PHB) in different media by *Streptococcus thermophilus* Ba21S strain. Journal of Applied Biological Sciences, 2(2), 7-10. https://dergipark.org.tr/en/download/article-file/415035

Zhou, X. Y., Yuan, X. X., Shi, Z. Y., Meng, D. C., Jiang, W. J., Wu, L. P., ... & Chen, G. Q. (2012). Hyperproduction of poly (4-hydroxybutyrate) from glucose by recombinant *Escherichia coli*. Microbial cell factories, 11(1), 1-8. https://dergipark.org.tr/en/pub/jabs/issue/34893/386884

Chapter 7 Effects of selenium on yield, seed size, and phenolic compound content of common bean (*Phaseolus vulgaris* L.)

Capítulo 7 Efectos del selenio en el rendimiento, tamaño de la semilla y contenido de compuestos fenólicos del frijol común (*Phaseolus vulgaris* L.)

GARCÍA-MORALES, Soledad´†, MACÍAS-GARCÍA, María Juventina´´´, LUGO-CERVANTES, Eugenia´´ and ALCÁZAR-VALLE, Elba Montserrat´´*

´CONACYT-Centro de Investigación y Asistencia en Tecnología y Diseño del Estado de Jalisco A. C., Plant Biotechnology, Zapopan 45019, Mexico.
´´Centro de Investigación y Asistencia en Tecnología y Diseño del Estado de Jalisco A. C., Food Technology, Zapopan 45019, Mexico.
´´´Universidad de Guadalajara, Chemistry Department, Boulevard Gral. Marcelino García Barragán 1421, 44430 Guadalajara, Mexico.

ID 1st Author: *Soledad, García-Morales* / **ORC ID**: 0000-0002-2551-2518, **CVU CONACYT ID**: 224490

ID 1st Co-author: *María Juventina, Macías-García* / **ORC ID:** 0000-0002-9657-2286

ID 2nd Co-author: *Eugenia, Lugo-Cervantes* / **ORC ID:** 0000-0003-3337-5872, **CVU CONACYT ID**: 57433

ID 3rd Co-author: *Elba Montserrat, Alcázar-Valle* / **ORC ID**: 0000-0003-2949-4799, **CVU-CONACYT ID**: 274400

DOI: 10.35429/H.2022.6.1.82.95

S. García, M. Macías, E. Lugo and E. Alcázar

* ealcazar@ciatej.mx

A. Marroquín, L. Castillo, S. Soto, L. Cruz. (Coord.) CIERMMI Women in Science TXIX Biological Sciences. Handbooks-

Abstract

Beans are some of the most important legumes in human nutrition since they contain various secondary metabolites with antioxidant activity, such as phenolic compounds, associated with the color of the seed coat. Several reports indicate that beans with dark colors (black, red, brown, etc.) provide the highest contents of phenolic compounds, while those with light-colored seed coats have the lowest contents. Furthermore, selenium (Se) is an essential microelement for humans since it acts as an antioxidant and can help prevent various types of cancer and maintain good immune system functioning. This work aims to determine the effects of selenium on the yield, seed size, and phenolic compound content of common bean varieties with white seed coats. Four (0, 2.5, 5, and 10 µM) concentrations of sodium selenite (Na_2SeO_3) were evaluated during the cultivation of three beans (*Phaseolus vulgaris* L.) varieties with white coats, named OX-7, OX-11, and OX-14. Selenium concentrations were applied along with irrigation every 15 days. The OX-7 variety had the longest seeds, while the OX-11 and OX-14 varieties had the highest and lowest numbers of pods, respectively, and the highest and lowest yields. The highest content of phenolic compounds was obtained in the OX-11 variety, with the application of 5 µM Na_2SeO_3. Moreover, the highest concentration of flavonoids was found in OX-11, with both 5 and 10 µM Na_2SeO_3 treatments, as well as in OX-14 treated with 2.5 µM Na_2SeO_3. These findings indicate that the beneficial effect of selenium depends on the concentration, variety, and stage of plant development.

Secondary metabolites, Phenolic compounds, Legumes, Beneficial element

Resumen

El frijol es una de las leguminosas más importantes en la nutrición humana debido a que contiene varios metabolitos secundarios con actividad antioxidante, como los compuestos fenólicos, asociados con el color de la testa de la semilla. Algunos reportes indican que los frijoles de colores oscuros (negro, rojo, café, etc.) proporcionan un alto contenido de compuestos fenólicos, mientras que aquellas semillas con testa de colores claros tienen contenidos bajos. Por otro lado, el selenio (Se) es un microelemento esencial para los humanos debido a que actúa como un antioxidante, puede ayudar a prevenir varios tipos de cáncer y mantener el funcionamiento del sistema inmune. El objetivo de este trabajo es determinar los efectos del selenio en el rendimiento, el tamaño de la semilla y el contenido de compuestos fenólicos de variedades de frijol común de testa blanca. Se evaluaron cuatro (0, 2.5, 5 y 10 µM) concentraciones de selenito de sodio (Na_2SeO_3) durante el ciclo de cultivo de tres variedades de frijol (*Phaseolus vulgaris* L.) con testa de color blanca, codificados como OX-7, OX-11 y OX-14. Las concentraciones de selenio se aplicaron junto con el riego cada 15 días. La variedad OX-7 presentó las semillas más grandes; mientras que, las variedades OX-11 y OX-14 tuvieron el mayor y el menor número de vainas, respectivamente, así como los mayores y menores rendimientos. El mayor contenido de compuestos fenólicos se obtuvo en la variedad OX-11, con la aplicación de 5 µM Na_2SeO_3. También, la mayor concentración de flavonoides se encontró en la variedad OX-11, con ambos tratamientos de 5 y 10 µM Na_2SeO_3, al igual que OX-14 tratada con 2.5 µM Na_2SeO_3. Estos hallazgos indican que los efectos benéficos del selenio dependen de su concentración, la variedad y el estado de desarrollo de la planta.

Metabolitos secundarios, Compuestos fenólicos, Leguminosas, Elemento benéfico

7.1 Introduction

7.1.1 General characteristics of selenium

Selenium (Se) can be found in five allotropic forms, two of which are amorphous with the remaining three crystalline. This element can form molecules with a ring structure consisting of eight atoms and chain molecules of considerable length. Ring-shaped molecules are unstable and occur in red α β crystalline forms (Kieliszek, 2019).

Selenium is an essential microelement for humans and very important for cell metabolism, especially for antioxidant reactions (Woch & Hawrylak-Nowak, 2019). Its deficiency in the human body can lead to heart disease, viral infections, hyperthyroidism, diabetes, and cancer (Pannico *et al*., 2020). This element enters the food chain mainly through the diet, and its level in food depends on the bioavailable reserves in the soil and the absorption and accumulation capacity of plants (Hajiboland *et al*., 2015). Moreover, it is commonly added to the diet as sodium selenite (Na_2SeO_3). However, there is growing interest in dietary supplementation with organic selenium. Organic sources are more efficiently assimilated than inorganic selenium sources and are considered less toxic and, therefore, more appropriate for use as food supplements (Shini *et al*., 2015).

The World Health Organization (WHO) recommends a daily selenium dose of 55 μg for adults. This required amount of Se changes with sex and age, 40-70 μg for men and 45-55 μg for women, while for children, the recommended daily dose is 25 μg (Kieliszek, 2019).

Selenium has been identified as a cofactor of the enzyme glutathione peroxidase, a catalyst in the reduction of peroxides that can damage cells and tissues, and can act as an antioxidant (Mezeyová *et al*., 2020). Besides, Se is incorporated into selenoproteins that exert antioxidant and anti-inflammatory effects. The selenoprotein family in humans includes the following enzymes: glutathione peroxidases (GPX1-GPX4 and GPX6), thioredoxin reductase (TXNRD1-2), thioredoxin-glutathione reductase (TXNRD3), iodothyronine deiodinases (DIO1-3), selenophosphate (SEPHS2), and methionine sulfoxide reductase B1 (MSRB1) (Zoidis *et al*., 2018). These selenoproteins depend mainly on Se intake through the diet. Selenoproteins are essential for human health, mainly due to their antioxidant activity (Mezeyová *et al*., 2020).

Furthermore, selenomethionine is the main chemical form of selenium in plants, while selenocysteine predominates in animals. Therefore, selenoamino acids (selenocysteine and selenomethionine) are necessary for the synthesis of selenium-containing peptides and proteins (Shini *et al*., 2015).

The effects of selenium have been addressed in many aspects of biomedicine, biochemistry, and environmental science. Selenium also has agricultural applications as a soil fertilizer and animal feed (Natasha *et al*., 2018). The application of Se at low concentrations has emerged as a possible alternative to synthetic fungicides for controlling plant diseases and reducing their potentially dangerous effects on the environment and human health (López-Velázquez *et al*., 2019)

7.1.2 Selenium in the soil

Selenium exists naturally in the Earth´s crust and is highly available to living things in arid areas with alkaline soils. Selenium concentrations are low, from 0.01 to 2.0 mg/kg, with an average of 0.4 mg/kg, although concentrations of 1200 mg/kg can be found in seleniferous soils (Becvort-Azcurra *et al*., 2012). Selenium in the soil exists in four oxidation states: selenite (Se^{4+}), selenate (Se^{6+}), elemental selenium (Se^0), and selenide (Se^{2-}). Plants can absorb selenium in the forms of selenite and selenate, both of which are components of the most common inorganic compounds present in the soil (León-Morales *et al*., 2019), but selenium can also be present in organic forms such as selenomethionine (SeMet), selenocysteine (SeCys), and methyl selenocysteine (MeSeCys) (Natasha *et al*., 2018). Selenium can bind with organic and inorganic elements and can form complexes with different elements, such as hydrogen, oxygen, iron, and halogens (Natasha *et al*., 2018).

Soil is the primary source of Se for plants, while plants are the main sources of Se for humans and animals (Shini *et al*., 2015). Application of fertilizer containing Se is the best possible strategy for enriching soils deficient in this element. The use of organic fertilizers amended with Se is widespread in countries with Se-deficient soils (Natasha *et al*., 2018).

7.1.3 Selenium uptake and metabolism in plants

Plants assimilate Se mainly in the form of Se^{6+} or Se^{4+}. Selenate is absorbed by the plasma membranes of root cells using sulfate (SO_4) assimilation pathways with the action of the enzyme sulfate permease, while selenite is absorbed through phosphate (PO_4) transporters (Pannico *et al*., 2019).

The selectivity of these transporters depends on the plant species and is affected by the concentration of sulfate and the salinity, pH, and redox potential of the soil (Pannico *et al*., 2020). Different types of sulfate carriers may have different selectivity for selenium and sulfur. However, compared to selenate, selenite is less soluble, more phytotoxic, and more difficult to transport and accumulate in plant tissues (Pannico *et al*., 2019).

Selenate can access the SO_4 assimilation pathway and be reduced through Se^{4+} to Se^{2-} (Malagoli *et al*., 2015) with greater incorporation of selenium into amino acids, especially in the accumulation of low molecular weight methylated species in plants (Wrobel *et al*., 2020). Methylated Se species have shown biological activity of great relevance to human health. Moreover, a defensive mechanism found in accumulator and hyperaccumulator plants is based on the synthesis of various methylated selenium species that cannot be integrated into the protein structure (Wrobel *et al*., 2020).

Some plants accumulate organic Se compounds such as methyl selenocysteine (MeSeCys), γ-glutamyl-MeSeCys, and selenocysteine (SeCys). Moreover, Se can also volatilize from plants in the form of dimethyl selenide or dimethyl diselenide, which are produced from SeMet and methyl SeCys, respectively (Malagoli *et al*., 2015).

The phytotoxicity of Se in plants is mainly due to its incorporation into the amino acids selenocysteine and selenomethionine, which replace their sulfur analogs in plant proteins (Pannico *et al*., 2020). Selenium uptake capacity depends mainly on plant species, with most agricultural and horticultural plants classified as nonaccumulators. At the same time, accumulators can grow in soils with high concentrations of salts (Mimmo *et al*., 2017). Plants have been classified according to their Se accumulation capacity as hyperaccumulators (1000-15000 mg/kg), accumulators (do not exceed 1000 mg/kg), and nonaccumulators (<100 mg/kg) (Wrobel *et al*., 2020).

Selenium accumulates mainly in the sprouts of plants. However, the degree of transfer of Se from the root to the aerial part of a plant depends on the plant species and the type and form of the Se species present in the soil (Natasha *et al*., 2018). Selenate accumulates more readily in the aerial part of the plant, while most of the selenite remains in the roots and is quickly converted to organic forms (Natasha *et al*., 2018).

7.1.4 The role of selenium in plant growth and physiology

Selenium, at low concentrations, acts as an antioxidant and can stimulate plant growth and improve tolerance to oxidative stress. In contrast, it acts as a pro-oxidant at high concentrations, which reduces plant growth by interfering with the sulfur metabolic pathway (Pannico *et al*., 2019). A low concentration of Se stimulates antioxidant activity and the potential of the plant to cope with biotic or abiotic stress. On the other hand, high Se concentrations are tolerated by accumulator and hyperaccumulator plants, causing adverse effects in nonaccumulator plants (Wrobel *et al*., 2020).

The growth of lettuce plants has been evaluated through the application of sodium selenite (Na_2SeO_3). The results showed that the optimal dose for plant growth was 7.35 μM (Nawaz *et al*., 2014). Furthermore, selenium has been applied to tomato and pepper plants in the form of sodium selenite (Na_2SeO_3) in a 50% nutrient solution with concentrations of 5, 10, and 20 μM After 20 days, greater root and sprout growth was observed, and increases in dry biomass in both tomato and pepper were observed with the 5 μM concentration (Saldaña-Sánchez *et al*., 2019).

Rice seedling growth has been evaluated with sodium selenate (Na_2SeO_4) applied at 15, 30, 45, 60, 75, 90, and 105 mg/kg. The results indicated that the highest growth occurred at a concentration of 15 mg/kg (Du *et al*., 2019). Furthermore, the effect of foliar application of Se at concentrations of 5, 10, and 20 mg/L Na_2SeO_4 on grape plants (*Vitis vinifera* L.) has been evaluated. The results showed that the application of Se had a positive effect on the height of the plant, the number of leaves, and the leaf area, especially at a concentration of 5 mg/L (Karimi *et al*., 2020).

To evaluate the germination and initial growth of pepper (*Capsicum annum* L.) and radish (*Raphanus sativus* L.), Na_2SeO_3 and Na_2SeO_4 were applied at concentrations of 1.25, 2.5, and 5 μM. In general, the germination percentage of pepper increased, but germination of radish remained unaffected. The addition of selenite increased the heights of the seedlings in both radish and pepper at a 5 μM concentration, while selenate at a 1.25 μM concentration improved length and number of roots in pepper and radish; height increased with this same concentration (León-Morales *et al*., 2019).

7.1.5 The importance of beans

Mexico has been recognized as the primary center of bean diversification. This crop is considered one of the oldest; some of the archaeological finds in Mexico and South America indicate that it was known 5000 years BC (Quintana-Blanco *et al*., 2016). In Mexico, beans are the legumes with the highest human consumption, ranging from 110 g to 10.38 kg per person in a year (SAGARPA, 2017). In Mexico, 70 species of the genus *Phaseolus* are reported out of the 150 species that exist in the world; of these, five have been domesticated: *Phaseolus vulgaris* (common bean), *P. coccineus* (ayocote bean), *P. lunatus* (lima bean), *P. acutifolius* (tepary bean), and *P. dumosus* (year-long bean) (Alcázar-Valle *et al*., 2020). Bean grains are sources of carbohydrates, proteins, lipids, B vitamins, fiber, minerals, and bioactive compounds with high antioxidant activity, such as flavonoids, anthocyanins, polyphenols, tannins, and flavones (García-Díaz *et al*., 2018). Among the *Phaseolus vulgaris* varieties, there are different types of grains. Commercial value is influenced by characteristics such as size, color, grain uniformity, cooking time, and flavor (Mederos, 2006). Depending on the type of bean, the protein content varies from 14 to 33%, being rich in amino acids such as lysine and phenylalanine but with deficiencies in sulfur amino acids such as methionine and cysteine. Nevertheless, according to biological evaluations, the protein quality of cooked beans can reach as high as 70% (Ulloa *et al*., 2011).

The color of the bean seed coat is often highly variable. This characteristic is determined by nine main genes that are responsible for generating changes in the patterns of seed color variation ranging from homogeneous primary colors or primary colors with secondary colors expressed as variegated spots, marks, stripes or patterns to combinations of two phenotypic expressions up to a uniform color (García-Díaz *et al*., 2018). The color of the bean seed coat is related to the contents of various phenolic compounds, mainly tannins, flavonoids, and anthocyanins (Chávez-Mendoza *et al*., 2019). Some authors, such as Xu & Chang (2009), have reported that black bean seeds provide a higher content of phenols, while white bean seeds have a lower content.

7.1.6 Phenolic compounds of beans

Phenolic compounds are molecules that contain one or more aromatic or benzene rings that are attached to one or more hydroxyl groups. These compounds are widely distributed in nature, especially in plants such as cereals, fruits, and vegetables, whether in stems, roots, flowers, fruits, or seeds. Therefore, they play various roles in metabolism, growth, reproduction, and protection against pathogenic organisms such as viruses, bacteria, and fungi (Abarca-Vargas & Petricevich, 2019). They contribute to some organoleptic properties of plant foods, for example, color and flavor.

Studies carried out by Xu & Chang (2009) indicate that the content of phenolic compounds in beans is higher than in other legumes, such as lentils, chickpeas, and soybeans. Phenolic compounds have a wide range of biological effects, with their anticarcinogenic and anti-inflammatory activities highlighted (Pérez-Pérez *et al*., 2019).

Phenolic compounds are divided into hydroxycinnamic acids and hydroxybenzoic acids. The mean phenolic compounds in bean are ferulic, p-coumaric, caffeic, and sinapic acids, which are hydroxycinnamic acids. Gallic, p-hydroxybenzoic, vanillin and syringic acid are hydroxybenzoic acids (Yang *et al*., 2018)

Flavonoids are low molecular weight compounds that can act as inhibitors of the growth of tumors and some types of cancer; together with phenolic acids and tannins, they increase the antioxidant capacity of foods due to their high redox potential (Pérez-Pérez *et al*., 2019). However, various factors can degrade these compounds, such as storage at high temperatures and exposure to light. The main flavonoids present in bean seed coats are quercetin and kaempferol (Capistrán-Carabarin *et al*., 2019).

Common bean is a food source rich in proteins, lipids, vitamins, minerals, bioactive molecules, and compounds with high antioxidant activity, such as phenolic compounds, which are associated with the color of the seed coat (Xu & Chang, 2009). Black bean seeds provide a higher content of phenolic compounds than white bean seeds. Phenolic compounds exert various biological effects, in particular, antioxidant, anticarcinogenic, and anti-inflammatory activities.

Selenium plays a vitally important role because it is an essential element for humans as a component of several enzymes, such as glutathione peroxidase (GSH-Px), which protects the human body against oxidizing agents. Selenium also has anticancer and anti-inflammatory properties, so a deficiency in this element can alter the body´s physiological functions, causing heart disease, diabetes, and cancer (Pannico *et al*., 2020).

An option for increasing Se intake is to consume crops enriched or supplemented with this element. Biofortification is the process of increasing the bioavailable content of specific elements in the edible parts of plants through agricultural intervention or genetic selection. Biofortification with Se seeks to improve the nutritional quality of vegetables, which implies the production of crops with more significant health benefits. The level of Se in food depends on the bioavailable reserves in the soil and the absorption and accumulation capacities of plants.

This work aimed to determine the effect of selenium on the phenolic content of the common white bean seed. Various concentrations of sodium selenite (Na_2SeO_3) were evaluated through application to the roots with irrigation every 15 days during bean cultivation until seeds were obtained.

7.2 Methodology

7.2.1 Establishment of the experiment

Bean seeds were sown in germination trays with a commercial substrate (SUNSHINE, 90% sphagnum and 10% vermiculite, dolomite, limestone) under greenhouse conditions at an average temperature of 24 °C and average relative humidity of 52.6%. At 21 days after sowing, seedlings of uniform size were selected and transplanted into pots with the commercial substrate (SUNSHINE), with two plants per pot. Four concentrations of sodium selenite (Na_2SeO_3) were used for this experiment: 0, 2.5, 5, and 10 µM, as well as three bean varieties (OX-7, OX-11, and OX-14). Different concentrations of Na_2SeO_3 were applied to the roots together with irrigation every 15 days. There were six replicates (six pots) for each bean variety and each Se treatment, for a total of 120 pots.

7.2.2 Determination of the number and lengths of pods

Four months after the establishment of the experiment, pods were collected. The lengths of 20 pods were measured for each combination of bean variety and treatment. A total of 240 pods were used. An electronic Vernier caliper was used to measure pod length.

7.2.3 Determination of bean seed size

The length, width, and thickness of each seed obtained were determined. Measurements were made on 20 seeds per replicate for each bean variety and for each treatment for a total of 1440 seeds. An electronic Vernier caliper was used to measure the seeds.

7.2.4 Determination of the weight of 100 seeds

For seed weight, 100 seeds were counted for each treatment for varieties OX-7 and OX-11. For variety OX-14, the weight of 50 seeds was recorded.

7.2.5 Preparation of extracts for the determination of phenolic compounds

Extracts were prepared from white bean seeds. First, each sample of seeds was ground in a coffee grinder until a very fine powder was obtained. Next, we weighed 1 g of fine powder and added 10 mL of a solution composed of acetone, water, and acetic acid in a 70:29.5:0.5 (v/v/v) ratio (Gu *et al*., 2002). Then, maceration was carried out at room temperature in the dark with stirring for 17 h. After this time, the extracts were centrifuged at 4000 rpm for 8 min, washed, and centrifuged again under the same conditions. Subsequently, the supernatants from the maceration and washing were combined for each sample. Finally, the extracts were concentrated at 40 °C in a rotary evaporator (Buchi, R-100, Switzerland). The extracts were stored at -20 °C until analysis (Alcázar-Valle *et al*., 2020).

7.2.6 Determination of total phenolic content

Total phenolic content was determined using the Folin-Ciocalteu (F-C) method. The previously obtained extracts were used; 50 µL of each sample was mixed with 3 mL of distilled water, 250 µL of the F-C reagent (2N), and 750 µL of the sodium carbonate solution (7%, w/v) and incubated at room temperature for 8 min. Next, 950 µL of distilled water was added to each sample, and the solutions were mixed and left in darkness for 2 h to read the absorbance at 765 nm with a spectrophotometer (Tecan, Infinite M200 Pro, Switzerland). Phenolic compounds were quantified using a gallic acid standard curve (0 to 500 mg L^{-1}) and reported in gallic acid equivalents (GAE) per gram of sample (Alcázar-Valle *et al*., 2020).

7.2.7 Determination of flavonoid content

Flavonoid content was determined using aluminum chloride ($AlCl_3$) solution. First, 133 mg of $AlCl_3$ and 400 mg of sodium acetate ($C_2H_3NaO_2$) were weighed and dissolved in 100 mL of diluent solution (methanol-water-acetic acid; 140:50:10 v/v). Then, fifty microliters of each sample, previously extracted, was mixed with 700 µL of deionized water, and 250 µL of $AlCl_3$ solution was added. The resulting solutions were mixed and kept at room temperature for 30 min to complete the reactions. Finally, absorbance values were read at 410 nm with a spectrophotometer (Tecan, Infinite M200 Pro, Switzerland). Flavonoid quantification was performed using a quercetin standard curve (0 to 80 µg mL^{-1}) and expressed as quercetin equivalents (QE) per gram sample (Alcázar-Valle *et al*., 2020).

7.2.8 Statistical analysis

An analysis of variance and comparison of means was performed with the Duncan multiple range test ($p \leq 0.05$) using the procedures of the SAS 9.1 statistical package.

7.3 Results

To evaluate the effect of sodium selenite (Na_2SeO_3), three bean varieties (OX-7, OX-11, and OX-14) were used, applying four concentrations of Na_2SeO_3 (0, 2.5, 5, or 10 µM). The treatments were applied by root application during the bean crop cycle. At the end, yield production, number, length of pods, and seed dimensions were obtained. Besides, the contents of total phenolic compounds and flavonoids in bean seeds were also determined.

7.3.1 Effect of selenium on the yield production of common bean

The OX-7 variety did not show significant variation in bean yield per plant among the 2.5, 5, and 10 µM Se concentrations; however, yields from these treatments differed significantly from that of the control (0 µM). In the OX-11 variety, no significant difference was observed between the 0 µM and 5 µM concentrations, but there were significant differences between the control (0 µM) and the 2.5 and 10 µM concentrations of Se. The OX-14 variety showed significant differences between the 0 and 10 µM concentrations, with a yield higher for the higher concentration of sodium selenite (Na_2SeO_3). The OX-11 variety had the highest yield, and OX-14 had the lowest yield (Graphic 7.1 A).

About the weight of 100 seeds for the OX-7 and OX-11 varieties, the OX-7 variety showed significant differences between the control (0 µM) and the 5 and 10 µM concentrations of Se, with a tendency for seed weight to increase as the concentration of sodium selenite (Na_2SeO_3) improved. In the OX-11 variety, a significant difference was observed between the control (0 µM) and the 2.5 µM Se concentration. In the OX-14 variety, the weight of 50 seeds was recorded because 100 seeds were not obtained for each replicate and treatment. Variety OX-14 did not show significant differences among the treatments applied (Graphic 7.1B).

Graphic 7.1 Total yield per plant (A) and 100-seed weight (B) of white bean varieties grown under the application of different concentrations of sodium selenite (Na_2SeO_3). Means with different letters indicate significant differences according to Duncan's test ($p<0.05$), ± standard deviation

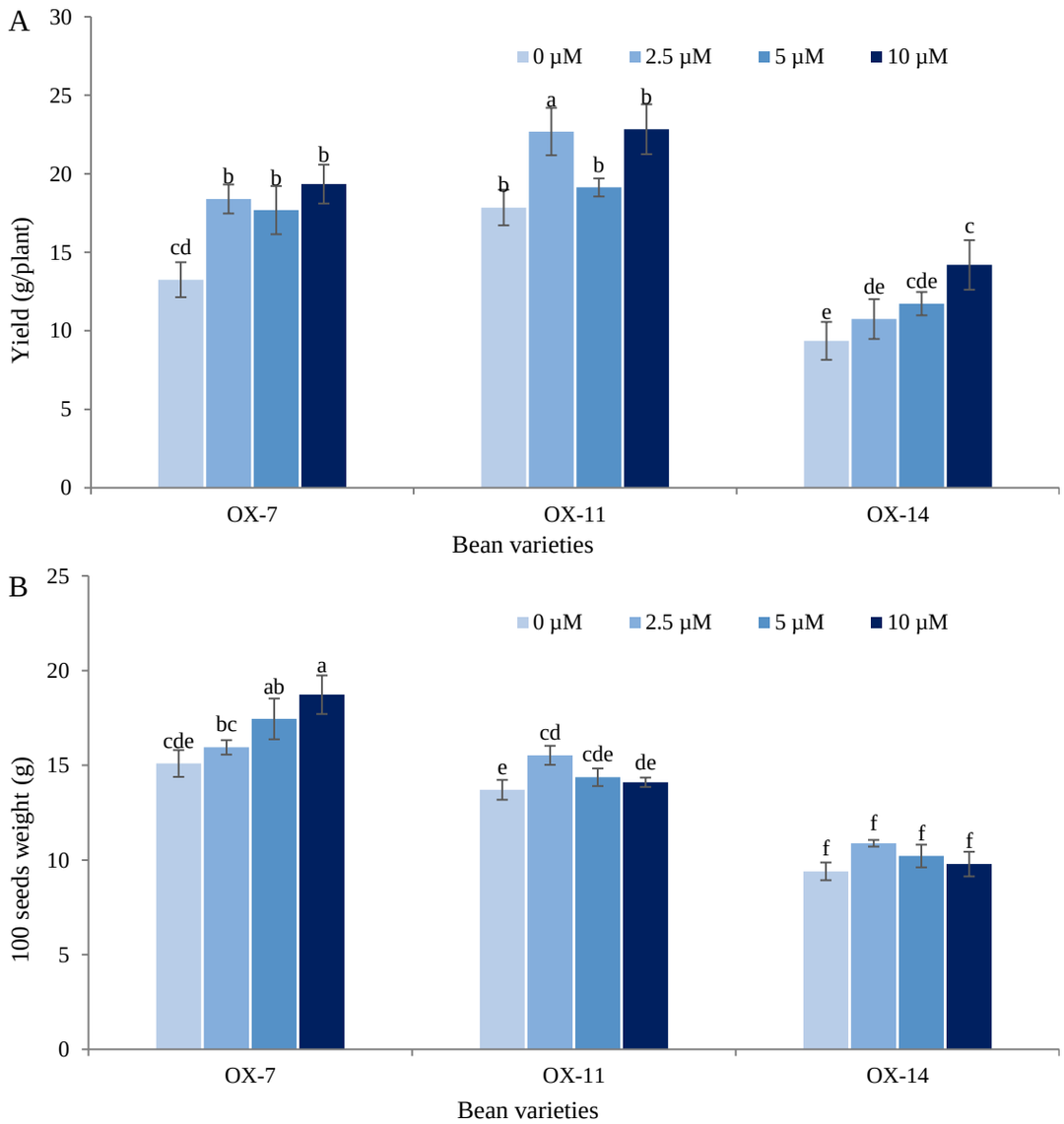

7.3.2 Characteristics of bean seeds due to the effect of selenium

In the OX-7 variety, the greatest seed length was observed with the 10 µM concentration, while in this same variety, there were significant differences between the 0 and 10 µM concentrations in seed width and thickness. Variety OX-11 did not show significant differences in seed length between the 0 and 10 µM concentrations, while significant differences were observed in seed width and thickness for the 2.5 µM concentration. In the OX-14 variety, no significant differences were observed in seed length or thickness between the 0 and 10 µM concentrations. In contrast, there was a significant difference in seed width between the same concentrations. In general, variety OX-7 had the longest seeds, while variety OX-14 had the widest and thickest seeds (Table 7.1).

In the OX-7 variety, a significant difference was observed between the 0 and 2.5 µM Se concentrations. Varieties OX-11 and OX-14 had the highest and lowest number of pods, respectively, with the 2.5 µM Se concentration, although there were no significant differences with respect to the control. In general, the OX-11 variety exhibited the highest number of pods among the varieties; OX-7 had an intermediate number, while OX-14 had the lowest number of pods (Table 7.1). Regarding pod length, the most significant differences in length were observed in the OX-7 variety with the 2.5 and 10 µM Se concentrations. In comparison, in the OX-14 variety, the greatest length occurred with the 2.5 µM Se concentration. In the OX-11 variety, there were significant differences between the control (0 µM) and the 10 µM Se concentration (Table 7.1).

Table 7.1 Seed and pod characteristics of white bean varieties supplemented with different concentrations of Na_2SeO_3 (Se)

Bean varieties	Se [µm]	Seed lenght (mm)	Seed width (mm)	Seed thickness (mm)	Pod number	Pod length (cm)
OX-7	0	9.61±0.33ab	5.64±0.23c	4.51±0.26d	22.67±2.02ef	7.51±0.45bcd
	2.5	9.30±0.29de	5.63±0.16c	4.74±0.18c	28.33±2.07cd	8.02±0.39ab
	5	9.06±0.35f	5.70±0.20c	4.87±0.24bc	23.00±3.22ef	6.87±0.30e
	10	9.77±0.42a	5.90±0.19b	4.86±0.19bc	26.17±1.53de	8.22±0.19a
OX-11	0	9.62±0.31ab	4.92±0.14e	3.96±0.19e	32.67±2.80abc	7.73±0.22abc
	2.5	9.30±0.37cde	5.32±0.31d	4.49±0.37d	36.33±1.91a	7.35±0.36cde
	5	9.50±0.34bc	4.95±0.14e	4.02±0.16e	30.67±0.61bc	7.50±0.18cd
	10	9.62±0.34ab	4.85±0.14e	3.97±0.16e	33.33±1.37ab	7.41±0.15de
OX-14	0	9.52±0.46bc	6.14±0.19a	5.22±0.19[a]	17.00±0.63g	6.89±0.34e
	2.5	9.11±0.68ef	5.73±0.39c	4.85±0.37bc	15.33±1.21g	7.76±0.27abc
	5	9.23±0.42def	5.91±0.20b	4.96±0.22b	19.33±0.93gf	7.46±0.28cd
	10	9.39±0.42bcd	5.99±0.20b	5.12±0.23[a]	19.83±1.83gf	7.16±0.21de

Means with different letters indicate significant differences according to Duncan's test ($p<0.05$), ± standard deviation

Source: Author's elaboration

7.3.3 Total phenol and flavonoid contents in bean seeds with different concentrations of Se

Concerning total phenols, the OX-7 variety showed a significant difference between the 0 and 10 µM concentrations, with a tendency for phenolic content to increase with increasing concentration of Se. Variety OX-11 showed significant differences for the 5 µM concentration of Se and the highest content of total phenols with this same concentration. In the OX-14 variety, no significant differences were observed among the applied treatments (Graphic 7.2A).

The content of flavonoids in bean seeds of variety OX-7 did not show significant differences among the applied treatments. The OX-11 variety showed significant differences at 5 and 10 µM Se concentrations. The variety OX-14 showed significant differences for the 2.5 µM Se concentration. In general, the highest flavonoid content was observed in the OX-11 variety at 5 µM, while at this same concentration, the OX-14 variety showed the lowest flavonoid content (Graphic 7.2B).

Graphic 7.2 Effect of Na_2SO_3 (Se) in the content of total phenolic compounds (A) and flavonoids (B) in seeds white bean varieties. Means with different letters indicate significant differences according to Duncan's test ($p<0.05$), ± standard deviation

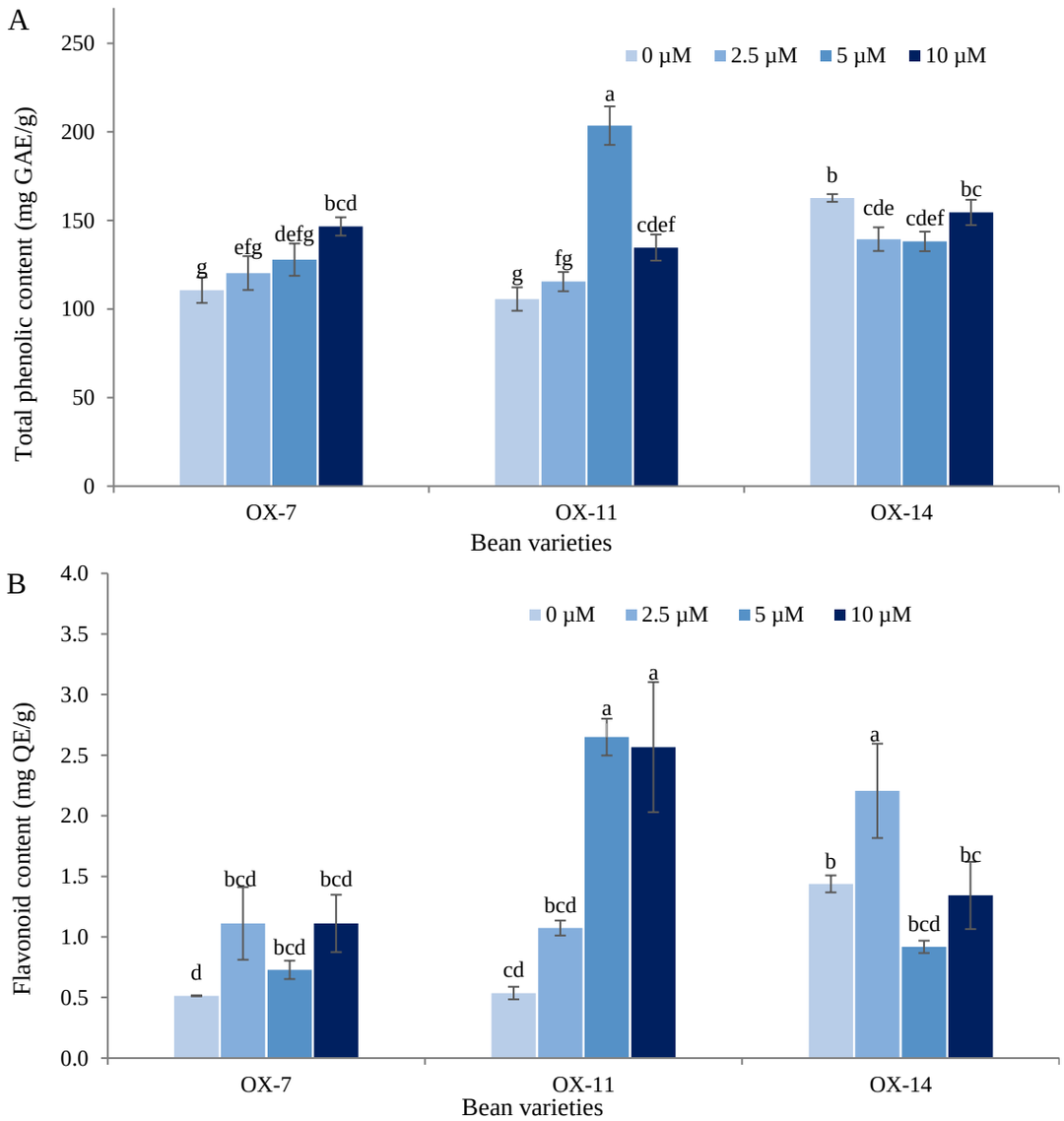

7.4 Discussion

Biofortification with Se is an excellent strategy for increasing the Se content in food and improving the nutritional quality of vegetables, which implies the production of crops with more significant health benefits (León-Morales *et al*., 2019). The application of Se in a nutrient solution in soilless cropping systems (SCS) is the most efficient approach, as it can be applied more reliably through precise management of the composition and concentration of the nutrient solution (Pannico *et al*., 2020). Studies by Pannico *et al*. (2019) reported that biofortification with a 40 µM concentration of Na_2SeO_4 increased the Se content in red lettuce plants. In an investigation of wheat plants reported by Poplaciones *et al*. (2014), the greatest effect was found with the 10 µM concentration of Na_2SeO_4.

Seed size and growth habit are related to the efficiency of biomass allocation to grain in the growth environment. Nevertheless, these attributes depend on other seed characteristics, such as vigor (Morales-Santos *et al*., 2017). Vigor is a seed's biological potential for rapid and uniform establishment even under unfavorable plant conditions (Morales-Santos *et al*., 2017).

In this work, the OX-7 variety had the longest seeds, while the OX-14 variety had the thickest and widest seeds. According to studies reported by Alcázar-Valle *et al*. (2020), the species *P. coccineus* had the longest seeds. However, *P. vulgaris* was distinguished as the most heterogeneous species in terms of size differences among varieties.

The total yield per plant of white bean varieties OX-7, OX-11, and OX-14 varied among varieties and concentrations of Na_2SeO_3. This work reports the highest yield for the OX-11 variety, while the lowest yield is reported for the OX-14 variety. Studies by Premarathna *et al*. (2012) reported that the optimum dose in rice plants was 15 µM Na_2SeO_3. In this work, the highest yield was with a concentration of 10 µM Na_2SeO_3.

The highest flavonoid content was found in the OX-11 variety at a concentration of 5 µM, while the lowest content was found in the OX-14 variety at the same concentration. For the total phenolic content, a tendency was observed in the OX-7 variety: as the concentration of Se increased, the total phenolic content increased. Particularly in beans, in studies by Alvarado-López *et al*. (2019), the purple variety of the ayocote bean (*P. coccineus*) exhibited high concentrations of total phenolic compounds and flavonoids and high antioxidant activity. Xu & Chang (2009) mention the relationship between bean color and phenolic compound content, with light-colored beans containing lower levels of phenols than in dark-colored beans. However, in studies reported by Pérez-Pérez *et al*. (2019), Peruvian beans with yellow pigmentation showed higher content of phenolic compounds than did black beans.

In other crops, Malagoli *et al*. (2015) reported that a concentration of 2 µM Na_2SeO_4 was the best treatment for increasing the flavonoid content in tomato. Chomchan *et al*. (2017) reported an increase in phenolic compounds with 10 and 20 µM Na_2SeO_3 concentrations in rice. Studies by Woch & Hamrylak-Nowak (2019) showed that the optimal dose of Na_2SeO_3 was 20 µM in alfalfa, while Pannico *et al*. (2020) reported that the concentrations of 16 µM in cilantro and 8 µM in green and purple basil were the most effective for biofortification with Se and for increasing the contents of bioactive compounds.

Several authors, such as Schiavon *et al*. (2013), have reported the effect of selenium on the content of phenolic compounds in tomato leaves, where the highest contents of phenolic compounds were obtained at concentrations of 5 and 10 µM, studies conducted by Ghasemi *et al*. (2015) with garlic plants reported that the highest contents of flavonoids and total phenols were obtained with 10 µM concentration of Na_2SeO_4. In this study, the highest phenolic compound content was obtained in the OX-11 variety with 5 µM Na_2SeO_3, while the highest flavonoid concentration was found in the OX-11 (5 and 10 µM Na_2SeO_3) and OX-14 (2.5 µM Na_2SeO_3) varieties. Thus, variation is observed concerning the concentrations and sources of selenium to obtain the highest content of phenolic compounds in the various cultivars.

7.5 Acknowledgments

This work was conducted at the Plant Biotechnology Department of the PLANTECC National Laboratory.

7.6 Funding

This work has been funded by the CONACYT-FORDECYT project [grant number 292474-2017]

7.7 Conclusion

Variety OX-7 had the longest seeds, and no significant differences in yield were observed among the applied treatments. Variety OX-11 had the highest number of pods, with no significant differences in pod length but with the highest yield. Variety OX-14 had the lowest number of pods and the lowest yield. Regarding flavonoid and total phenolic contents, variety OX-11 exhibited the highest phenol and flavonoid contents, while variety OX-12 had the lowest flavonoid content. Therefore, the beneficial effect of Se depends on the concentration and the variety and stage of development of the plant.
Future studies will consider including another source of selenium, such as sodium selenate (Na_2SeO_4), and other forms of selenium application, with foliar application being an alternative, and will determine the contents of inorganic and organic Se in bean seeds.

7.8 References

Abarca-Vargas, R., & Petricevich, V.L. (2019). Importancia biológica de los compuestos fenólicos. Inventio, 14(34),33-38. DOI: 10.30973/inventino/2018.14.34/4

Alcázar-Valle, M., Lugo-Cervates, E., Mojica, L., Morales-Hernández, N., Reyes- Ramírez, H., Enríquez-Vara. J.N., & García-Morales, S. (2020). Bioactive compounds, antioxidant activity, and antinutritional content of legumes: a comparison between four *Phaseolus* species. Molecules, 25(15), 3528. DOI: 10.3390/molecules25153528

Alvarado-López, A. N., Gómez-Oliván, L. M., Heredia, J. B., Baeza-Jiménez, R., Garcia-Galindo, H. S., & Lopez-Martinez, L. X. (2019). Nutritional and bioactive characteristics of Ayocote bean (*Phaseolus coccienus* L.): An underutilized legume harvested in Mexico. CYTA - Journal of Food, 17(1), 199–206. DOI: 10.1080/19476337.2019.1571530

Becvort-Azcurra, A., Fuentes-Lara, L., Benavides-Mendoza, A., Ramírez, H., & Robledo-Torres. (2012). Aplicación de selenio en tomate: crecimiento, productividad y estado antioxidante del fruto. Terra Latinoamericana, 30,291-301. https://www.scielo.org.mx/pdf/tl/v30n4/2395-8030-tl-30-04-00291.pdf

Capistrán-Carabarin, A., Aquino-Bolaños, E. N., García-Díaz, Y. D., Chávez-Servia, J. L., Vera-Guzmán, A. M., & Carrillo-Rodríguez, J. C. (2019). Complementarity in phenolic compounds and the antioxidant activities of *Phaseolus coccineus* L. and *P. vulgaris* L. landraces. Foods, 8(8):295. DOI: 10.3390/foods8080295

Chávez-Mendoza, C., Hernández-Figueroa, K. I., & Sánchez, E. (2019). Antioxidant capacity and phytonutrient content in the seed coat and cotyledon of common beans (*Phaseolus vulgaris* L.) from various regions in Mexico. Antioxidants, 8(1), 5. DOI: 10.3390/antiox8010005.

Chomchan, R., Siripongvutikorn, S., Puttarak, P., & Rattanapon, R. (2017). Influence of selenium bio-fortification on nutritional compositions, bioactive compounds content and anti-oxidative properties of young ricegrass (*Oryza sativa* L.). Functional Foods in Health and Disease, 7(3),195-209. DOI: 10.31989/ffhd.v7i3.321

Du, B., Luo, Du, H., H He, Luo, L., Zhang, He, L., Liu, Zhang, Y., Mo, Liu, Z., Pan, Mo, S., Tian, Pan, H., Duan, Tian, M., Tang, & Duan, X. (2019). Rice seed priming with sodium selenate: Effects on germination, seedling growth, and biochemical attributes. Scientific Reports, 9, 4311. DOI: 10.1038/s41598-019-40849-3

García-Díaz, Y. D., Aquino-Bolaños, E. N., Chávez-Servia, J. L., Vera-Guzmán, A. M., & Carrillo-Rodríguez, J. C. (2018). Bioactive compounds and antioxidant activity in the common bean are influenced by cropping season and genotype. Chilean Journal of Agricultural Research, 78(2), 255–265. DOI: 10.4067/S0718-58392018000200255

Ghasemi, K., Bolandnazar, S., Tabatabaei, S. J., Pirdashti, H., Arzanlou, M., Ebrahimzadeh, M. A., & Fathi, H. (2015). Antioxidant properties of garlic as affected by selenium and humic acid treatments. New Zealand Journal of Crop and Horticultural Science, 43(3),173-181. DOI: 10.1080/01140671.2014.991743.

Gu, L., Kelm, M., Hammerstone, J., Beecher, G., Cunningham, D., Vannozzi, S., & Prior, R. (2002). Fractionation of polymeric procyanidins from lowbush blueberry and quantification of procyanidins in selected foods with an optimized normal-phase HPLC-MS fluorescent detection method. Journal of Agricultural and Food Chemistry, 50(17):4852-60. DOI: 10.1021/jf020214v.

Hajiboland, R., Ramhat, S., Aliasgharzad, N., & Hartikainen, H. (2015). Selenium-induced enhancement in carbohydrate metabolism in nodulated alfalfa (*Medicago sativa* L.) as related to the glutathione redox state. Soil Science and Plant Nutrition, 61,676-687. DOI: 10.1080/00380768.2015.1032181.

Karimi, R., Ghaboli, M., Rahimi, J., & American, M. (2020). Effects of foliar selenium application on some physiological and phytochemical parameters of *Vitis vinifera* L. cv. Sultana under salt stress. Journal of Plant Nutrition, 43(14), 2226-2242. DOI: 10.1080/0190416.2020.1766072

Kieliszek, M. (2019). Selenium–fascinating microelement, properties and sources in food. Molecules, *24*(7). DOI: 10.3390/molecules24071298

León-Morales, J., Panamá-Raymundo, W., Langarica-Velázquez, E., & García-Morales, S. (2019). Selenium and vanadium on seed germination and seedling growth in pepper (*Capsicum annuum* L.) and radish (*Raphanus sativus* L.). Revista Bio Ciencias, *6*(33), 0–2. DOI: 10.15741/revbio.06.e425

López-Velázquez, J.C., Navarro-López, D.E., Qui-Zapata, J.A., León-Morales, J.M., Saavedra-Loera, D.I., & García-Morales, S. (2019). Efecto del selenito e inulina en la interacción *Capsicum annuum* L. - *Phytophthora capsici* en invernadero. Biotecnología Vegetal, 19,25-34. https://revista.ibp.co.cu/index.php/BV/article/view/598/pdf

Malagoli, M., Schiavon, M., dallÁcqua, S., & Pilon-Smits, E.A. (2015). Effects of selenium biofortification on crop nutritional quality. Frontiers in Plant Science, 6:280. DOI: 10.3389/fpls.2015.00280

Mederos, Y. (2006). Indicadores de la calidad en el grano de frijol (*Phaseolus vulgaris* L.). Cultivos tropicales, 27,55-62. https://www.redalyc.org/pdf/1932/193215825009.pdf

Mezeyová, A., Hegedusova, O., Hegedus, A., Vargova, M., Timoracka, M., Slosar, A., Andrejiova, T., Juríkova, J., & Mezey. (2020). Basil seeds as a source of antioxidants affected by fortification with selenium. Folia Horticulturae, 32,1-10. DOI: 10.2478/fhort-2020-0002

Mimmo, T., Tiziani, R., Valentinuzzi, F., Lucini, L., Nicoletto, C., Sambbo, P., Scampicchio, M., Pi, Y., & Cesco, S. (2017). Selenium Biofortification in *Fragaria* × *ananassa*: Implications on Strawberry Fruits Quality, Content of Bioactive Health Beneficial Compounds and Metabolomic Profile. Frontiers in Plant Science, 8: 1887. DOI: 10.3389/fpls.2017.01887

Morales-Santos, M.E., Peña-Valdivia, C.B., García-Esteva, A., Aguilar-Benitez, G., & Kohashi-Shibata, J. (2017). Características físicas y de germinación en semillas y plántulas de frijol (*Phaseolus vulgaris* L.) silvestre, domesticado y su progenie. Agrociencia, 51,43-62. https://www.scielo.org.mx/pdf/agro/v51n1/1405-3195-agro-51-01-00043-en.pdf

Natasha, Shahid, M., Niazi, N. K., Khalid, S., Murtaza, B., Bibi, I., & Rashid, M. I. (2018). A critical review of selenium biogeochemical behavior in soil-plant system with an inference to human health. Environmental Pollution, *234*, 915–934. DOI:10.1016/j.envpol.2017.12.019

Nawaz, M., Ashraf, R., Ahmad, E., & Ahmad, R. (2014). Selenium (Se) Regulates Seedling Growth in Wheat under Drought Stress. Advances in Chemistry, 2014:143567. DOI:10.1155/2014/143567

Pannico, A., El-Nakhel, C., Kyriacou, M. C., Giordano, M., Stazi, S. R., De Pascale, S., & Rouphael, Y. (2019). Combating Micronutrient Deficiency and Enhancing Food Functional Quality Through Selenium Fortification of Select Lettuce Genotypes Grown in a Closed Soilless System. Frontiers in Plant Science, 10:1495. DOI: 10.3389/fpls.2019.01495

Pannico, A., El-Nakhel, C., Graziani, G., Kyriacou, M. C., Giordano, M., Soteriou, G. A., Rouphael, Y. (2020). Selenium biofortification impacts the nutritive value, polyphenolic content, and bioactive constitution of variable microgreens genotypes. Antioxidants, 9(4). DOI: 10.3390/antiox9040272

Pérez-Perez, L. M., Del Toro, S.C. L., Sánchez, C. E., González, V. R. I., Reyes, D. A., Borboa, F. J., Soto, P. J. M. & Flores-Cordova, M. A. (2019). Bioaccesibilidad de compuestos antioxidantes de diferentes variedades de frijol (*Phaseolus vulgaris* L.) en México, mediante un sistema gastrointestinal *in vitro*. Biotecnia, 22(1), 117–125. DOI: 10.18633/botecnia.v22il.1159

Premarathna, L., McLaughlin, M.J., Kirby, J.K., Hettiarachch, G.M., Stacey, S., & Chittleborough, D.J. (2012). Selenate-enriched urea granules are a highly effective fertilizer for selenium biofortification of paddy rice grain. Journal of Agricultural and Food Chemistry, 60(23),6037-6044. DOI:10.1021/jf3005788

Quintana-Blanco, W. A., Pinzón Sandoval, E. H., & Fernando Torres, D. (2016). Evaluación del crecimiento de fríjol (*Phaseolus vulgaris* L.) cv. Ica Cerinza, bajo estrés salino. Revista U.D.C.A Actualidad & Divulgación Científica, 19(1), 87–95. DOI: 10.31910/rudca.v19.n1.2016.113

SAGARPA. 2017. Planeación agrícola nacional 2017 2030: Frijol mexicano. Disponible en https://www.gob.mx/cms/uploads/attachment/file/255625/Planeaci_n_Agr_cola_Nacional_2017-2030-_parte_dos.pdf (accessed April 25, 2022)

Saldaña-Sánchez, W.D., León-Morales, J.M., López-Bibiano, Y., Hernández-Hernández, M., & Langarica- Velazquez, E.C. (2019). Effect of V, Se, and Ce on Growth, Photosynthetic Pigments, and Total Phenol Content of Tomato and Pepper Seedlings. Journal of Soil Science and Plant Nutrition, 19, 678–688. DOI:10.1007/S42729-019-00068-1

Schiavon, M., dall´Aqua, S., Mietto, A., Pilon-Smits, E.A. H., Sambo, P., Masi, A., & Malagoli, M. (2013). selenium fertilization alters the chemical composition and antioxidant constituents of tomato (*Solanum lycopersicon* L.). Journal of Agricultural and Food Chemistry, 61 (44),10542–10554. DOI:10.1021/jf4031822

Shini, S., Soultan, A., & Bryden, W. (2015). Selenium Biochemistry and Bioavailability: Implications for Animal Agriculture. Agriculture, 5,1277-1288. DOI: 10.3390/agriculture5041277

Ulloa, J. A., Petra, M. C., Ulloa, R., Carmen, J., Ramírez, R., Blanca, I. B. Q., & Ulloa, E. (2011). El frijol (*Phaseolus vulgaris*): su importancia nutricional y como fuente de fitoquímicos. Revista Fuente, *3*(8), 5–9. http://dspace.uan.mx:8080/jspui/handle/123456789/582

Woch, W., & Hawrylak-Nowak, B. (2019). Selected antioxidant properties of alfalfa, radish, and white mustard sprouts biofortified with selenium. Acta Agrobotanica, 72(2), 1–11. DOI: 10.5586/aa.1768

Wrobel, K., Guerrero, M., Yañez-Barrientos, E., & Corrales-Escobosa, A.R. (2020). Different approaches in metabolomic analysis of plants exposed to selenium: a comprehensive review. Acta Physiologiae Plantarum, 42,1-20. DOI: 10.1007/s11738-020-03113-0

Xu, B., & Chang, S. K. C. (2009). Total phenolic, phenolic acid, anthocyanin, flavan-3-ol, and flavonol profiles and antioxidant properties of pinto and black beans (*Phaseolus vulgaris* L.) as affected by thermal processing. Journal of Agricultural and Food Chemistry, 57(11):4754-4764. DOI: 10.1021/jf900695s

Yang, Q. Q., Gan, R. Y., Ge, Y. Y., Zhang, D., & Corke, H. (2018). Polyphenols in common beans (*Phaseolus vulgaris* L.): chemistry, analysis, and factors affecting composition. Comprehensive Reviews in Food Science and Food Safety, 17(6), 1518–1539. DOI: 10.1111/1541-4337.12391

Zoidis, E., Seremelis, I., Kontopoulos, N., & Danezis, G. (2018). Selenium-Dependent Antioxidant Enzymes: Actions and Properties of Selenoproteins. Antioxidants, 7,2-26. DOI:10.3390/antiox7050066

Chapter 8 Genetic improvement of polyester degrading enzymes

Capítulo 8 Mejoramiento genético de enzimas degradadoras de poliésteres

VÁZQUEZ-ALCÁNTARA, Laura†* & PEÑA-MONTES, Carolina

Tecnológico Nacional de México - I. T. Veracruz, Unidad de investigación y Desarrollo de Alimentos, Av. Miguel Ángel de Quevedo No. 2779, Col. Formando hogar, 91987 Veracruz, Ver, México

ID 1er Author: *Laura, Vázquez-Alcántara* / **ORC ID:** 0000-0001-9920-7703, **CVU CONACYT ID:** 714254

ID 1er Co-author: *Carolina, Peña-Montes* / **ORC ID:** 0000-0002-4767-1210, **CVU CONACYT ID:** 277236

DOI: 10.35429/H.2022.6.1.96.108

* carolina.pm@veracruz.tecnm.mx

A. Marroquín, L. Castillo, S. Soto, L. Cruz. (Coord.) CIERMMI Women in Science TXIX Biological Sciences. Handbooks-

Abstract

Synthetic polymers usage has increased according to modern society to have basic applications such as high technology in generating different plastic materials. Therefore, plastic debris accumulates in the environment while biodegradation occurs very slowly. Therefore, the application of hydrolases in the degradation of polyesters has been limited by the ranges of pH and temperature of the environment where these contaminants are found; for this reason, changes have been made in the sequence of some enzymes, resulting in modifications in the structure and change in its characteristics, using molecular techniques such as site-directed mutagenesis, error-prone PCR and random mutagenesis. Many enzymes with polyester degradation activity have been discovered, characterized and designed. However, the classification and integrated knowledge of these enzymes are of interest. For this reason, this paper summarizes the currently known improvement of polyester-degrading enzymes, focusing on their structural and activity modifications.

Mutagenesis, PCR, Enzyme, Mutation, Polyesters

Resumen

El uso de polímeros sintéticos como los poliésteres está en aumento acorde a la sociedad moderna, teniendo tanto aplicaciones básicas como de alta tecnología en la generación de diferentes materiales plásticos. Por lo tanto, los desechos plásticos se acumulan en el medio ambiente en grandes cantidades mientras que su degradación ocurre muy lentamente. La aplicación de hidrolasas en la biodegradación de polímeros sintéticos se ha visto limitada por los rangos de pH y temperatura del ambiente donde se encuentran estos contaminantes, por lo que se han realizado cambios en la secuencia de algunas enzimas, resultando en modificaciones en la estructura. y cambio en sus características, utilizando técnicas moleculares como la mutagénesis sitio-dirigida, la PCR propensa a errores y la mutagénesis aleatoria. Se han descubierto, caracterizado y diseñado enzimas con actividad de degradación de poliésteres. Sin embargo, la clasificación y el conocimiento integrado de estas enzimas son de interés. Por esta razón, en este artículo presentamos una revisión sobre el mejoramiento de enzimas degradadoras de poliésteres actualmente conocidas, centrándonos en sus modificaciones estructurales y de actividad.

Mutagénesis, PCR, Enzima, Mutación, Poliésteres

8.1 Introduction

According to modern society, synthetic polymers have increased to have had basic applications such as high technology. This increase is because of the low production costs of plastic from fossil feedstock, besides the material's high durability, being both relevant advantages and becoming a burden on the global ecosystem (Moharir and Kumar, 2019). Therefore, plastic debris accumulates in the environment to a large extent, while biodegradation occurs very slowly (Lebreton *et al*., 2018).

Among these contaminants are heteroatomic plastics such as polyamides, polyurethanes and polyesters, which contain groups of greater reactivity and therefore are more easily biologically degraded (Wei and Zimmermann, 2017). In recent years, enzymes have been used for the degradation of polyesters, such as carboxylic ester hydrolases (E.C.3.1.1) that have degraded PCL (polycaprolactone), PLA (polylactic acid) and PET (polyethylene terephthalate) (Nikolaivits *et al.* al., 2018). However, some polyesters have not been hydrolyzed efficiently, which is why the structure and functioning of enzymes have been investigated through enzymatic engineering to improve the hydrolysis activity of polyesters (Dubey *et al*., 2019).

The application of hydrolases in the degradation of polyesters has been limited by the ranges of pH and temperature of the environment where these contaminants are found; for this reason, changes have been made in the sequence of some enzymes, resulting in modifications in the structure and change in its characteristics, using molecular techniques such as site-directed mutagenesis, error-prone PCR and random mutagenesis (Lu *et al*., 2022).

One of the most studied enzymes regarding the degradation of polyesters has been the esterase of *Ideonella sakaiensis*, which without making modifications, can degrade PET but only under certain conditions, for which they decided to make modifications in its sequence with the help of molecular techniques such as site-directed mutagenesis changing the amino acids (S160A, D206A, H237A) thus obtaining better results of enzyme degradation activity and stability (Liu *et al.*, 2019).

Many enzymes with polyester degradation activity have been discovered, characterized and designed. However, the classification and integrated knowledge of these enzymes are of interest. For this reason, we present a review of currently known improved polyester-degrading enzymes, focusing on their structural and activity modifications.

8.2 Site-directed mutagenesis

It is a technique that is one of the most used for the modification of enzymes, which allows the selective engineering of gene sequences and has been used to investigate the catalytic properties of proteins. One of the most critical steps in this technique is selecting and identifying the site of the mutations. Bioinformatics-based 3D modeling of the enzyme structure can be carried out using the PDB protein database (Dubey *et al.*, 2019; Liu *et al.*, 2008). In this technique, two independent PCR reactions are performed. The resulting first PCR products are used for an overlapping extension PCR reaction, with the products of the overlapping extension PCR reaction finally cloned into plasmids and expressed. Commonly in bacteria and yeasts, figure 8.1 (Tseng *et al*., 2008; Tee *et al*., 2013).

Figure 8.1 Principles of molecular cloning: (A) complementary overhangs, (B) homologous sequences, (C) overlapping PCR and (D) megaprimer

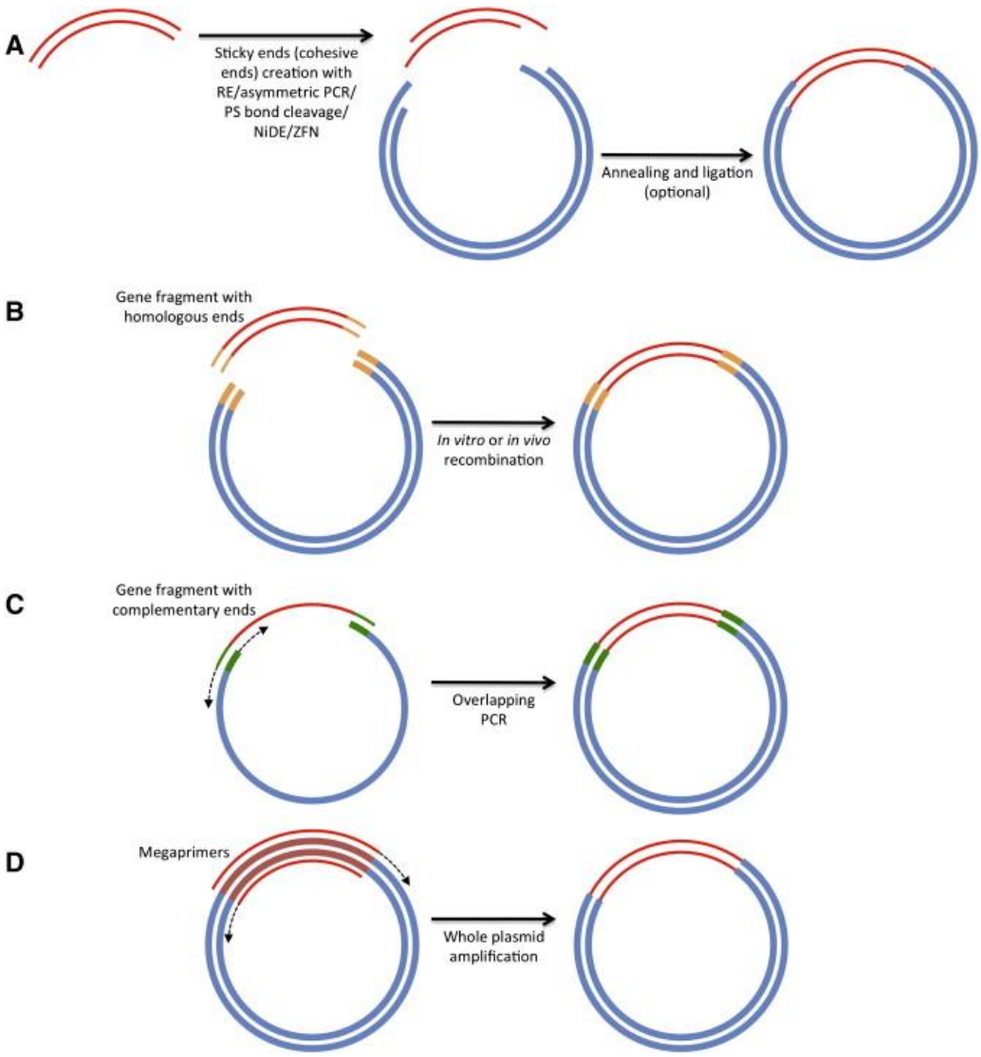

Source: (Tee et al., 2013)

The position of the bound ligand in the active site of RPA1511 and analysis of PLA hydrolysis products suggest that this enzyme can cleave PLA with both endo- and exoesterase. Using structure-based site-directed mutagenesis, we identified several residues of RPA1511 that were essential for PLA hydrolysis but not required for activity against a soluble monoester substrate. These residues represent a potential structural motif for PLA binding, and further characterization will help narrow the search for new PLA depolymerase based on sequence analysis (Hajighasemi *et al*., 2016).

Studies were also carried out on a *Clostridium botulinum* polyesterase in which the Cbotu_EstA zinc-binding domain was modified by site-directed mutagenesis, and a specific domain consisting of 71 amino acids at the N-terminus of the enzyme was also removed. A combination of substitution of residues in the zinc-binding domain synergistically increased enzyme activity in PET seven-fold when combined with truncation of 71 amino acids at the N-terminus of the enzyme alone. Compared to the native enzyme, the combination of truncation and substitutions in the zinc-binding domain leads to a 50-fold improvement in activity (Biundo *et al.*, 2018).

This technique was used with a carboxylic ester hydrolase from a marine bacterium *Pseudomonas aestusnigri* (VGXO14T), modified by mutagenesis to improve the potential for PET degradation, obtaining a variant (Y250S) in which changes were made to stabilize the MHET at the catalytic site with the help of hydrophobic interactions. After making these changes, the production of MHET was measured, resulting in 5.4 mg/L in 48 h at 30 ºC, compared to the unmodified enzyme, which was 4.2 mg/L of MHET (Bollinger *et al.*, 2020).

Figure 8.2 Predicted ligand binding modes in wild-type PE-H and variant Y250S. The predicted binding poses of BHET (magenta), MHET (yellow), and 2-HE(MHET)4 (brown) in WT PE-H (navy) and the variant Y250S (cyan). In (A, C, F), S171 is shown in orange, and in (B, D, E), the catalytic triad (S171, D217, and H249) is shown in orange and interacting residues are shown in white. (A) In wild-type PE-H, BHET and MHET bind to a groove adjacent to the catalytic site (white arrow). (B) BHET and MHET bind to the hydrophobic groove and are stabilized by hydrogen bonding interactions with S103, D106, S248, and S256. 2-HE(MHET)4 binds similarly to BHET and MHET in the groove adjacent to the catalytic site. (C) In the variant Y250S, MHET binds to the catalytic site, while BHET occupies the hydrophobic groove. (D) MHET binds to the catalytic site and is stabilized by hydrophobic interactions to F98, V99, M172, and I219 such that S171 can attack the carbonyl carbon for ester hydrolysis. (E) A second binding pose of BHET binds similarly to MHET. (F) Proposed mechanism of PET polymer interaction. Residues G254, Y258, and N259, which, when substituted, decrease esterase activity, are shown in red. One polymer unit (stylized green rectangle) binds to the groove adjacent to the catalytic site, a second unit bridges the distance to the catalytic site, and a third unit cleaves from the polymer chain at the catalytic unit

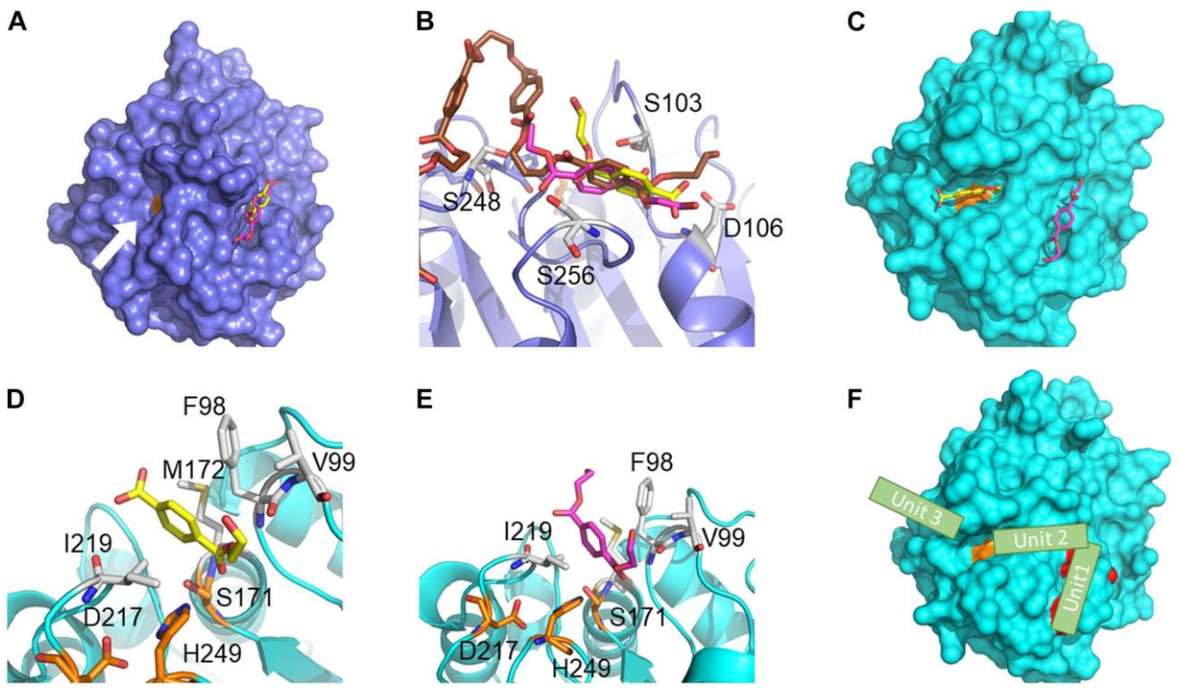

(Bollinger et al., 2020)

Another enzyme modified by this method was a PET hydrolase from I*deonella sakaiensis* (6THS), which managed to degrade 90% in 10 h, achieving productivity of 16.7 grams of terephthalate per liter per hour (200 grams per kilogram of PET suspension). , with an enzyme concentration of 3 milligrams per gram of PET), the changes made to this enzyme were in the amino acids D238 and S283, where these amino acids carry out the formation of disulfide bonds (Fig. 8.2), which allows the thermal stabilization of 94.4 ºC, 9.8 ºC higher than the wild-type enzyme, with a decrease in the activity of only 28% (Tournier *et al*., 2020).

Figure 8.3 Improvement of LCC thermostability by addition of a disulfide bridge. (a), The leading figure shows the locations of putative sites that coordinate divalent metal ions in the crystal structures of identified PET hydrolases. On wild-type LCC (ribbon), catalytic residues (S165, D210 and H242) and the C-terminal disulfide bond (C275–C292) are shown as blue rods. Divalent metal ions are shown as green spheres. In the upper inset, residues that bind metal ions in *Thermobifida alba* Est119 (PDB ID 3WYN) are shown as purple sticks, with the residues indicated with an asterisk; metal-binding residues in *Thermobifida cellulosilytica* Thc Cut1 (PDB ID 5LUI) are shown as yellow sticks, with the residues underlined in black; and the metal-binding sites in *Saccharomonospora viridis* Cut190 variants (PDB ID 4WFJ and 5ZNO) are shown as grey sticks, with residue names underlined in red. The left panels show a putative calcium-binding site formed by E208, D238 and S283 in LCC (with calcium shown as a blue sphere) and the disulfide bond (yellow) introduced here

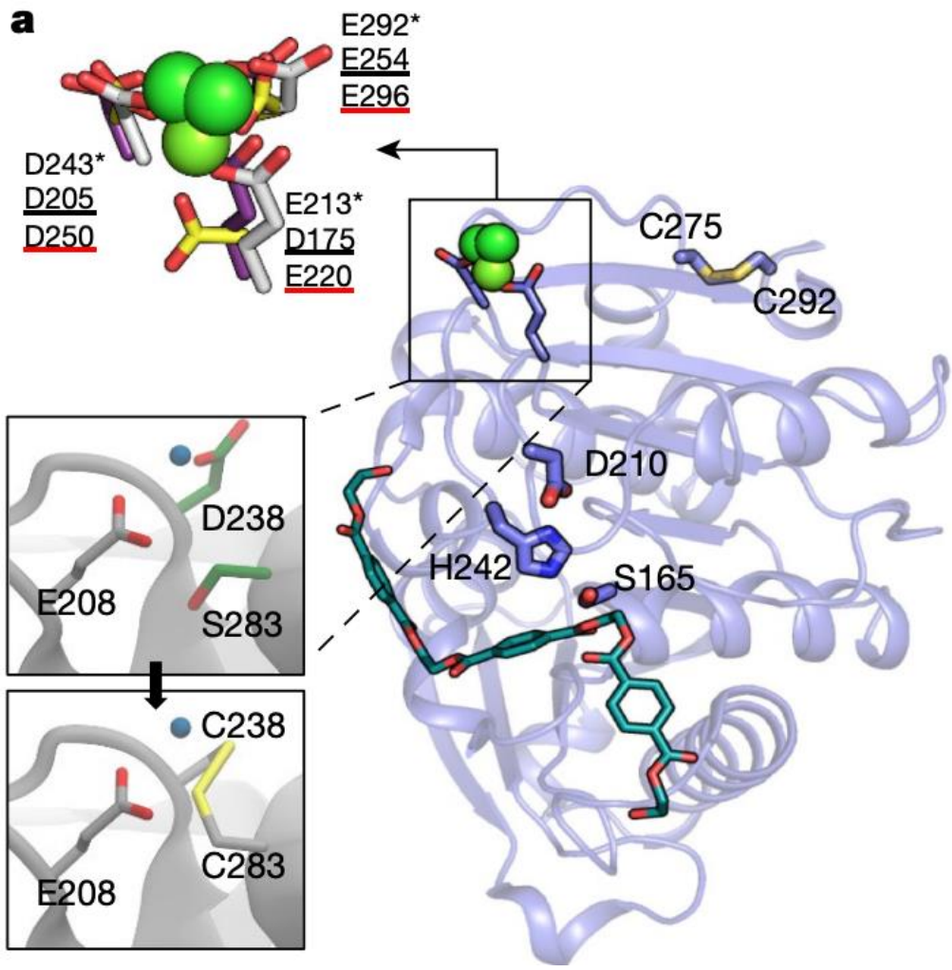

Source: (Tournier et al., 2020)

In 2019 Hajighasemi and collaborators conducted a study on 90 microbial hydrolases, selecting 2 enzymes (ABO2449 and RPA1511) from *Alcanivorax borkumensis* and *Rhodopseudomonas*, respectively. These were selected for the study due to the polyesters PLA (polylatic acid) and PCL (polycaprolactone) degradation power. These enzymes underwent site-directed mutagenesis changes where they identified several other residues necessary for the hydrolysis of both substrates, including His113, Leu182 and Tyr198 in RPA1511 and Leu32 and Leu249 in ABO2449. In the structure of RPA1511, the His113 side chain is located close to the catalytic Ser114. In contrast, the Leu182 and Tyr198 side chains are part of the alcohol-binding pocket, suggesting that these residues contribute to the binding of alcohol substrates. monoester and polyester.

RPA1511-V202A showed significantly higher activity against PLA and lower activity towards α-naphthyl propionate than the wild-type protein, suggesting that the Val202 side chain might interfere with PLA binding. The crystal structure of RPA1511 revealed the presence of an active site-bound polyethylene glycol molecule near the Ser114 catalyst, likely mimicking the bound PLA substrate (Figure 8.4) (Clarke, D. J., y Dobson, A. D., 2020). In the case of the ABO2449 enzyme, it was able to completely degrade the solid and emulsified PLA substrates in 2 days.

Figure 8.4 Crystal structure of RPA1511: overall fold and catalytic triad. (A) The overall structure of the RPA1511 protomer is shown in three views related by a 90° rotation. The protein core domain is shown in gray, whereas the lid domain is colored in cyan. The position of the active site is indicated by the side chain of the catalytic Ser114. (B) RPA1511 protomer with bound PEG 3350 (dodecaethylene glycol, shown as sticks). 2Fo-Fc map contoured at 1.0 σ displayed (shown as a blue mesh) around the dodecaethylene glycol molecule (colored in orange). (C) The surface presentation of the RPA1511 protomer reveals the entrance into the active site with bound PEG 3350 (shown as green sticks). Electrostatic potential mapped onto the solvent-accessible protein surface with red color representing potential below 5 kT, blue above 5 kT, and white as neutral. (D) Close-up view of the dodecaethylene glycol molecule (PEG 3350) bound close to the catalytic triad Ser114, His270, and Asp242 (shown as sticks along the protein ribbon colored in gray). (E) Close-up view of the RPA1511 active site with bound PEG 3350

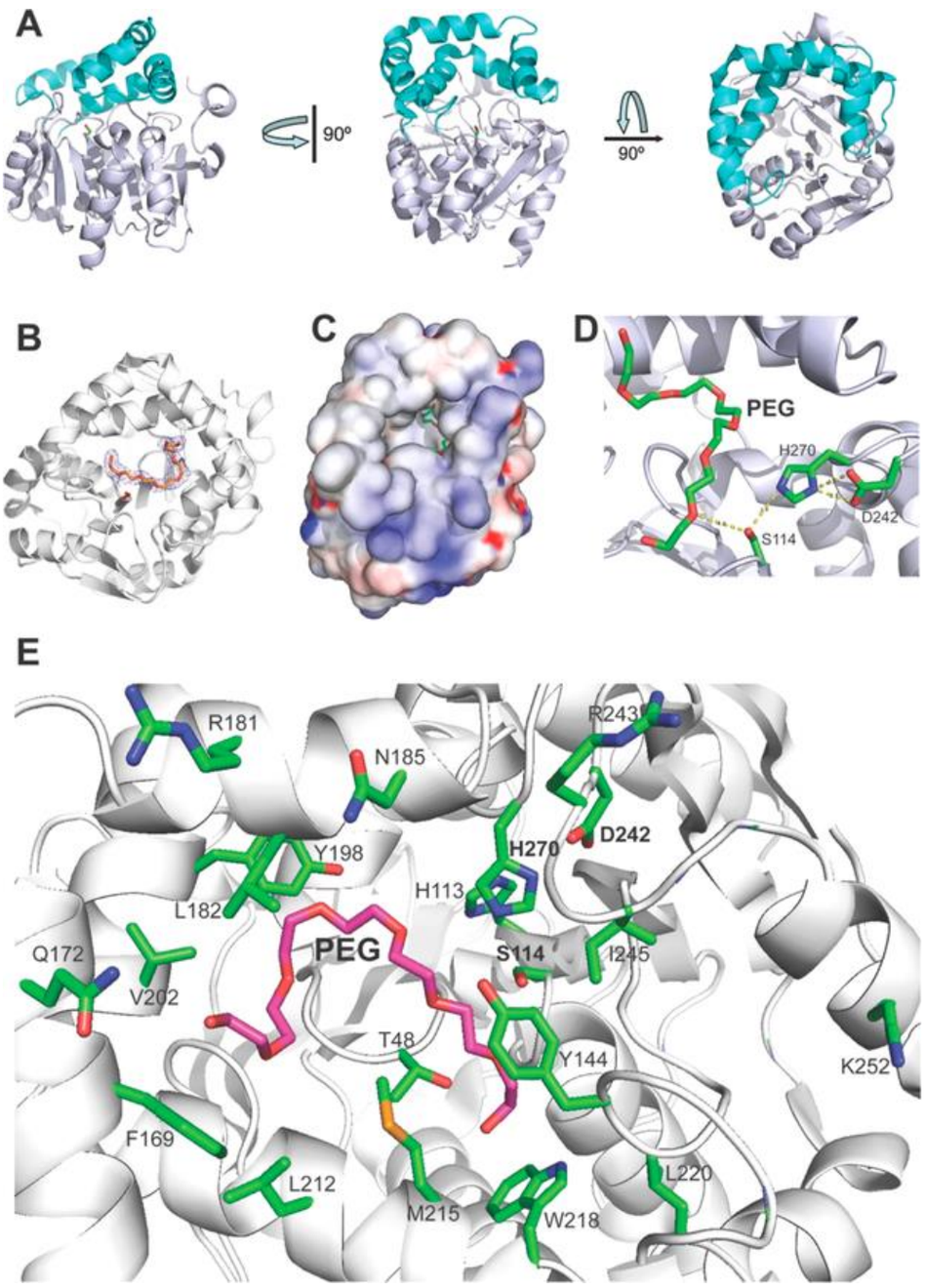

Source: (Clarke, D. J., y Dobson, A. D., 2020)

8.3 Error-prone PCR

This method introduces random mutations in a DNA segment >100 bp that are too long to be synthesized chemically (Wilson and Keefe *et al*., 2000). It is a method based on the polymerase chain reaction (PCR), in which the gene of interest is amplified under conditions that the enzyme adds wrong nucleotides randomly throughout the entire gene sequence and in the copies generated during replication cycles. The conditions that can change the fidelity of DNA polymerase $MgCl_2$, the presence of Mn_{2+}, a high concentration or asymmetric concentrations of deoxyribonucleotide triphosphates (dNTPs) and high concentrations of primers figure 8.4 (Cadwell & Joyce, 1992; Jaeger *et al*., 2001).

Figure 8.5 Asexual methods to generate point mutations. A) ep-PCR and mutagenic strains introduce errors at random positions along the gene sequence. Several random sequences are modified, so a group of mutagenic primers is used, hybridizing in the template's homologous regions

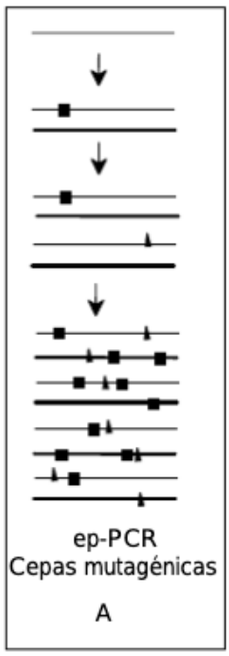

Source: (Cadwell y Joyce, 1992)

In 2006, the depolymerase enzyme obtained from *Ralstonia pickettii* responsible for degrading poly[(R)-3-hydroxybutyrate] (PHB) was mutated. It was modified to improve PHB degradation, changing amino acids found in its domain of Substrate binding (SBD), changing the Ser, Tyr, Val, Ala and Leu residues in the SBD for amino acids with high frequency in other enzymes, as can be seen in figure 8.4. The PhaZRiT1 variant was obtained from these mutations. It degrades PHB through hydrogen bonding between the hydroxyl groups of Ser on the enzyme and the carbonyl groups on the PHB polymer, but also hydrophobic interaction between the enzyme residues and the methyl groups on the PHB polymer. With these changes, the kinetic analysis of PHB degradation resulted in a decrease in the affinity of SBD towards dPHB (denatured PHB), causing a decrease in the degradation rate of dPHB without loss of its hydrolytic activity for the polymer chain (Hiraishi *et al.*,2006).

Similarly, in 2010 Hiraishi and coworkers investigated the effects of mutations in Leu441, Tyr443 and Ser445 on PHB degradation, as shown in Figure 8.5. They predicted that the modified residues would form a beta-sheet structure and be oriented in the same direction to interact directly with the PHB surface possibly. Mutant enzymes L441H, Y443H and S445C, were prepared. The hydrolytic activities for water-soluble substrates were identical to those of the wild-type enzyme, indicating that these mutations do not influence their structures and ability to break the bond ester.

Figure 8.6 Proposed mechanism of PHB degradation by PhaZRpiT1 (A) wild-type and (B) S445C enzymes based on the present kinetic studies. Inset shows a plausible model of the interaction between amino acid residues at positions 441, 443, and 445 in the SBD of the S445C enzyme and the PHB polymer chain. A predicted tertiary structure of SBD depicts only the R carbon, and the R carbons at positions 441, 443, and 445 in SBD of S445C are indicated in green, blue, and orange spheres, respectively

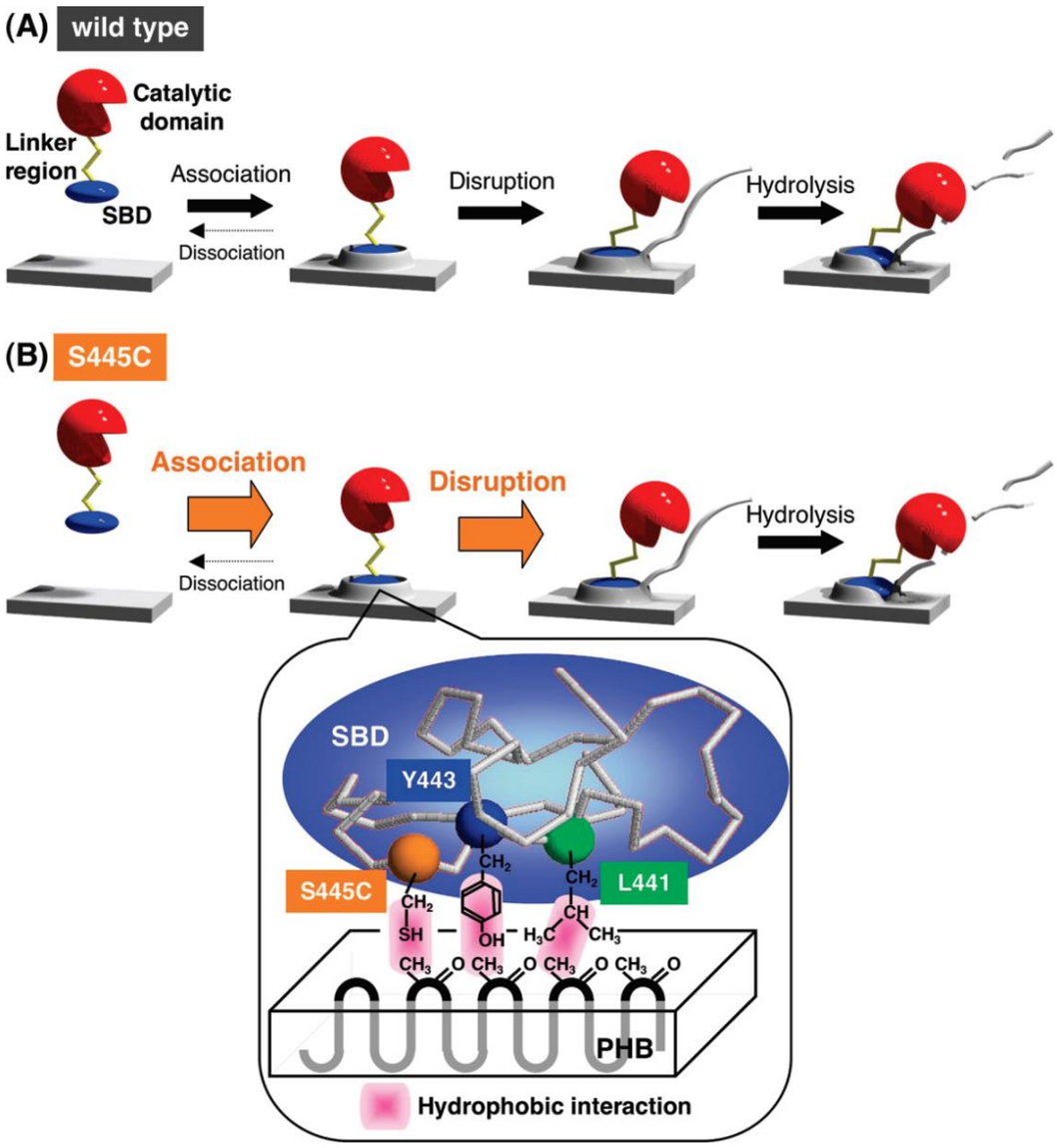

Source: (Hiraishi et al., 2010)

The PHB-degrading activity of the mutants differed from the wild-type enzyme, enzyme L441H and Y443H had lower PHB-degrading activity than their wild-type counterpart, while S445C had higher activity. Kinetic analysis of PHB degradation by the mutants suggested that hydrophobic residues at these positions are essential for the adsorption of enzymes on the PHB surface, and substitutions such as Y443H and S445C may more effectively alter the PHB surface to enhance the hydrolysis of PHB polymer chains than the wild-type enzyme (Hiraishi *et al*., 2010).

Another enzyme modified by the error-prone PCR method was a PETase obtained from *Ideonella sakaiensis* (IsPETase), where a mutant library based on a thermostable triplet mutant (TM) of IsPETase was obtained. Four variants showed higher melting points; the most promising IsPETAse TMK95N/F201I had a melting point of 5 ºC higher than IsPETAseTM. This variant showed slightly lower activity in PET at lower incubation temperatures; its thermostability makes it a more active PET hydrolase at higher action temperatures of up to 60°C.

The degradation of the amorphous PET film was carried out with the TMK95N/F201I variant at an incubation temperature of 60 ºC for 72 h, where a higher concentration of products (2500 mM) was observed, which are the sum of MHET, TA, and BHET released (Brott *et al*., 2022).

8.4 Modified enzyme degraded polyesters

Enzymes that can degrade polyesters have amino acids and critical bonds that allow them to carry out this activity; some enzymes are modified using the techniques mentioned in the previous sections. Depending on the requirement or use of the enzymes, they can be modified so that these enzymes change their characteristics, such as thermostability, halotolerant or increase the affinity to the substrate. In Table 8.1, mutated polyester-degrading enzymes are shown; PETases can be observed first since these were studied for their significant activation on PET (Han *et al*., 2017).

Table 8.1 Modified enzymes for improvement of polyesters degradation

Enzyme	Mutation	Substrate	Reference
IsPETase	C203S, C2395,W185A, S214H, I208A, W159A, M161A, Y87A, T88A, W168H.	PET Film	Han *et al*., 2017
IsPETase	S160A, D206A, H237A, Y87A, M161A, W185A, I208A, W159A, S238A, N241A, R280A, C203S, C239S, S238F, W159H	PET Film	Joo *et al*., 2018
IsPETase	S238F/W159H, W185A.	PET Film	Austin *et al*., 2018
IsPETase	P181A, S121D/D186H, S121E, D186H, D186F, P181G, P181S, P181A/S121D/D186H.	PET Film	Son *et al*.,2019
IsPETase	S160A,D206A, H237A, Y87B, M161A, W185A, I208A, W159A, S238A, N241A, R280A, C203S, C239S, S238F, W159H.	BHET	Sagong *et al*., 2020
IsPETase	S160A, D206A, H237A, W159A, W159H, M161A, A209I, Q119A.	BHET	Liu *et al*., 2018
IsMHETase	R411K, F415S, F424D, F424E, F424H, F424I, F424L, F424N, F424T, F424V, R411K/F424N, R411K/F424V, F415H/F424N.	MHET	Sagong *et al*., 2020
	S225A, D492A, H528A, W397A, R411A, R411Q, F415A, F415H, S416A, S416G, S419G, F424Q, H488A		Palm *et al*., 2019
PaPETase	G254S, S256N, I257S, Y258N, N259Q, Y250S,	*p*-NPB	Bollinger *et al*., 2020
PaPETase	S256N, I257S, Y258N, N259Q, Y250S	BHET	Bollinger *et al*., 2020
PaPETase	G254S, S256N, I257S, Y258N, N259Q, Y250S	Amorphous PET	Bollinger *et al*., 2020
CutinasaSvCut190	S226P/R228S/S176	Succinate	Numoto *et al*.,2018
Cutinasa SxCut190	S226P/R228S	NPB	Kawai et al.,2014
CutinasaSvcut190	S226P/R228s/E184R	PBSA, PET	Oda *et al*., 2018
Cutinasa TcCut1	S131A	PBA	Perz *et al*., 2015
Cutinasa TcCut1	R29D/A30V	*p*-NPA	Herrero *et al*.,2013
Esterase TaEst1	A68V/t253P	3PET	Thumarat *et al*., 2015
Esterase TaEst1	A68V/T253P	3PET	Thumarat *et al*., 2015
Esterase TaEst1	A68V/M259K	3PET	Thumarat *et al*., 2015
Lipase TlLip	E109A	*p*-NPB	Skjold *et al*., 2017
Lipase TlLip	I108c/I277c	*p*-NPDecanoate	Skjold *et al*., 2017
Esterase TfCa	E184Q	*p*-NPB	Billig *et al.*, 2010
Esterase TfCa	E319D	*p*-NPB	Billig *et al.*, 2010
Esterase TfCa	E184H/A186M	*p*-NPB	Billig *et al*., 2010

8.5 Acknowledgment

CONACyT

8.6 Funding

Laura Vázquez received a CONACyT grant during her Ph.D. [277236]. CONACYT has funded this work [Project A1-S-47929].

8.7 Conclusions

The enzymes have been improved to meet industrial requirements. These improvements have been made through various molecular techniques, such as site-directed mutagenesis and error-prone PCR. For the modifications, it is necessary to consider strategies and selective practices imitating the evolutionary processes of nature, thus creating enzymes with new characteristics of industrial interest.

For the use of enzymes in an industrial context, high temperatures close to the glass transition temperature of polyesters are desirable. For this reason, modified enzymes are required for the efficient hydrolysis of polyesters at high temperatures and in extreme conditions since most polymeric contaminants are found in extreme environments such as wastewater.

8.8 References

Araújo, R., Casal, M., & Cavaco-Paulo, A. (2010). Design and engineering of novel enzymes for textile applications. In *Advances in Textile Biotechnology* (pp. 3-31). Woodhead Publishing. https://doi.org/10.1533/9780857090232.1.3; URL: https://www.sciencedirect.com/science/article/pii/B9781845696252500012?via%3Dihub

Austin, H.P.; Allen, M.D.; Donohoe, B.S.; Rorrer, N.A.; Kearns, F.L.; Silveira, R.L.; Pollard, B.C.; Dominick, G.; Duman, R.; El Omari, K.; Mykhaylyk, V.; Wagner, A.; Michener, W.E.; Amore, A.; Skaf, M.S.; Crowley, M.F.; Thorne, A.W.; Johnson, C.W.; Woodcock, H.L.; McGeehan, J.E.; Beckham, G.T. Characterization and Engineering of a Plastic-Degrading Aromatic Polyesterase. Proc. Natl. Acad. Sci. U. S. A., 2018, 115, E4350–E4357.
https://doi.org/10.1073/pnas.1718804115; URL: https://www.pnas.org/doi/10.1073/pnas.1718804115

Billig, S.; Oeser, T.; Birkemeyer, C.; Zimmermann, W. Hydrolysis of Cyclic Poly(Ethylene Terephthalate) Trimers by a Carboxylesterase from Thermobifida Fusca KW3. Appl. Microbiol. Biotechnol., 2010, 87, 1753–1764. DOI: https://doi.org/10.1007/s00253-010-2635-y
URL: https://link.springer.com/article/10.1007/s00253-010-2635-y

Biundo, A., Reich, J., Ribitsch, D., & Guebitz, G. M. (2018). Synergistic effect of mutagenesis and truncation to improve a polyesterase from Clostridium botulinum for polyester hydrolysis. *Scientific reports*, *8*(1), 1-7. https://doi.org/10.1038/s41598-018-21825-9;
URL: https://www.nature.com/articles/s41598-018-21825-9

Bollinger, A., Thies, S., Knieps-Grünhagen, E., Gertzen, C., Kobus, S., Höppner, A., ... & Jaeger, K. E. (2020). A novel polyester hydrolase from the marine bacterium Pseudomonas aestusnigri–structural and functional insights. *Frontiers in microbiology*, *11*, 114. DOI: 10.3389/fmicb.2020.00114.
URL: https://www.frontiersin.org/articles/10.3389/fmicb.2020.00114/full

Brott, S., Pfaff, L., Schuricht, J., Schwarz, J. N., Böttcher, D., Badenhorst, C. P., ... & Bornscheuer, U. T. (2022). Engineering and evaluation of thermostable IsPETase variants for PET degradation. Engineering in life sciences, 22(3-4), 192-203. DOI: https://doi.org/10.1002/elsc.202100105
URL: https://onlinelibrary.wiley.com/doi/10.1002/elsc.202100105

Cadwell C & Joyce G (1992) Randomization of genes by PCR mutagenesis. PCR Methods and Applications, 2: 28-33. DOI: https://doi.org/10.1101/gr.2.1.28.,
URL: https://pubmed.ncbi.nlm.nih.gov/1490172/

Dubey, K. K., Pramanik, A., & Yadav, J. (2019). Enzyme Engineering. In Advances in Enzyme Technology (pp. 325-347). Elsevier. DOI: https://doi.org/10.1016/B978-0-444-64114-4.00012-1
URL: https://www.sciencedirect.com/science/article/pii/B9780444641144000121?via%3Dihub

Liu, B.; He, L.; Wang, L.; Li, T.; Li, C.; Liu, H.; Luo, Y.; Bao, R. Protein Crystallography and Site-Direct Mutagenesis Analysis of the Poly(Ethylene Terephthalate) Hydrolase PETase from Ideonella Sakaiensis. Chembiochem, 2018, 19, 1471–1475. DOI: 10.1002/cbic.201800097; URL: https://pubmed.ncbi.nlm.nih.gov/29603535/.

Lu, H., Diaz, D. J., Czarnecki, N. J., Zhu, C., Kim, W., Shroff, R., ... & Alper, H. S. (2022). Machine learning-aided engineering of hydrolases for PET depolymerization. *Nature*, *604*(7907), 662-667.URL: https://pubmed.ncbi.nlm.nih.gov/35478237/ DOI: 10.1038/s41586-022-04599-z.

Oda, M.; Yamagami, Y.; Inaba, S.; Oida, T.; Yamamoto, M.; Kitajima, S.; Kawai, F. Enzymatic Hydrolysis of PET: Functional Roles of Three Ca2+ Ions Bound to a Cutinase-like Enzyme, Cut190*, and Its Engineering for Improved Activity. Appl. Microbiol. Biotechnol., 2018, 102, 10067–10077. DOI: https://doi.org/10.1007/s00253-018-9374-x; URL: https://pubmed.ncbi.nlm.nih.gov/30250976/

Palm, G.J.; Reisky, L.; Böttcher, D.; Müller, H.; Michels, E.A.P.; Walczak, M.C.; Berndt, L.; Weiss, M.S.; Bornscheuer, U.T.; Weber, G. Structure of the Plastic-Degrading Ideonella Sakaiensis MHETase Bound to a Substrate. Nat. Commun., 2019, 10, 1717. DOI: https://doi.org/10.1038/s41467-019-09326-3; URL: https://pubmed.ncbi.nlm.nih.gov/30979881/.

Peña-Montes, C., & Gonzalez-Saravia, A. F. (2008). Evolución Dirigida en la generación de biocatalizadores: Biocatalizadores hechos a medida. DOI:
URL:
https://www.researchgate.net/publication/260249630_Evolucion_Dirigida_en_la_Generacion_de_Biocatalizadores_Biocatalizadores_Hechos_a_Medida

Perz, V.; Zumstein, M.T.; Sander, M.; Zitzenbacher, S.; Ribitsch, D.; Guebitz, G.M. Biomimetic Approach to Enhance Enzymatic Hydrolysis of the Synthetic Polyester Poly(1,4-Butylene Adipate): Fusing Binding Modules to Esterases. Biomacromolecules, 2015, 16, 3889–3896. DOI: https://doi.org/10.1021/acs.biomac.5b01219 URL: https://pubs.acs.org/doi/full/10.1021/acs.biomac.5b01219

Skjold-Jørgensen, J.; Vind, J.; Moroz, O. V; Blagova, E.; Bhatia, V.K.; Svendsen, A.; Wilson, K.S.; Bjerrum, M.J. Controlled Lid-Opening in Thermomyces Lanuginosus Lipase- An Engineered Switch for Studying Lipase Function. Biochim. Biophys. acta. Proteins proteomics, 2017, 1865, 20– 27. DOI: 10.1016/j.bbapap.2016.09.016; URL: https://europepmc.org/article/med/27693248

Son, H.F.; Cho, I.J.; Joo, S.; Seo, H.; Sagong, H.-Y.; Choi, S.Y.; Lee, S.Y.; Kim, K.-J. Rational Protein Engineering of Thermo-Stable PETase from Ideonella Sakaiensis for Highly Efficient PET Degradation. ACS Catal., 2019, 9, 3519–3526.DOI: https://doi.org/10.1021/acscatal.9b00568
URL: https://pubs.acs.org/doi/abs/10.1021/acscatal.9b00568.

Tee, K. L., & Wong, T. S. (2013). Polishing the craft of genetic diversity creation in directed evolution. *Biotechnology advances*, *31*(8), 1707-1721. DOI: 10.1016/j.biotechadv.2013.08.021 URL: https://pubmed.ncbi.nlm.nih.gov/24012599/.

Thumarat, U.; Kawabata, T.; Nakajima, M.; Nakajima, H.; Sugiyama, A.; Yazaki, K.; Tada, T.; Waku, T.; Tanaka, N.; Kawai, F. Comparison of Genetic Structures and Biochemical Properties of Tandem Cutinase-Type Polyesterases from Thermobifida Alba AHK119. J. Biosci. Bioeng., 2015, 120, 491–497.

Tournier, V., Topham, C. M., Gilles, A., David, B., Folgoas, C., Moya-Leclair, E., ... & Marty, A. (2020). An engineered PET depolymerase to break down and recycle plastic bottles. *Nature*, *580*(7802), 216-219. https://pubmed.ncbi.nlm.nih.gov/32269349/ DOI: 10.1038/s41586-020-2149-4

Farres, A., Peña, M, C., Hernández, D, E., García, M, S., Sánchez, S, M., Solís, B,I. 2018. Cutinasas recombinantes de aspergillus nidulans para biodegradación de poliésteres. WO2017204615A2.
URL: https://patentimages.storage.googleapis.com/12/c1/88/fe23159e6c8ac6/WO2017204615A2.pdf

Gaeger KE, Eggert T, Eipper A & Reetz MT (2001).Directed evolution and the creation of enantioselective biocatalysts. Appl. Microbiol. Biotechnol. 55: 519-530. DOI: 10.1007/s002530100643 URL: https://pubmed.ncbi.nlm.nih.gov/11414315/

Han, X.; Liu, W.; Huang, J.-W.; Ma, J.; Zheng, Y.; Ko, T.-P.; Xu, L.; Cheng, Y.-S.; Chen, C.-C.; Guo, R.-T. Structural Insight into Catalytic Mechanism of PET Hydrolase. Nat. Commun., 2017, 8, 2106. DOI: 10.1038/s41467-017-02255-z URL: https://pubmed.ncbi.nlm.nih.gov/29235460/

Hajighasemi, M., Nocek, B. P., Tchigvintsev, A., Brown, G., Flick, R., Xu, X., ... & Yakunin, A. F. (2016). Biochemical and structural insights into enzymatic depolymerization of polylactic acid and other polyesters by microbial carboxylesterases. *Biomacromolecules*, *17*(6), 2027-2039. DOI: 10.1021/acs.biomac.6b00223 URL: https://pubmed.ncbi.nlm.nih.gov/27087107/

Herrero Acero, E.; Ribitsch, D.; Dellacher, A.; Zitzenbacher, S.; Marold, A.; Steinkellner, G.; Gruber, K.; Schwab, H.; Guebitz, G.M. Surface Engineering of a Cutinase from Thermobifida Cellulosilytica for Improved Polyester Hydrolysis. Biotechnol. Bioeng., 2013, 110, 2581–2590. DOI: 10.1002/bit.24930 URL: https://pubmed.ncbi.nlm.nih.gov/23592055/

Hiraishi, T., Hirahara, Y., Doi, Y., Maeda, M., & Taguchi, S. (2006). Effects of mutations in the substrate-binding domain of poly [(R)-3-hydroxybutyrate](PHB) depolymerase from Ralstonia pickettii T1 on PHB degradation. *Applied and Environmental Microbiology*, *72*(11), 7331-7338. DOI: 10.1128/AEM.01187-06 ; URL: https://www.ncbi.nlm.nih.gov/pmc/articles/PMC1636158/

Hiraishi, T., Komiya, N., Matsumoto, N., Abe, H., Fujita, M., & Maeda, M. (2010). Degradation and adsorption characteristics of PHB depolymerase as revealed by kinetics of mutant enzymes with amino acid substitution in substrate-binding domain. *Biomacromolecules*, *11*(1), 113-119. DOI: 10.1021/bm900967a; URL: https://pubmed.ncbi.nlm.nih.gov/20058938/

Joo, S.; Cho, I.J.; Seo, H.; Son, H.F.; Sagong, H.-Y.; Shin, T.J.; Choi, S.Y.; Lee, S.Y.; Kim, K.-J. Structural Insight into Molecular Mechanism of Poly(Ethylene Terephthalate) Degradation. Nat. Commun., 2018, 9, 382. DOI: https://doi.org/10.1038/s41467-018-02881-1 URL: https://www.nature.com/articles/s41467-018-02881-1

Kawai, F.; Oda, M.; Tamashiro, T.; Waku, T.; Tanaka, N.; Yamamoto, M.; Mizushima, H.; Miyakawa, T.; Tanokura, M. A Novel Ca2+-Activated, Thermostabilized Polyesterase Capable of Hydrolyzing Polyethylene Terephthalate from Saccharomonospora Viridis AHK190. Appl. Microbiol. Biotechnol., 2014, 98, 10053–10064. DOI: 10.1007/s00253-014-5860-y; URL: https://pubmed.ncbi.nlm.nih.gov/24929560/

Lebreton, L., Slat, B., Ferrari, F., Sainte-Rose, B., Aitken, J., Marthouse, R., et al. (2018). Evidence that the Great Pacific Garbage Patch is rapidly accumulating plastic. *Sci. Rep.* 8:4666. DOI: https://doi.org/10.1038/s41598-018-22939-w
URL: https://www.nature.com/articles/s41598-018-22939-w

Liu, H., & Naismith, J. H. (2008). An efficient one-step site-directed deletion, insertion, single and multiple-site plasmid mutagenesis protocol. *BMC biotechnology*, *8*(1), 1-10.DOI: 10.1186/1472-6750-8-91; URL: https://bmcbiotechnol.biomedcentral.com/articles/10.1186/1472-6750-8-91.

Meng,X., Yang, L., Liu, H., Li, Q., Xu, G., Zhang, Y., ... & Tian, J. (2021). Protein engineering of stable IsPETase for PET plastic degradation by Premuse. *International Journal of Biological Macromolecules*, *180*, 667-676. DOI: 10.1016/j.ijbiomac.2021.03.058; URL: https://pubmed.ncbi.nlm.nih.gov/33753197/

Moharir, R. V., and Kumar, S. (2019). Challenges associated with plastic waste disposal and allied microbial routes for its effective degradation: a comprehensive review. *J. Clean. Prod.* 208, 65–76. DOI: https://doi.org/10.1016/j.jclepro.2018.10.059; URL: https://www.sciencedirect.com/science/article/abs/pii/S0959652618330737

Nikolaivits, E., Kanelli, M., Dimarogona, M., and Topakas, E. (2018). A middle-aged enzyme still in its prime: recent advances in the field of cutinases. *Catalysts* 8:612. DOI: https://doi.org/10.3390/catal8120612 URL: https://www.mdpi.com/2073-4344/8/12/612

Numoto, N.; Kamiya, N.; Bekker, G.-J.; Yamagami, Y.; Inaba, S.; Ishii, K.; Uchiyama, S.; Kawai, F.; Ito, N.; Oda, M. Structural Dynamics of the PET-Degrading Cutinase-like Enzyme from Saccharomonospora Viridis AHK190 in Substrate-Bound States Elucidates the Ca2+-Driven Catalytic Cycle. Biochemistry, 2018, 57, 5289–5300. DOI: 10.1021/acs.biochem.8b00624 URL: https://pubmed.ncbi.nlm.nih.gov/30110540/

Sagong, H.-Y.; Seo, H.; Kim, T.; Son, H.F.; Joo, S.; Lee, S.H.; Kim, S.; Woo, J.-S.; Hwang, S.Y.; Kim, K.-J. Decomposition of the PET Film by MHETase Using Exo-PETase Function. ACS Catal., 2020, 10, 4805–4812. https://doi.org/10.1021/acscatal.9b05604
URL: https://pubs.acs.org/doi/abs/10.1021/acscatal.9b05604

Tseng WC, Lin JW, Wei TY, Fang TY. A novel megaprimed and ligase-free, PCR-based, site-directed mutagenesis method. Anal Biochem. 2008 Apr 15;375(2):376-8. DOI: 10.1016/j.ab.2007.12.013; URL: https://pubmed.ncbi.nlm.nih.gov/18198125/

Wei, R., and Zimmermann, W. (2017). Microbial enzymes for the recycling of recalcitrant petroleum-based plastics: how far are we? *Microb. Biotechnol.* 10, 1308–1322. DOI: 10.1111/1751-7915.12710; URL: https://pubmed.ncbi.nlm.nih.gov/28371373/

Wilson, D. S., & Keefe, A. D. (2000). Random mutagenesis by PCR. *Current protocols in molecular biology*, *51*(1), 8-3. DOI: https://doi.org/10.1002/0471142727.mb0803s51;

Zhang, K., Yin, X., Shi, K., Zhang, S., Wang, J., Zhao, S., ... & Deng, W. (2021). A high-efficiency method for site-directed mutagenesis of large plasmids based on large DNA fragment amplification and recombinational ligation. *Scientific Reports*, *11*(1), 1-16. DOI: https://doi.org/10.1038/s41598-021-89884-z; URL: https://www.nature.com/articles/s41598-021-89884-z.

Chapter 9 *Staphylococcus carnosus* study as an alternative bio-collector for metal minerals

Capítulo 9 Estudio de *Staphylococcus carnosus* como un bio-colector alternativos para minerales metálicos

RAMOS-ESCOBEDO, Gema Trinidad*, ESCALANTE-IBARRA, Griselda Berenice, ROSALES-SOSA Ma. Gloria and REYES-GUZMAN, Claudia Verónica

Facultad de Metalurgia-Universidad Autónoma de Coahuila. Carretera 57 Km 5 C.P. 25710, Monclova, Coah., México.

ID 1st Author: *Gema Trinidad, Ramos-Escobedo* / **ORC ID**: 0000-0003-2902-6928, **CVU CONACYT ID:** 94696

ID 1st Co-author: *Griselda Berenice, Escalante-Ibarra* / **ORC ID:** 0000-0002-6329-5294, **CVU CONACYT ID:** 321452

ID 2nd Co-author: *Ma. Gloria, Rosales-Sosa* / **ORC ID**: 0000-0002-6654-3433- **CVU CONACYT ID:** 63212

ID 3rd Co-author: *Claudia Verónica, Reyes-Guzman* / **ORC ID**: 0000-0001-5470-0510, **CVU CONACYT ID:** 176351

DOI: 10.35429/H.2022.6.1.109.123

* gema_ramos@uadec.edu.mx

A. Marroquín, L. Castillo, S. Soto, L. Cruz. (Coord.) CIERMMI Women in Science TXIX Biological Sciences. Handbooks-©ECORFAN-México, Querétaro, 2022.

Abstract

Biotechnology has been explored as a potential low cost, environmentally benign alternative to many of the current mineral processing techniques. Recent investigations have shown that selected bacteria may also assist in the beneficiation of these minerals through bioflotation bioflocculation. Bioflotation represents an innovative in the minerals benefit process, where the bacteria are generally used as a collector avoiding the use of conventional reagents. The aim of this study was to evaluate the use of *Staphylococcus Carnosus* as bio-reagent in the flotation process of sulfides such as galena (PbS), pyrite (FeS_2) and chalcopyrite ($CuFeS_2$). To evaluate the bacterial influence on minerals floatability Hallimond flotation test was carried out. The absorption zeta potential and adhesion measurements were useed to determine the adhesion of the bacteria from each mineral. The assays were carried out with and without bacteria. The results showed that *S. Carnosus* has a hydrophobic behavior and different affinity grade to sulfides mineral substrates. This interaction allowed the bacteria to act as a collector. The biomodified sulfides show the following floatability in decreasing order: galena>chalcopyrite>pyrite. These differences point out the possibility of future application of *S. carnosus* in selective separation of sulfide minerals to depress the gangue type ores (pyrite among others).

Biotechnology, Bioflotation, Hydrophobic, Alternative, Processing

Resumen

La biotecnología ha sido explorada como una alternativa potencial de bajo costo y benigna para el medio ambiente a muchas de las técnicas actuales de procesamiento de minerales. Investigaciones recientes han demostrado que bacterias también pueden ayudar en el beneficio de estos minerales a través de la biofloculación de bioflotación. La bioflotación representa un proceso innovador en beneficio de los minerales. Donde las bacterias se utilizan generalmente como un colector evitando el uso de reactivos convencionales. El objetivo de este estudio fue evaluar el uso de *Staphylococcus Carnosus* como agente biológico en el proceso de flotación de sulfuros como galena (PbS), pirita (FeS_2) y calcopirita ($CuFeS_2$). Para evaluar la influencia de las bacterias en la flotabilidad de minerales, la prueba de flotación de Hallimond fue llevado a cabo. Las mediciones de absorción del potencial zeta y de adhesión se utilizaron para determinar la adhesión de las bacterias de cada mineral. Las experiencias se llevaron a cabo con y sin bacterias. Los resultados mostraron que la bacteria *S. Carnosus* tiene un comportamiento hidrofóbico y un grado de afinidad diferente a los sustratos minerales sulfurosos. Esta interacción permitió que las bacterias actuaran como colectoras. Los sulfuros biomodificados muestran la siguiente flotabilidad en orden decreciente: galena> calcopirita> pirita. Estas diferencias señalan la posibilidad de una futura aplicación de *S. carnosus* en la separación selectiva de minerales de sulfuro para deprimir los minerales de tipo ganga (pirita, entre otros).

Biotecnología, Bioflotación, Hidrofóbico, Alternativa, Procedimiento

9.1 Introduction

Today, Mexico continues to stand out as one of the world's largest producers of different minerals such as: copper, bismuth, fluorite, celestite, wollastonite, cadmium, molybdenum, lead, zinc, diatomite, barite, graphite, gypsum, gold and silver. Being the latter who occupies the first place of productive demand worldwide.

However, today mining companies are required to comply with newer and more stringent environmental legislation in order to ensure that exploration and mining activities have a reduced impact on the environment.

A very promising alternative with a lower environmental impact that requires less infrastructure and resources than traditional technologies is the biomining process.

Biomining comprises a series of microbiological processes that can be used for the extraction and recovery of metals from very low-grade minerals. And this process can be applied in three different areas of mining activity, such as: Bioflotation, Biolleaching and Biooxidation.

9.1.1. Bioflotation

The gradual depletion of high-grade deposits makes interesting the benefit of complex sulfides. Thus, it is important the development of better flotation schemes in order to beneficiate and process complex ores, which are represented by polymetallic sulfide associations. Along with the industrial necessity to develop new technologies for the processing of ores, the design of methods, which accomplish to strict environmental regulations is unavoidable. (Pecina *et al*., 2009).

In Mexico, the use of these biological reagents as bacteria and their manipulation for their selective adhesion on mineral surfaces are relatively important aspects for mineral beneficiation. Considering that there are serious concerns regarding the availability of these mineral elements in the future due to their low abundance, complexity or low-grade ores and difficult access, viable alternative methods are required.

Traditionally, the benefit of low-grade sulfides ores has been carried out through the conventional flotation process. Which employ highly selective inorganic modifiers, such as cyanides, sulfides and ferro-cyanides (Bradshaw *et al*., 1998). Despite the many advantages of flotation process, the hazardous chemicals used limits the development of this process and other minerals.

Nowadays the industry is trying to develop environmentally friendly technology for processing ores, different from traditional separation methods. Many previous attempts have been made to replace hazardous materials in the flotation processes, using environmentally friendly reagents, instead of harmful chemicals. The biotechnology has opened up possibilities for the utilization of microorganisms in mineral beneficiation as flotation collectors.

The use of microorganisms as a bio-collector could be an alternative in mineral flotation. This process offers various advantages such as, as lower operating costs in the processing of low grade ores, mineral selectivity in the processing of fine and ultrafine mineral particles and to the constant quest of reagents that attends the rigorous specifications for production of concentrates and stricter environmental legislation (Gericke and Govender, 2011; Lopez *et al*., 2015; Ramos-Escobedo *et al*., 2016).

Bioflotation can be used as an alternative to the conventional process and consists of the selective separation of commercial minerals (Cu, Pb, etc.) from the gangue (pyrite, etc.) through microorganisms interactions (Deo and Natarajan., 1997). Where the adhesion is governed by physicochemical interactions (most likely electrostatic interactions) (Botero *et al*., 2008, de Mesquita *et al*., 2003); Dwyer *et al*., 2012; Merma *et al*., 2013).

Generally, the three mechanisms used during biomodifaction of minerals surface are: a) the adhesion of hydrophilic bacteria to the mineral substrate; b) the oxidation that directly or indirectly, generates the biomodifaction of sulfur; and c) adsorption or chemical reaction with metabolic products on the substrate (Rao *et al*., 2010).

Some microorganisms such as Acidithiobacillus ferrooxidans, Leptospirillum ferrooxidans, Polymyxa Paenibacillus, Acidithiobacillus thiooxidans, among others (Ramos Escobedo *et al*., 2012, Nagaoka *et al*., 1999, Subrahmalannian *et al*., 2003, Pecina *et al*., 2009, 2010; Santhiya *et al*., 2001a, 2001b, 2001c, 2002) were reported for sulfidic ores benefit.

In the case of bioflotation of sulfides minerals, the most common minerals and some non-metallic minerals systems employed the bacteria Acidithiobacillus ferrooxidans and Acidithiobacillus thiooxidans, reaching a successfully separation of sphalerite (ZnS)-galena (PbS). Sphalerite without promoter/collector is selectively floated from lead ores, especially as galena is oxidized (PbS to PbSO4), highlighting the importance of parallel single bacterial adhesion (Santhiya *et al*., 2001). While for pyrite and arsenopyrite systems, using xanthate as a collector emphasizes that Acidithiobacillus ferrooxidans acts as a pyrite depressant.

This reaction is established because bacteria have greater affinity for iron-rich substrates, showing a descending effectiveness of the next minerals: pyrite>galena≈millerite> molibdenite≈calcocite. The tests were performed at pH 2 without collector (Nagaoka *et al*., 1999). The depressant effect is interpreted in terms of surface free energy decrease that weakens contact with the Xanthate. Moreover, Vilinska, (2007) mention that bacteria, achieve superficial chemical changes and could be manipulated for specific purposes in flotation, depending on the concentration and composition of medium culture, as well as bacteria adaptation to a mineral type.

Possible interaction mechanisms based on the interaction of carbohydrate metabolite/galena to acid / base model are set based using xanthate as a collector. (Subrahmanian *et al*., 2003). The depressant effect is interpreted according to the decrease in surface free energy diminishing the contact with the xanthate. The advantage of bioflotation is that bacteria can have the same functions as conventional reagents and provides specificity for different type of minerals. The aim of this study was to evaluate the use of S. carnosus as froth flotation reagent for sulfide minerals (galena (PbS), pyrite (FeS_2), chalcopyrite ($CuFeS_2$)).

9.1.2. *Staphylococcus carnosus* description

9.1.2.1. Characteristics and taxonomy

Staphylococcus carnosus is a unicellular non-pathogenic, Gram-positive bacteria. It comes of the *Staphylococacceae* family. Schleifer and Fischer (1982) describe *Staphylococcus carnosus* morphologically as cocci from 0.5 to 1.5 μm in diameter, presented mainly in pairs or individually. *Staphylococcus carnosus* is a facultative aerobic microorganism may develop NaOH concentrations more than 15%, with the ability to reduce nitrates and produce acetoin. In addition, these micro-organism has polysaccharides, carboxylic acids, and lipid groups (Ramos-Escobedo *et al.*, 2016). The peptidoglycan represents the major component of the cell wall (50-80 wt%) (Madigan *et al*., 2004)

Exist very few studies on the use of *S. carnosus* as a biocollector in the mineral processing research.). The aim the purpose of this investigation is to evaluate the *S. carnosus* floatability in systems of sulfide minerals of commercial interest (chalcopyrite and galena) and gangue type (pyrite, etc.) under similar conditions used in chemical flotation. The importance of this investigation is to find an alternative flotation bio-reagent applied to sulfidic ores.

Figure 9.1 Growth curve of *S. carnosus* bacteria

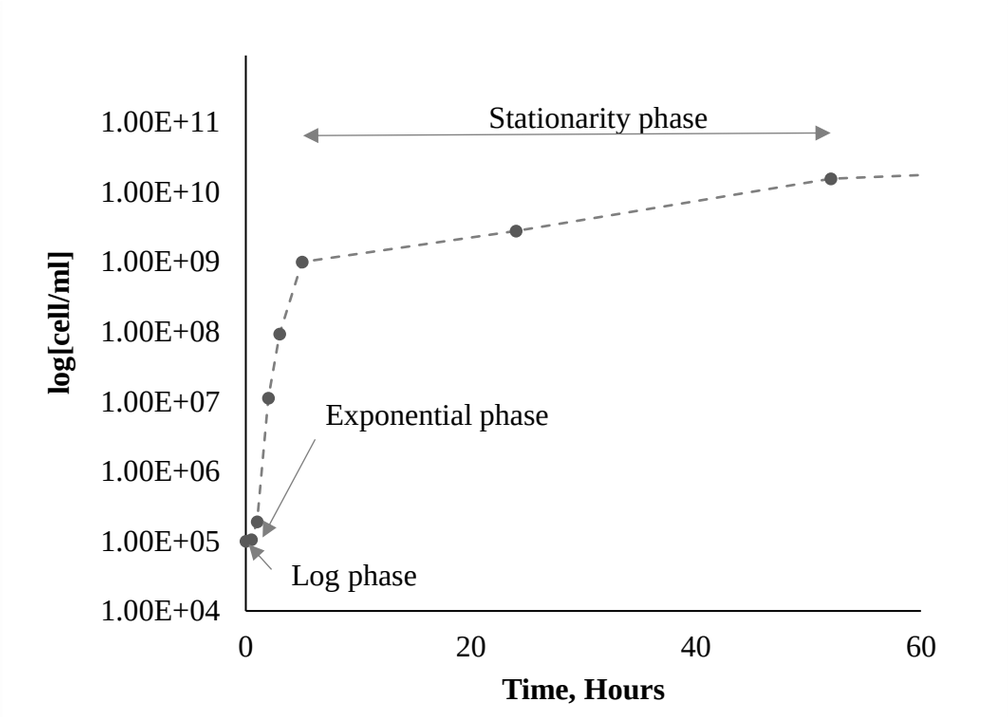

Figure 9.2 Hydrophobicity of the bacteria as a function of pH

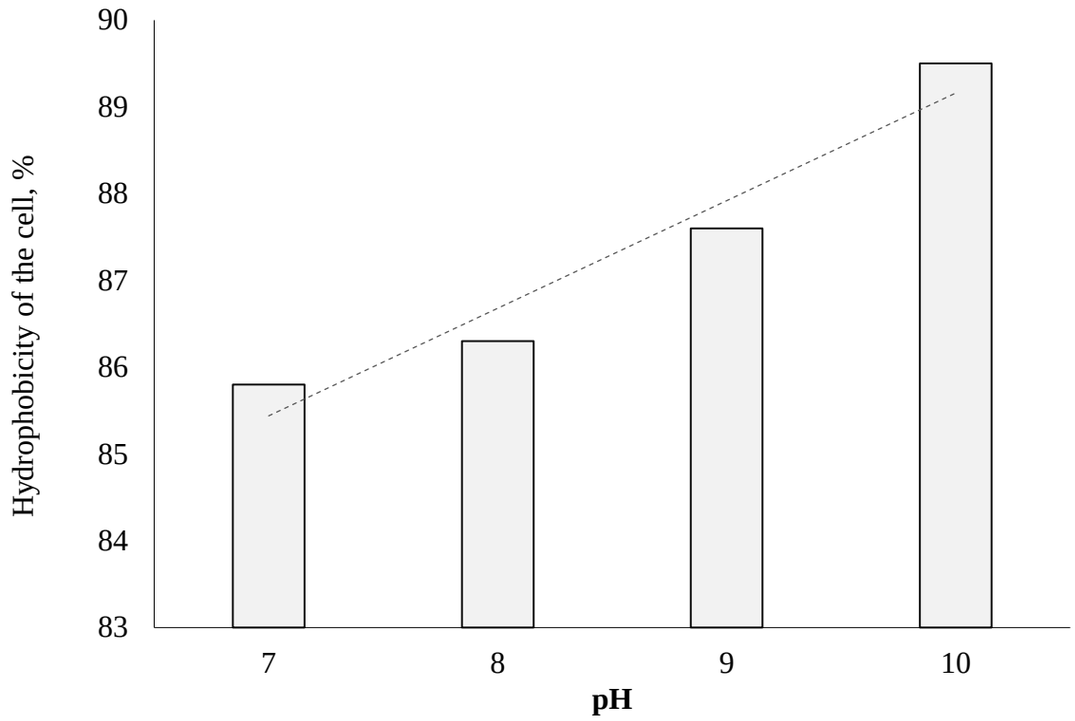

Figure 9.3 Effect of the culture period the bacteria in the floatability of the chalcopyrite with fresh bacteria (culture medium) and washed bacteria (without culture media)

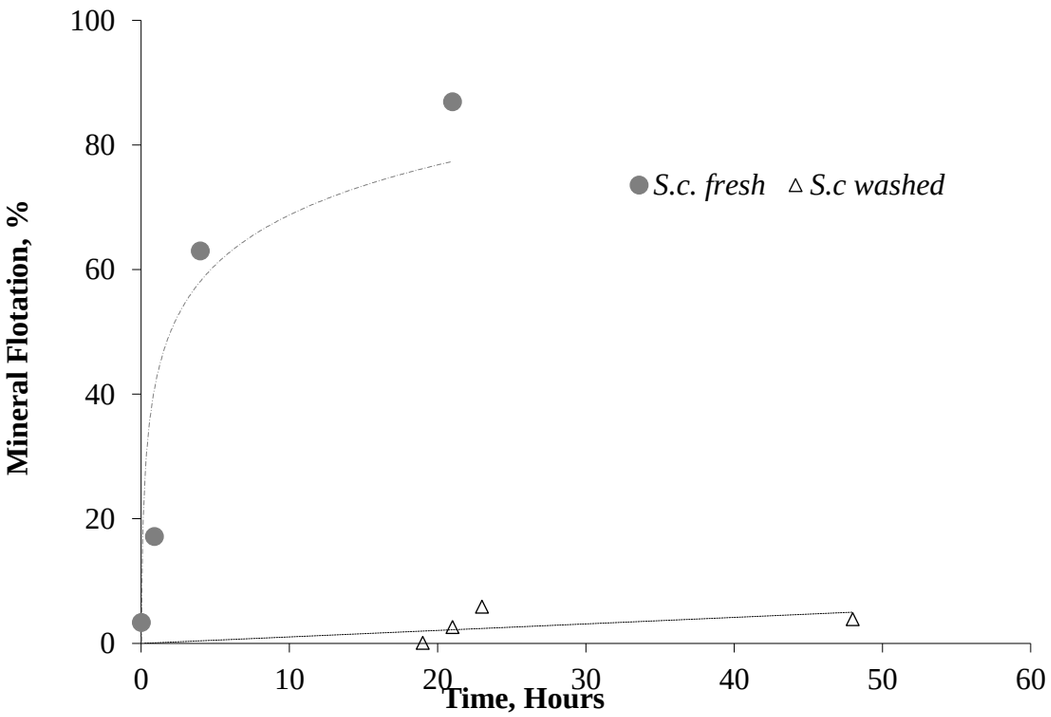

Figure 9.4 Effect of the floatability of *S. carnosus* + $CuFeS_2$ bacteria with culture medium and without culture medium at pH 9

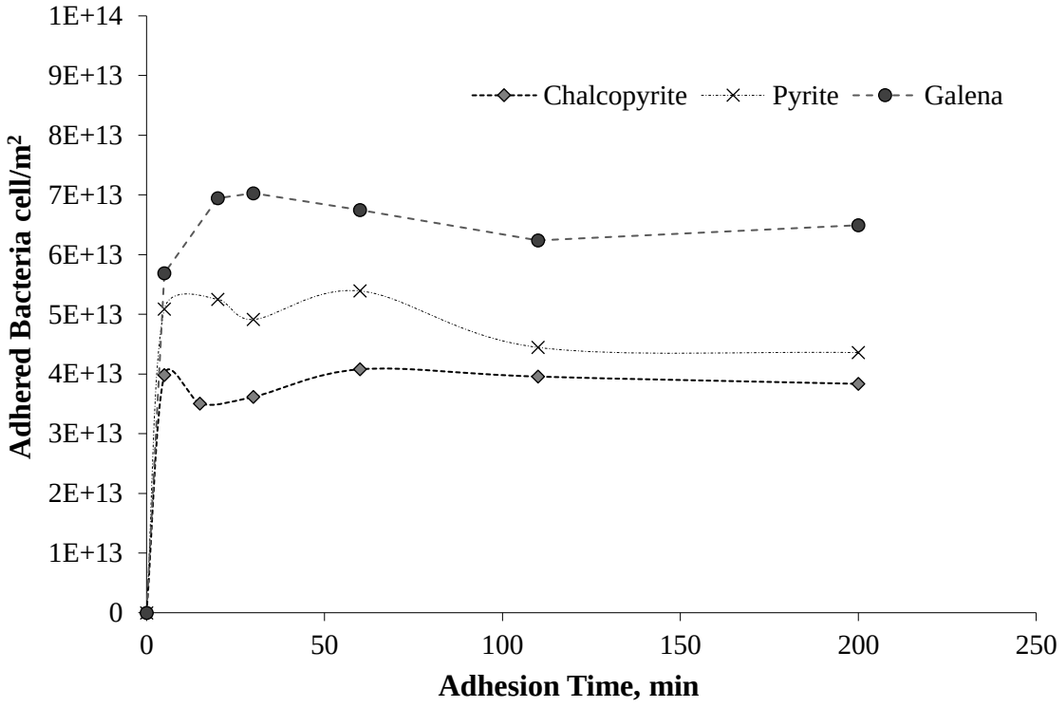

Figure 9.5 Adhesion isotherms of *S. carnosus* bacteria with minerals of interest at pH 9

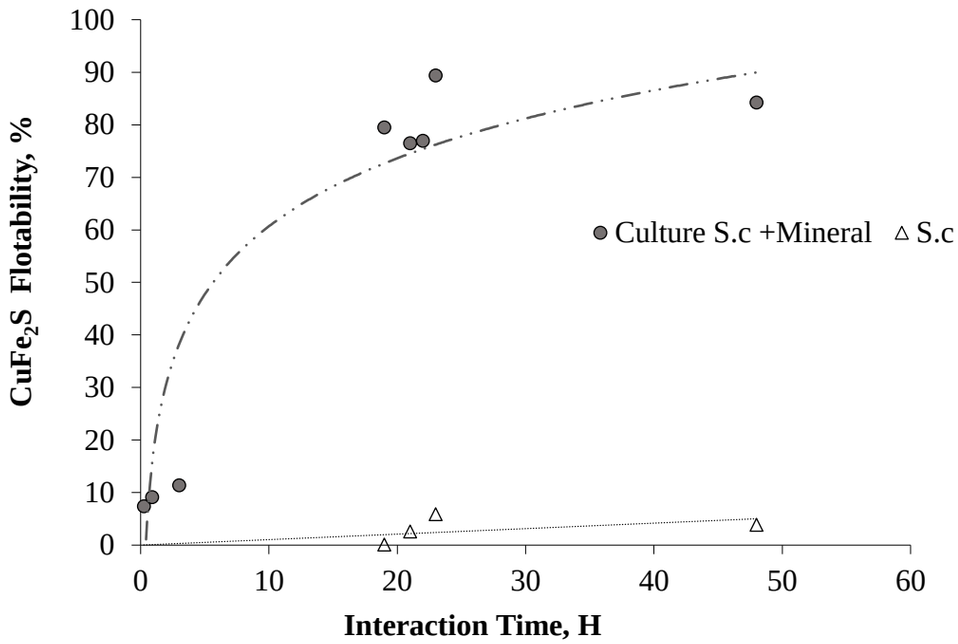

Figure 9.6 Zeta potential of *S. carnosus* bacteria (control) depending on: a) pH and b) Time (H)

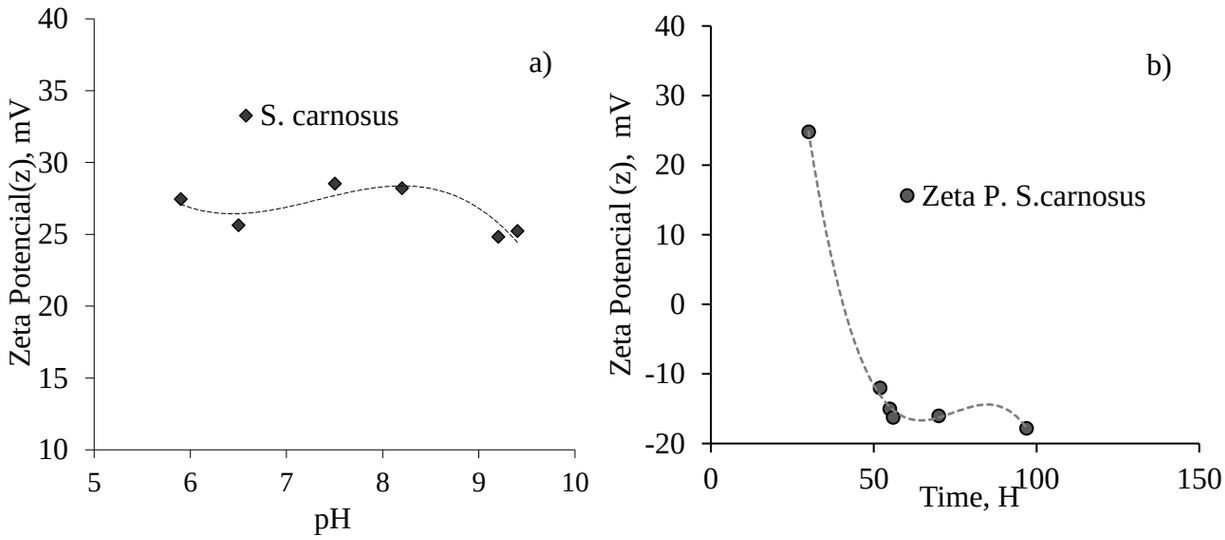

Figure 9.7 Zeta potential of S. *carnosus* bacteria with the mineral of interest. a) Before the interaction and b) after the interaction

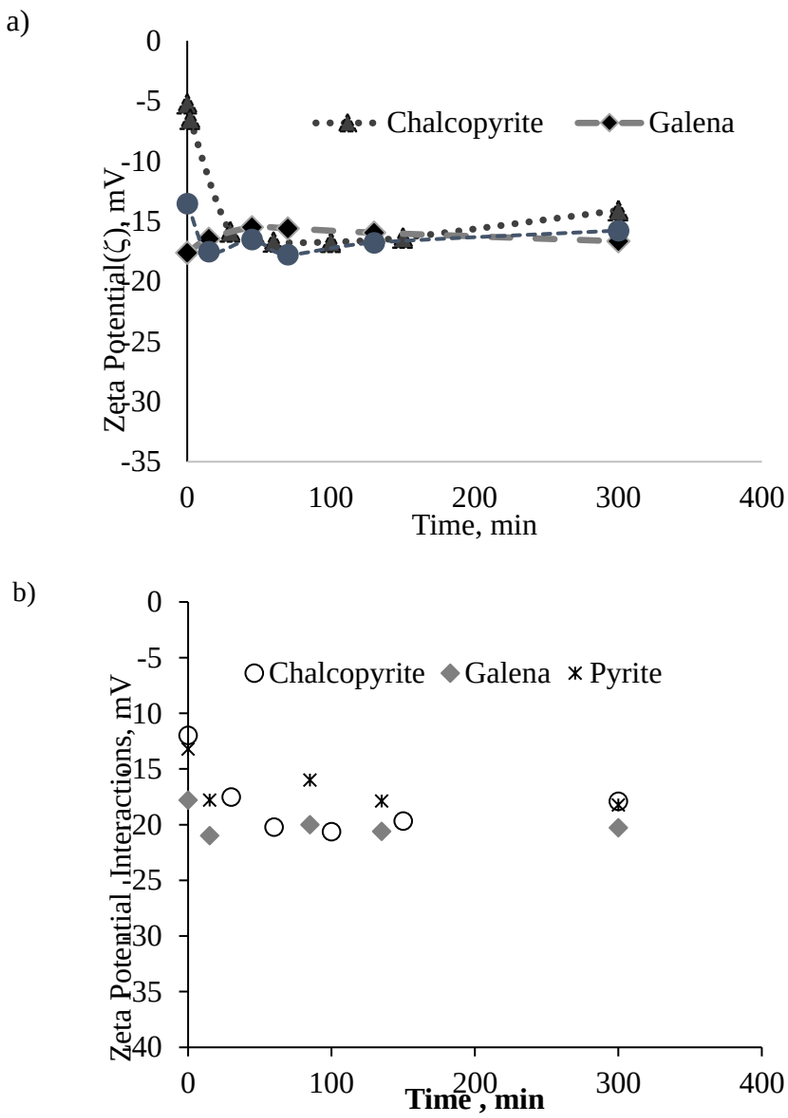

Figure 9.8 Floatability of the natural mineral at pH 9. Minerals conditioned in a 1 x 10^{-3} M solution of $NaNO_3$ at pH 9, in the absence of bacteria

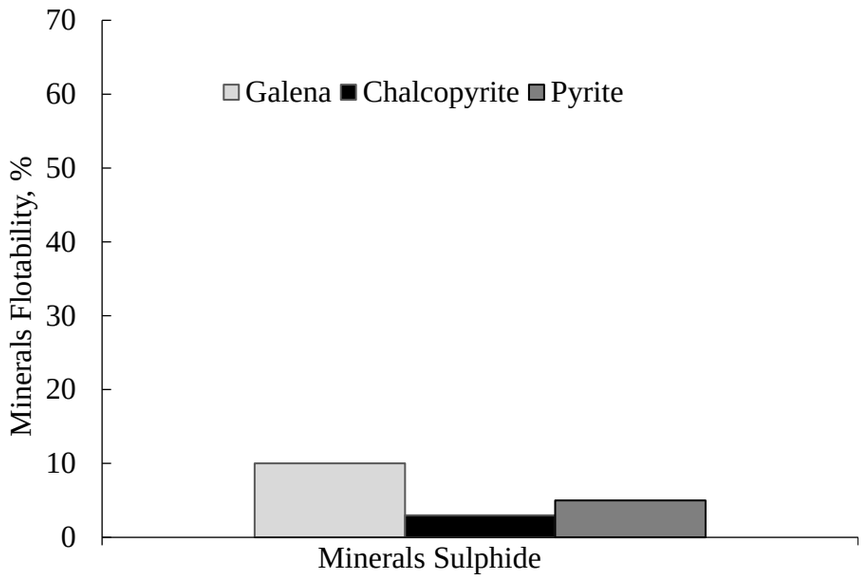

Figure 9.9 Floatability of bio-modified minerals. After interaction with *S. carnosus* bacteria at a pH of 9

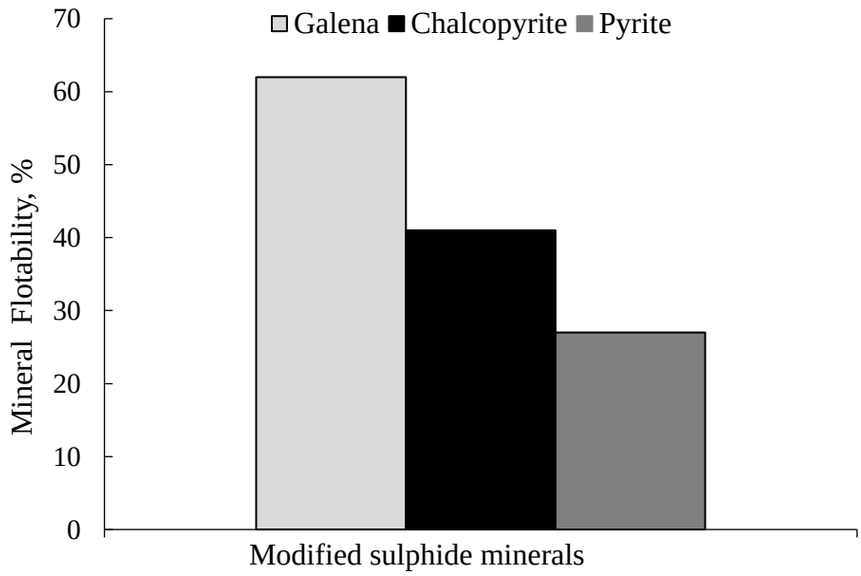

Table 9.1 Chemical analysis of minerals

Minerals	Formula	Cu%	Zn%	Fe%	S%	Pb%	Purity %
Chalcopyrite	$CuFeS_2$	31.24	0.22	32.58	30.45	0.01	90
Galena(+)	PbS	0.009	0.157	0.135	12.39	73.01	85
Pyrite(+)	FeS_2	0.002	0.004	40.42	47.439	0.006	88
(+) Associated gangue silicates.							

Table 9.2 Surface area of the mineral fraction used

Minerals	Surface area, m^2/g
Chalcopyrite	0.0109
Pyrite	0.00874
Galena	0.00673

9.2 Methodology

9.2.1 Reagents and minerals

Three pure mineral samples of chalcopyrite ($CuFeS_2$), pyrite (FeS_2) were obtained from Santa Eulalia, Chihuahua, while the galena (PbS) was attained from the Plomosas Mine at Chihuahua. The chemical compositions of the chalcopyrite, pyrite and galena used during the microflotation tests are presented in Table 9.1. Other chemical reagents used for this test were distilled water was used to prepare the solutions and n-hexadecane was used as foaming agent.

9.2.2 Microorganism

The bacteria used was *Staphylococcus carnosus* ATCC No. 51365 strain. Bacteria was cultured in tryptone soy broth with yeast extract (ATCC Medium No 1887). The culture media consisted of 30 g tryptone and 3 g yeast, which were diluted in 1 L of distilled water and the pH was adjusted to 7. The medium was autoclaved (Model No 25 x All American Autoclave) for 15 min. After annealing the culture, broth was inoculated with the lyophilized bacterium *Staphylococcus carnosus* (ATCC 51365) and then incubated for 24 h at 37 ° C. (Ramos-Escobedo *et al.*, 2016).

9.2.3 Growth Kinetics

The kinetics of bacteria growth was conducted by counting the microorganisms in the culture medium at different times in a period between 0 to 60 h, using the Neubauer chamber (Neubauer Reichert) and phase contrast microscopy (Axioskop 40, ZEISS). Cell counting was performed in 14.5 μl of sample.

9.2.4 Preparation of minerals

The crystals were crushed in porcelain mortar and then wet sieved using -100 + 200 mesh, -200 + 400, and -400. The fraction between -100 +200 mesh was separated for flotation test. A sample of 5 g of each mineral (-400 mesh) was analyzed by atomic absorption spectroscopy (AAS) to determine its chemical composition (Table 9.1).

9.2.5 Bacterial adhesion

For bacterial adhesion test, 1 g of each mineral was collected in 50 ml of fresh bacterial culture, over a period of 5 to 1440 min. The initial concentration of bacteria at time t was determined by direct counting in a Neubauer chamber. The amount of attached bacteria was determined by Eq. (1):

$$B_{Ad} = \frac{(B_0 - B)V}{wA_m} \tag{1}$$

Where: B_{Ad} is adhering bacteria (cell/m^2); B_0 and B are the concentration of free bacteria at zero time and t, respectively (cell/ml); V is the volume of sample in ml; w is the exact weight of mineral in grams, A_m is the surface area determined by Coulter counter mineral (Table 9.2).

9.2.6 Zeta potential

Prior to the measurement of zeta potential, microorganisms were washed to eliminate the culture medium used in culture of bacteria. To accomplish this, a solution of $NaNO_3$ at pH 7 was prepared and the sample was centrifuged for 5 min at 2,000 rpm, the supernatant was pulled, and the precipitate was washed with the appropriate solution (pH 6, 7, 8, 9). Then, the samples were shaken in a Vortex to re-suspend the bacteria, which were placed in test tubes and refrigerated. After that, samples of 20 ml of the microorganisms in suspension were analyzed for zeta potential in the equipment Zetaphoremeter IV (CAD Instruments). The effect of the mineral-bacterium interaction was determined by contacting 5 g of each mineral (38 μm) in 250 ml of fresh culture. At a given time (0-1440 min), a sample of 3 ml was centrifuged at 1000 rpm for 5 min to remove bacteria and ore. Subsequently, they were separately suspended in 30 ml of 10^{-3} M $NaNO_3$ at pH 9 and its zeta potential was measured.

9.2.7 M.A.T.H. (Microbial adhesion to hydrocarbons)

Hydrophobicity was measured by MATH, for which, 1 ml of suspended bacteria and 0.16 ml of solvent n-hexadecane, were mixed in a vortex for 20, 45, 60 and 90 seconds. Tests were performed at pH 7. The concentration of bacteria was recorded as a function of conditioning time by counting microorganisms in the aqueous phase using a Neubauer chamber. (Ramos-Escobedo *et al.*, 2016).

9.2.8 Microflotation

Microflotation tests were performed using a Partridge microcell (Partridge and Smith, 1972), which is superimposed on a magnetic stirring grid. For this purpose, the sample was conditioned before floatation, using a 25 ml beaker with 25 ml of sample (culture medium with bacteria in suspension) at different pH values (6, 7, 8, 9) and 1 g of the mineral of interest, (chalcopyrite, pyrite, galena and). The mixture was conditioned for 24 h at 160 rpm.

During flotation, the mixture bacteria / mineral was poured in the flotation cell, which was regulated at a nitrogen pressure of 60 psi and flow rate of 60 ml/min. After solution was added to the respective pH to the sample to reach the volume optimal for flotation. Flotation was carried out for two min. The not floated and floated minerals, were filtered, dried and floatability was calculated according to Eq. (2)

$$\%\ Mineral\ flotability = \frac{C}{A}\ \text{X}\ 100 \qquad (2)$$

Where: A is the weight fed in grams of ore and C is the weight in grams of concentrated ore (float).

9.3 Results and discussion

9.3.1 Growth phases and kinetic of *S. carnosus*

The kinetics of *S. carnosus* growth is presented in Figure 9.1, which shows the bacterial concentration versus incubation time. This figure shows how the exponential phase starts at 2 h and ends at about 6 h. According to the results, it was determined that the optimal incubation time for the bacterium was about 20 h, as the bacteria concentration remained practically constant for larges times.

The concentration of the bacteria was determined using the optical density method in a UV-1800 Shimadzu spectrophotometer, at a wavelength of 620 nm. Each of the experimental tests was done in triplicate.

In the Figure 9.2 can be observed and the concentration of the bacterium of *Staphylococcus carnosus* with respect to pH.

9.3.2 Hydrophobicity of *S. carnosus*

The hydrophobicity of bacteria was determined by affinity of *S. carnosus* to n-hexadecane (nonpolar solvent) (Ramos-Escobedo *et al., 2016).* The results are presented in Figure 9.2, showing a high percentage of bacteria removal from aqueous phase, obtaining values from 87.5 to 89.5%, noting a slight increase as more alkaline is the pH. This indicates that the surface of *S. carnosus* has hydrophobic characteristics, which are accentuated in alkaline conditions, property suitable for conventional flotation of sulfides minerals.

Key features of great importance for using *S. carnosus* in this research are the hydrophobic characteristics of bacteria, which are necessary for flotation. Therefore, it may function as a collector in sulfides systems, resulted by the adherence of bacteria to the ore, hydrophobic properties. On this aspect, Langwaldt and Kalapudas, 2007 reported the application of *S. carnosus* in the nickel concentration of shales by flotation. No report has documented the use of *S. carnosus* in sulfides systems (Thewes *et al., 2014).*

9.3.3 Effect of *S. carnosus* in the preparation time of bacteria and in the presence of a hydrophobic medium

In Figure 9.3 the test results for chalcopyrite floatability are presented, respect to subsequent washout observed using fresh bacteria (wash and application of bacteria) and washed bacteria after 48 h (bacteria stale). Results indicate that fresh bacteria remains hydrophobic causing chalcopyrite recoveries up to 80% after an interaction period of 10 h. Ore floated with washed bacteria after 48 h is not significant, which shows that the surface of the bacteria undergoes changes that decrease the hydrophobicity due to the separation of the cells from the medium, i.e. absence of nutrients generated by means culture in which the microorganism was cultured.

The floatability of the chalcopyrite generates information on the hydrophobic effect of *S. carnosus,* an increase in the mineral floatability can be interpreted as optimizing the hydrophobic effect of the mineral-bacterium interaction.

The change in the hydrophobic surface of *S. carnosus* is unknown. Moreover, whereas in an industrial system conditioning chemical collectors is relatively fast (minutes order), the results with *S. carnosus* indicate that biomodification of the mineral surface requires a very long period to generate optimal conditions flotation.

9.3.4 Effect of culture on the floatability of minerals

In Figure 9.4, the culture medium effect on the biomodification and the percentage of chalcopyrite floatability is presented. The results of the curve sharper were performed using bacteria suspensions in culture medium. The percentage of chalcopyrite floatability increased, reaching 86% with the culture medium. Less favorable results were observed using washed bacteria, preserved in solution at pH 9, which significantly reduces its ability to float chalcopyrite, that in the absence of nutrients during experimentation. Based on these results, it was determined carrying out the experimentation using bacterial culture, since the results show that the bacteria retain their hydrophobicity and achieve longer adhesion to mineral generating good floatability.

9.3.5 Characterization of the adhesion of *S. carnosus*

The rate of bacterial adhesion of *S. carnosus* on various sulfide ores were determined by adhesion isotherms as shown in Figure 9.5. The adhesion of *S. carnosus* is almost completed in the first 5 min of the bacteria-mineral interaction by chalcopyrite and pyrite. While in the case of galena the adhesion of the bacteria is reached after of 20 min. Adhesion speed can be represented as *galena >> pyrite> chalcopyrite*

The results suggest that the adhesion of the bacteria is favored in the galena mineral. Because the galena has more adhesion bacterias at pH alkaline (Patra *et al.*, 2008). Followed by a lower adhesion to iron containing minerals ($CuFeS_2$, FeS, FeS_2). The results indicate that *S. carnosus* exhibits different rates of adhesion sulfide ores, which may be used to generate a selective adhesion during the separation of mineral mixtures in future work.

9.3.6 *S. carnosus* and biomodified minerals Zeta potential

Figure 9.6 shows the results of zeta potential of the bacterium *S. carnosus* varying the pH. It shows a positive charge along pH values evaluated. The utility of measuring the zeta potential is primarily determining the surface charge of both controls (bacteria and mineral) as that of bioengineered mineral (mineral + bacteria), their behavior explains the interaction mechanisms between the mineral-bacteria. Some interesting aspects are evident due to the evolution of the zeta potential with *S. carnosus.* Where for the case of fresh bacterium, the bacterium ζ exhibits a positive charge independent of pH (Fig. 9.6 (a)). In the case of separate culture medium and suspended in electrolyte solution (10^{-3}M $NaNO_3$) and adjusted to pH 9 with NaOH, changes to a negative value were observed (Fig. 9.6 (b)). The reason for this result is due to the bacterial wall of *S. carnosus*, which consists of peptidoglycan and polysaccharide, and the strain reducing action by nitrate (Schleifer, 1982) is highlighted. Liu et al, 2000; mentioned that the absorption of polysaccharides on the surface of mineral can happen by some beneficial mechanisms such as hydrogen bonding, or chemical complexation.

In the case of the polysaccharides, these commonly establish equilibrium between cyclic and linear forms; therefore, due to the bacteria conditions with the electrolyte ($NaNO_3$), and the susceptibility of the aldehyde group of polysaccharide to chemical interaction with ions (NO^{3-}). This could promote the release of H^+ ions (Wade, 2004), affecting the modification of the bacterial surface with the consequent change in the value of the zeta potential.

Moreover, the bacteria with negative charge is less hydrophobic than fresh cells or cells in their culture medium stored under refrigeration, indicating that the separation of the bacteria from the medium and resuspension of the cells in the electrolyte generates an alteration on the surface characteristics of *S. carnosus*.

The results of biomodified minerals (Figure 9.7) reveal changes in both surfaces, mineral and bacterial. It shows that the zeta potential of mineral evaluated is modified to the value generated by the ζ of bacteria, indicating that the surface is covered with *S. carnosus*. In addition, the zeta potential of the modified bacteria to negative values could be due to the modification described above. The authors consider the possibility that the ions released from minerals contribute to the modification of the zeta potential of the bacteria

The correlation of the results suggests that in the initial stage of modification with *S. carnosus* could be characterized by a physical process due to the attractive forces generated between the positive bacterial cell and the negative charge of mineral substrate. Subsequently loading the bacterium, modifies the complex to negative values, however, the release of the bacteria is observed, indicating the adherence of *S. carnosus* to ore. See Figure 9.7.

9.3.7 Effect of Biomodification floatability mineral sulfides

Figure 9.8 shows the results of the natural floatability of mineral conditioned at pH 9 in the absence of bacteria. The results indicate a lower floatability than 10% of the sulfides evaluated (pyrite, chalcopyrite and galena). The hydrophilicity of sulfide ores relates to the precipitation of metal hydroxides in the mineral surface (Senior and Trahar, 1991).

The effect of biomodification mineral sulfides by conditioning with *S. carnosus* are shown in Figure 9. The results indicate that floatability of all minerals evaluated increases due to bio-modification, corroborating the hydrophobicity of *S. carnosus.*

The floatability of minerals in descending order is as follows:

galena >> chalcopyrite> pyrite>

The highest floatability is obtained by the biomodified galena (61.17%), followed by that reported for the chalcopyrite (41.2%) and 27% for the pyrite. It should be noted that faster floatability of chalcopyrite and galena are desirable because they are valuable minerals. Instead, the floatability of the pyrite is not desirable because they are gangue mineral type (unmarketable).

Galena has the highest adhesion of bacteria (see isotherms results) which causes a significant increase in the floatability of the mineral. No correlation was found with the results of the floatability of the other minerals (chalcopyrite and pyrite) and adhesion isotherms. Because the hydrophobicity of the biomodified minerals is influenced by the alteration of the bacterial surface itself species from the mineral with which it interacts, as demonstrated in tests zeta potential, in these cases, the hydrolysis of iron species (Fe (II)) of iron ore (pyrite) counteracts the hydrophobicity conferred by bacterial cells.

9.4 Acknowledgement

Our thanks and editorial to PhD Emma Teresa Pecina Treviño, teacher-researcher at the U.A de C. for all her patience, doctrine and learning for this research work.

9.5 Conclusions

From the results, it can be concluded that *S. carnosus* has a hydrophobic effect on minerals, resulting on its adherence on surface minerals and acting as a natural collector. The bio-modification generates different degrees of minerals hydrophobicity, which indicates the possibility to control the bio-collector for selective separation of minerals. The magnitude of the floatability of minerals showed the descending order as follows:

galena >> chalcopyrite> pyrite

The sulfides mineral bio-modification mechanism was evaluated in the presence of *S. carnosus* and the results shows a physical mechanism, due to the electrostatic attraction generated between the bacterial surface charge or positive zeta mineral powder and negative surface charge (negative zeta potential).

It is concluded that the usage of this strain are promising for environmentally friendly bioreagent, thus being applicable for the eco-friendly development of the bioflotation of sulfide minerals.

9.6 Acknowledgments

The authors thank to PhD Emma Teresa Pecina Treviño† for her contribution to this work, distinguished researcher who failed to see complete this manuscript. We also thank CIMAV-CHIHUAHUA y UAdeC for the support given to this project.

9.7 Nomenclature

A	Weight fed mineral in grams
C	Weight of the mineral concentrate in grams
B_{Ad}	Number of bacteria Adhered cells /m^2
B_0	Concentration of free bacterial at zero time cells/m^2
B	Concentration of free bacterial at time t in cells/m^2
V	Sample volume, mL
w	Ore weight, g
A_m	Specific surface area of the mineral, g/m^2
t	Time, h
h	hour
g	grams
wt%	percentage in weight
min	minutes

Greek symbols

ζ	Zeta Potential

9.8 References

Botero, A.E.C., Torem, M.L., de Mesquita, L.M.S., (2008). Surface chemistry fundamentals of biosorption of Rhodococcus opacus and its effect in calcite and magnesite flotation. Minerals Engineering 21, 83-92. https://doi.org/10.1016/j.mineng.2007.08.019

Bradshaw, D.J., Harris, P.J., O'Connor, C.T., (1998). Synergistic interactions between reagents in sulphide flotation. The Journal of South African Institute of Mining and Metallurgy, 189–194. https://www.saimm.co.za/Journal/v098n04p187.pdf

de Mesquita, L.M.S., Lins, F.F., Torem, M.L., (2003). Interaction of a hydrophobic bacterium strain in a hematite-quartz flotation system. International Journal of Mineral Processing 71, 3144. https://doi.org/10.1016/S0301-7516(03)00028-0

Deo, N., Natarajan, K.A., (1997). Interaction of Bacillus polymyxa with some oxide minerals with referente to mineral beneficiation and environmental control. Minerals Engineering 10, 1339-1354. https://doi.org/10.1016/S0892-6875(97)00125-8.

Dwyer, R., Bruckard, W.J., Rea, S., Holmes, R.J., (2012). Bioflotation and bioflocculation review: microorganisms relevant for mineral beneficiation. Mineral Processing and Extractive Metallurgy (IMM Transactions section C) 121, 65-71. https://doi.org/10.1179/1743285512Y.0000000005

Gericke, Y., Govender, M., 2011. Extracellular polymeric substances (EPS) from bioleaching systems and its application in bioflotation. Minerals Engineering 24 (11), 1122–1127. https://doi.org/10.1016/j.mineng.2011.02.016

Langwaldt, J., Kalapudas, R. (2007). Bio-beneficiation of multimetal black Shale ore by flotation. Physicochemical Problems of Mineral Processing. 41, 291-299.
http://www.minproc.pwr.wroc.pl/journal/pdf/2007/291-299.pdf

Liu, Q., Zhang, Y. Laskowski, J.S. (2000), The adsorption of polysaccharides onto mineral surfaces: an acid/base interaction. Int. J. Miner. Process, 60, 229-245. https://doi.org/10.1016/S0301-7516(00)00018-1

Lopez, Leslie Y., Merma, Antonio G., Torem, Mauricio L., Pino, Gabriela H., 2015. Fundamental aspects of hematite flotation using the bacterial strain Rhodococcus ruber as bioreagent. Minerals Engineering 75, 63–69. https://doi.org/10.1016/j.mineng.2014.12.022

Madigan, M.T., Martinko, J.M., y Parker, J., (2004). Book Brock, Biologia de los Microorganismos Biología de los microorganismos Pearson Prentice Hall. 10 Edición. España. ISBN 10: 8420536792 / ISBN 13: 9788420536798
https://www.academia.edu/39077515/Biolog%C3%ADa_de_los_microorganismos_BROCK

Merma, A.G., Torem, M.L., Morán, J.J.V., Monte, M.B.M., (2013). On the fundamental aspects of apatite and quartz flotation using a gram-positive strain as a bioreagent. Minerals Engineering 48, 61-67. https://doi.org/10.1016/j.mineng.2012.10.018

Nagaoka, T., Ohmura, N., Saiki, H., (1999). A Novel mineral flotation process using Thiobacillus ferrooxidans. Applied and Environmental Microbiology 65, 3588-3593. https://doi.org/10.1016/S1572-4409(99)80123-0

Partridge, A.C. y Smith. G.W. (1972). Technical Note. Small sample flotation testing: a new cell. Trans of IMMC 80, 199-200.

Pecina, E.T., Rodríguez, M., Castillo, P., Díaz, V., and Orrantia, E. (2009). Effect of Leptospirilum ferrooxidans on the flotation kinetics of sulphide ores. Minerals Engineering 22: 462-468. https://doi.org/10.1016/j.mineng.2008.12.008

Ramos Escobedo, G., Gallegos-Acevedo, P.M., López Saucedo, F.J., Orrantia-Borunda, E. (2012). Bioflotation of sulfide minerals with Acidithiobacillus ferrooxidans in relation to Cu-activation and surface oxidation. Canadian Journal of Microbiology 58, 1073-1083. http://doi.org/10.1139/w2012-072

Ramos-Escobedo, G.T., Pecina-Treviño, E.T., Bueno-Tokunaga, A., Concha-Guerrero, S.I., Ramos-Lico, D., Guerra-Balderrama, R., Orrantia-Borunda, E. (2016). Bio-collector alternative for the recovery of organic matter in flotation processes. Fuel, 176, 165-172. https://doi.org/10.1016/j.fuel.2016.02.018

Rao, K.H., Subramanian, S. (2007). Bioflotation and bioflocculation of relevance to mineral bioprocessing. In: Micobial Processing of Metal Sulfides, (E.R. Donati, y W. Sand, eds.), Springer, Paises Bajos 267-286. https://link.springer.com/book/10.1007/1-4020-5589-7

Rao K. H., Vilinska A., Cheryshova I.V. (2010) Minerals Bioprocessing: R&D needs in mineral biobeneficiation. Hydrometallurgy, 104, 467-470. https://doi:10.1016/j.hydromet.2010.01.016

Santhiya, D., Subramanian, S., Natarajan, K.A. (2001a). Surface chemical studies on sphalerite and galena using Bacillus polymyxa: I. Microbially induced mineral separation. Journal of Colloid and Interface Science. 235 (2), 289–297. https://doi.org/10.1006/jcis.2000.7374

Santhiya, D., Subramanian, S., Natarajan, K.A. (2001b). Surface chemical studies on sphalerite and galena using Bacillus polymyxa: II. Mechanisms of microbe–mineral interactions. Journal of Colloid and Interface Science. 235 (2), 298–307. https://doi.org/10.1006/jcis.2000.7256

Santhiya, D., Subramanian, S., Natarajan, K.A., Rao, K.H., Forssberg, K.S.E. (2001c). Biomodulation of galena and sphalerite surfaces using Thiobacillus thiooxidans. International Journal of Mineral Processing. 62 (1–4), 121–141. https://doi.org/10.1016/S0301-7516(00)00048-X

Santhiya, D., Subramanian, S., Natarajan, K.A. (2002). Surface chemical studies on sphalerite and galena using extracellular polysaccharides isolated from Bacillus polymyxa. Journal of Colloid and Interface Science. 256 (2), 237–248. https://doi.org/10.1006/jcis.2002.8681

Santhiya, D., Subramanian, S., y Natarajan, K.A. (2001). Surface chemical studies on galena and sphalerite in the presence of Thiobacillus thiooxidans with reference to mineral beneficiation. Minerals Engineering 13, 747-763. https://doi.org/10.1016/S0892-6875(00)00059-5

Schleifer, K.H., Fischer, U. (1982). Description of a New Species of the Genus Staphylococcus: Staphylococcus carnosus. International Journal of Systematic Bacteriology. 32, 153-156. https://www.microbiologyresearch.org/content/journal/ijsem/10.1099/00207713-32-2-153

Senior, G.D., and Trahar, W.J. (1991). The influence of metal hydroxides and collector on the flotation of chalcopyrite. International Journal of Minerals Process. 33, 321-341. https://doi.org/10.1016/0301-7516(91)90061-M

Subrahmanian, S., Santhiya, D., Natarajan, K.A. (2003). Surface modification studies on sulphide minerals using bioreagents. International Journal of Mineral Processing 72, 175-188. https://doi.org/10.1016/S0301-7516(03)00097-8

Thewes, N., Loskill P., Jung P., Peisker H., Bischoff M., Herrmann M. Jacobs K. (2014). Hydrophobic interaction governs unspecific adhesion of staphylococci: a single cell force spectroscopy study. Beilstein Journal of Nanotechnology 5, 1501—1512.

https://www.researchgate.net/publication/265908161_Hydrophobic_interaction_governs_unspecific_adhesion_of_staphylococci_A_single_cell_force_spectroscopy_study
http://doi.org/10.3762/bjnano.5.163

Vilinska A. (2007) Bacteria-Sulfide Mineral Interactions with Reference to Flotation and Flocculation. Licentiate Thesis. Luleå University of Technology, Luleå, Swaden. http://www.diva-portal.se/smash/get/diva2:998994/FULLTEXT01.pdf

Wade, L.G. (2004). Química Orgánica. 5ed, Ed. Pearson Prentice Hall, España. ISBN: 84-205-4102-8 https://clea.edu.mx/biblioteca/files/original/54cf5e0505683274cf95b8f0fb580034.pdf

[Title in Times New Roman and Bold Type No. 14 in English and Spanish]

Last Name (IN CAPITAL LETTERS), First Name of 1st Author†*, Last Name (IN CAPITAL LETTERS), First Name of 1st Co-Author, Last Name (IN CAPITAL LETTERS), First Name of 2nd Co-Author and Last Name (IN CAPITAL LETTERS), First Name of 3rd Co-Author.

Author's Institution of Affiliation including dependency (in Times New Roman No.10 and Italics)

International Identification of Science - Technology and Innovation

1st Author ID: (ORC ID - Researcher ID Thomson, arXiv Author ID - PubMed Author ID - Open ID) and CVU 1st Author: (Scholar-PNPC or SNI-CONACYT) (No.10 Times New Roman)

1st Co-author ID: (ORC ID - Researcher ID Thomson, arXiv Author ID - PubMed Author ID - Open ID) and CVU 1st Co-author: (Grantee-PNPC or SNI-CONACYT) (No.10 Times New Roman)

2nd Co-author ID: (ORC ID - Researcher ID Thomson, arXiv Author ID - PubMed Author ID - Open ID) and CVU 2nd Co-author: (Scholar-PNPC or SNI-CONACYT) (No.10 Times New Roman)

3rd Co-author ID: (ORC ID - Researcher ID Thomson, arXiv Author ID - PubMed Author ID - Open ID) and CVU 3rd Co-author: (Grantee-PNPC or SNI-CONACYT) (No.10 Times New Roman)

(Indicate Date of Submission: Month, Day, Year); Accepted (Indicate Date of Acceptance: Exclusive Use by ECORFAN)

Citation: First letter (IN CAPITAL LETTERS) of the Name of the 1st Author. Last Name, First Letter (IN CAPITAL LETTERS) of the 1st Co-author's Name. Last name, first letter (IN CAPITAL LETTERS) of the 2nd Co-author's name. Last Name, First Letter (IN CAPITAL LETTERS) of the Name of the 3rd Co-author. Last name

Institutional Mail [Times New Roman No.10].

First letter (IN CAPITAL LETTERS) of the Name Editors. Surname (eds.) *Title of the Handbook [Times New Roman No.10]*, Selected Topics of the corresponding area ©ECORFAN-Filial, Year.

Abstract

Text written in Times New Roman No.12, single spaced, in English.

Indicate (3-5) keywords in Times New Roman and Bold No.12.

1 Introduction

Text written in Times New Roman No.12, single spaced.

Explanation of the topic in general and explain why it is important.

What is its added value with respect to other techniques?

Focus clearly on each of its characteristics.

Clearly explain the problem to be solved and the central hypothesis.

Explanation of the sections of the Chapter.

Development of Sections and Sections of the Chapter with subsequent numbering.

[Title in Times New Roman No.12, single space and Bold].

Development of Chapters in Times New Roman No.12, single space.

Inclusion of Graphs, Figures and Tables-Editables

In the content of the Chapter, all graphs, tables and figures must be editable in formats that allow modifying size, type and number of letters, for editing purposes, these must be in high quality, not pixelated and must be noticeable even if the image is reduced to scale.

[Indicating the title in the upper part with Times New Roman No.12 and Bold, indicating the font in the lower part centered with Times New Roman No. 10].

Table 1.1 Title

Variable	Description	Value
P_1	Partition 1	481.00
P_2	Partition 2	487.00
P_3	Partition 3	484.00
P_4	Partition 4	483.50
P_5	Partition 5	484.00
P_6	Partition 6	490.79
P_7	Partition 7	491.61

Source:

(They should not be images, everything should be editable)

Figure 1.1 Title

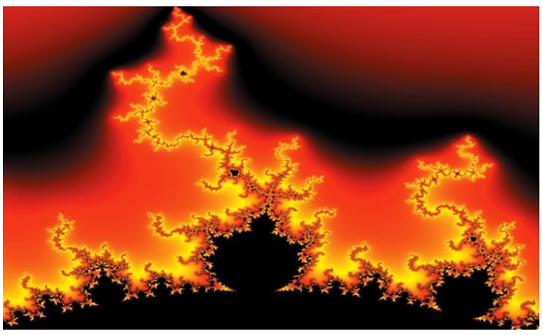

Source:

(They should not be images, everything should be editable)

Graphic 1.1 Title

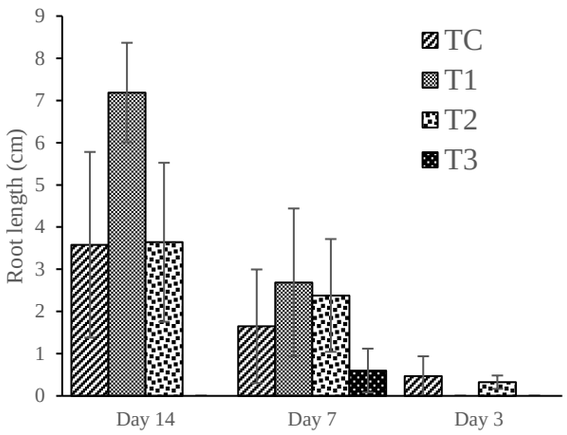

Source:

(They should not be images, everything should be editable)

Each Chapter should be presented separately in **3 Folders:** a) Figures, b) Graphs and c) Tables in .JPG format, indicating the number in Bold and the sequential Title.

For the use of Equations, indicate as follows:

$$\int_{lim^{-1}}^{lim^{1}} = \int \frac{lim^{1}}{lim^{-1}} = \left[\frac{1\,(-1)}{lim}\right]^{2} = \frac{(0)^{2}}{lim} = \sqrt{lim} = 0 = 0 \rightarrow \propto \quad (1)$$

They should be editable and with numbering aligned on the far right.

Methodology to be developed

Give the meaning of the variables in linear wording and it is important to compare the criteria used.

Results

The results should be per section of the Chapter.

Annexes

Tables and appropriate sources.

Acknowledgements

Indicate if they were financed by any Institution, University or Company.

Conclusions

Clearly explain the results obtained and the possibilities for improvement.

References

Use the APA system. They should not be numbered or bulleted, however, if numbering is necessary, it will be because there is a reference or mention in some part of the Chapter.

Technical Data Sheet

Each Chapter should be presented in a Word document (.docx):

Name of the Handbook
Title of the Chapter
Abstract
Keywords
Sections of the Chapter, e.g:

1. *Introduction*
2. *Description of the method*
3. *Analysis based on demand curve regression*
4. *Results*
5. *Acknowledgement*
6. *Conclusions*
7. *References*

Name of Author(s)
Correspondence E-mail to Author
References

Intellectual Property Requirements for its edition:

- Author's and co-authors' autographic signature in blue colour of the originality form.

- Author's and co-authors' autgraphic signature in blue colour of the author and co-authors' acceptance form.

Reservation to the Editorial Policy

ECORFAN Handbooks reserves the right to make any editorial changes required to bring the Scientific Work into compliance with the ECORFAN Handbooks Editorial Policy. Once the Scientific Work has been accepted in its final version, ECORFAN Handbooks will send the author the proofs for review. ECORFAN® will only accept the correction of errata and errors or omissions arising from the editing process of the journal, reserving in its entirety the rights of authorship and dissemination of content. Deletions, substitutions or additions that alter the formation of the Scientific Work will not be accepted.

Code of Ethics - Good Practices and Statement of Solution to Editorial Conflicts

Declaration of Originality and unpublished character of the Scientific Work, of Authorship, on the obtaining of data and interpretation of results, Acknowledgements, Conflict of interests, Assignment of rights and distribution.

The Management of ECORFAN-Mexico, S.C. claims to the Authors of the Scientific Work that its content must be original, unpublished and of Scientific, Technological and Innovation content in order to submit it for evaluation.

The Authors signing the Scientific Work must be the same who have contributed to its conception, realization and development, as well as to the obtaining of the data, the interpretation of the results, its writing and revision. The Corresponding Author of the proposed Scientific Work should fill in the following form.

Title of the Scientific Work:

- The submission of a Scientific Paper to ECORFAN Handbooks implies the author's commitment not to submit it simultaneously to the consideration of other serial publications. To do so, he/she must complete the Originality Form for his/her Scientific Paper, unless it is rejected by the Referee Committee, it may be withdrawn.

- None of the data presented in this Scientific Work has been plagiarized or invented. The original data are clearly distinguishable from those already published. And we are aware of the PLAGSCAN test, if a positive plagiarism level is detected, we will not proceed to refereeing.

- The references on which the information contained in the Scientific Work is based are cited, as well as theories and data from other previously published Scientific Works.

- The authors sign the Authorization Form for their Scientific Work to be disseminated by the means that ECORFAN-Mexico, S.C. in its Holding Mexico considers pertinent for the dissemination and diffusion of their Scientific Work, ceding their Scientific Work Rights.

- Consent has been obtained from those who have provided unpublished data obtained through verbal or written communication, and such communication and authorship are properly identified.

- The Author and Co-Authors signing this work have participated in its planning, design and execution, as well as in the interpretation of the results. Likewise, they critically reviewed the work, approved its final version and agree with its publication.

- No signature responsible for the work has been omitted and the criteria for Scientific Authorship have been met.

- The results of this Scientific Work have been interpreted objectively. Any results contrary to the views of the signatories are stated and discussed in the Scientific Work

Copyright and Access

The publication of this Scientific Work implies the assignment of the copyright to ECORFAN-Mexico, S.C. in its Holding Mexico for its ECORFAN Handbooks, which reserves the right to distribute on the Web the published version of the Scientific Work and the availability of the Scientific Work in this format implies for its Authors the compliance with the provisions of the Law of Science and Technology of the United Mexican States, regarding the obligation to allow access to the results of Scientific Research.

Title of the Scientific Work:

Name and surname(s) of Contact Author and Co-authors	Signature
1.	
2.	
3.	
4.	

Principles of Ethics and Editorial Conflict Resolution Statement

Editor's Responsibilities

The Editor undertakes to guarantee the confidentiality of the evaluation process, and may not reveal the identity of the Authors to the Referees, nor may he/she reveal the identity of the Referees at any time.

The Editor assumes the responsibility of duly informing the Author of the stage of the editorial process in which the submitted text is, as well as of the resolutions of the Double Blind Arbitration.

The Editor must evaluate manuscripts and their intellectual content without distinction of race, gender, sexual orientation, religious beliefs, ethnic origin, nationality, or political philosophy of the Authors.

The Editor and its editorial staff of ECORFAN® Holdings will not disclose any information about the submitted Scientific Work to anyone other than the corresponding Author.

The Editor must make fair and impartial decisions and ensure a fair peer review process.

Responsibilities of the Editorial Board

The description of the peer review process is made known by the Editorial Board so that the Authors are aware of the evaluation criteria and will always be ready to justify any controversy in the evaluation process. In case of Plagiarism Detection to the Scientific Work, the Committee notifies the Authors for Violation of the Right of Scientific, Technological and Innovation Authorship.

Responsibilities of the Referee Committee

The Referees undertake to notify any unethical conduct on the part of the Authors and to point out any information that may be a reason to reject the publication of the Scientific Work. In addition, they must undertake to keep confidential the information related to the Scientific Work they evaluate.

Any manuscript received for refereeing must be treated as a confidential document, not to be shown or discussed with other experts, except with the permission of the Editor.

Referees should conduct themselves in an objective manner; any personal criticism of the Author is inappropriate.

Referees should express their views clearly and with valid arguments that contribute to the Scientific, Technological and Innovation achievements of the Author.

Referees should not evaluate manuscripts in which they have conflicts of interest and which have been notified to the Editor before submitting the Scientific Work for evaluation.

Responsibilities of Authors

Authors must guarantee that their Scientific Works are the product of their original work and that the data have been obtained in an ethical manner.

Authors must guarantee that they have not been previously published or that they are not being considered in another serial publication.

Authors must strictly follow the rules for the publication of Scientific Works defined by the Editorial Board.

Authors should consider that plagiarism in all its forms constitutes unethical editorial conduct and is unacceptable; consequently, any manuscript that incurs in plagiarism will be eliminated and will not be considered for publication.

Authors should cite publications that have been influential in the nature of the Scientific Work submitted for refereeing.

Information Services

Indexing - Bases and Repositories

RESEARCH GATE (Germany)
MENDELEY (Bibliographic Reference Manager)
GOOGLE SCHOLAR (Citation Indexes-Google)
REDIB (Ibero-American Network of Innovation and Scientific Knowledge- CSIC)

Editorial Services

Citation Identification and H Index
Originality and Authorization Format Management
Handbooks Testing with PLAGSCAN
Evaluation of Scientific Work
Issuance of Referee Certificate
Scientific Work Editing
Web Layout
Indexing and Repository
Publication of Scientific Work
Scientific Work Certificate
Invoicing for Publishing Services

Editorial Policy and Administration

143 - 50 Itzopan, Ecatepec de Morelos - Mexico. Tel: +52 1 55 6159 2296, +52 1 55 1260 0355, +52 1 55 6034 9181; E-mail: contact@ecorfan.org www.ecorfan.org

9 786078 695867
ISBN: 978-607-869-58-67